Kalbassi, Mohammed Ali (1987) Distillation sieve tray efficiencies. PhD thesis, University of Nottingham.

Access from the University of Nottingham repository:
http://eprints.nottingham.ac.uk/13540/1/376628.pdf

UNIVERSITY OF NOTTINGHAM

DEPARTMENT OF CHEMICAL ENGINEERING

DISTILLATION SIEVE TRAY EFFICIENCIES

by

Mohammad. Ali. Kalbassi B.Sc.

A thesis presented to the University of Nottingham
for the degree of Doctor of Philosophy.

May 1987

VOLUME CONTAINS CLEAR OVERLAYS

OVERLAYS HAVE
BEEN SCANNED
SEPERATELY
AND
THEN AGAIN OVER
THE RELEVANT PAGE

Dedicated to my dear mother Ezzat,

and to the memory of my beloved

father Mohammad Reza.

ACKNOWLEDGEMENTS

It is with pleasure that I record my sincere gratitude to Dr. M. W. Biddulph for his kind and enthusiastic guidance throughout this work.

I would also like to express my thanks and gratitude to:

- Professor W. Smith, the head of department.

- My friend Dr. M. M. Dribika.

- Highly skilled members of the lab especially Mr. W. Thomson, Mr. J. Luger, Mr. M. Jefferies, Mr. B. Wilson and Mr. D. Wood who made this highly experimental research possible.

- Mrs. W. Mason for her computing assistance.

- Mrs. L. Watson for typing this thesis.

- Acknowledge the provision of tray material by B.O.C. Cryoplants Ltd., London.

The sieve tray distillation column is one of the most widely used separation devices throughout the chemical and petrochemical industry. Although an enormous amount of research has been carried out in order to understand the behaviour of the sieve trays, there are still many uncertainties. One of these uncertainties is concerned with the prediction of the tray efficiency for binary and multicomponent systems. It has been shown that the methods available at present have deficiencies for binary system predictions and have hardly been tested against large scale experimental data for ternary distillation. There is no theoretical method available to predict efficiencies of systems comprising more than three components. The prediction of tray efficiency can be divided into two parts. In the first part the 'point efficiency' is obtained by a theoretical or experimental method. In the second part this point efficiency is incorporated into a mixing model taking into account the hydraulics, which may include the uniformity of flow across the tray.

In this thesis the point efficiencies for atmospheric operation in the mixed flow regime are presented based on measurements in two sieve tray distillation columns operating under similar hydrodynamic condition as follows:-

A - A small scale Oldershaw column modified to inhibit surface tension induced 'wall effects'.

B - A large rectangular tray distillation column with narrow width and about one meter flow path length.

Three binaries, two ternaries and a quaternary alcohol-water systems have been studied experimentally using these two columns.

The ternary point efficiencies for the system $MeOH/n.PrOH/H_2O$ are

predicted using the methods available and compared with actual large scale experimental efficiencies. The point efficiencies from the modified Oldershaw column are also compared with actual large scale experimental point efficiencies in the ternaries and the quaternary systems to study the feasability of incorporating them into the design of large scale columns.

Further steps are also described to improve the gas and liquid contact on the modified column to obtain better point efficiencies.

In order to improve the uniformity of flow across a circular tray, an expanded aluminium material tray has been studied experimentally with different hydraulic conditions during distillation. The small diamond shaped holes in this material are corrugated, thus allowing the vapour momentum assist the liquid flow.

SUMMARY

The distillation point efficiencies for the alcohol-water binary, ternary and quaternary systems were measured using a modified Oldershaw column. This column is expanded above the tray to separate the newly formed bubbles from the column wall, thus eliminating the surface tension induced wall effects for positive systems and discouraging wetted wall effects. The excessive and recirculating foam and froth found in the conventional Oldershaw column is due to these wall effects and does not represent conditions in large scale distillation.

The point efficiencies measured using this column for the system methanol/water were lower than the point efficiencies deduced from the composition profiles across a large and narrow rectangular distillation column using an eddy diffusion model.

The narrow rectangular column had a liquid flow path length of about one meter, thus avoiding stagnant zones and flow non-uniformities. The lower efficiencies were due to the shorter contact time between the gas and the liquid. This contact time was increased markedly by fitting an outlet weir to the modified Oldershaw column, thus increasing the tray liquid hold-up and the point efficiencies. These point efficiencies were about 10 per cent lower than those on the large tray at a similar value of the F. Factor. The eddy diffusion model predicted rectangular tray efficiencies about 10 to 20 per cent lower than those measured, when using the improved modified column point efficiencies. Using a suitable model, the improved point efficiencies were scaled-up to the conditions existing on the rectangular tray. This resulted in the large tray values of 2 to 4 per cent lower tray efficiencies than those measured.

The surface tension effect on the point efficiencies of the binary systems MeOH/H_2O, EtOH/H_2O. The systems n.PrOH/H_2O and MeOH/n.PrOH were

investigated using the original modified Oldershaw column in the absence of wall effects using the concept of the Marangoni stabilising index. The surface tension of these systems were measured using a glass tensiometer. The system $MeOH/H_2O$ had the highest Marangoni index and showed the highest point efficiencies throughout the composition range, with the $EtOH/H_2O$ system following closely. However, the systems $n.PrOH/H_2O$ and $MeOH/n.PrOH$, with low values of the Marangoni index, showed comparable point efficiencies throughout the composition range. These systems demonstrate all the possible types of surface tension behaviour.

The effects of the outlet weir height and hole size on the point efficiencies in the rectangular column operating under similar hydrodynamic conditions were also investigated using the system $MeOH/H_2O$. There was an increase in point and tray efficiencies on increasing the outlet weir height from 2 mm to 12.7 mm. There was also small increase in point and tray efficiencies on decreasing the hole size from 6.4 mm to 1 mm at the expense of higher pressure drops. The point efficiencies of these trays under different hydraulic conditions were in the range 85 to 95 per cent, with subsequent high tray efficiencies. This provides further evidence of the high tray efficiencies available to the design engineer, if the detrimental effects of stagnant zones and flow non-uniformities were eliminated.

Two highly non-ideal ternary systems and quaternary system were also studied using the original modified Oldershaw and the rectangular columns. Considerable differences between the individual component point efficiencies were observed. These differences are probably caused by the interactive nature of the mass transfer in these systems. These systems also exhibited equal component point efficiencies in parts of the composition range, which illustrates the composition dependency of these systems.

The individual component tray efficiencies for these systems were noticeably different, even with equal component point efficiencies operating across the tray. These differences were simulated using the eddy diffusion model, highlighting the effects of limited liquid back mixing on the tray.

The composition profile for the system MeOH/EtOH/H_2O were predicted and compared with the measurements across the rectangular column using three methods derived from the original Maxwell and Stephan mass transfer equations. These predictions were in good agreement with the measurements. However, as the comparison is only based on a one meter flow path length, the actual design of distillation column using these methods would be conservative. The prediction of the composition profiles using the point efficiencies from the original version of the modified Oldershaw column yielded a similar observation for both the ternaries and the quaternary system.

An expanded aluminium tray (Expamet 607A) was also subject to preliminary efficiency tests in the rectangular column. This material has corrugated angled holes, thus encouraging the liquid flow across the tray by using the vapour momentum. This material showed much lower pressure drops, due to its high open area compared with conventional sieve trays, and discourages weeping and entrainment.

CONTENTS

LIST OF SYMBOLS

a, b, c and d	Defined by equation 3.4	-
a1 and a2,	Interfacia mass transfer area for small and large scale columns.	(L^{-1})
aC	Defined by equation 7.8	-
AR	Area Ratio	-
A	Sugden equation constant (Equation 3.1)	-
ACC	Deviation from a known value	-
AD, BD, CD, DD, FD, GD and HD	Defined by the equation C3	-
b 0	Weir length per unit bubbling area	(L^{-1})
B	Second Virial Coefficient	$(FL/mole)$
C1, C2 and C3	Antoine equation constants	-
C_v	Discharge coefficient	-
D_e	Eddy diffusivity	(L^2/θ)
D_H	Hole Diameter	(L)
D_B	Characteristic diameter of a bubble	(L)
D_g	Binary gas diffusivity	(L^2/θ)
e and f	Coefficients of equation D.1	-
E	Characteristic energy parameter	-
Eog	Point efficiency	-
Emv	Tray efficiency	-
F	Characteristic length	(L)
F_i^L	Liquid phase fugacity	(F/L^2)
F_i^{OL}	Standard state fugacity	(F/L^2)
F(0), F(1) and F(2)	Emperial correlation for second virial equation	-

Symbol	Description	Units
$[G]$	Matrix 9.10	–
G	Vapour rate	(L^3/θ)
g	Acceleration due to gravity	(L^2/θ)
H	Coefficient of the equation C9	–
H_L	Liquid enthalpy	$(FL/mole)$
H_V	Vapour enthalpy	$(FL/mole)$
H_{Vb}	Vapourisation heat	$(FL/mole)$
H_1 and H_2	Manometer differences through the fine and large capillary	(L)
H_f	Froth height	(L)
h_D	Dry pressure drop	(L)
h_L	Tray liquid head	(L)
h	Surface tension pressure drop	(L)
h_T	Total tray pressure drop	(L)
h_W	Weir height	(L)
Kog_1, Kog_2	Overall mass transfer coefficient of the small and large scale columns	(L/θ)
K	Volatility (Equilibrium constant)	–
K_s	$Vs \left(\dfrac{\rho_V}{\rho_L - \rho_V}\right)^{\frac{1}{2}}$	(L/θ)
k	Boltzmann constant	–
L	Liquid rate	(L^3/θ)
L'	Liquid rate	$(moles/\theta/L^2)$
LPR	Liquid phase resistance	–
M	Marangoni stabilising index	(F/L)
Mo	Defined by equation 7.5	–
Mi, Mj	Molecular weights	$(M/mole)$
m	Slope of the equilibrium line	–
n	Tray number	–

NOG	Overall number of transfer units	–
NTG	Ternary equivalent number of gas phase transfer units	–
NTL	Ternary equivalent number of liquid phase transfer units	–
NL	Binary number of liquid phase transfer units	–
NG	Binary number of vapour phase transfer units	–
P	Pressure	(F/L^2)
P_c	Reduced pressure	(F/L^2)
P_i	Partial pressure	–
P^s	Saturation pressure	(F/L^2)
P_e	Peclet number	–
QL	Liquid flowrate per unit length of weir	$(L^3/\theta/L)$
Q_F	Relative froth density	–
R	Gas constant	$(FL/mole.T)$
r, s and t	Coefficients of the equation B18	–
r2	Radius of large capillary	(L)
S	Defined by equation 9.5	–
t_L	Residence time	(θ)
T	Temperature	(T)
T_R	Reduced temperature	–
T_C	Critical temperature	(T)
V_S	Superficial gas velocity	(L/θ)
V_H	Hole Velocity	(L/θ)
w	Relative position on the tray	–
W	Weight fraction	–
W_j	Weight ratio	–

X or x	Mole fraction of the liquid	–
Y or y	Mole fraction of the vapour	–
Y^*	Equilibrium vapour mole fraction of the liquid X	–
Z	Compressibility	–
Z_1	Liquid path length	(L)

GREEK SYMBOLS

α, β	Parameters of Polar contribution	-
γ	Activity coefficient	-
δ	Surface tension	(L/θ)
η	Parameter of equation 6.4	-
λ	Flow parameter	-
ν	Molar volume	$(L^3/mole)$
ρ	Density	(M/L^3)
ψ	Wilson equation parameters	-
Ψ	Flow ratio parameter	-
ω	Acentric factor for polar component	-
φ	Vapour phase fugacity coefficient	-
Φ_e	Effective relative froth density	-
Γ	Ratio of driving forces	-
Ω_D	Diffusion collusion coefficient	-
Λ	Wilson equation factor	-
Δ	Difference in quantity	-

SUBSCRIPTS

BUB	Bubble point
B	Bottom sample point
boil	Boiling condition
Calib	Calibrated value
c	Critical value
i	Component, i
ij	Cross property of the components i and j
L	Liquid
M, Mix	Mixture property
Max	Maximum
Modi	Modified Oldershaw Column
Meas	Measured
n	Tray number
PO	Standard state
Recta	Rectangular column
s	Saturation property
T	Top sample point
v	Vapour

Also:		
	MeOH	Methanol
	EtOH	Ethanol
	n.PrOH	Normal Propanol
	H_2O	Water

CHAPTER 1

INTRODUCTION

INTRODUCTION

Distillation is the most widely used sparation process. Using about 3% of the world's energy (Mix et. al. 1980), and so even small small improvements in the technology are significant.

Sieve trays have been used in the chemical and petrochemical industry for over 30 years replacing the bubble cap columns, and generally preferred to other contacting devices such as valve trays and packed columns. This is because sieve trays are easy to fabricate and maintain, they can operate under different loading conditions and tolerate reasonable turndown ratios (Eagle and Lemieux, 1964). These trays generally have lower pressure drops, and consequently have lower running costs.

An enormous amount of research has been carried out to establish the behaviour of these trays under various loading conditions. Extensive studies were carried in the early 1960's in the laboratories of Fractionation Research Incorporated (F.R.I.), where the behaviour of trays with hole sizes in the range 6.4 to 19.1 mm was investigated. Design procedures have been formulated which are available in most chemical engineering design texts (Smith 1963, Lockett, 1986). However, since these early studies, some success has been achieved in understanding the behaviour of the biphase on sieve trays. The presence of stagnant zones and flow non-uniformities (Porter et. al. 1972, Lockett et. al. 1973 and Bell, 1972) has been found to reduce the efficiency of trays in large scale operation. Various attempts have also been made to use small laboratory scale sieve tray columns to study different distillation systems. Efficiency results from these studies have not agreed closely with those from large trays. This is due to the shorter vapour and liquid contact, and also surface tension induced wall effects. The biphase observed in small laboratory columns, for a surface tension positive system, is foamy

and deep, (Haselden and Thorogood, 1964). These conditions are not usually found on large industrial sieve trays (Zuiderweg, 1979) operating under similar loading conditions, but instead a biphase of liquid, fairly short-lived "froth" and spray co-exist.

Although separation processes in the chemical and petrochemical industries often involve multicomponent distillation, there is very limited information on the efficiencies of multicomponent systems as compared with binary systems, particularly for large columns. This lack of data has resulted in the usual assumption that the component efficiencies are equal to each other. This is true for thermodynamically ideal systems, if complete liquid mixing is achieved on the tray. However, for thermo-dynamically non-ideal systems, made up of components of different molecular size and nature, significant differences exist between these efficiencies. In the case of large trays with longer liquid flow paths, where partial liquid mixing exists, the components exhibit different tray efficiencies (Biddulph, 1975).

In order to predict point efficiencies for a multicomponent system, there are models available based on the Maxwell-Stephan mass transfer equation, (Diener and Gerster 1968). These models can only be used for ternary systems, and incorporate a large number of assumptions, and have hardly been tested against large tray data (Lockett, 1986). There is no method available to compute efficiencies in systems comprising four or more components where significant interactions between the components exist.

The main purpose of the work reported in this thesis is to investigate the hydraulic effects on efficiency in the mixed froth regime on a large sieve tray in the absence of stagnant zones and flow non-uniformities. The variables studied are the hole size and the outlet weir height.

Point efficiencies, composition and temperature profiles, pressure drop and liquid hold-ups are reported.

In order to eliminate "wall supported froth" common in small Oldershaw column, a new design of column is described in which an expansion of the column above the tray separate the newly formed bubbles from the glass wall. The efficiencies measured in this column are compared with those from the standard Oldershaw column, and are compared with large scale measurements. The possibility of using improved form of this column to predict point efficiencies for the design of a large scale distillation column is discussed. A new efficiency classification of positive, negative and neutral systems as defined by Zuiderweg and Harmens (1958), is also suggested based on measurements from this column.

Studies of three non-ideal multicomponent systems are also described. The prediction methods are tested for a ternary systems using the large tray data. The point efficiencies measured using the modified column on these systems were also used to predict the composition profiles across the rectangular tray. These point efficiencies were incorporated into an eddy diffusion model simulating distillation runs on the large rectangular column, and the resulting tray efficiencies and composition profiles were compared with actual measurements. The point efficiencies predicted by the method of Diener and Gerster (1968), Krishna et. al. (1977) and Medina et. al. (1979), using rectangular tray binary distillation data for the pairs comprising the system MeOH/n.PrOH/H_2O were also used as above to predict composition profiles and compared with actual measurements.

Preliminary work on a expanded aluminium tray is also introduced. The holes on this tray are angled at about 45° to the direction of vapour flow. This means that the vapour momentum encourages the liquid on the tray to move forward faster than on the normal sieve tray. It is hoped

that, if correct hydraulic conditions can be found, this tray will reduce flow non-uniformities, and may eliminate the stagnant zones on circular, chordal weir trays.

CHAPTER 2

LITERATURE SURVEY

LITERATURE SURVEY

2.1   The Effects of Outlet Weir Height and Hole Size on the Operation

and Efficiencies of Distillation Sieve Trays

The effects of hydraulic parameters, such as the outlet weir height
and hole size, have been studied by many investigators. The outlet weir
is used to maintain an appropriate liquid depth on the tray, (Huang et. al.,
1958), and it has been found that an increase in its height increases the
tray efficiency; (Umholtz and Van Winkle, 1957; Hellums et. al., 1958;
Finch and Van Winkel, 1964; Brown and England, 1961; Jeromin et. al., 1969;
Sargent et. al., 1964; Haselden and Thorogood, 1964; and Fane and
Sawistowski, 1964). Outlet weirs of the order of 25 to 50 mm are commonly
used in large distillation columns. In the low temperature distillation
of air much lower outlet weir heights are used to facilitate small tray
spacing.

Hole size, another important hydraulic parameter, has attracted
considerable attention in the past. Large perforations have been rec-
ommended on the grounds of ease of fabrication, lower cost, less suscept-
ibility to fouling and corrosion, (Patton and Pritchard, 1960), and low
pressure drop. However, weeping and low turn-down ratios have been
associated with such trays. Eagle and Lemieux (1964), demonstrated that
columns with holes as small as 6.4 mm in diameter can operate in dirty
services and tolerate larger turn-down ratios. Friend and Lemieux (1956)
found that poor performance from small hole trays could occur because of
rust and sediment deposits when operating with corrosive systems. They
recommended trays with perforations larger than 6.4 mm for such services.
Hunt et. al., (1955) and Mayfield et. al., (1952) concluded that tray
stability increases with decreasing hole size.

The effect of hole size on tray efficiency has also been a subject

of interest in the past, and Table 2.1 summarises some column features of these studies.

TABLE 2.1

Reference Year	Hole sizes mm	Column Equipment size m	% Free Area
Finch and Van Winkle (1964)	1.6 to 8.0	0.15 x 0.73 rectangular	7.0
Hellums et. al. (1958)	1.6 to 4.8	0.153 dia. circular	5.7 to 12.5
Umholtz and Van Winkle (1957)	1.6 to 4.8	0.076 dia. circular	12.5 to 16.5
Pruden et. al. (1974)	3.2 to 24.5	0.153 dia. circular	5.6

Umholtz, (1957) used 1.6 to 4.8 mm hole size perforated trays with the system octane-toluene and found no effect of hole size on tray efficiency. Hellums et. al., (1958) used the same system and range of hole sizes. At the lower vapour rates, smaller holes exhibited higher efficiencies, but at high vapour rates they found no effect of hole size. It was suggested that smaller holes, at low vapour rates, prevent the liquid being dumped due to the capillary surface tension effects, thus increasing the tray liquid hold-up and the efficiencies. Finch and Van Winkle (1964) used the methanol-air-water system for their studies, and stagnant zones were absent during their experiments. They detected no significant effect of hole size on tray efficiency. They also computed point efficiencies, assuming plug flow in the liquid phase. Pruden et. al.,

(1974) used an absorption system, finding the effect of hole size on tray efficiencies to be negligible. The range of hole size used was 3.2 to 24.5 mm, but wall effects were present during their experiments. Zenz (1972), in his comprehensive absorption review, suggested that higher efficiencies be used for smaller perforated tray design purposes. Fryback and Hufnagel (1960), using data from some confidential reports, reported that large perforations of 12.7 to 24.5 mm to be as efficient and flexible as 2.4 and 6.4 mm hole size trays. Kreis and Raab (1979), using the examples of six industrial air separation columns and petrochemical plants, found no effect of hole size on tray efficiency. Their columns employed trays with a hole size range of 1 mm to 25 mm. Patton and Pritchard (1960) indicated that trays with smaller holes provide a greater degree of mixing and a wider range of flexibility. Fell and Pinczewski (1977), recommended small hole trays for distillation of surface tension positive systems as they have high capacity advantage (Lemieux and Scotti, 1969). Burgess and Calderbank (1975), measured bubble properties and concluded that the hole size had a negligible effect on mass transfer. An examination of the bubbling process on a tray may however suggest that the rate of mass transfer could markedly increase as the perforation size decreases. Lockett et. al., (1979) proposed that the mass transfer on a sieve tray takes place in two regions, the "formation" and the "bulk froth". In the formation region they suggested that the mass transfer is highly sensitive to hole size. Smaller jets are issued by small holes which increase the mass transfer process. Their absorption experiments were carried out in small scale columns where froth heights of up to 20 cm, presumably due to the wall effects, were reported.

2.2   Small-column Efficiencies

For many years workers in the field of distillation have tried to
simulate the behaviour of large distillation columns by using laboratory
scale studies. Recent mathematical simulation of tray behaviour using
point efficiencies (Biddulph, 1975) and the short-comings of prediction
methods (Lockett and Ahmed, 1983; Dribika, 1986), together with the
scarcity of field data, necessitate an easy method of obtaining point
efficiency data for the design of distillation columns. Small columns
have been used for years to study distillation systems. One of the most
famous of these is the sieve tray Oldershaw column (1941), and many
systems and flow condition studies have been made over the years using
this type of laboratory arrangement. Zuiderweg and Harmens (1958),
Ellis and Legg (1962) and Medina et. al., (1978) studied surface tension
effects using an Oldershaw column arrangement. Ellis and Bennett (1960),
Ellis and Contractor (1959), and Ellis and Catchpole (1964), used this type
of arrangement to study vapour velocity, performance at reduced pressure,
composition effects and mass transfer effects. Meanwhile other laboratory
scale studies with novel designs or Oldershaw columns were carried out.
Brown and England (1961) used a small sieve tray column to investigate
the effect of vapour velocity, outlet weir height and mixture composition
on the efficiencies of the nitrogen/oxygen system. Fane and Sawistowski
(1969) and Bainbridge and Sawistowski (1964) studied surface tension and
other effects at high vapour velocities. Haseldon and Thorogood (1964),
and Hart and Haseldon (1969) tried to represent the behaviour of large
sieve trays by installing a foam baffle at the outlet of their small
tray, and hence study the liquid hold-up and composition effects on
point efficiencies. However, the use of the efficiencies measured in
small columns to design large tray columns has always been difficult.
This is because the dispersion stability, its hold-up and character are

sufficiently different to make translation of the results to industrial scale columns difficult. One of the important reasons for this is the presence of "wall effects" referred to by Standart (1974), Ashley and Haseldon (1972), Thomas and Haq (1976), Lockett and Ahmed (1983), Young and Weber (1972), Zuiderweg (1969), Sargent et. al., (1964), The Bubble Tray Design Manual (1958), Pruden et. al., (1974), Finch and Van Winkle (1964) and Dribika and Biddulph (1986).

2.2.1   The Scale-up of Plate Efficiency from Small Column Data

Veatch et. al., (1960) reported that Oldershaw columns had been used successfully in scale-up studies for the acrylonitrile process. Martin (1964) showed that laboratory studies with a glass Oldershaw column were in good agreement with plant studies of a high-vacuum solvent-water fractionator. Similar conclusions were reached by Andrew, (1969). Finch and Van Winkle (1964) proposed a model based on residence times and efficiency coefficients for the gas and liquid phases to obtain scaled-up tray efficiencies. The more significant studies, however, have been published in recent years. Fair et. al., (1983) measured point efficiencies using an Oldershaw column and compared them with the Fractionation Research Inc. (F.R.I.) results (Sakata and Yanugi, 1979; and Yanugi and Sakata, 1981). The efficiencies in both devices were comparable. They proposed a scale-up model based on mass transfer, tray spacing and the approach-to-flooding of the two columns. Dribika and Biddulph, (1986) measured point efficiencies of surface-tension-neutral systems in an Oldershaw column and compared them with measurements from a large rectangular column. They proposed a model based on the hydrodynamics of columns using penetration theory. The efficiencies of the Oldershaw column were some-what lower than those in the larger column.

2.3   Surface Tension Effects on Tray/Point Efficiencies

2.3.1   Surface Tension Systems

Early studies of surface tension effects in distillation by
Zuiderweg and Harmens (1958) resulted in a classification of systems
according to their surface tension characteristics. The systems are
defined as positive if the surface tension of the reflux increases down
the column, negative if it decreases and neutral if it remains unchanged.
The latter occurs if the pure components have similar surface tensions,
or if the mass transfer driving force is insufficient to cause a major
surface tension change. Their work with supported area (i.e. packed
columns) or unsupported area (i.e. laboratory Oldershaw sieve tray)
columns revealed higher efficiencies for the positive systems. This was
explained in terms of Marangoni effects on the stabilisation of the
liquid films or froth in the positive systems. Similar conclusions were
also made by Ellis and Bennett, (1960); Hart and Haseldon,(1969), Medina
et. al., (1978); and Young and Weber,(1972). The reverse, however, was
observed by Bainbridge and Sawistowski,(1964). They operated their
column in the spray regime, and their higher efficiencies for the negative
systems were explained in terms of "Marangoni" effects on droplet form-
ation. Fane and Sawistowski (1969) corrected the above statement by
defining the foam (liquid-phase continuous) and spray regime (vapour-
phase continuous). In the spray regime the negative systems obeyed the
Bainbridge and Sawistowski (1964) rule but in the froth regime Zuilderweg
and Harmens (1958), observations were repeated. Boyes and Ponter (1970)
obtained photographs of the retarded re-coalescence of ejected droplets
in a negative system. This gave longer exposure times between liquid
and gas. In some cases entrance of a droplet caused secondary ejection
of more droplets from the liquid. Boyes and Ponter (1970 and 1971) also

succeeded in measuring contact angles under the conditions obtaining

in distillation and successfully correlated the column efficiency against

the contact angle for positive systems in both supported and unsupported

interfacial area equipment. For negative systems, however, the production

of satellite droplets and sprays becomes important and hence were not

related to contact angles.

Macroscopic applications of these surface tension systems are also

considered. Fell and Pinczewski (1977), based on the above findings,

provided the following design strategy:-

a) For surface tension positive systems, the tray should be designed to

operate at low F.Factor. The tray spacing was rather moderate (300 to

460 mm) as the entrainment for such systems is low. Small holes and low

free area should be used as higher tray capacities are possible. Under

these circumstances large tray efficiencies are obtained which lead to

savings in cost. This also applies to low driving force, high surface

tension systems.

b) For surface tension negative systems the tray should be designed to

operate at a high F.Factor, with large holes and free area to encourage

spraying effects. Large tray spacing is hence required to accommodate

higher entrainment. The saving in cost results from a reduction in the

column diameter. This will also apply for surface tension neutral system.

2.3.2 Surface Tension Renewal Effects

Biddulph (1966), photographed, and hence measured, eddies arriving

at the surface for positive and negative systems in a glass-sided cell.

The eddies were the dyed liquid of the system to be examined injected by

hypodermic needle at the bottom of the cell. The spreading of the dye

on the surface was then measured by photographic techniques. The positive

systems with the highest difference in individual component surface tension

showed the maximum spreading effect. The surface tension negative systems

showed no spreading but rather a repulsion of the eddies. He then followed

this work by experimenting using a constant area pool column. There was

no abrupt change in terminal efficiencies of the positive and the negative

systems. This was explained as the result of a constant interfacial area.

For the negative systems, larger liquid phase-resistances to mass transfer

due to the lack of interfacial turbulance were measured. Higher point

efficiencies were obtained for the positive systems. Moens and Bos (1972),

accepting the above criteria, added that in macro-scale operation, the

efficiency most probably changes as a result of interfacial flow generated

by the surface tension gradient parallel to the liquid flow. They also

used a surface tension stabilising index to explain their findings using

a pool column. Similar conclusions to those of Biddulph (1966) and Ellis

and Biddulph (1967), were reached. In general, the larger the stabilising

index, the larger the efficiencies of the pool columns due to the surface

tension turbulances. Moens (1972) also studied the effect of composition

and driving force on the performance of packed distillation columns.

2.3.3   Surface Tension Effects on Mass Transfer

Both Ellis and Biddulph (1967) and Moens and Bos (1972) demonstrated

how surface renewal effects can enhance efficiencies of the positive

systems. Sawistowski (1973), in two reports, emphasised the importance

of Marangoni-induced instability and renewal. In the first report it

was stressed that these Marangoni effects affect both the mass transfer

coefficient and the effective interfacial area. It was stated that these

surface tension effects increase the mass transfer coefficient several times, that is from similar predictions using film or penetration theory. In the second report he confirmed the previous speculation (Fane and Sawistowski,1969)in terms of the effect of Marangoni instabilities on droplet sizes. Zuiderweg (1983) reported a large enhancement of point efficiency owing to the Marangoni effect. Dribika (1986) compared the distillation of a surface tension neutral system, methanol/n.propanol, with the highly surface tension positive system methanol/water. These two systems were very similar in physical properties, and their equilibrium relationship shows a similar form. Higher point and tray efficiencies were measured for the positive system. His measurement of mass transfer coefficient confirmed the conclusions reached by Sawistowski (1973).

2.4   Multicomponent Distillation Efficiencies

In designing a column for a multicomponent system, it is the normal procedure to calculate the number of theoretical stages from the equilibrium data for a required separation, a constant column efficiency is then used to estimate the required number of trays. Nord (1946) and Qureshi and Smith (1958) were among the first investigators to point out that, in multicomponent systems, individual components may operate with different efficiencies. Toor (1957) showed theoretically that, for thermodynamically non-ideal multicomponent systems, there are marked differences between binary and ternary mass transfer, arising out of interactions between the diffusing species. These interactions were designated as, firstly, "diffusion barrier" (no mass transfer occurs despite there being a driving force), secondly, "osmotic diffusion" (mass transfer when there is no driving force) and thirdly, "reverse diffusion" (mass transfer against the direction of the driving force). Toor and Buchard (1960) studied the

mass transfer behaviour of the non-ideal system methanol-isopropanol-water to demonstrate these effects. They computed different component point efficiencies existing in this system. Haselden and Thorogood (1964), using the system nitrogen-oxygen-argon, and Dribika (1986), using the system methanol-ethanol-n.propanol, measured equal component point efficiencies. This is the expected result since both these systems are thermodynamically ideal. Meanwhile, different component point efficiencies were measured for the thermodynamically non-ideal systems methanol-acetone-water, (Diener and Gerster 1968, Vogelpohl 1979), acetone-methanol-ethanol, (Free and Hutchinson 1960), methanol-isopropanol-water, (Vogelpohl 1979, Vogelpohl and Cerettor 1972), methanol-ethanol-n.propanol-butanol-water, (Gelbin 1965), ethanol-tetra-butanol-water, (Krishna et. al., 1977), cyclohexane-toluene-n.heptane, (Medina et. al., 1979), cyclohexane-toluene-ethanol and hexane-methylcyclopentane-ethanol-benzene (Young and Weber 1972).

Different individual component efficiencies were also reported by Miskin et. al., (1972), Cilianu et. al., (1974), Cermak (1970), and Konstantinov and Nikolae (1968) working on different ternary systems. These efficiencies were found to have values outside the (0, 1) internal, especially when a maximum in concentration occurred for one of the components. Medina et. al., (1979) have pointed out that the composition of the component exhibiting the maxima is independant of the precise values of its efficiency in this region.

Mixing effects on the tray have an important influence on the individual component tray efficiencies. In a series of papers Biddulph (1975, 1977) and Biddulph and Ashton (1977) used an eddy diffusion model to allow for the extent of the liquid back mixing on the tray and to simulate conditions corresponding to those in large industrial applications. They computed different component tray efficiencies despite equal component

point efficiencies operating across the tray. Dribika (1986) measured different component tray efficiencies across the tray despite the existence of equal component point efficiencies for the system methanol-ehanol-n.propanol.

2.4.1 Prediction Methods

These methods lead to the calculation of individual component point efficiencies, taking into account diffusional interactions. The procedure involves using the Maxwell-Stefan diffusion equations. These equations were derived by Diener and Gerster (1968), Krishna et. al. (1977) and Medina et. al. (1979). They assumed equimoler mass-transfer, no influence of finite mass-transfer rate on mass transfer equations, neglected thermodynamic correction factors and, most important of all, no liquid-phase resistance to mass transfer. The latter is still unknown and requires further research to take into account the interactions in the liquid phase. A method for the calculation of the liquid phase resistance is given by Krishna and Standart, (1979), but there are still complications. Krishna et. al. (1977) and Medina et. al. (1979) used these equations and their predictions were in agreement with experimental measurements. Aittama (1981) used this theory taking into account the liquid phase resistance satisfactorily. In a recent report, Lockett (1986) used this theory from first principles to calculate efficiencies for the system methanol-ethanol-water. These efficiencies were different for different components and similar to industrial data. The mass transfer process in this system was reported to be vapour phase controlled (Kutsarov and Tasev, 1986).

2.5 The Effect of Liquid Flow Maldistribution on Tray Efficiency

Kirschbaum (1934) was the first investigator to recognise that the liquid flow on a circular tray is far from uniform, and that maldistribution causes a loss of efficiency. It was not, however, until 1972 that Bell (F.R.I.) published some experimental results from a 2.4 m diameter tray which showed significant concentration changes at right angles to the direction of flow. Lines of constant concentration were U shaped. (i.e. composition at the sides of the tray was similar to that of the liquid leaving.) Porter et. al. (1972) and Lockett et. al. (1973) suggested a model which not only predicted the above behaviour, but also predicted a loss of tray efficiency on scaling up single pass sieve trays above about 3 meter in diameter. This is because as the liquid flows onto a single-pass tray from the downcomer, it tends to take the shortest route to the other downcomer by channelling down the centre of the tray. This leaves slower moving, stagnant or circulating liquid at the sides of the tray Lockett (1986). Since there is no bulk flow of liquid through these regions, they reach equilibrium with the vapour flowing through them. This obviously reduces the tray efficiency. There were other reports confirming the above criteria Lockett and Safekourdi (1976), Bell (1972a, b), Weiler et. al. (1973) and Neuburg and Chuang (1982). Smith and Delnicki (1975) and Weiler and Lockett (1985), of Union Carbide Co., used slotted trays to promote liquid movement at the sides of the tray. This was reported to increase the tray efficiencies. Porter and Davies (1986) are currently investigating the effect of changing the shape of the bottom of the inlet downcomer to encourage liquid flow round the curved walls, raising the outlet weir to allow some liquid to escape from underneath and using inclined trays in order to linearise the liquid flow on the tray. It is worth noting that all the above problems are associated with operation in the froth regime (Hofhuis and Zuiderweg, 1979). Porter et. al. (1974) reported no liquid channelling in the spray regime.

2.6   Conclusions

a)   Although the effect of variation of the outlet weir height and the hole size have been the subject of thorough studies in the past, there seems to be considerable experimental inconsistancies. The comparison made by Hellums et. al. (1958) and Umholtz and Van Winkle (1957) used trays with different free areas, although it can be assumed that the flow non-uniformities were non-existant on their small circular tray. Pruden et. al. (1974) used baffles on the test tray. It was reported that wall effects affected their experiments. The same can be said about the works of Lockett et. al. (1979).

b)   Various authors have reported the existance of "wall effects" in small Oldershaw columns. These small columns do not represent the distillation process on a large tray. No attempt has ever been made to tackle this problem. There is a large number of conclusions made about the effect of different factors using small Oldershaw distillation column data. Serious doubts may be cast on the validity of these conclusions, in the light of the "wall effects" and their influence on the mass transfer process.

c)   The Marangoni effects on mass transfer in the froth regime, where the liquid phase is dominant, was studied by Dribika (1986). A large number of columns operate in the spray regime, and there seems to be a lack of information about the nature of the mass transfer in these columns. This may involve studying the cumulative droplet distribution for different surface tension systems, and their effects on mass transfer.

d)   Surface renewal effects play an important role in the distillation of different positive systems, Biddulph (1966), Moen and Bos (1972), and these effects require further investigation under distillation conditions in order to obtain a clearer picture.

e) In recent years, there has been growing attention paid to the behaviour of multicomponent systems. Recent reports emphasise that equal individual component tray efficiency is an unrealistic assumption and better design methods are required to take into account:-

    i) The effect of the interaction on individual component point/tray efficiencies.

    ii) The effect of liquid back mixing on individual component composition gradients and tray efficiencies.

f) The multicomponent point efficiency prediction methods are limited to ternary systems. These methods require testing against large tray data (Lockett 1986).

g) There is no method reported to predict point efficiencies for multicomponent systems comprising more than three components.

h) The effect of flow non-uniformities and stagnant zones on tray efficiencies have been studied by Porter and co-workers (1972, 1972). The Union Carbide Company have been using slotted sieve trays as one means of overcoming this problem.

Further research is required to find other means and understand the effect of these flow non-uniformities under different hydrodynamic conditions, (Lockett, 1986).

CHAPTER 3

BOILING POINT SURFACE TENSION

MEASUREMENTS ON THE AQUEOUS ALCOHOL

SYSTEMS

BOILING POINT SURFACE TENSION MEASUREMENTS ON THE AQUEOUS ALCOHOL SYSTEMS

3.1   Introduction

The Marangoni effect has been attracting increased attention because

of its influence on mass transfer in the field of distillation (Zuiderweg

and Harmens 1958, Biddulph 1966, Boyes and Ponter 1971, Fane and

Sawistowski 1969, Bainbridge and Sawistowski 1964, Zuiderweg 1983),

humidification, absorption of gases, and liquid-liquid extraction (Liddel,

J. 1985). It has been shown to occur in many systems of commercial

interest, affecting interfacial turbulence and droplet-droplet coalescence

rates, froth formation and droplet size, thus altering the interfacial

area available for mass transfer. Marangoni effects occur when large

surface tension differences exist between the pure components, and is

intensified by large mass transfer driving forces. Examples of such

systems are alcohol-water combination, and considerable effort has been

made in the past to develop suitable correlation to describe the surface

tension behaviour of these systems (Winterfield et. al. 1978, Tamura,

1955). Due to the highly non-linear nature of these systems, arising from

the complexity of the structure of the hydrogen bonding of water, the

correlations are not very successful. In the field of distillation the

surface tension/composition relationship is required at the boiling point

and most of the measurement technique, such as capillary rise, cannot

be used. Sugden (1922-1924) gave details of a tensiometer which was

reported by Adam (1941) to "combine the advantages of speed, simplicity

and accuracy to a greater extent than any other method". Although the

apparatus was originally designed for room temperature determinations,

with some modification it was used successfully for measurements at the

boiling point by Catchpole (1962) and Biddulph (1966).

Using this equipment the surface tensions of the binary and ternary

alcohol-water mixtures were measured. In addition the surface tension of the system MeOH/n.PrOH was also determined. For the binary systems correlations are proposed which predict the surface tension at the boiling point.

3.2   Apparatus

The overall equipment is shown in figure 3.1. Photographs in figures 3.3 and 3.4 illustrate a general view, the tensiometer in operation and a close up of the tensiometer. The glass tensiometer (G) consists of a vessel provided with a variable electrical heating element (H), side condensers (F) and a drain line. Into the top of the vessel is fitted a B.40 general glass stopper through which are sealed two tubes and a thermometer pocket (Figure 3.2). One tube has a short length of precision bore capillary tube of 1.52 mm hole diameter, the other is drawn out until its diameter is about one-third of that of the capillary section. This diameter need not be known. The length of these tubes are identical, so their depth of immersion in the boiling liquid is the same. A two-way tap is used to divert the gas flow from one tube to the other.

Nitrogen from the gas cylinder (A) is passed through a drying tower (B) containing calcium chloride, and then passes through a fine needle valve (C) and a manometer (D) immersed in a constant temperature water bath (E), to the tensiometer (G).

3.3   Procedure

A liquid mixture is introduced into the tensiometer vessel, and a small amount of mercury is introduced into the vessel to fill the drain

arm, thus avoiding "dead-space" liquid. The heating mantle (H) is then switched on and the current varied to maintain a non-vigorous boiling of the liquid. The gas flow rate is adjusted to maintain a bubbling rate of one bubble every five seconds. The manometer level fluctuates, registering a pressure difference corresponding the maximum pressure required for a bubble to break. The water bath temperature was kept at 30°C. The mixture boiling temperature was measured by a pre-calibrated thermocouple with an error of $\pm$ 0.1°C. The manometer pressure difference was measured by using a travelling microscope. The equipment was carefully cleaned and free from contamination, and all the tensiometer joints were scaled with P.T.F.E. sleeving. The tensiometer fitted in the heating mantle was maintained upright by using a spirit level mounted in a circular, flat stainless steel disc. The pressure drops were taken as nitrogen bubbles break and leave the capillaries. The procedure was repeated up to five times to check for reproducibility.

3.4   Sugden Equation

The emperical equation developed by Sugden (1922-1924), and reported by Catchpole (1962), has an accuracy of 0.1% for the surface tension is as follows:-

$$\delta_m = A \ \rho_m \ g \ (\triangle H_1 - \triangle H_2) \left[1 + \frac{0.69 \ r_2 \ \rho_{mix}}{g(\triangle H_1 - \triangle H_2)} \right] \qquad 3.1$$

When: A_1: Constant of apparatus, determined by calibration with dried distilled toluene.

   δ_m: surface tension of the mixture (mN/m) or (Dyne/cm)

   $\triangle H_1$: manometer difference through fine capillary (cm)
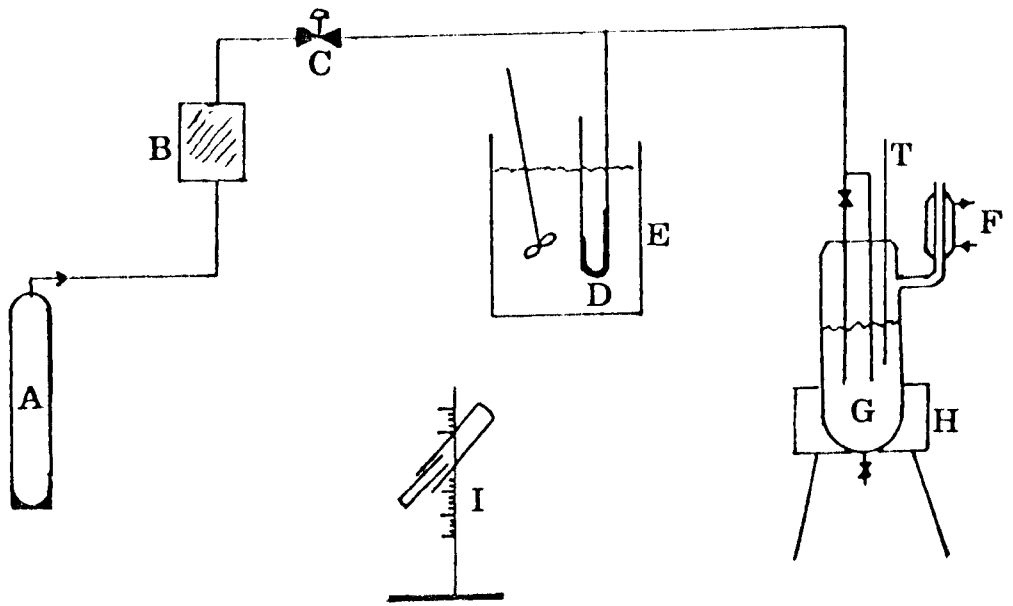
FIGURE 3.1   Surface Tension Apparatus
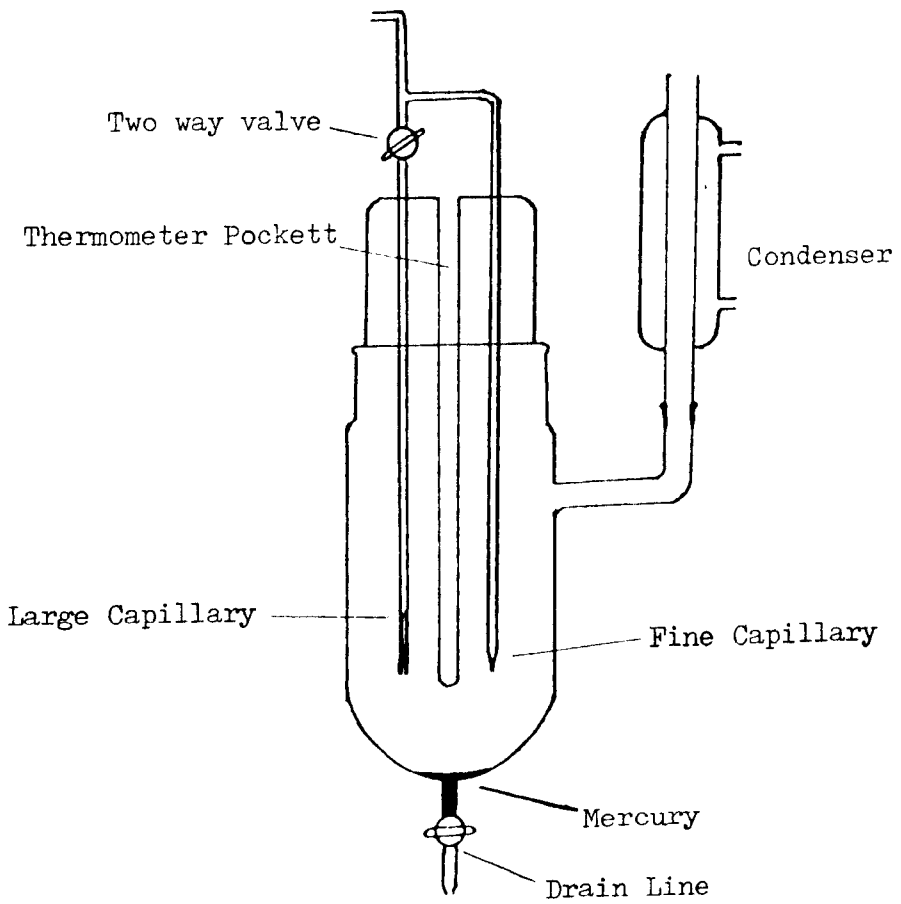
FIGURE 3.2   The Tensiometer
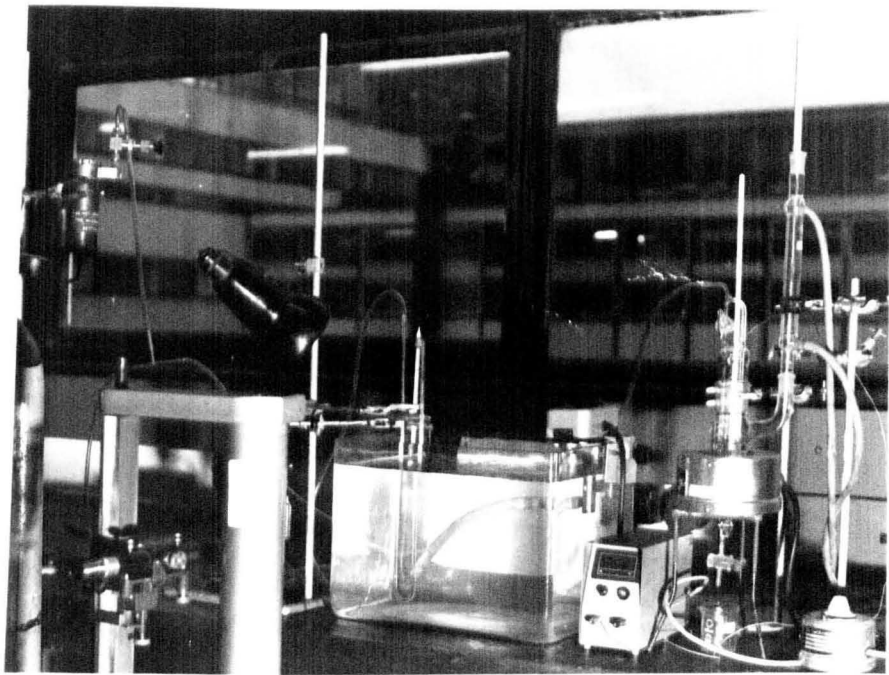
Figure 3. 3   A View of the Apparatus.
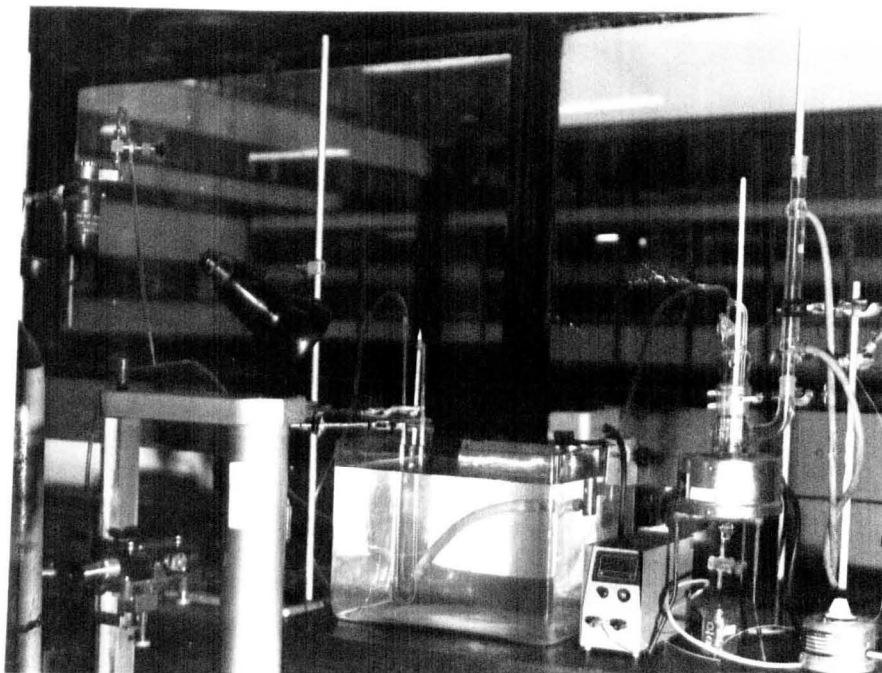
Figure 3. 3   A View of the Apparatus.
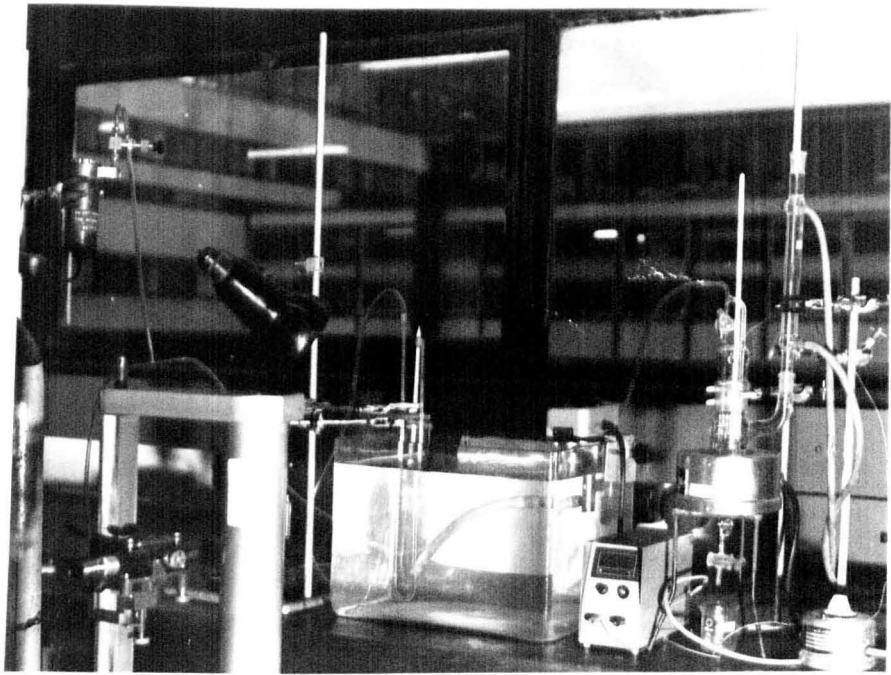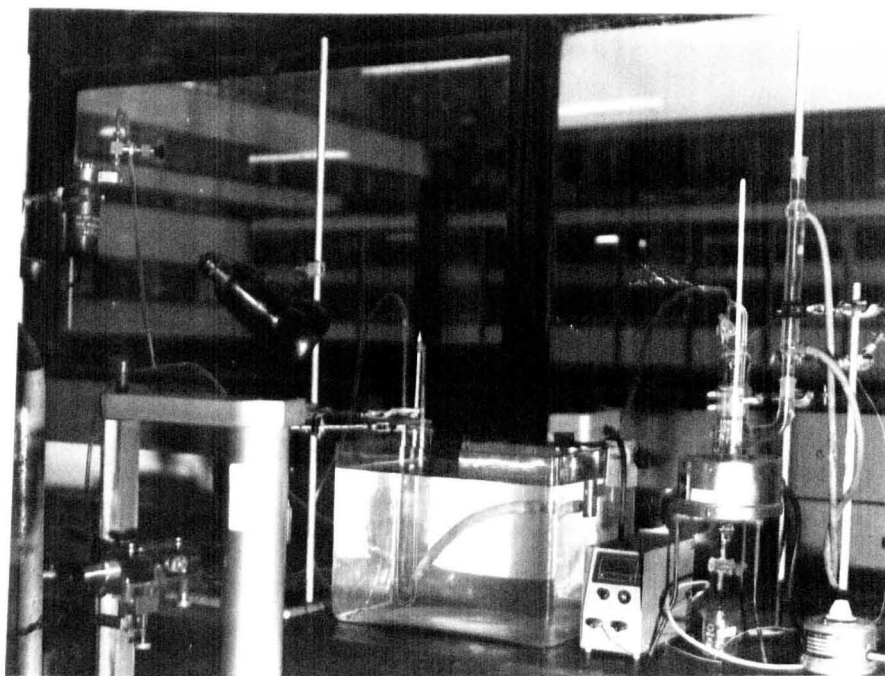
Figure 3. 3   A View of the Apparatus.
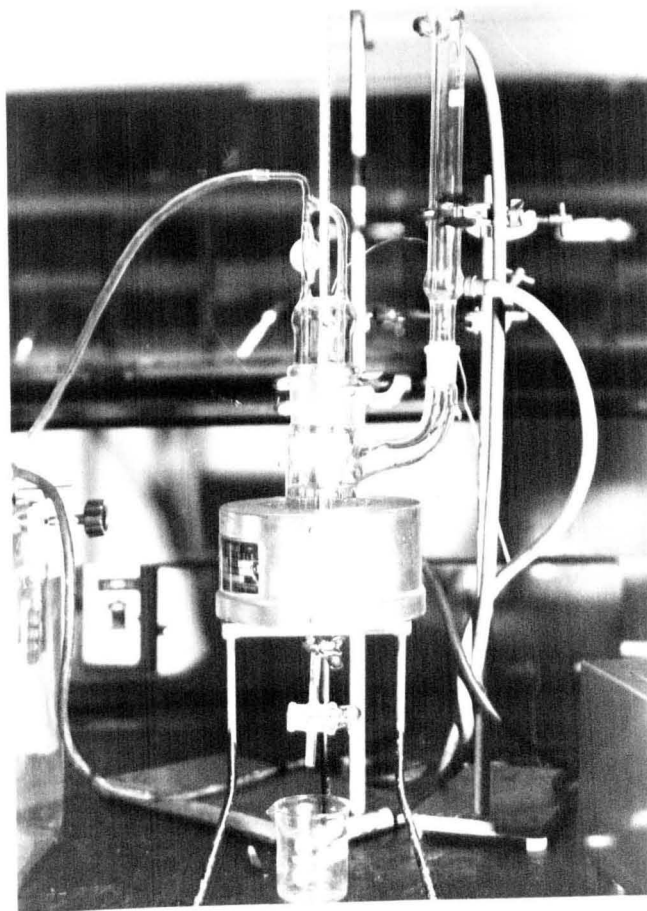
Figure 3.4.a   A View of the Tensiometer in Operation .
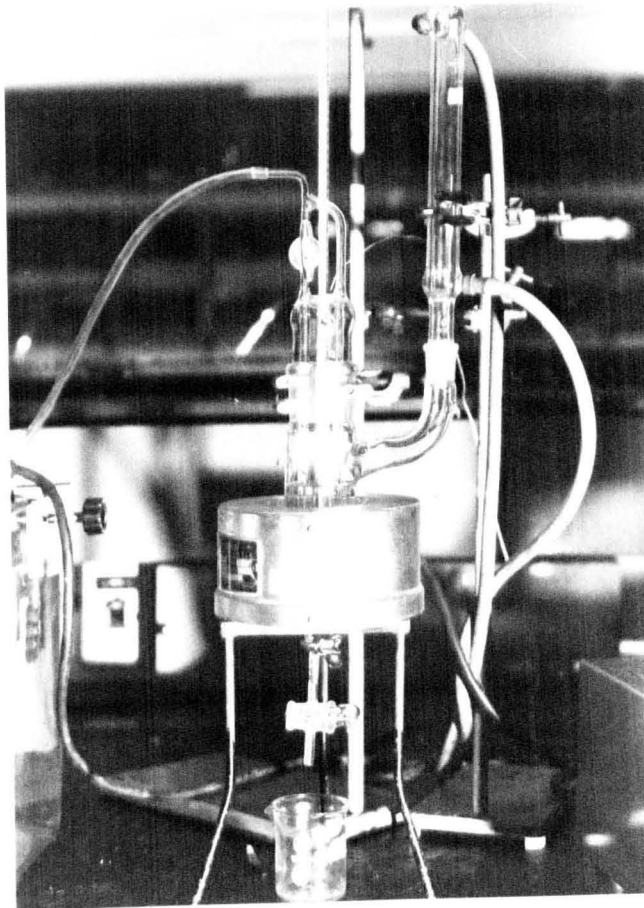
Figure 3.4.a   A View of the Tensiometer in Operation .
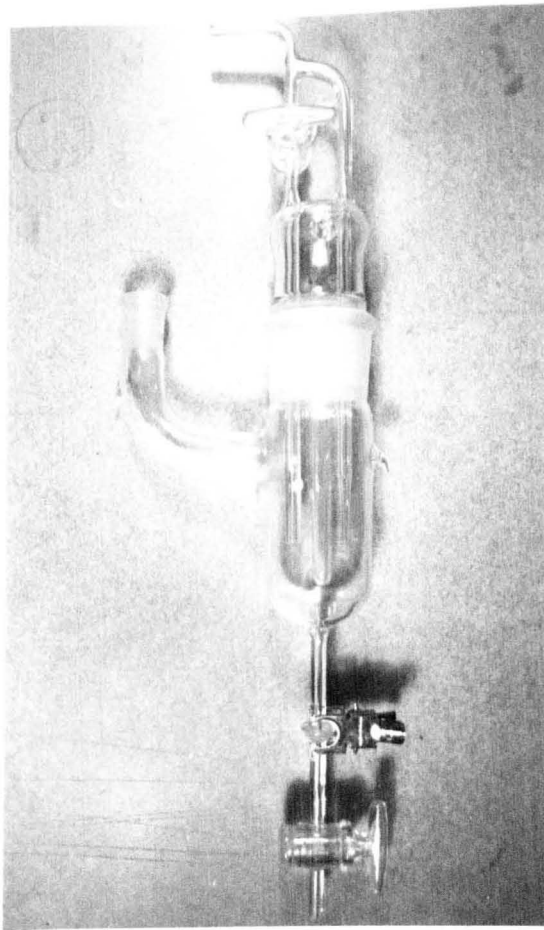
Figure 3.4.b   The Glass Tensiometer.
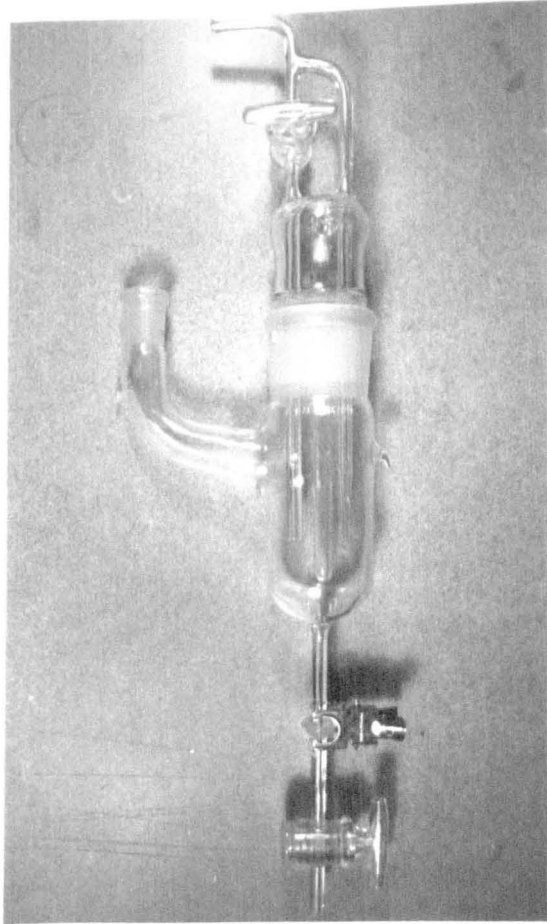
Figure 3.4.b The Glass Tensiometer.

$\triangle H_2$: manometer difference through larger capillary (cm)

r_2: radius of larger capillary = 0.076 (cm)

ρ_{mix}: density of liquid (gr/ml), (see appendix C for calculation)

ρ_m: density of manometer liquid = 0.784 (g/ml) (kerosine)

g: 981 (cm/sec^2)

incorporating the values of g , ρ_m and r_2, equation 3.1, reduces to the following:-

$$\delta_m = A \ 769.104 \ (\triangle H_1 - \triangle H_2) + 51.44 \ \rho_{mix} \qquad 3.2$$

3.5 Calibration

The calibration of the tensiometer was carried out using dried distilled Toluene, supplied by Fisons Ltd., over a range of temperatures up to and including the boiling point. The pure component surface tension data for this system was reported by Jasper (1972) and the density data by Gallant (1970). Table 3.1 summarises all the measurements. The constant A was found to have a value of 0.03519, which produced a maximum error in surface tension evaluation of 3.4 %. Using this constant, the surface tensions at the boiling points of water, methanol and ethanol were determined and compared with the measurements reported by Jasper (1972). This comparison is shown in Table 3.2, and the agreement is satisfactory The percentage error was calculated from this equation:-

$$\% \ Error = \frac{(\delta^* - \delta_m)100}{\delta^*} \qquad 3.3$$

AR grade alcohol and deionised water was used throughout this work.

3.6 Analysis of the Samples

Details of the analysis of the samples are given in appendix D.

3.7 Results

The surface tensions of the binary systems, MeOH/n.PrOH, MeOH/H_2O, EtOH/H_2O and the ternary system MeOH/n.PrOH/H_2O were determined. These results are tabulated in tables 3.3, 3.4, 3.5, 3.6 and 3.7. The tables also include the bubble point temperatures of the test mixture, determined by the thermocouple. The results of the binary surface tension determinations are plotted in figure 3.5 and for the ternary system in the triangular diagram 3.6. The bubble point temperature of the test mixture was also calculated, taking into account the non-idealities in the phases (see appendix B). These temperatures are plotted against the measurements by the thermocouple in the figure 3.7. It can be seen that the agreement is good.

3.8 Binary Surface Tension Correlations

An attempt was made to correlate the surface tension behaviour of the binary systems studied here. The non-linear behaviour of the aqueous systems made it impossible to derive a relationship which covered the whole of the composition range adequately. However, since the surface tension of these aqueous systems decreases sharply at high water concentration as a result of an increase in alcohol composition, it was decided to use two forms of correlation to describe this behaviour. Using a Least Mean Square method the following relations were obtained:-

a) Composition range 0 - 0.1 mole fraction more volatile component.

$$\delta = \frac{1}{x_1 + a} + b \qquad\qquad 3.4$$

b) Composition range 0.1 - 1.0 mole fraction more volatile component.

$$\delta = EXP \left(c - d \ln x_1 \right) \qquad\qquad 3.5$$

The constants for equations 3.4 and 3.5 are tabulated in table 3.8.

Table 3.8   Constants of the Equations 3.4 and 3.5

System	a	b	c	d
MeOH/H_2O	0.0394	33.81	2.990	0.3238
EtOH/H_2O	0.0270	22.35	2.850	0.2133
n.PrOH/H_2O	0.0214	12.481	2.943	0.0968

The boiling point surface tensions calculated from these equations are in a good agreement with the measurements, as illustrated in figure 3.5. The following equation was used for the MeOH/n.PrOH system:-

$$\delta = 17.44 + 7.739\, x1 - 11.96\, x^2 \qquad\qquad 3.5a$$

3.9   Discussion

Boiling point surface tensions of the aqueous systems of interest were measured using the tensiometer described. The use of this equipment is quick, easy and precise. There have been a few attempts to measure

the surface tension of the systems at boiling point under man transfer

conditions in the past. Ling and Van Winkle (1958) developed a method

designed to bring the liquid and the vapour into equilibrium contact while

measuring the surface tension. This equipment was rather complicated.

Aquiler et. al. (1983) measured the surface tension of their mixtures

at lower temperatures and extrapolated them to the boiling point. They

used the ring method. Both authors measured the boiling point surface

tension of the system n.PrOH/H_2O and a comparison of their measurements is

made in figure 3.8, and compared with the measurements reported here.

There is good agreement between these measurements, but a very important

feature of the measurements using the tensiometer described here is the

ease of use under boiling conditions.

Table 3.1   Summary of Tensiometer Caliberation

with Dried Distilled Toluene

T °C	δ* mN/m	δ_m mN/m	% Error	A
26.1	27.80	27.76	0.14	0.03524
28.6	27.50	27.70	0.69	0.03495
35.3	26.70	26.75	0.19	0.03512
37.6	26.43	26.56	0.49	0.03502
41.7	25.94	25.32	2.40	0.03605
47.9	25.21	25.89	2.71	0.03564
50.3	24.92	24.64	1.11	0.03559
53.4	24.55	24.59	0.15	0.03514
56.2	24.22	24.28	0.26	0.03510
59.0	23.88	23.88	0.00	0.03519
63.1	23.39	23.53	0.67	0.03500
69.4	22.65	22.86	0.95	0.03485
74.4	22.05	22.27	0.99	0.03485
80.3	21.35	21.69	1.59	0.03464
84.6	20.84	21.55	3.41	0.03404
89.3	20.28	20.01	1.33	0.03566
110.00**	17.70	17.21	2.74	0.03618

A average = 0.03519

Deviation of the measured
Surface Tension   = ± 0.26

*   Jasper 1972

**   Boiling Point

Table 3.2   Deviation of Measured Surface Tension

from Published Works

Liquid	T $^{\circ}C$	δ [**] mN/m	δ_m mN/m	$\|\delta^* - \delta_m\|$ mN/m
Ethanol	78.0*	17.56	17.69	0.13
Methanol	65.0*	18.98	19.47	0.50
"	47.0	20.37	20.71	0.34
Water	100.0*	58.85	59.21	0.3

*   Boiling Point

**   Jasper (1972)

Table 3.3   Methanol/n.propanol Surface Tension at

Boiling Point

Test No.	X1	δ_m (mN/m)	T $1^{\circ}C$
68	0.0428	19.72	66.0
69	0.1594	19.35	68.6
70	0.2971	19.82	72.5
71	0.5276	18.63	77.8
72	0.6579	18.85	82.0
73	0.7825	18.82	86.6
74	0.8640	18.15	90.5
75	0.935	18.18	93.1
76	0.9659	17.38	95.0

Table 3.4   Methanol/Water Boiling Point Surface Tension

Test No.	X1	δ_m (mN/m)	T $^{\circ}$C
1	0.0218	49.23	96.6
2	0.04345	45.69	92.6
3	0.0384	49.69	92.2
4	0.0760	42.43	88.0
5	0.1696	37.14	82.6
6	0.1980	34.03	82.8
7	0.2667	32.53	79.1
8	0.2974	30.06	78.0
9	0.3630	27.85	76.0
10	0.6004	23.20	70.8
11	0.5026	24.40	73.0
12	0.7293	21.63	68.6
13	0.8162	20.40	67.8
14	0.8959	20.52	66.8
15	0.9480	20.31	66.0

Table 3.5   Ethanol/Water Surface Tension

at the Boiling Point

Test	X1	δ_m (mN/m)	T °C
34	0.0143	46.95	96.2
35	0.0206	45.17	94.8
36	0.0423	38.26	91.0
37	0.0576	34.15	88.7
38	0.1076	28.44	85.4
39	0.1347	28.58	84.4
40	0.17505	25.88	83.2
41	0.1830	24.96	82.0
42	0.3027	21.59	81.1
43	0.5269	20.58	79.3
44	0.7029	18.19	78.5
45	0.8982	18.10	78.0

Table 3.6   n.propanol/Water Surface Tension at the Boiling Point

Test	X1	δ_m (mN/m)	T
16	0.00	59.21	99.8
17	0.0088	54.75	96.4
18	0.0194	38.32	90.7
19	0.0300	30.05	89.4
20	0.0495	26.66	88.0
21	0.0663	24.35	"
22	0.0830	23.84	"
23	0.0874	24.23	"
24	0.1136	26.30	87.7
25	0.1351	22.77	87.4
26	0.2306	22.55	87.3
27	0.4990	21.12	87.4
28	0.6621	21.08	88.6
29	0.8125	19.18	90.2
30	0.9033	19.10	92.4
31	0.2306	20.985	87.7
32	0.0851	22.66	88.3
33	0.078	28.39	88.7
33a	1.000	17.53	99.0

Table 3.7   Surface Tension of the Ternary

System MeOH/n.PrOH/H_2O

Test	X1	X2	δ_m (mN/m)	T °C
46	0.8458	0.0053	19.77	68.00
47	0.7880	0.0720	19.50	69.00
48	0.7044	0.1272	19.06	72.0
49	0.1780	0.8015	17.40	89.0
50	0.1110	0.5433	19.07	87.7
52	0.3972	0.3445	19.99	77.9
53	0.4689	0.3023	18.57	76.8
54	0.5544	0.2522	19.61	74.3
55	0.4132	0.1979	21.31	77.5
56	0.2177	0.1116	26.18	81.0
57	0.1805	0.0979	24.45	82.0
58	0.1317	0.0718	24.08	83.2
59	0.0830	0.0458	28.08	85.0
60	0.0528	0.0293	31.16	88.0
61	0.0298	0.0152	37.32	90.5
63	0.3690	0.0184	34.55	89.0
64	0.1395	0.0129	34.50	84.00
65	0.2691	0.0100	30.56	78.4
66	0.3727	0.0079	28.45	73.2
67	0.4339	0.1155	23.23	76.2
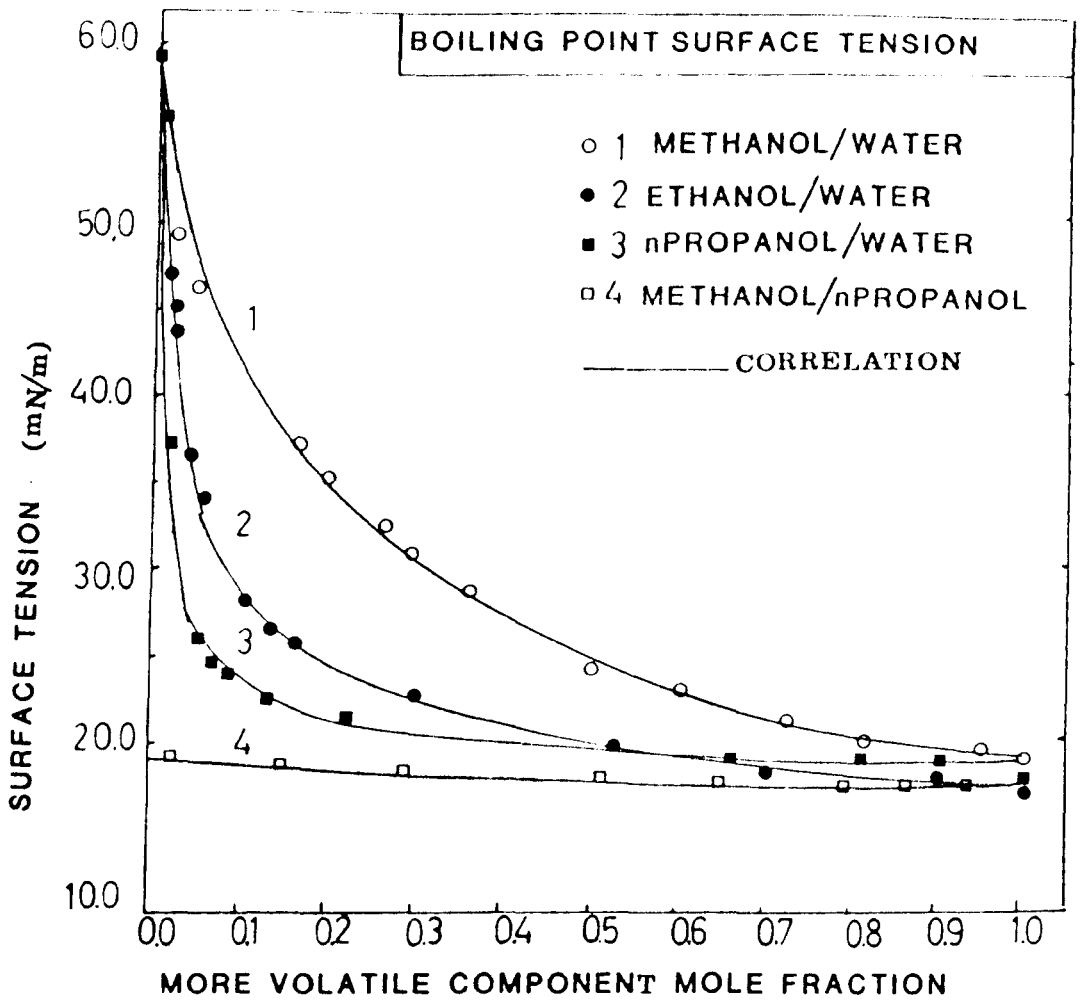
FIGURE 3.5   Binary Surface Tensions
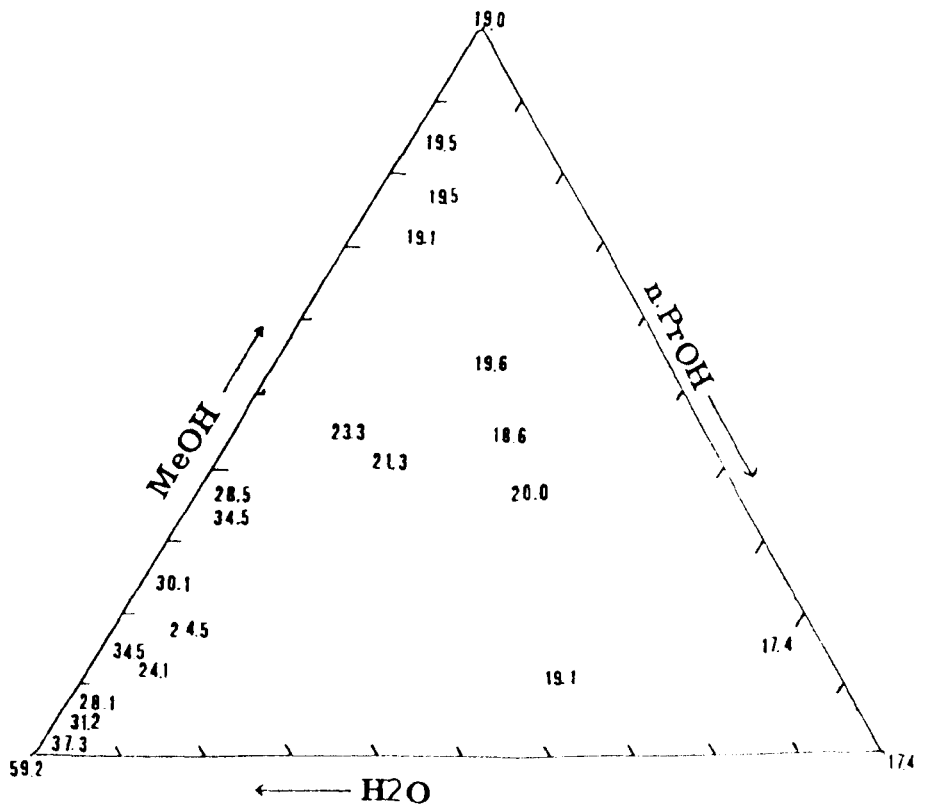
FIGURE 3.6   Surface tension (mN/m) of MeOH/n-PrOH/H_2O system at boiling point
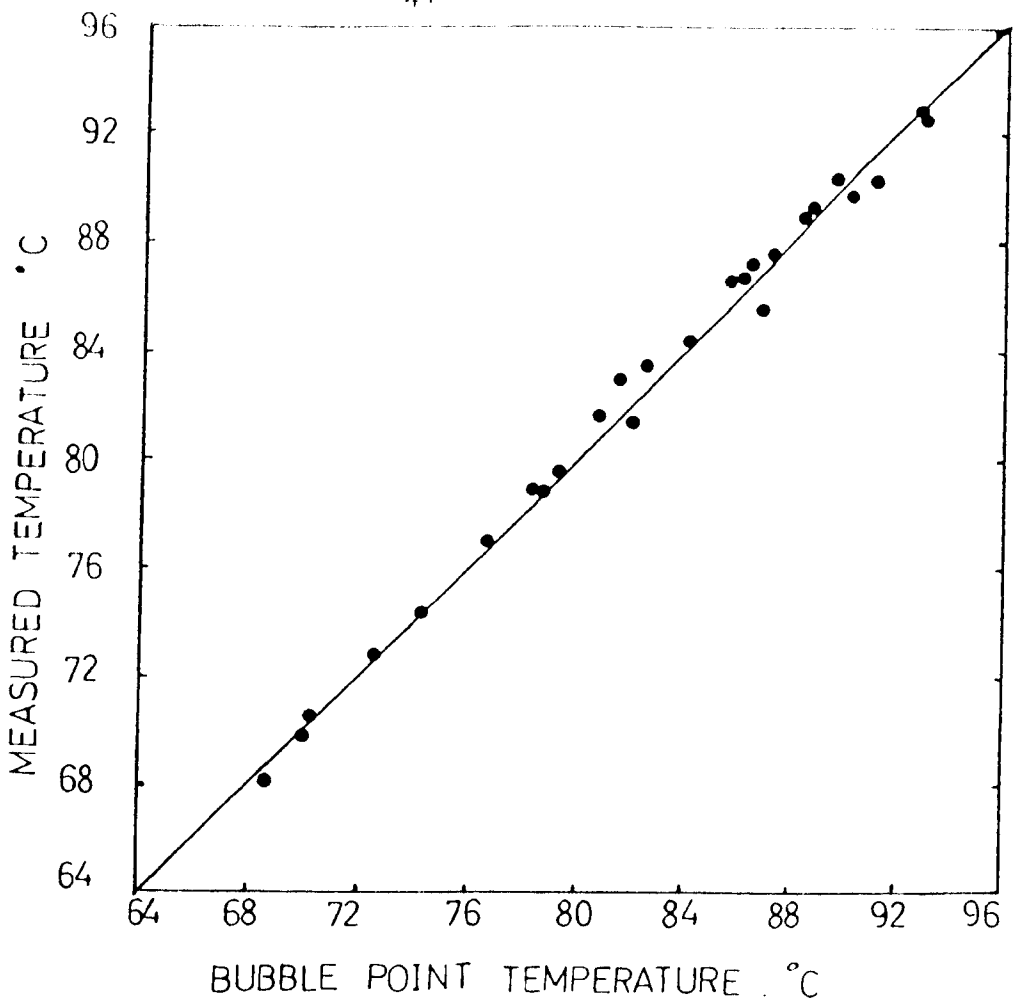
FIGURE 3.7   Comparison of bubble and measured temperatures
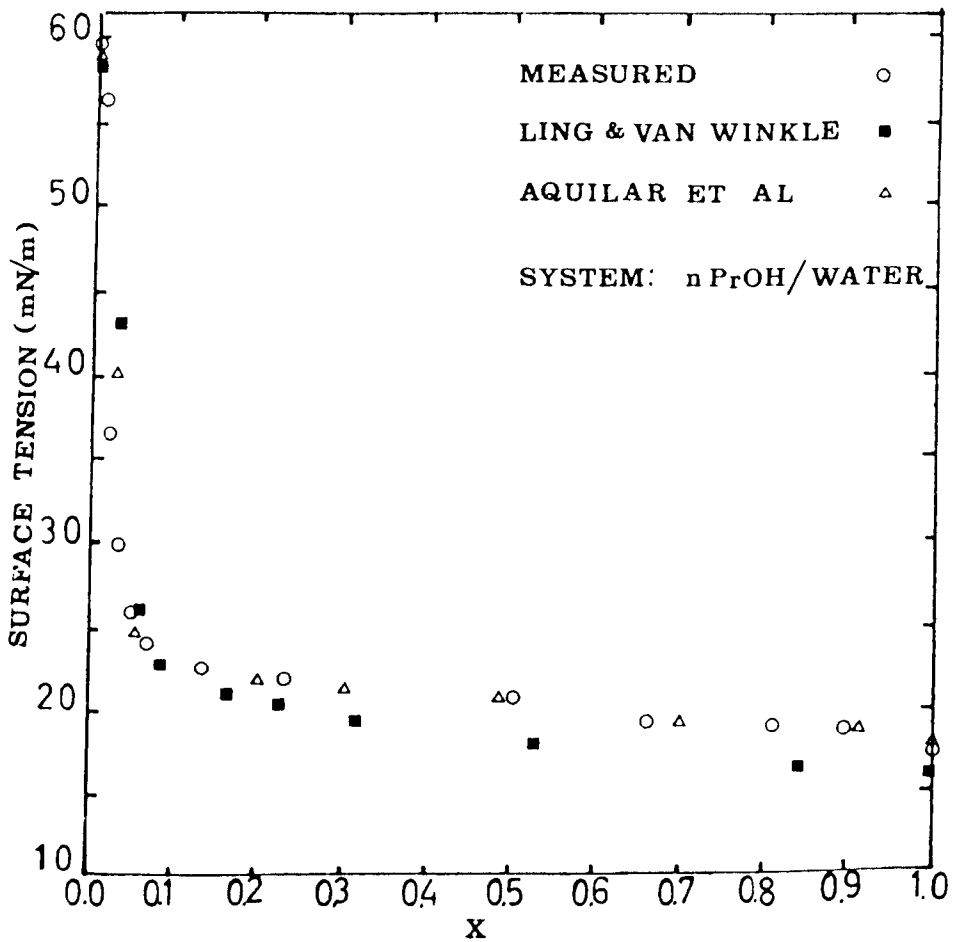
FIGURE 3.8   n.Propanol-Water Surface Tension

CHAPTER 4

A MODIFIED OLDERSHAW COLUMN FOR

DISTILLATION EFFICIENCY MEASUREMENTS

A MODIFIED OLDERSHAW COLUMN FOR DISTILLATION EFFICIENCY MEASUREMENTS

4.1   Introduction

A considerable amount of research has been carried out into efficiency measurements using small sieve tray columns during past 30 years to study the characters of different systems under closely controlled conditions. Ease of fabrication and lower costs have been the main attraction of this sort of arrangement. The literature survey in Chapter 2 covers a number of published works concerning the use of such equipment. One of the disadvantages of small sieve tray distillation columns, distilling "high" surface tension positive and neutral systems, Zuiderweg and Harmens (1958), is the phenomenon of wall-supported froth. The froth height in a large sieve tray distillation column is partly a function by the liquid-hold up on the tray. The liquid hold-up is a direct function of the outlet weir height, as shown by the recent correlations of the Bennett et. al. (1983) and Zuiderweg (1982). Therefore much lower froth heights should be expected in a small laboratory size distillation column, usually having no outlet weir and having a short flow path length.

4.2   Systems Investigated

The methanol/water, ethanol/water, n.propanol/water, and methanol/ n.propanol systems were investigated. The aqueous systems are defined as highly positive according to the Zuiderweg and Harmens, (1958) classification. The system n.propanol-water is especially interesting since it is positive up to the azeotropic composition, neutral at the azeotrope and negative at high n.propanol concentrations. The system methanol-n.propanol is surface tension neutral since both the constituents possess similar and low pure component surface tensions.

4.3 The Properties of the Systems

The physical properties of methanol, ethanol, n.propanol and water are given in appendix C. In addition, the surface tension of these systems was measured at the boiling point using a glass tensiometer. The surface tension measurement detials are given in Chapter 3, and the change of surface tension with composition is shown in figure 3.5.

4.4 Vapour/Liquid Equilibrium Data

The equilibrium data for the systems methanol/water, ethanol/water and n.propanol/water were provided by Maripuri and Ratcliff (1972), Stabinkov et. al. (1972) and Smirnov et. al. (1959) respectively. These data, in form of the Wilson parameters, according to the recent compilation of equilibrium data by Gemhling and Onken (1977) are thermodynamically consistant. The VLE data of Dribika and Biddulph (1986) were used for the system MeOH/n.PrOH. These parameters are given in table 4.1 and will be used in subsequent multicomponent work (see later).

TABLE 4.1   BINARY WILSON PARAMETERS

System	Wilson Parameter	Reference
Methanol-n.propanol	421.821, -245.905	Dribika and Biddulph 1986
Methanol-water	216.851, 468.601	Gemhling and Onken 1977 Part 2a
Ethanol-water	276.756, 975.488	Gemhling and Onken 1977 Part 2a
n.propanol-water	906.526, 13969.639	Gemhling and Onken 1977 Part 2a

4.5   Computation of the Equilibrium Vapour Composition

A computer model taking into account the non-idealities in both phases (Prausnitz et. al. 1967) was used to carry out the required computation of the activity coefficient using the Wilson model. The key equations involved in such computation, and the data required, are given in appendix B.

4.6   The Modified Oldershaw Column

The idea that a modification is desirable grew after calculating the point efficiencies of highly positive aqueous systems using a standard Oldershaw column (Figure 4.1a) and studying the mechanism of froth formation in small columns. One of the systems of interest, methanol/water, had been studied before and point efficiencies had been measured in larger scale columns (Lockett and Ahmed 1983, Biddulph and Dribika 1986). Clearly the point efficiencies measured from small column experiments (see later) were excessive.

Based on our observations, it was decided to design a column with a similar form to that of the standard Oldershaw column used during our earlier experiments but with an expansion above the tray to try to avoid the wall supporting the froth. Figure 4.1.b shows the new column and compares it with the previous arrangement. The two columns are compared in Table 4.2.

The experiments with the modified column appeared to give a much more representative froth for the outlet weir height used. A froth height of 1.5 to 2.5 cm was obtained as compared with 12 to 15.5 cm with the unmodified column, see Figure 4.2.

a STANDARD   b MODIFIED
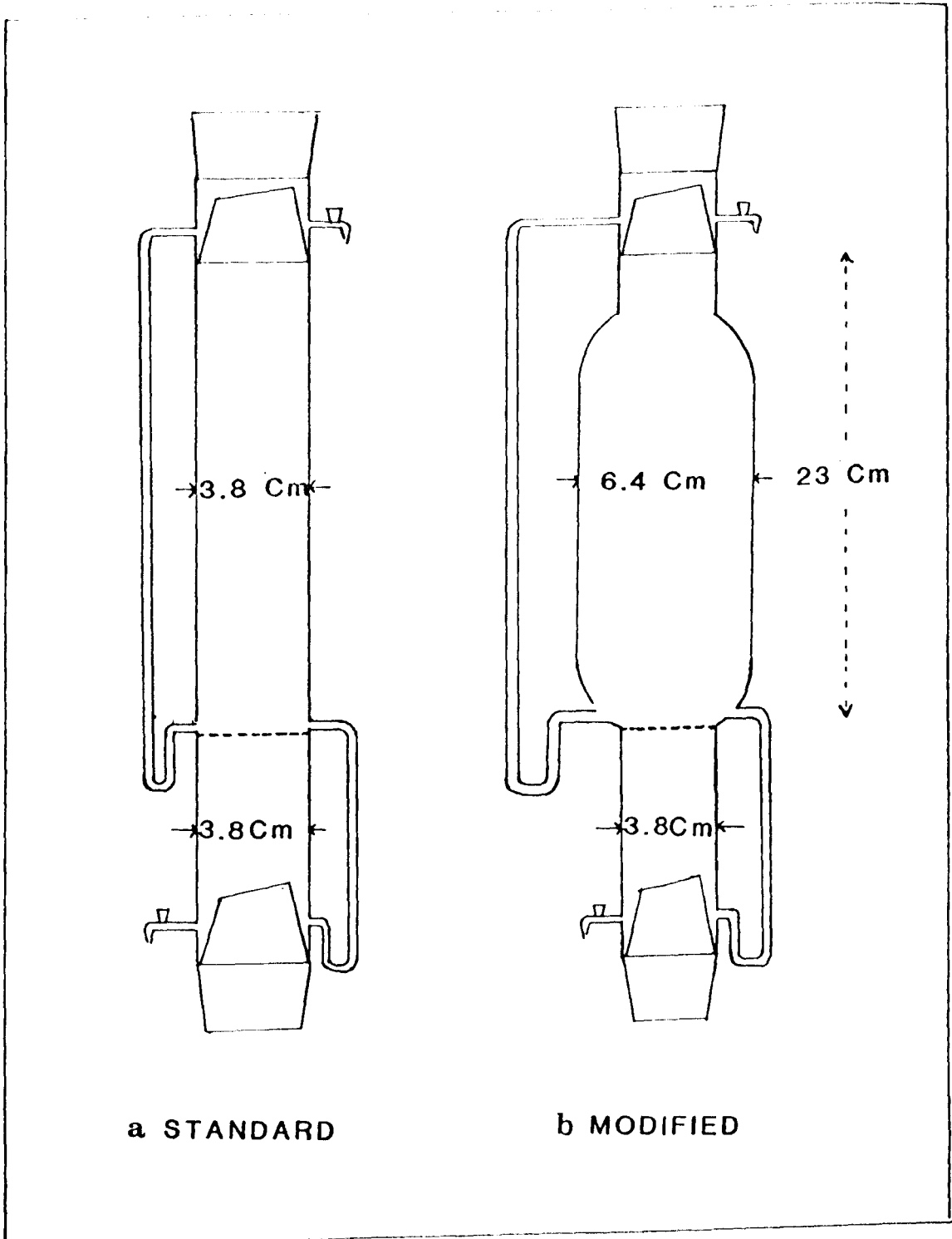
Figure 4.1   Standard and Modified Oldershaw Columns
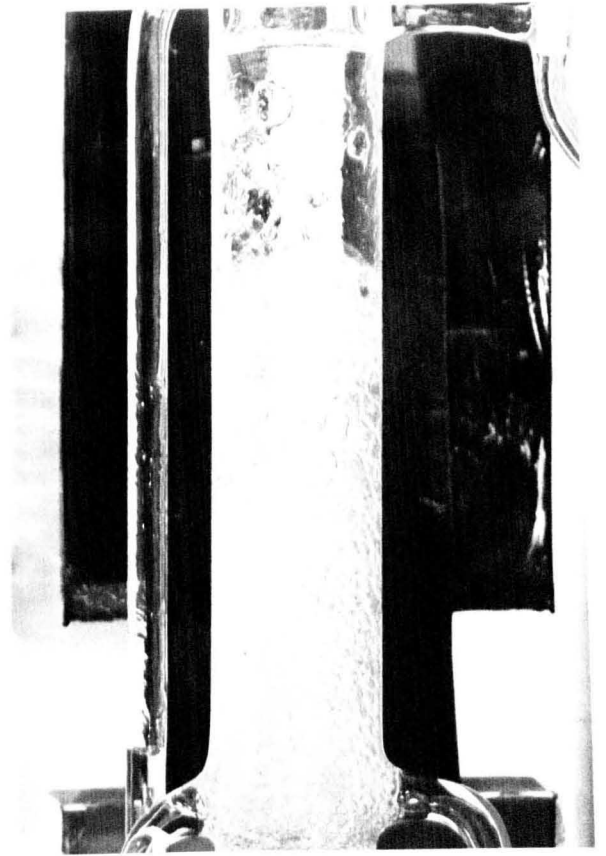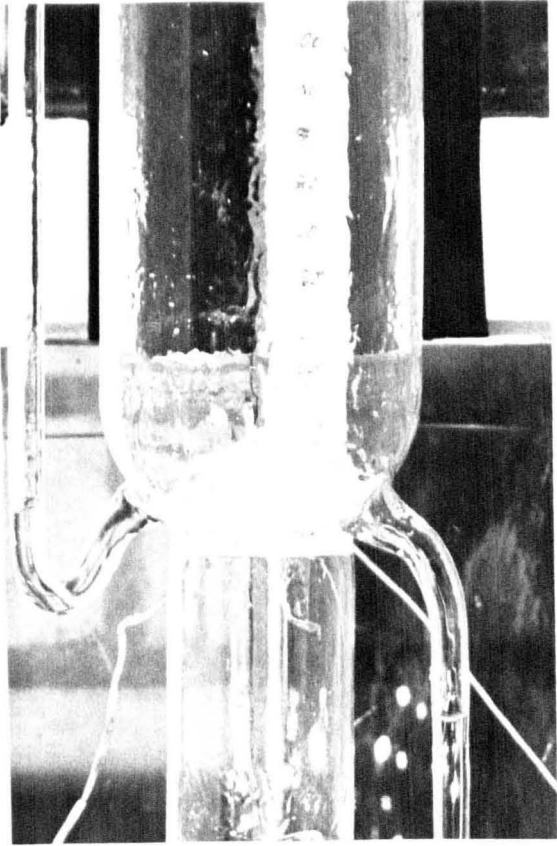
System:Methanol/Water

Run:112a
Froth Height:2 cm
Point Efficiency: 0.77
Vapour Velocity:0.41 m/s
X:0.8356

Run:112b
Froth Height:15 cm
Point Efficiency: 1.01
Vapour Velocity:0.45 m/s
X:0.8268

Figure 4.2   Operation of the Standard and the Modified
            Oldershaw Columns.
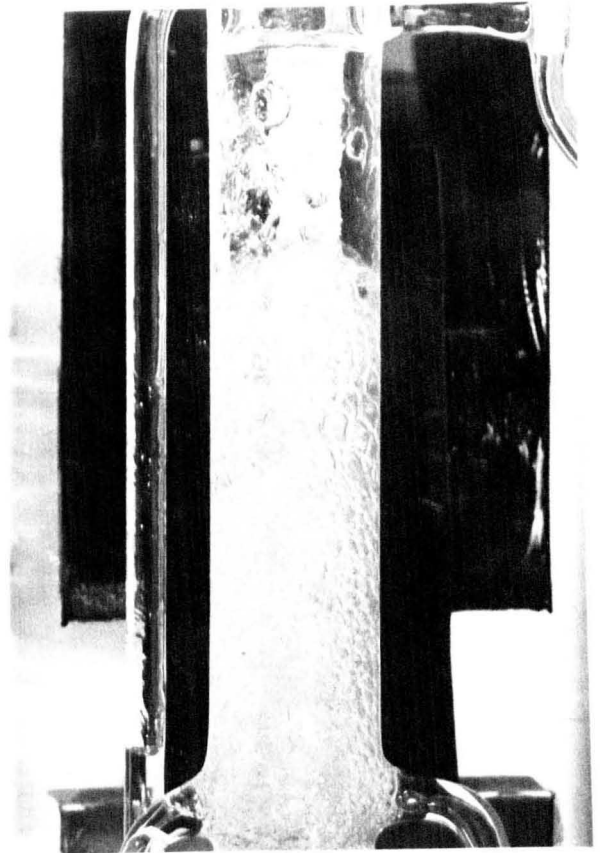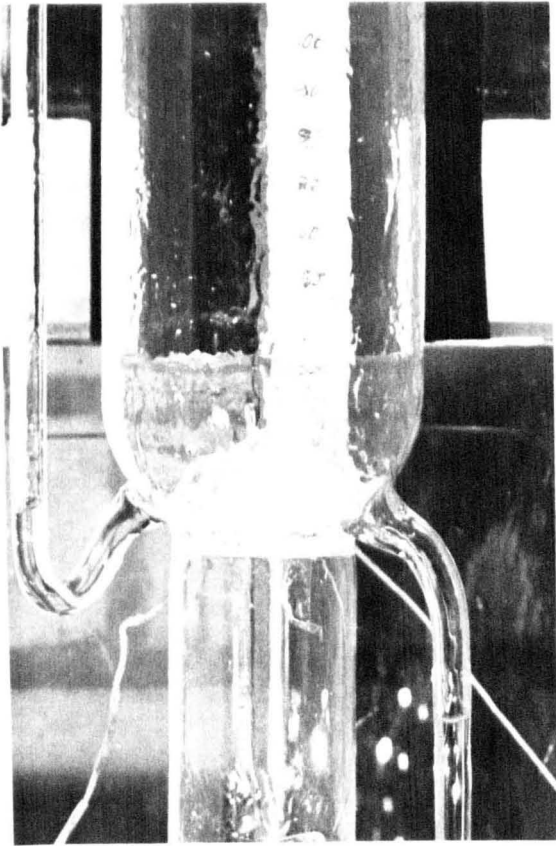
System:Methanol/Water

Run:112a
Froth Height:2 cm
Point Efficiency: 0.77
Vapour Velocity:0.41 m/s
X:0.8356

Run:112b
Froth Height:15 cm
Point Efficiency: 1.01
Vapour Velocity:0.45 m/s
X:0.8268

Figure 4.2   Operation of the Standard and the Modified
Oldershaw Columns.

TABLE 4.2   A COMPARISON OF THE STANDARD AND MOFIFIED OLDERSHAW COLUMNS

	Oldershaw	Modified
Tray Diameter (cm)	3.8	3.8
Column Dia. (cm) above the tray	3.8	6.4
No. of holes	46	46
Hole Diameter (mm)	1.1	1.1
Weir Height (mm)	2.5	2.0
% Free Area	8%	8%
Hole Pitch (mm)	3.8	3.8

Biddulph and Dribika (1986), and Lockett and Ahmed (1983), reported froth heights of the order 8 to 9 cm on their large distillation columns with high outlet weirs.

4.7   The Apparatus

The apparatus is shown diagramatically in figure 4.3. A 10 litre reboiler (R) was provided with a heating mantle and covered with a heating jacket, together generating a heat input of 1300 watts, controlled by a variac. The vapour from the reboiler passed through a calming section (CS) and then through the test tray. The vapour then passed through the space above the tray (S), and an elbow (E) before being totally condensed above (CO). The condensed liquid then passed through a flowmeter (F) before returning to the column at the top sample point (ST). Here a chimney keeps liquid and vapour apart. The reflux then returned to the test tray after passing through the external downcomer made in a U-shape at the bottom to seal the downcomer. A similar arrangement was made for the liquid leaving the test tray to the bottom sample point (SB). The reflux

then returned to the reboiler by overflowing the top of the chimney. The column section was enclosed in an air heated cabinet to minimise heat losses. The electrical heater (H) was controlled manually, the temperature gradient across the cabinet being monitored by thermocouples installed at T1 and T2. Two additional thermocouples T3 and T4 measured the reboiler and the vapour temperatures.

4.8   The Materials

For the aqueous system experiments, Fisons SLR grade alcohol was used, with water being the major impurity. De-ionised water was provided by the water treatment plant in the laboratory. Similar materials were used for the large scale binary and multicomponent experiments (see later chapters). For the experiments on the system methanol/n.propanol and analysis Fisons AR grade alcohols were used with purities of up to 99.8% W/W.

4.9   The Experimental Procedure

About 6 litres of the test mixture was placed in the reboiler and brought to boiling. Each experiment was of 4 hours duration to achieve steady-state conditions, the cabinet and the reboiler temperatures providing a guide to steady-state condition, these being monitored regularly and adjustments made if necessary. The experiments were carried out at atmospheric pressure and total reflux. The froth height was measured using a scale placed behind the column. The samples were collected in precooled bottles. Prior to sampling a small amount of liquid was withdrawn from each sample point to ensure representative
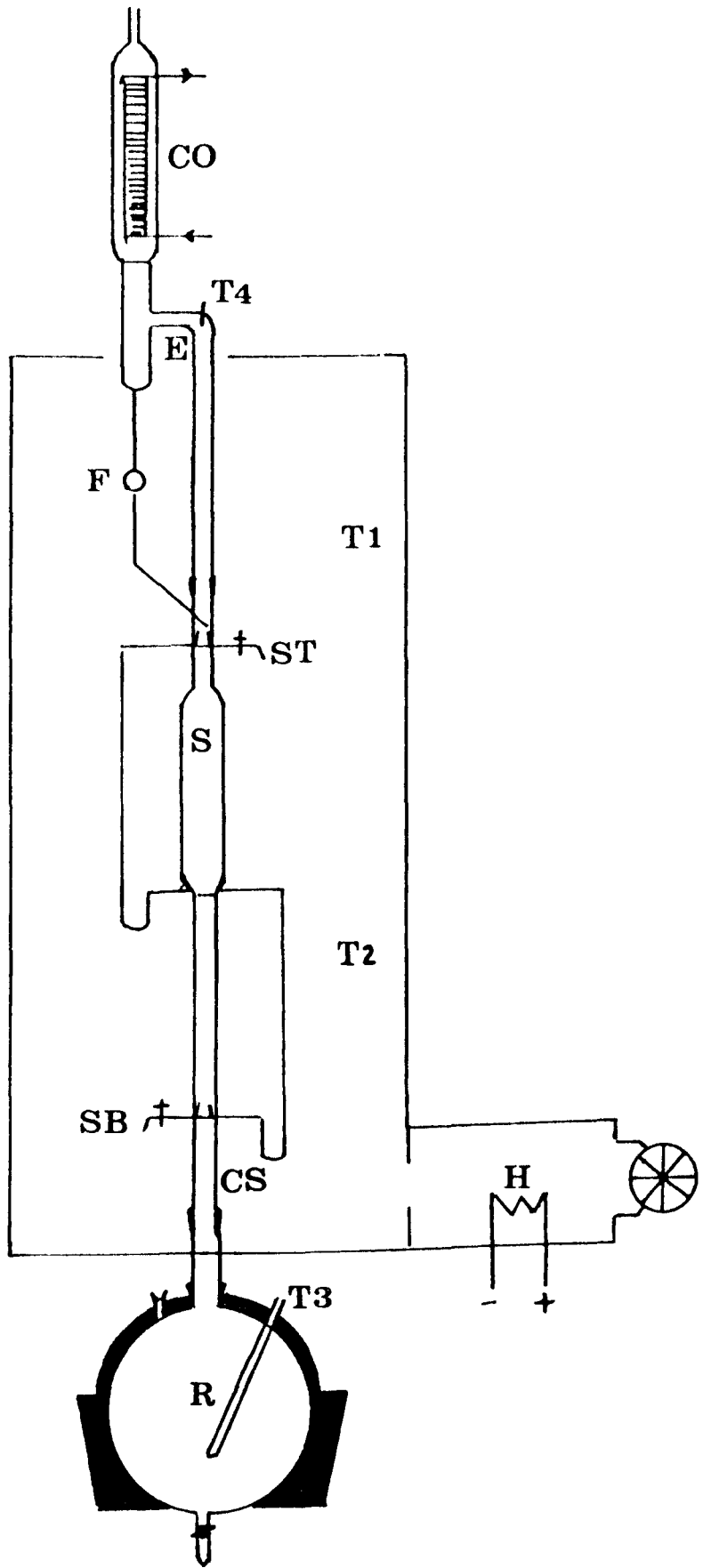
Figure 4.3 The Overall View of the Apparatus

sampling. The boil up rate was measured by direct collection of the reflux. There were the usual measurement errors involved in measuring the reflux rate, and the froth height.

4.10   The Analysis

The analysis of the samples was carried out by gas liquid chromatography. The average error in mole fraction calculations are tabulated in Table 4.3.

TABLE 4.3   ACCURACY OF THE ANALYSIS

System	ACC (mole fraction)
MeOH/n.PrOH	± 0.0020
MeOH/H_2O	± 0.0038
EtOH/H_2O	± 0.0028
n.PrOH/H_2O	± 0.0043

Details of the gas-liquid-chromatography and the analysis techniques are given in appendix D.

4.11   Results

All the experiments were carried out at a F.Factor of about 0.4 m/s $(Kg/m^3)^{0.5}$ except for n.propanol-water when a lower F.Factor of about 0.25 m/s $(Kg/m^3)^{0.5}$ was also investigated. Figures 4.4, 4.5 and 4.6 show comparisons of the point efficiencies and froth heights for the

aqueous systems using two columns, the standard Oldershaw column and the modified column.

It is apparent that the "wall supported" froth gives rise to high efficiencies by providing extra interfacial area. Figure 4.7 shows a comparison of the point efficiencies for the system methanol/water measured by the modified column with those of Biddulph and Dribika (1986), inferred from measurements in a one meter long rectangular sieve tray simulator column with 2.5 cm high outlet weir, and Lockett and Ahmed (1983), where point efficiencies were deduced from measurements in a 59 cm diameter sieve tray column with 5 cm high outlet weir providing a much greater liquid hold-up. A comparison is shown in Figure 4.8 for the sui.. e tension neutral system of methanol/n.propanol based on experiments with an Oldershaw column similar to Figure 4.1.a by Dribika (1986) and our modified column. This illustrates that the expansion above the plate in the modified column has no effect on the point efficiency measurements where non-frothing neutral or slightly positive and negative systems of low pure component surface tension are concerned. Finally the results on the n.propanol/water system, using the modified column, confirm that in the "froth regime", (Hofhuis and Zuiderweg 1979), the column superficial F-Factor appears to have no significant effect on the point efficiency. This is in agreement with the experimental observations of Lockett and Uddin (1980), Biddulph and Dribika (1986) and Dribika and Biddulph (1986). It is also worth noting that in the positive and negative composition ranges on either side of the azeotrope (Figure 4.6), the efficiencies are comparable.

The behaviour of the biphase on the test tray is shown and compared by the photographs in Figure 4.2. The biphase in the standard Oldershaw column consists of the supported froth and some recirculation, whereas the modified column biphase consists of froth and droplets. These droplets seemed to form as a direct atomisation of the liquid on the tray by the high speed vapour, or as a result of froth breakage. Smaller droplets were related to the latter. Figure 4.9 clearly demonstrates the foamy nature of the froth. Figures 4.10 compares the positive and negative surface tension system n.propanol/water during distillation. The biphase, in contradiction of previous reports (Zuiderweg and Harmens 1958), seems very similar in nature and casts serious doubts in the efficiency definition of these systems (Zuiderweg and Harmens, 1958). They referred to the positive systems on "foaming" and negative systems as "non-foaming", and reported lower efficiencies for the negative system. All the efficiency measurements concerning these two columns are tabulated in appendix A, Tables A.1.1, A.1.2, A.1.3, A.2.1, A.2.2, A.2.3 and A.2.4.

4.12   Discussion

4.12.1   Wall Effects

The measurements reported here clearly demonstrate the contribution of the "wall supported" froth to the high efficiencies evaluated. Furthermore, the modification encourages steady operating conditions. It seems likely that with the conventional column, the wetted wall effects due to returning small droplets colliding with the wall, some being carried over to the top sampling point, contributed to fluctuating point efficiencies. However, with the expansion above the plate reducing the vapour velocity, these effects have been markedly reduced.

Other studies have indicated that the size of the pilot test column
has a direct influence on wall effects, and consequently on the measured
point efficiency. Studies of the surface tension positive system
n.heptane-toluene were carried out by Medina et. al. (1978), Zuiderweg
and Harmens (1958) and Fane and Sawistowski (1969). Figure 4.11
illustrates the measured efficiencies which resulted from these studies.
Medina et. al. (1978) and Zuiderweg and Harmens (1958) used columns very
similar to the unmodified column described here and reported efficiencies
of the order of 80 to 90% whereas Fane and Sawistowski (1969), despite a
large liquid hold up on their tray, reported lower efficiencies from their
larger tray. Another surface tension positive system, N_2/O_2, had been
studied extensively in the past by Brown and England (1961), Ellis and
Catchpole (1964) and Haselden and Thorogood (1964). A comparison of those
results in terms of point efficiencies and froth heights is shown on
Figure 4.12. The same trend is observed, the larger tray with the greater
liquid hold-up but lower froth heights exhibits the lowest point efficiencies.
Haselden and Thorogood (1964) used a foam supporting baffle in an attempt
to represent the behaviour of an industrial air separation distillation
column, and obtained efficiencies of about 90%. Hart and Haselden (1969)
used the same arrangement for their efficiency studies. One of the surface
tension positive systems used in their study, benzene-n.hexane, showed
efficiencies above 100% at mid composition range. These efficiencies were
discarded from their studies due to the probability of inaccurate phase
data. However, Zuiderweg (1969) discussed Hart and Haselden's work (1969)
and concluded that the foam conditions produced on their plate did not
resemble those of large industrial sieve plates since the drainage patterns
and foam heights were different. It seems very likely that the foam
supporting gauze baffle compensated for the lack of liquid hold-up in
simulating point efficiencies measured on the larger trays (Biddulph 1975).

It also seems likely that the column wall can help to support bubbles due to surface tension forces and reduced vapour velocities near the wall. These supported bubbles assist the bubbles nearer the centre of the plate to stabilize. However, in the case of larger diameter plates the supporting effect is quickly lost and the froth height is determined by the rate of build-up and break-down of froth on the main part of the plate. The modified column described here appears to provide more reliable point efficiency values, within its definition (Standart 1974), representative of the conditions found in the centre of a large plate. Several studies have reported increased tray efficiencies as a result of increased froth heights due to increased outlet weir heights or increased vapour velocities. The amount of froth is also expected to be a function of the liquid hold up on the tray and the vapour velocity (Haselden and Thorogood, 1964; Fane and Sawistowski, 1969; Brown and England, 1961; Finch and Van Winkle, 1964; Umholtz and Van Winkle, 1957; Jeromin et. al., 1969; Sargent et. al., 1964). To explain the above phenomena we refer to the results of Lockett and Ahmed (1983) and Biddulph and Dribika (1986). Using the system methanol/water a comparison is made between their results and our measured point efficiencies, in Figure 4.7, using the modified Oldershaw column. It is likely that the lower point efficiencies measured here are due to the much shorter gas and liquid contact on the tray due to lower froth height and smaller liquid hold-up present. The point efficiencies measured in the modified column can be used for the conservative design of a distillation column or be scaled-up by the recent method of Dribika and Biddulph (1986) for more accurate design. It is evident that such a column can actually measure point efficiencies very close to the ones operating on an industrial tray for any system, including those of extractive distillation.

In Chapter 8 this work has been taken further by increasing the height of the outlet weir on the modified column tray.

4.12.2   Surface Tension Effects

Figures 4.13 and 4.14 illustrate the change in surface tension and the Marangoni stabilising index (M), at boiling point, for the systems studied. The surface tension measurements were carried out in a tensiometer as reported in Chapter 3. The Marangoni stabilising index, defined as the change in the mixture surface tension with time (Hart and Haselden, 1969), is a measure of the surface behaviour of a system, as a result of the local change in surface tension due to mass transfer.

$$M = \frac{d\,\delta}{dx}\ (Y - Y^{*}) \qquad\qquad (4.1)$$

Y   - Mole fraction of the more volatile component in the vapour phase.

Y*   - Mole fraction of the more volatile component in the vapour phase in equilibrium with the liquid.

δ   - Surface tension at the boiling point (mN/m).

x   - Mole fraction of the more volatile component in the liquid phase.

M   - Marangoni stabilising index (mN/m).

Systems were defined by Zuiderweg and Harmens (1958) as positive if the surface tension of the reflux increases in the column, negative for the reverse and neutral either if the constituent of the mixture are of the same order of surface tension or if the driving force tends to zero. The azeotropic system n-propanol/water exhibits all the behaviour described here, being positive at low and negative at high n-propanol concentrations, it is neutral at the azeotropic point. The system ethanol/water also exhibits the same behaviour but only measurements on the positive side were feasible. The system methanol/water and methanol/n-propanol are

"highly positive" and "neutral" respectively.

Note that with the conventional column high froths were formed for the positive and neutral aqueous system whereas the "surface tension neutral" system of methanol/n-propanol was reported (Dribika and Biddulph 1986) to form no froths. This confirms that the froth supported by the column wall is partly a surface tension phenomena and its extent a function of pure component surface tension difference between the constituents of the mixture studied. The comparison of the point efficiencies of the neutral system methanol/n.propanol with the highly positive systems of methanol/water and ethanol/water (Figure 4.15) suggests that the positive systems exhibit higher point efficiencies due to the Marangoni surface renewal effects (Ellis and Biddulph, 1967). The comparison of the positive and the negative composition range point efficiencies of the n.propanol/ water system indicates that since the system properties are unchanged and the variation in the mixture surface tension, and consequently the stabilising index, is low in the composition range studied, similar point efficiencies result.

- 58 -
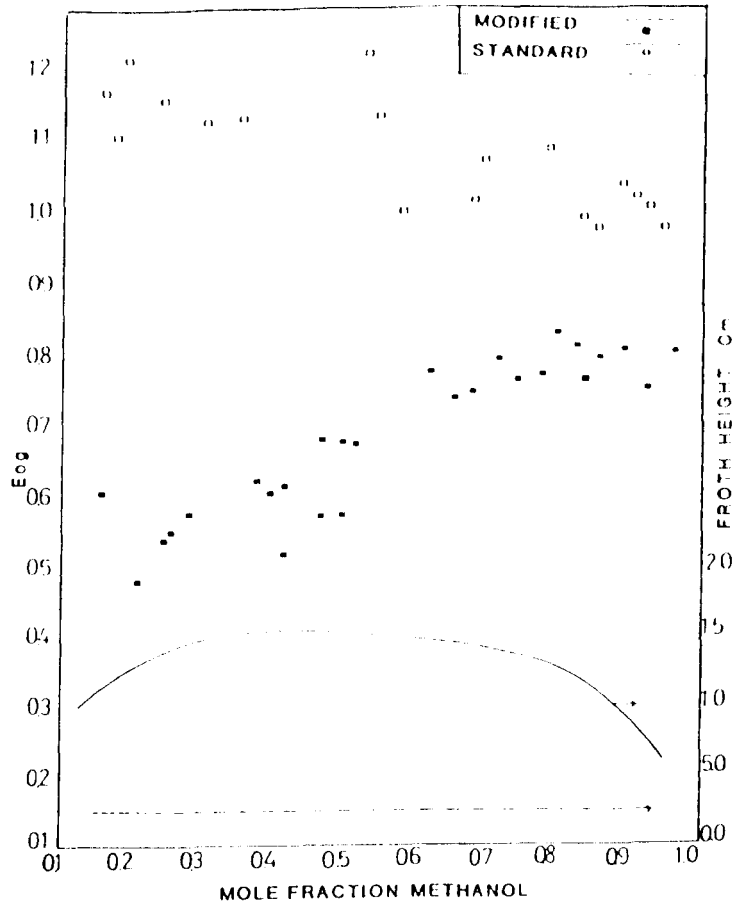
Figure 4.4 MeOH/H2O System Point Efficiencies and Froth heights
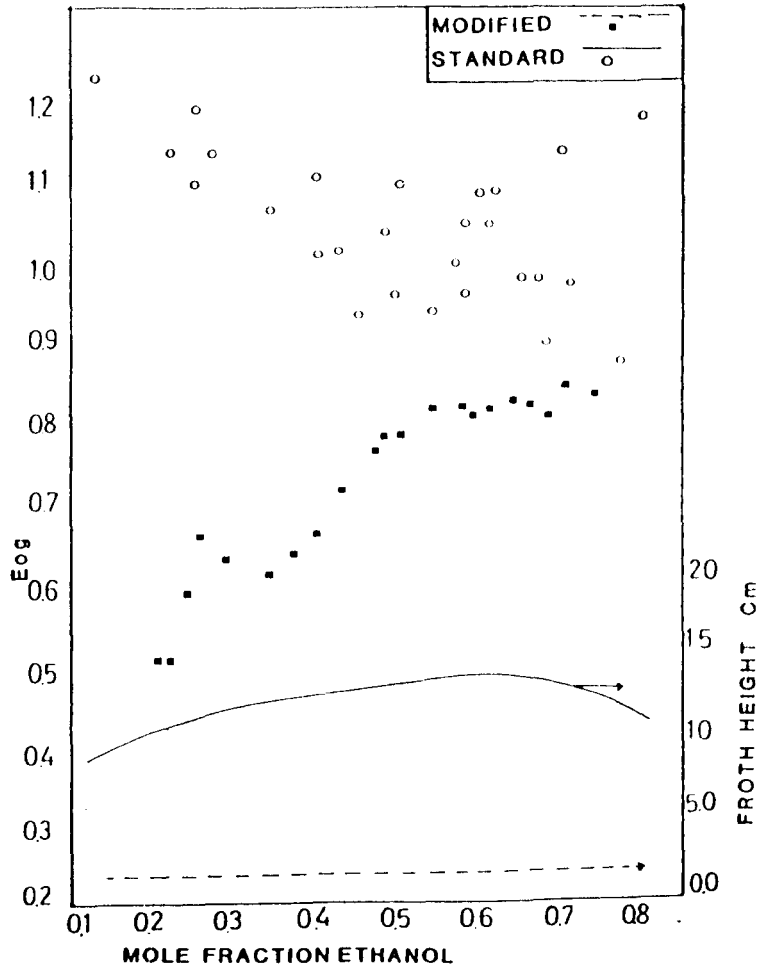
Figure 4.5 EtOH/H2O System Point Efficiencies and Froh Heights
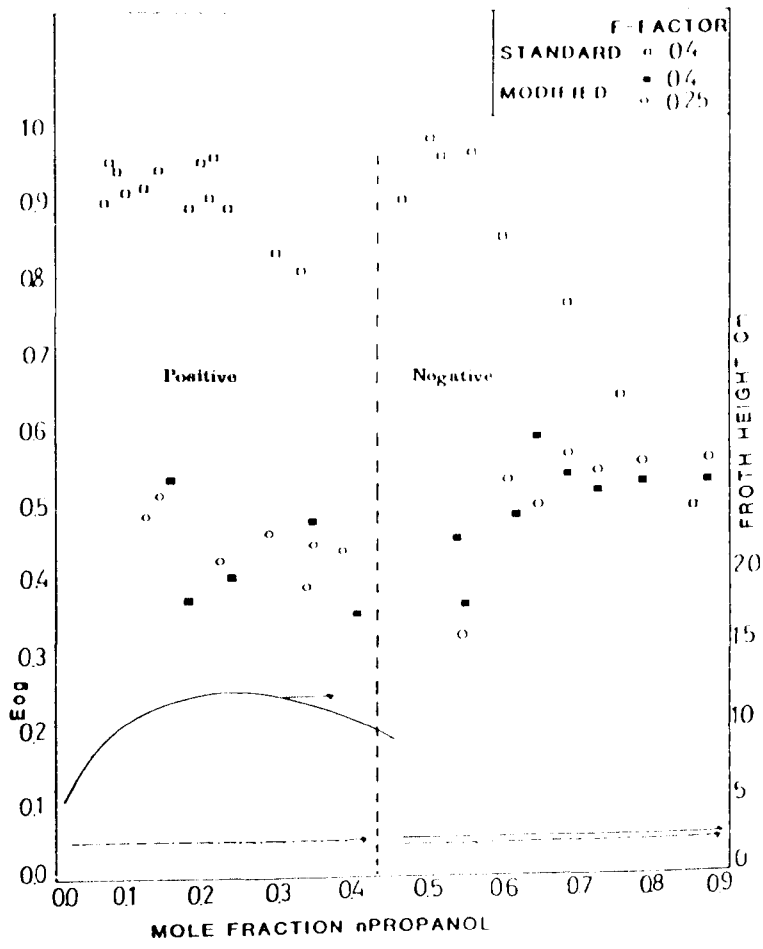
Figure 4.6   n.PrOH/H2O System Point Efficiencies and Froth Heights
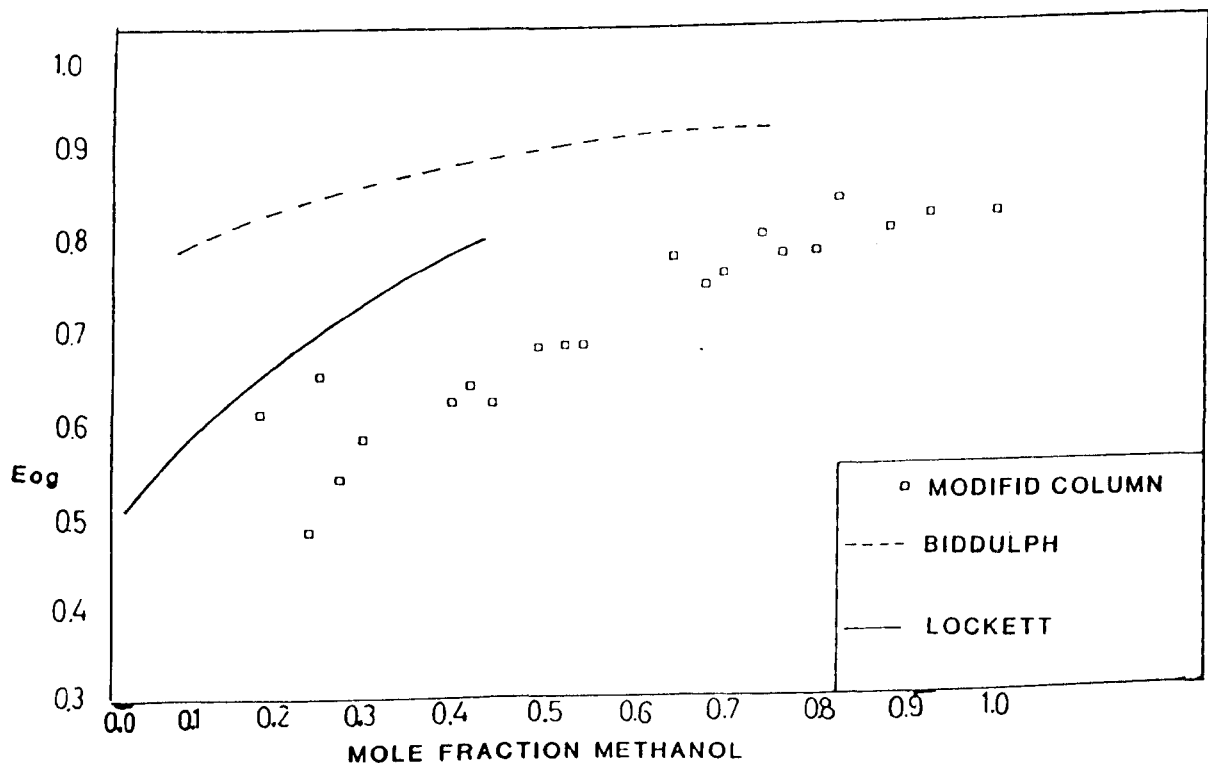
Figure 4.7   MeOH/H2O System Point Efficiencies
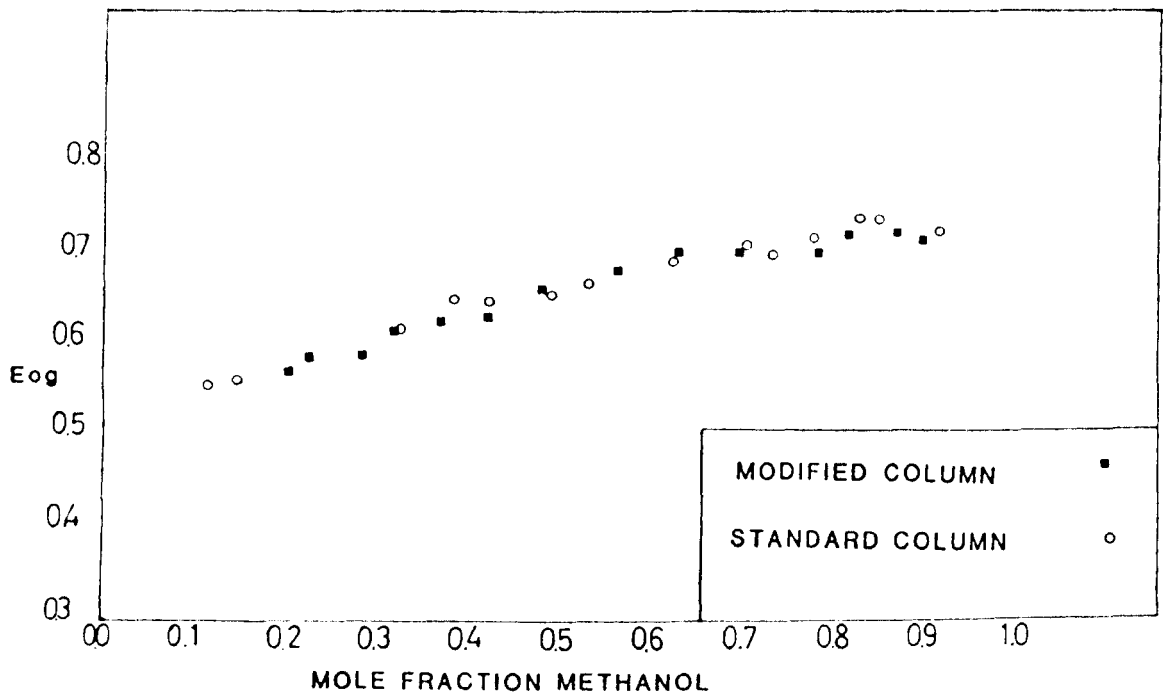
Figure 4.8 MeOH/n.PrOH System Point Efficiencies
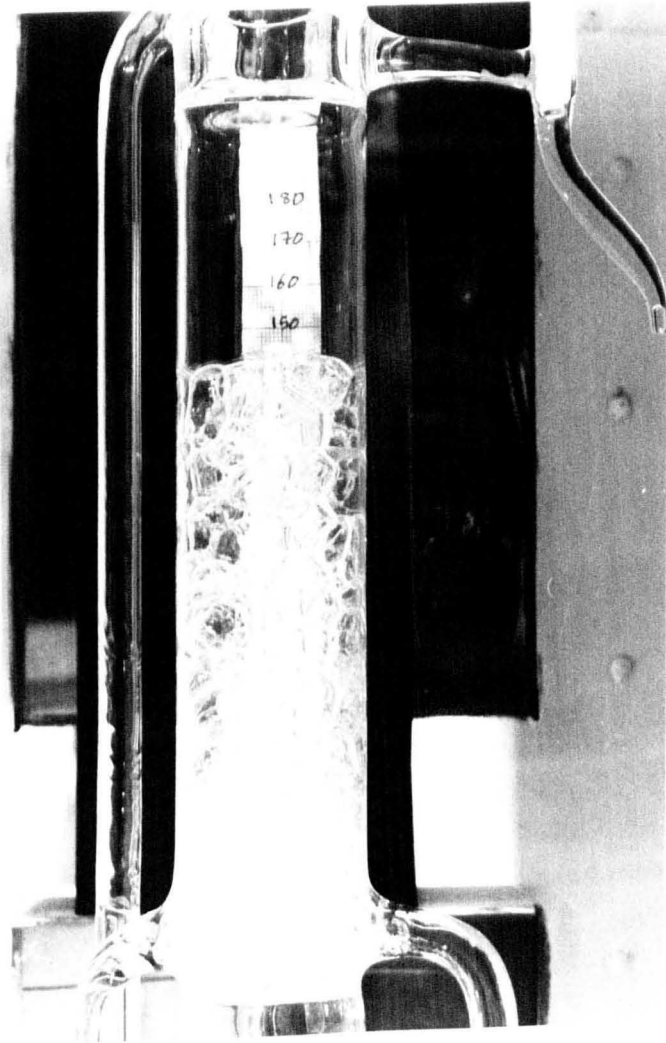
Run:12   System: n.Propanol/Water
              Vapour Velocity:0.37 m/s
              X=0.2044
              Eog=0.97

Figure 4.9 Operation of Standard Oldershaw Column.
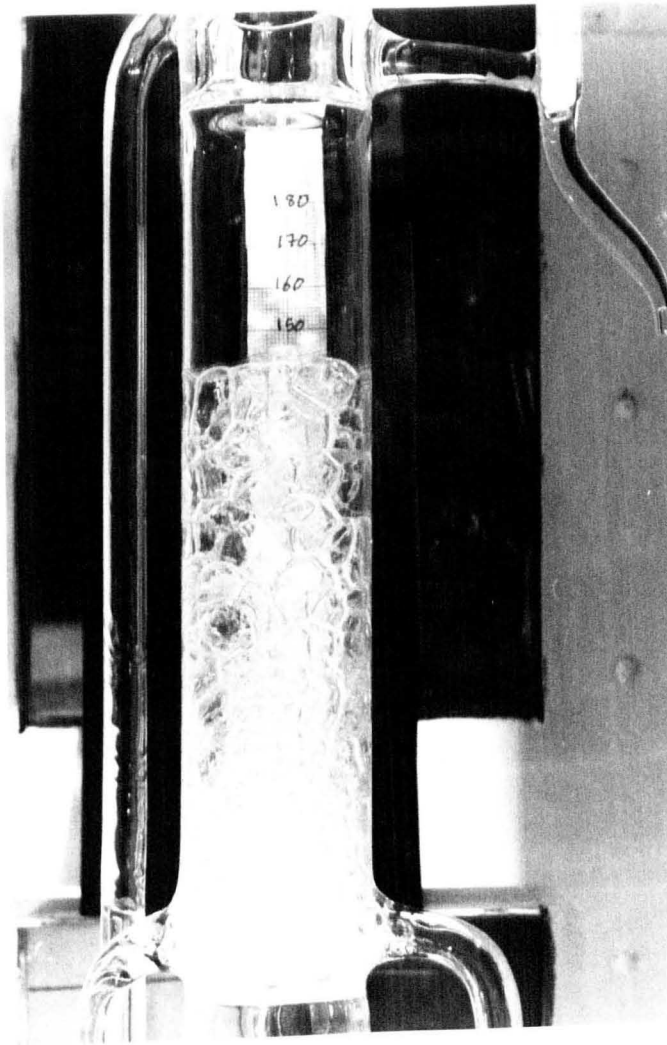
Run:12   System: n.Propanol/Water
              Vapour Velocity:0.37 m/s
              X=0.2044
              Eog=0.97

Figure 4.9 Operation of Standard Oldershaw Column.

Figure 4.10.a   Run:131
                       System:n.Propanol/Water(positive)
                       Vapour Velocity:0.49 m/s
                       X:0.3887
                       Eog:0.44
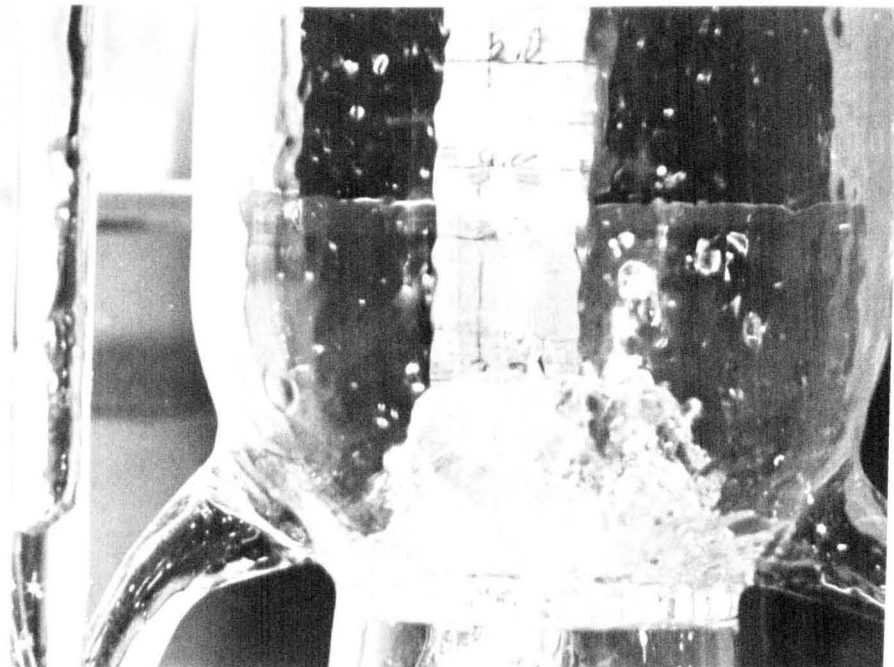
Figure 4.10.a

Run:131
System:n.Propanol/Water(positive)
Vapour Velocity:0.49 m/s
X:0.3887
Eog:0.44

Figure   4.10.b   Run:155
                       System:n.Propanol/Water (negative)
                       Vapour Velocity: 0.48 m/s
                       X: 0.5424
                       Eog: 0.32
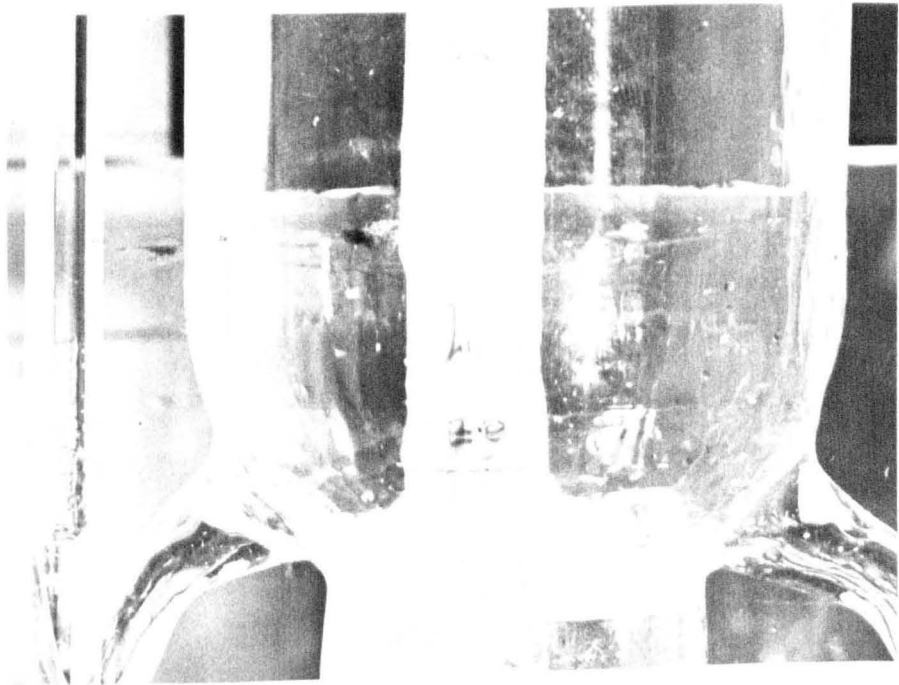
Figure   4.10.b

Figure 4.10.c   Run: 156
                       System:n.Propanol/Water (negative)
                       Vapour Velocity:0.26 m/s
                       X: 0.5448
                       Eog:0.36

Figure 4.10.c

Run: 156
System:n.Propanol/Water (negative)
Vapour Velocity:0.26 m/s
X: 0.5448
Eog:0.36
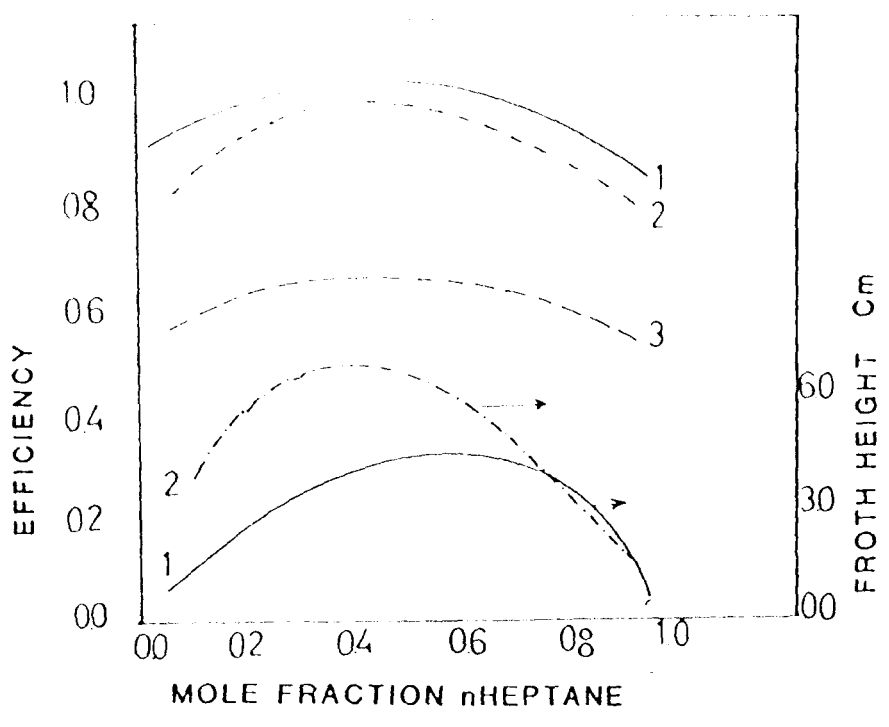
```
1  -  Medina et al
2  -  Zuiderweg and Harmens
3  -  Fane and Sawistowski
```

	REF. NO.		
	1	2	3
Column diameter or dimension cm	3.81	2.54	11x19
Outlet weir height cm	0.5	0.2	1.9
Vapour velocity ms^{-1}	-	0.3	-
No. of holes	55	-	148
Hole diameter m.m.	1.1	-	3

Figure 4.11   Efficiencies and Froth Heights of n.Heptane/Toluene System
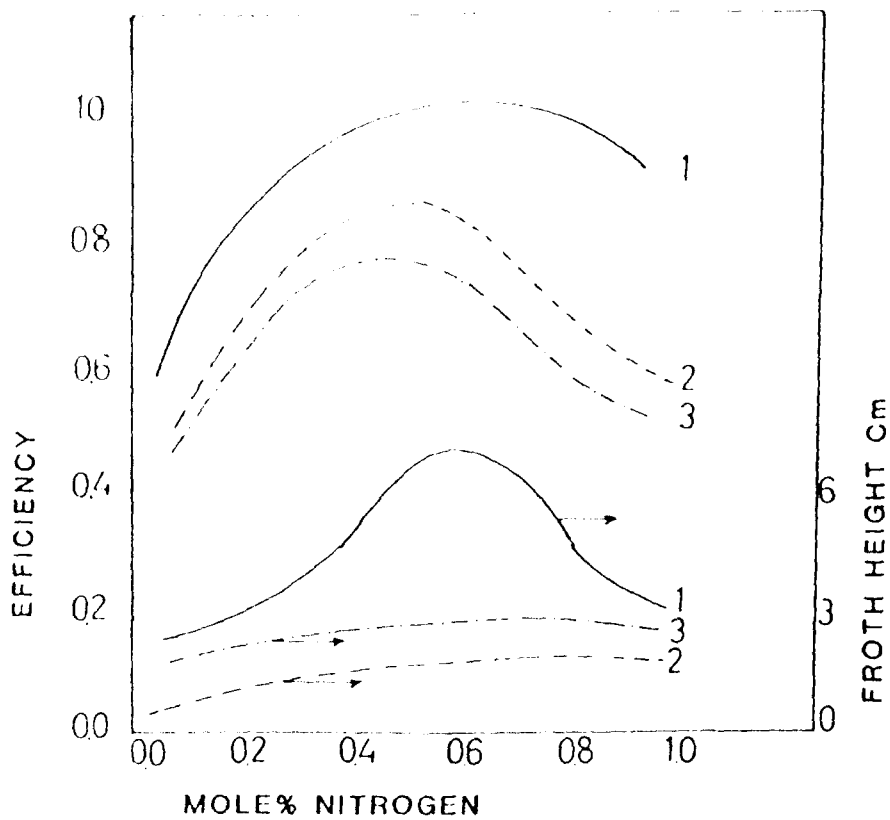
1 - Haselden and Thorogood
2 - Ellis and Catchpole
3 - Brown and England

	REF. NO.		
	1	2	3
Column diameter or dimension cm	1.7x1.8	3.81	7.62
Outlet weir height cm	2.54	0.635	2.54
Vapour velocity ms^{-1}	0.4	0.33	0.35
No. of holes	26	46	-
Hole diameter m.m.	1.00	1.1	-

Figure 4.12 Efficiencies and Froth Heights of N2/O2 System
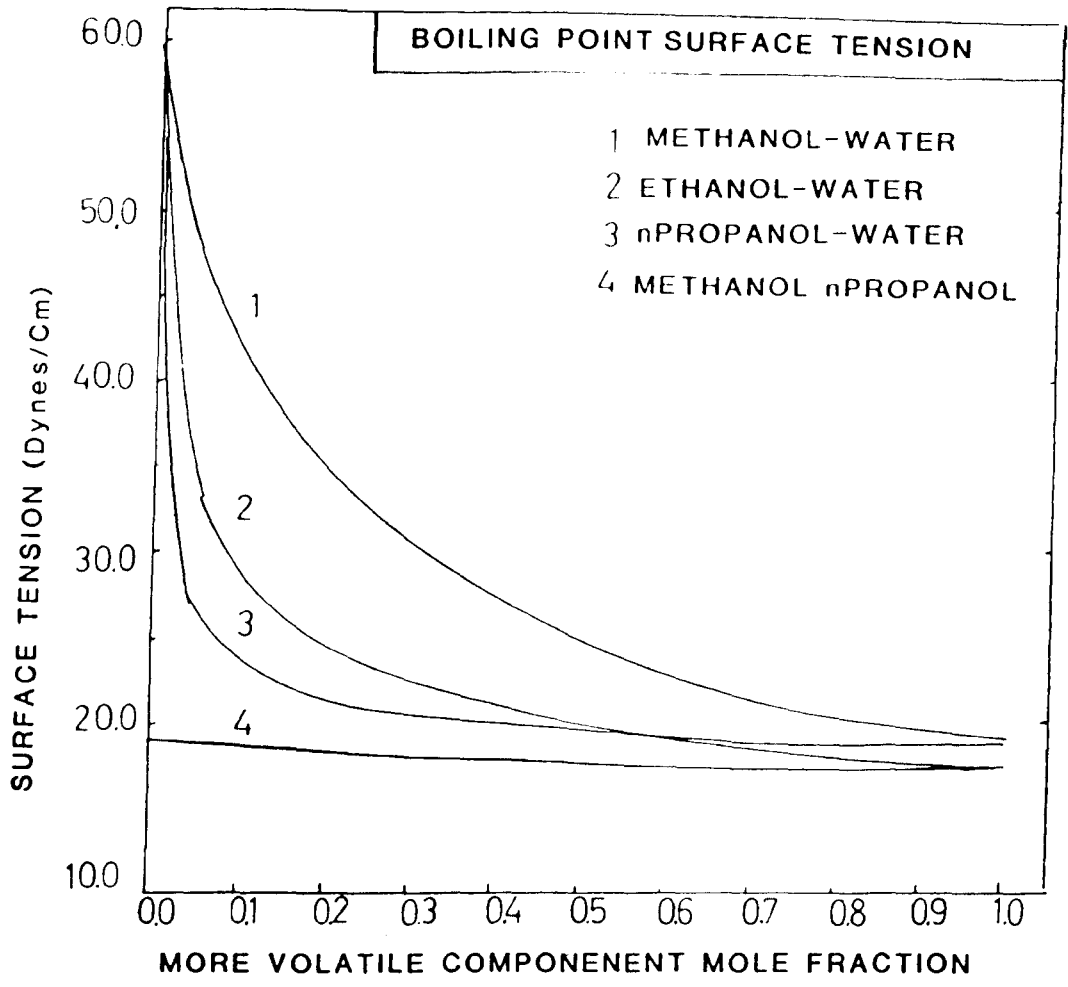
Figure 4.13 Boiling Point Surface Tension
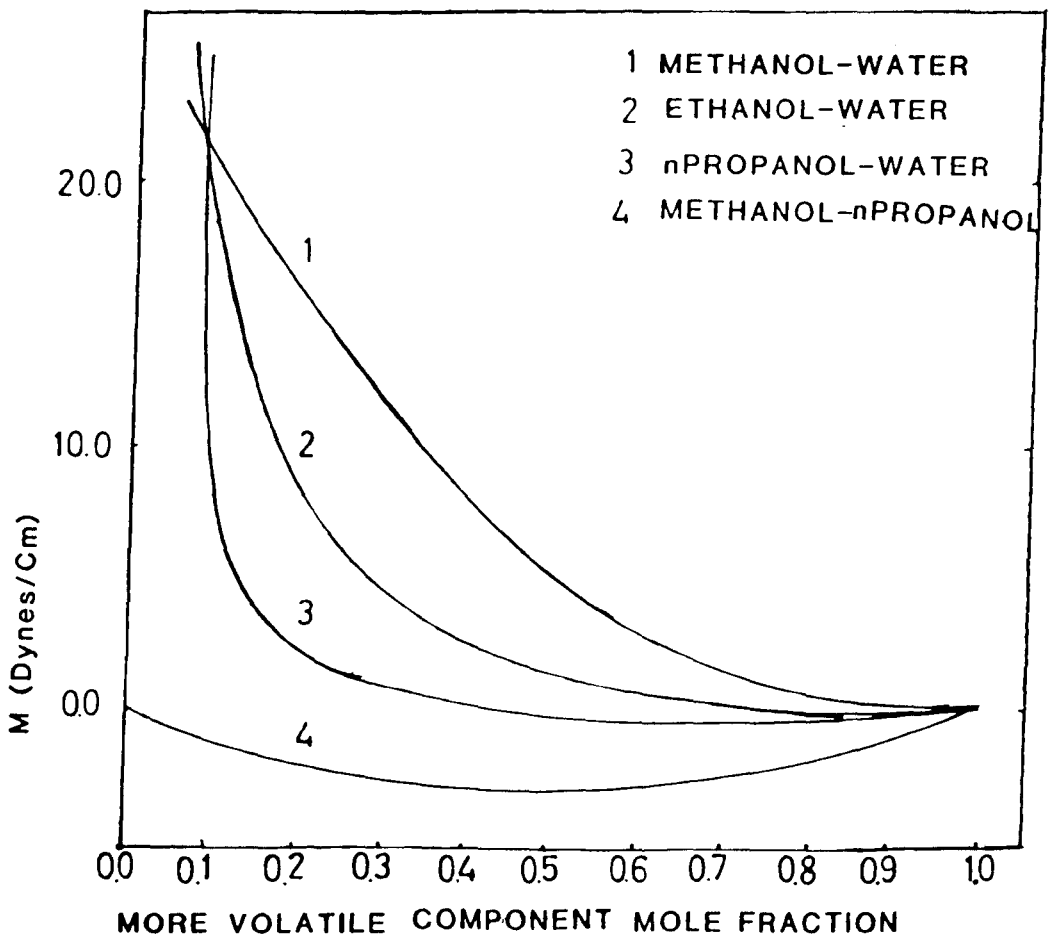
Figure 4.14 Marangoni Stabilising Index
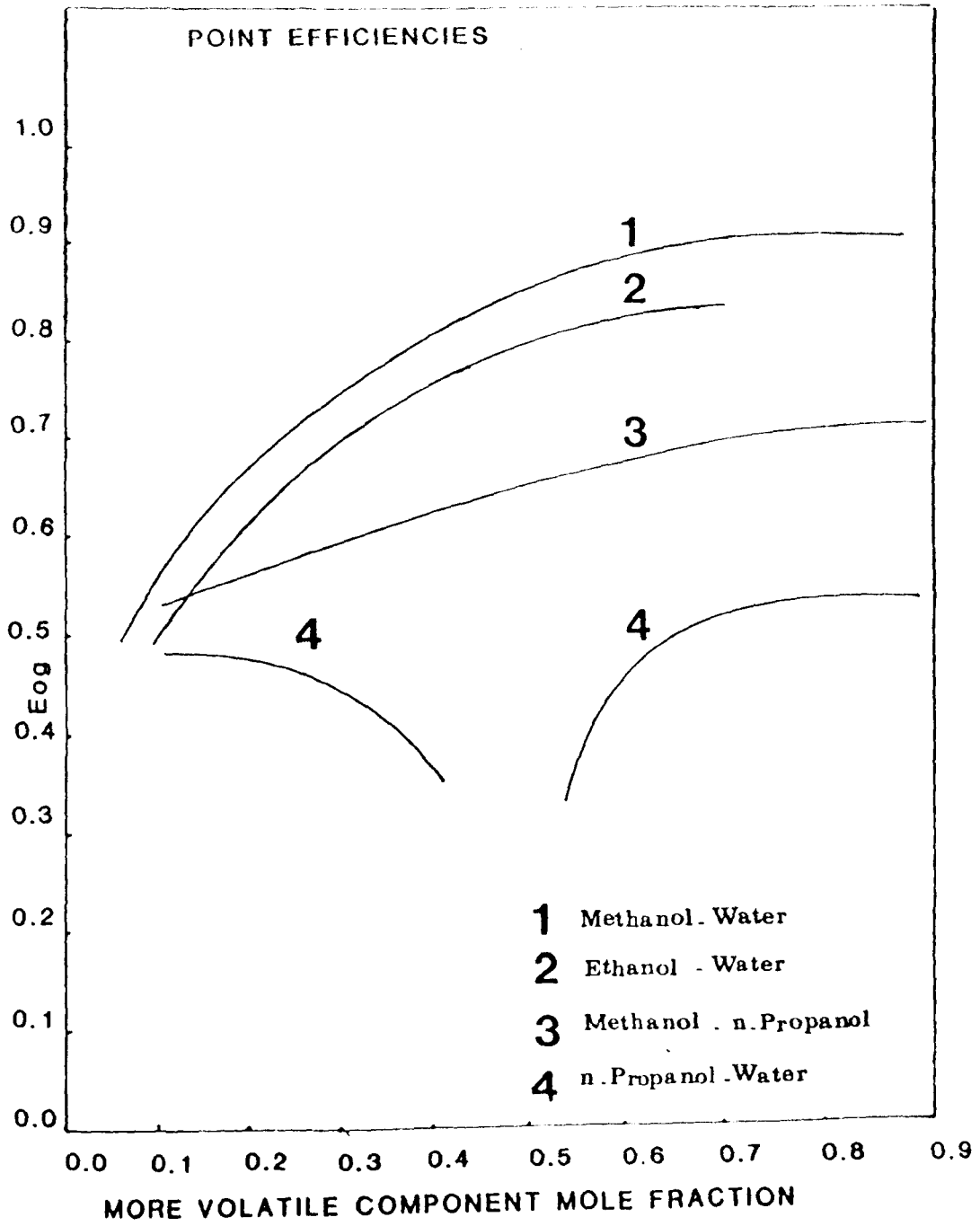
Figure 4.15 Point Efficiencies of Modified Column

CHAPTER 5

RECTANGULAR DISTILLATION COLUMN

RECTANGULAR DISTILLATION COLUMN

5.1 Introduction

The distillation equipment used here has been described previously by Biddulph and Dribika (1986), and Dribika (1986). A general flow sheet of the arrangement is given in Figure 5.1 and a photograph of the equipment is shown in Figure 5.2. Briefly it consists of the following sections:-

    1. Reboiler

    2. Rectangular Distillation Column

    3. Condensers

The vapour from the reboiler (R), passed through the rectangular distillation column (D) containing three trays and then to the condensers (C) where it was totally condensed. The resulting condensate formed the reflux and returned to the column via a calibrated rotameter.

5.2 The Reboiler

This vessel was constructed of stainless steel and was cylindrical in shape, having equal length and diameter of 0.76 metre. It had a capacity of 450 litres and could withstand working pressures of up to 100 p.s.i. The outside of the reboiler was insulated with 50 mm thick fibre-glass enclosed in aluminium cladding. The reboiler was steam jacketted with an automatic air vent for high efficiency operation. It was equipped with a pressure gauge, a sight glass, filling and drainage valves, a safety valve on the boiler mixture side, locations for the steam inlet and outlet condensate, a thermocouple pocket, and a steam pressure safety valve.

C   CONDENSERS
D   DISTILATION COLUMN
F   FLOW METER
R   REBOILER
W   WINDOWS

S   SAMPLE·POINT

C

WATER OUT

WATER IN

D

W ○   ○   ○   ○

S2   S3 S4 S5 S6 S7 S8   S9

F

S10

S1

STEAM IN

R

CONDENSATE

S11
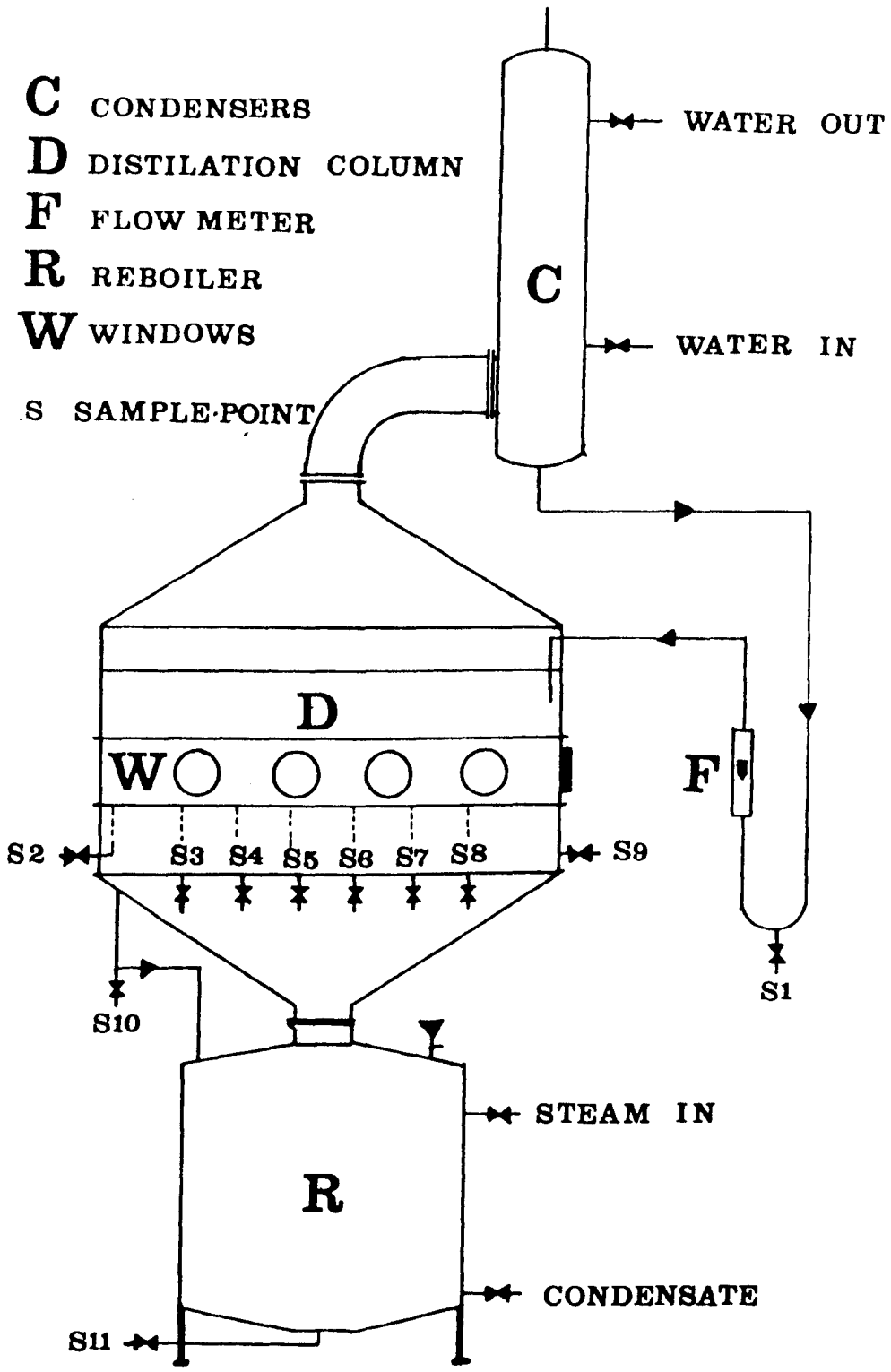
Figure 5.1   General   view of the rectangular column

Figure 5.2   General View of the Rectangular Column.

Figure 5.2 General View of the Rectangular Column.
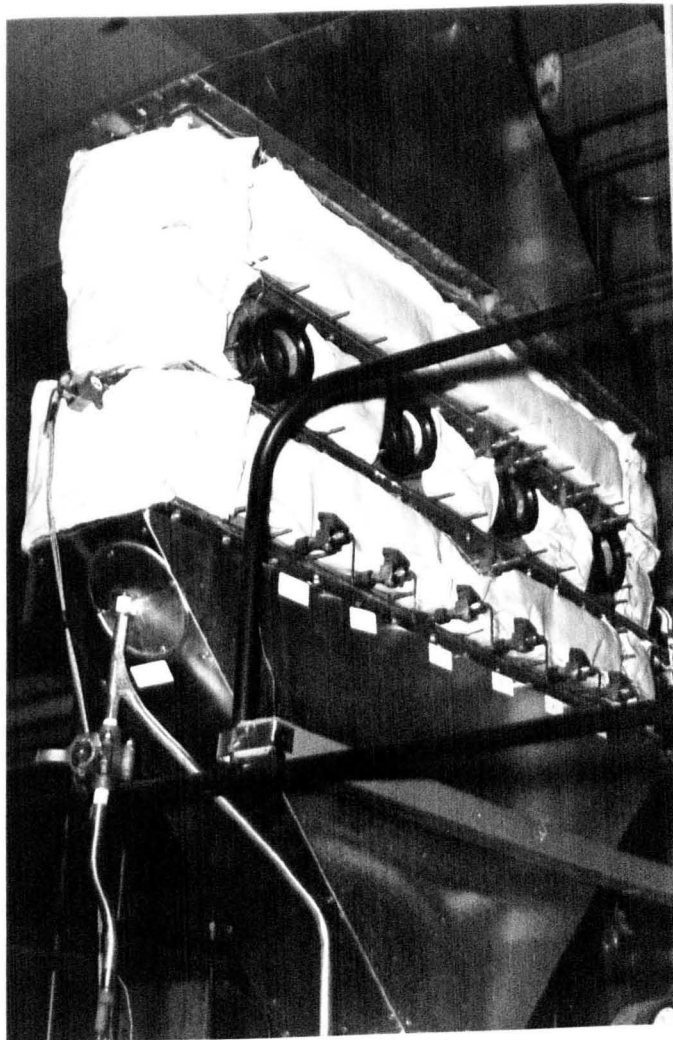
Figure 5.3 Front view of the Rectangular Column.
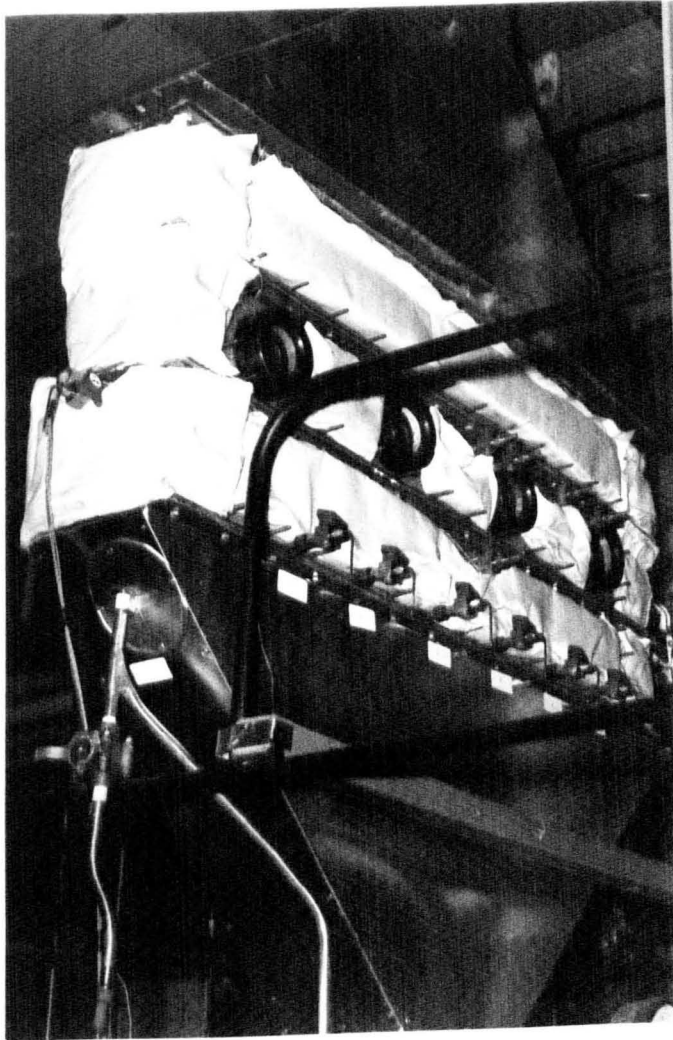
Figure 5.3 Front view of the Rectangular Column.

5.3   The Column Section

The rectangular distillation column, of dimensions 1.067 x 0.089 metre, had three trays, the middle being the test tray. The bottom tray acted as a vapour straightener, the top tray duty is to calm the liquid prior to entering to the test tray for stable hydrodynamic operation. The column itself was made up of three sections, in order to allow easy access to the internals. It had removable sides between the trays, each bolted to the main body frame and sealed with a silicon rubber gasket. This allowed minor changes/checks, such as moving the outlet weir to a new height or inspecting the sample lines or the thermocouples. If a major change, such as changing the tray, was required, the column could be dismantled easily. The modifications to the column could then be made by raising the section. Afterwards, these sections were bolted back together, including a neoprene rubber gasket.

The tetrahedral shaped upper and lower parts of the column had a height of 0.5 metre with rectangular base and circular top 0.15 metre in diameter, and were insulated with 50 mm thick fibre glass and aluminium cladding. The rectangular body of the column was also insulated with removable fibre glass, (Figure 5.3).

Observation of the biphase on the test tray was possible through five double-glazed windows made from borosilicate glass discs. Four of these windows were placed at equal distances of 50 mm apart on the front (Figure 5.3), and there was one at the end. Froth height measurements, observation of weeping and entrainment, and a close study of the froth and spray formation was then possible. A light beam could be directed through the end window to illuminate the biphase

The top of the column was connected to the condensers via a combination of a 90° glass bend and a tee. The lower part of the tee was connected to a reducer and then a stainless steel reflux line of 25 mm

in diameter. The rotameter was fitted to this line. The line delivered the liquid to the inlet downcomer of the top tray. The return liquid to the reboiler left the outlet bottom downcomer also via a 25 mm in diameter stainless steel line.

The test tray (Figure 5.4) was fitted with an inlet weir of 4.8 mm height. This reduced velocity of the entering liquid across the tray and encouraged uniform bubbling.

The liquid samples were withdrawn from the test tray, inlet and outlet downcomer, the reflux line and the liquid returning to the reboiler after achieving steady state conditions. These samples were collected in pre-chilled sample bottles. Six equally spaced sample tubes were fitted along the centre line of the tray, the liquid samples flowing by gravity. These stainless steel lines had 3 mm inside diameter. In addition two more sample points were also available in the inlet and outlet downcomers of the test tray. This allowed the measurement of the tray efficiency directly and a study of the concentration profiles across the tray. These sample lines where insulated with polymer sleeving below the test tray to avoid evaporation in the sample line and they were fitted with P.T.F.E. stainless steel valves.

5.4   Condensers

Three shell and spiral-wound tube glass condensers were connected in series, and provided a cooling area 5.3 square metres. The first two Quickfit condensers provided 2.5 m^2 of cooling area each, and the third, connected to the middle condenser by a reducer, provided the extra 0.3 m^2 surface area. These condensers were reported (Dribika, 1986) to be satisfactory even when operating at high boil-up rates. The cooling water supplied to these condensers was continuously recycled to a cooling tower
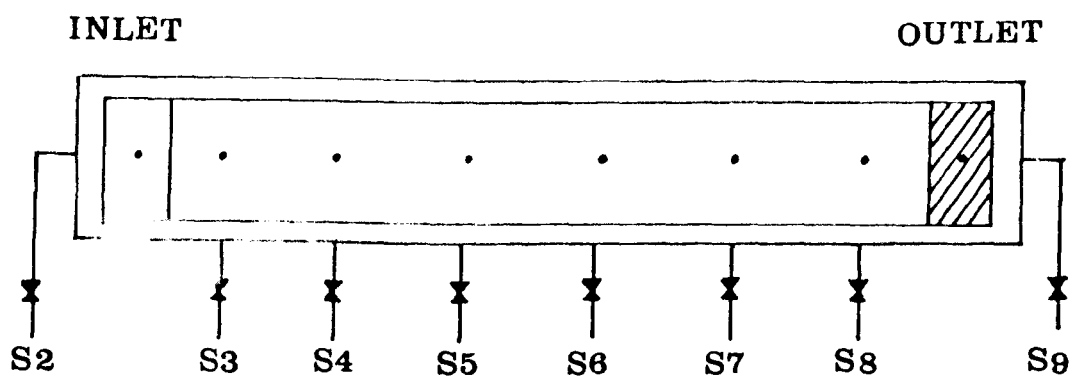
Figure 5.4 Sampling across the tray

to maintain a constant low temperature.

Chrome-aluminium thermocouples were available to measure the simult-
aneous temperature profiles in the test tray, the temperature of the
liquid inlet and outlet to the test tray downcomers, and the reboiler
temperature. Each thermocouple on the test tray was placed in the nearest
perforation available to a sample point, and 3 mm above the test tray.
The thermocouples were pre-calibrated against boiling distilled water to
an accuracy of $0.1^{o}C$.

Two vapour connection points, one above the test tray and the other
below it, were also available for pressure drop measurements. In addition
two perforated tracer injection probes were available for liquid mixing
studies on the tray. These lines were all fitted with P.T.F.E. valves.

5.5   Operation of the Column

The distillation experiments were carried out at total reflux and
atmospheric pressure. About 180 litres of the test mixture was used, and
the steam pressure was adjusted to give the required boil-up rate, which
was measured by using a calibrated rotameter placed in the reflux line.
The column was run for about four hours during which the boil up rate,
temperatures, froth heights and manometric readings, if required, were
noted at regular intervals. Steady-state conditions were achieved during
this period. The operation of the column was carried out at a vapour
F.Factor of about 0.5 (m/s) $(kg/m^{3})^{0.5}$, which was found to produce a
hydrodynamically stable biphase of decreasing height from the inlet to
the outlet. The mixed froth biphase (Hofhuis and Zuiderweg, 1979) consisted
of froth and spray. The samples were collected into pre-chilled bottles
at the end of each run to be analysed by G.L.C. methods. The sample

probes were regularly inspected to ensure proper insulation, and the thermocouples were also recalibrated after a major change involving removal and replacement of the test tray.

5.6   Safety of the Column

The reboiler was treated as a pressure vessel fitted with a steam safety valve and a mixture bursting disk safety valve connected to the top condenser and open to the atmosphere outside the laboratory through a pipe. This pipe also provided a safety measure against cooling water failure to release the volatile vapour to the atmosphere. The cooling water was also fitted with an automatic valve connected to the mains water supply in case of cooling water failure.

CHAPTER 6

DISTILLATION OF ETHANOL-WATER AND n.PROPANOL-WATER

IN THE LARGE RECTANGULAR COLUMN

DISTILLATION OF ETHANOL/WATER AND n.PROPANOL/WATER IN THE LARGE RECTANGULAR COLUMN

6.1 Introduction

Following the satisfactory development of the modified Oldershaw column to eliminate wall effects (see Chapter 4), and in order to study the relationship between the efficiencies of different columns for these highly surface tension affected systems, a series of experiments was conducted in the large distillation column (see Chapter 5). The components comprising these two systems also constitute the multicomponent systems studied (see Chapters 9 and 10). The distillation experiments were carried out similar F-Factors to those used in the small column and rectangular column experiments on the multicomponent systems. In addition the same tray percentage free area was used. The rectangular tray had a flow path length of about one metre and was narrow to avoid stagnant zones and flow non uniformities which are known to affect the performance of large circular trays (Lockett et. al. 1973). Mixing studies carried out on this tray by Biddulph and Dribika (1986) indicated that the conditions were approaching plug flow, so the AICHE partially-mixed flow model was used to deduce component point efficiencies from the measured tray efficiencies. It was originally intended to use the rigorous eddy diffusion model (Biddulph, 1975) as described in Chapter 7, but due to the non-linear behaviour of the 'K' values in these systems the less satisfactory AIChE model was used. The rigorous eddy diffusion model required a linear relationship between the temperature and K-value in order to make the predictor-corrector method stable.

6.2 Systems Used

Two systems, ethanol/water and methanol/water were used here. The equilibrium data for these systems are quoted in Chapter 4. The surface tension of these systems at the boiling points measured by a glass tensiometer (Chapter 3) are given in Figure 3.5.

6.3 Equipment

The rectangular sieve tray column has been described in detail in Chapter 5. The test tray (Table 6.1) material is typical of that commonly used in low temperature air distillation.

Table 6.1   Tray Details of the Rectangular Column

Weir Length	83 mm
Liquid flow-path length	991 mm
Tray Spacing	154 mm
Hole Diameter	1.8 mm
% Free area	8 %
Outlet weir height	25 mm
Inlet weir height	4.8 mm

6.4 Experimental

The experiments were carried out at an F-Factor of about 0.5 m/s $(kg/m^3)^{0.5}$. This provided stable hydrodynamic conditions on the tray. The experiments were conducted at total reflux and atmospheric pressure.

The flow of the reflux, temperatures along the tray and the froth heights were monitored regularly as a guide to steady-state operation. The reflux rate was measured using a rotameter placed in the reflux line and the froth height was observed through the windows of the test tray. These measurements were subject to the usual judgment errors. The samples at the end of each run were collected in pre-chilled bottles after a small quantity of the liquid was discarded from each sample point to ensure a representative sample. These samples were analysed by G.L.C., the accuracy of the mole fraction measurements being $\pm$ 0.0028 and $\pm$ 0.0034 for the EtOH and n.PrOH systems respectively. The details of the analysis and calibrations are given in appendix D.

6.5   The Tray Model

Assuming complete vapour stream mixing, the Murphree tray efficiency (Emv) is defined as the ratio of actual change in vapour composition through the tray to the change which would have occurred if the vapour had actually reached a state of equilibrium with the liquid leaving the tray.

$$Emv = \frac{Y_n - Y_{n-1}}{Y_n^* - Y_{n-1}} \qquad 6.1a$$

Where the subscripts n and n-1 refer to the outlet and inlet vapour streams (see the next page). Y_n^* is the concentration of the vapour in equilibrium with the liquid of composition Y_n, which at total reflux, is equal to Y_n. Thus at total reflux the equation 6.1a can be written as:-

$$Emv = \frac{x_{n+1} - x_n}{Y_n^* - x_n} \qquad 6.1b$$
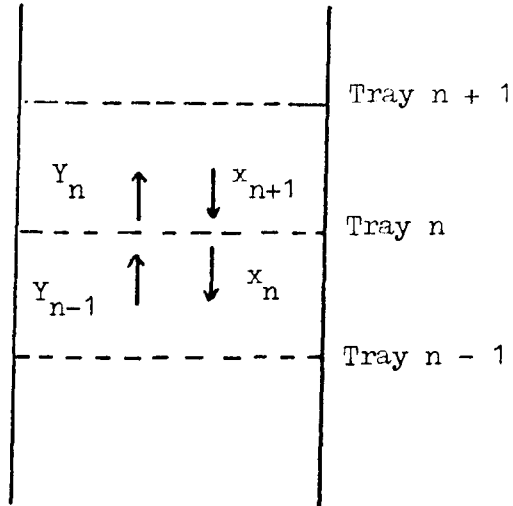
A Typical Stage

If complete mixing were achieved on the tray, equations 6.1a and 6.1b could be rewritten as:-

$$Emv = Eog = \frac{Y_n - Y_{n-1}}{Y_n^* - Y_{n-1}} \qquad 6.2a$$

$$Emv = Eog = \frac{x_{n+1} - x_n}{Y_n^* - x_n} \qquad 6.2b$$

As complete mixing is never achieved on a long flowpath tray, equation 6.2b can only describe a point on a test tray where complete mixing of the liquid can be assumed. Thus Eog is referred to as the point efficiency. As stagnant zones and flow non-uniformities were absent, a knowledge of

the extent of liquid mixing on the tray is required to predict the relationship between the tray and point efficiencies.

6.5.1 Partially Mixed Model

The final report of the University of Delaware (1958) research team, incorporating the extent of liquid back-mixing in terms of a Peclet number (pe) suggests:

$$\frac{Emv}{Eog} = \frac{1 - e^{-(\eta - Pe)}}{(\eta - Pe)(1 + \frac{\eta + Pe}{\eta})} + \frac{e^{\eta} - 1}{\eta(1 + \frac{\eta}{\eta + Pe})} \qquad 6.3$$

$$\text{where} \quad \eta = (\frac{Pe}{2})(\sqrt{1 + \frac{4\lambda Eog}{Pe}} - 1) \qquad 6.4$$

$$\text{total reflux} \quad \lambda = m \qquad 6.4a$$

$$Pe = \frac{Z_1^2}{D_E t_L} \qquad 6.5$$

D_E is the eddy diffusion coefficient, which is a measure of the amount of back-mixing.

6.6 The Relationship Between the Point Efficiency (Eog) and Overall Number of Transfer Units (NOG)

The overall number of transfer units is given by:

$$NOG = \int \frac{d_y}{Y^* - Y} \qquad 6.6$$

Assuming that the liquid concentration is constant in the vertical direction (i.e. completely mixed), the vapour enters the tray completely mixed and the vapour passing upwards through the liquid along any vertical section is in plug flow (i.e. no vertical mixing of the vapour), equation 6.6 can be integrated along any vertical line on the tray from the tray deck $(Z = 0, y = y_{n-1}, x = x)$ to the top of the froth $(Z = Z, y = y, x = x)$. Since x is constant y^* is a constant and:

$$NOG = -\ln \frac{y_n^* - y_n}{y_n^* - y_{n-1}} \qquad 6.7$$

$$\text{or } NOG = -\ln (1 - Eog) \qquad 6.8$$

Two film theory suggests that

$$\frac{1}{NOG} = \frac{1}{NG} + \frac{m}{L_m} \frac{G_m}{N_L} \qquad 6.9$$

where $1/NG$ and $\frac{m}{L_m} \frac{G_m}{N_L}$ are the vapour and the liquid phase resistances to mass transfer respectively. A knowledge of m and Eog enables the evaluation of N_G and N_L by the slope and intercept method. This facilitates the study

of binary systems and permits the identification of the elements of equation 6.9.

6.7 Mixing Study

The mixing studies on the 1.8 mm hole diameter tray was carried out by Biddulph and Dribika (1986). They used the system water/steam with sodium nitrate tracer injection. Using the well-established method of Barker and Self (1962), a Peclet number of about 39 was evaluated for the loadings used here from eddy diffusivity measurements. This result indicates that conditions are approaching plug flow on this tray, and a small variation in Peclet number, perhaps due to slightly different vapour velocities in different runs, will not greatly affect the predicted composition profiles.

6.8 Results

In order to cover a wide range of composition, a large number of runs was carried out at total reflux and atmospheric pressure. The F-Factor was approximately 0.5 m/s $(kg/m^3)^{0.5}$ in all cases, except for the n. propanol-water runs at high alcohol concentration where a slightly lower F-Factor was required to stop excessive foaming. However the results from the small column (Chapter 4) indicated that this would have a negligible effect on the point efficiencies. All the results are tabulated in Tables 6.2 and 6.3.

6.8.1 Observation of the Biphase

The froth heights were measured by using a metre rule and using the four observation windows available. These measurements were for each

individual run averaged as shown in Figure 6.1. The system ethanol/water exhibited large froth heights, especially in the higher ethanol composition range, whereas lower froth heights were obtained for the n.propanol/ water system. The system n.propanol/water, as discussed in Chapter 4, exhibits all surface tension characteristics.

It is positive at low n.propanol concentration, neutral at the azeo-tropic point and slightly negative in the higher alcohol composition range. The froth heights measured for this system indicated lower heights in the negative surface tension composition range presumably due to slightly lower F-Factor used. Further discussion of the surface tension characteristics of these systems appears in Chapter 4. The biphase itself consists of mixed flow of the froth and droplets. The froth had different bubble sizes and the droplets, some of them fairly large, were thought to be produced either as a result of the atomisation of the liquid by high speed vapour in the perforations or as a result of the bubbles bursting. Smaller droplets were associated with the latter phenomenon. As expected, the biphase declined in height from the inlet to outlet due to the hydraulic gradient.

6.8.2   Composition and Temperature Profiles Across the Tray

The temperature profiles across the tray were measured directly using the thermocouples installed on the test tray next to the sample points. These are plotted on Figure 6.2. A comparison between these measured temperatures and the calculated bubble-point temperatures (see Appendix B) are presented in Figure 6.3. They compare very well and indicate that heat losses from the column are minimal. The concentration profiles for the runs are presented in Figures 6.4 and 6.5. They indicate that the sampling technique was satisfactory.

6.8.3   Tray Efficiency Measurements

Equation 6.1b was used to calculate Murphree tray efficiencies, by incorporating the inlet and outlet compositions measured experimentally. The equilibrium value of the vapour leaving the tray, or the liquid entering the tray since operation was at total reflux, was calculated by using a series of computations outlined in Appendix B. These tray efficiencies are presented in Figures 6.6 and 6.7. The average liquid composition on the test tray was calculated by the following relationship (Lockett and Ahmed 1983):-

$$\bar{x}_i = \int_0^1 x_{wi} \, dw \qquad\qquad 6.10$$

where w, is the relative position in the tray.

6.8.4   Component Point Efficiencies

The partially mixed flow model was used to evaluate component point efficiencies. The slope of the equilibrium line was directly calculated using x, y data, (see Figure 6.8) using the following equation:-

$$m = \frac{Y_1^* - Y_2^*}{x_1 - x_2} \qquad\qquad 6.11$$

Small changes in x were used in the above evaluation. To calculate each point efficiency, the average composition on the tray was calculated by incorporating the measured profiles into equation 6.10 and corresponding m from Figure 6.8. These point efficiencies are plotted on the Figures 6.9 and 6.10. These point efficiencies follow the same trend observed

Table 6.2   Results of EtOH/H_2O Runs

RUN	$\bar{x}$	m	Emv	Eog(AIChE)	$1/N_{OG}$	H_f (cm)
EA	0.4570	0.42	1.05	0.87	0.49	5.5
EB	0.3052	0.49	1.01	0.82	0.58	5.5
EC	0.2527	0.55	1.01	0.74	0.74	5.5
ED	0.4149	0.41	1.02	0.85	0.52	7.0
EE	0.4750	0.43	1.02	0.85	0.53	8.5
EF	0.5132	0.44	1.03	0.85	0.53	9.0
EG	0.5235	0.45	1.02	0.84	0.55	8.5
EH	0.5324	0.46	1.04	0.85	0.55	9.0
EI	0.5450	0.46	1.02	0.84	0.55	9.0
EJ	0.5670	0.47	1.05	0.85	0.54	9.0
EK	0.5880	0.49	1.09	0.87	0.50	9.5
EL	0.6243	0.52	1.16	0.91	0.42	10.0
EM	0.5510	0.47	1.08	0.88	0.48	10.0
EN	0.6229	0.52	1.19	0.93	0.38	10.0
EO	0.6792	0.56	1.25	0.95	0.33	10.0
EP	0.2193	0.66	1.11	0.83	0.86	5.5
EQ	0.1701	1.1	1.21	0.77	0.68	5.5

Table 6.3   Results of n.Propanol/H_2O Runs

RUN	$\bar{x}$	m	Emv	Eog(AIChE)	$1/_{NOG}$	H_f (cm)
PA	0.8515	1.26	1.24	0.75	0.73	4.0
PB	0.8172	1.12	1.17	0.75	0.73	4.0
PC	0.7943	0.935	1.16	0.79	0.65	4.0
PD	0.6682	0.485	1.09	0.88	0.48	4.0
PE	0.3970	0.242	0.85	0.77	0.68	7.0
PF	0.3490	0.232	0.84	0.77	0.68	7.0
PG	0.2435	0.228	0.89	0.82	0.58	6.5
PK	0.110	1.62	1.86	0.86	0.51	5.5
PL	0.1523	0.554	1.06	0.84	0.55	5.5

in the small column measurements (Chapter 4). The point efficiencies of the system ethanol/water shows the expected composition dependency, but the system n.propanol/water does not show any specific trend, and both positive and negative surface tension regions exhibit fairly similar efficiencies.

6.8.5 Individual Number of Transfer Units and Percentage of Liquid Phase Resistance

The overall number of transfer units (NOG) was calculated using the point efficiencies for these two systems. The reciprocal of these NOG's were plotted against the slope of the equilibrium line m, (Figure 6.11). Using the slope and intercept method, the individual number of the transfer units N_L and N_G were calculated and tabulated in Table 6.4.

Table 6.4 N_L and N_G Values

System	N_L	N_G
$EtOH/H_2O$	4.83	2.3
$n.PrOH/H_2O$	7.05	1.88

The percentage of the liquid phase resistance is calculated from:-

$$\% \ LPR \ = \ \frac{m N_G}{N_L + m N_G} \qquad\qquad 6.13$$

6.9   Discussion

a)   The component point efficiencies obtained here are in very good agreement with the ones calculated in a small Oldershaw column described in Chapter 4. This indicates that a modified column can be used to obtain direct design data for a large distillation column, or be scaled-up using the proposed method of , Dribika and Biddulph, (1986,Chapter 8).

b)   The measured component point efficiencies for the system ethanol/ water are composition dependent (Hart and Haselden, 1969). The variations observed here can be explained in terms of the extent of phase resistance. At the lower ethanol end of the composition range there is a greater resistance to mass transfer from the liquid phase. The system n.propanol/ water does not show much variation and there is of course a much lower liquid phase resistance to mass transfer throughout the composition range. These findings are in agreement with the works of Biddulph (1966), Dribika (1986) and Mostafa (1979).

c)   The influence of the slope of the equilibrium line on tray efficiency is noticeable (Mostafa 1979). Which is in agreement with the theoretical equation used here.

d)   In the absence of stagnant zones and flow non-uniformities which are known to decrease the tray efficiency (Porter et. al. 1972, Lockett et. al. 1973) better efficiencies are to be expected from circular sieve trays, operating in the mixed flow regime, if these detrimental effects are eliminated.
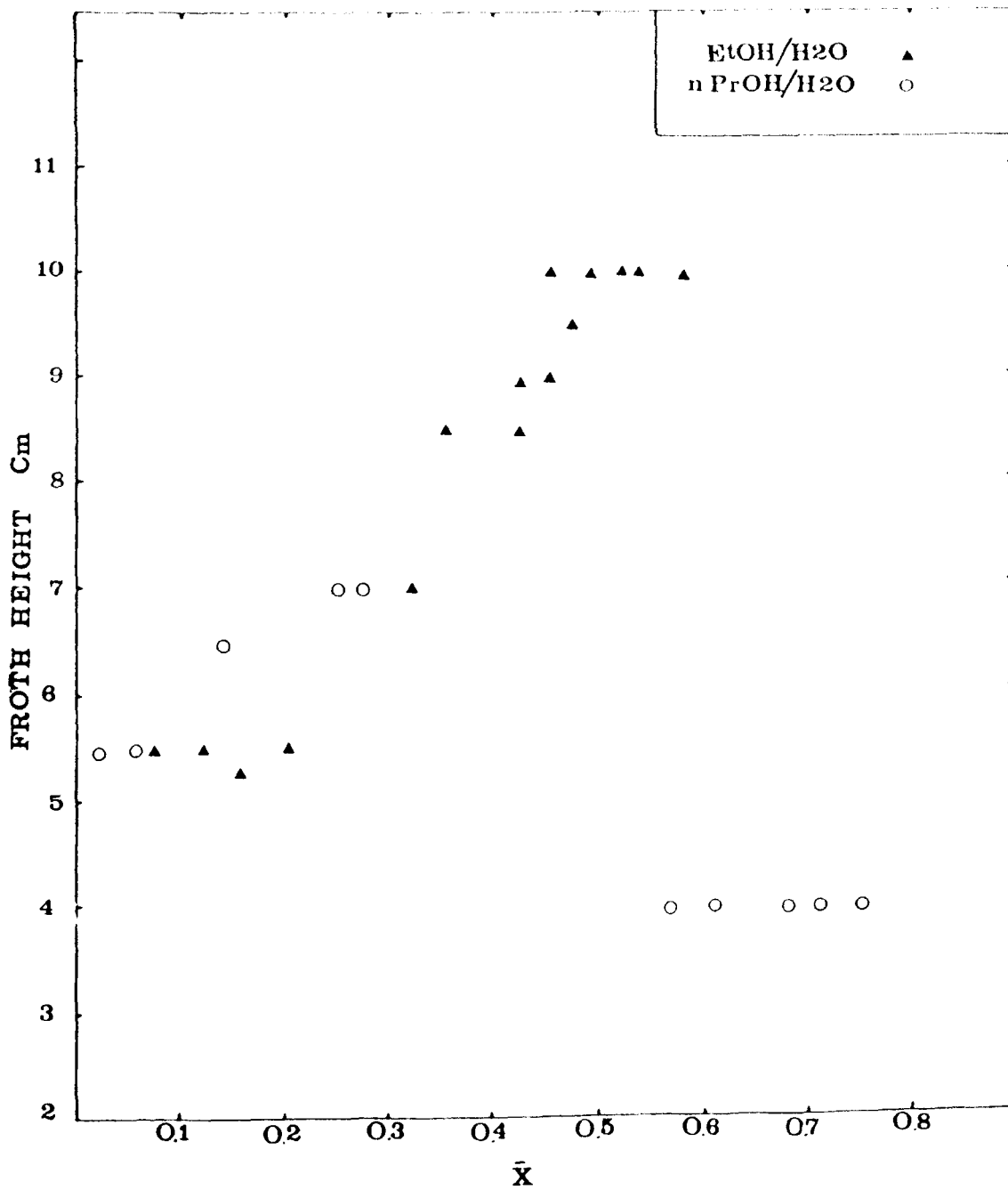
Figure 6.1 Froth heights
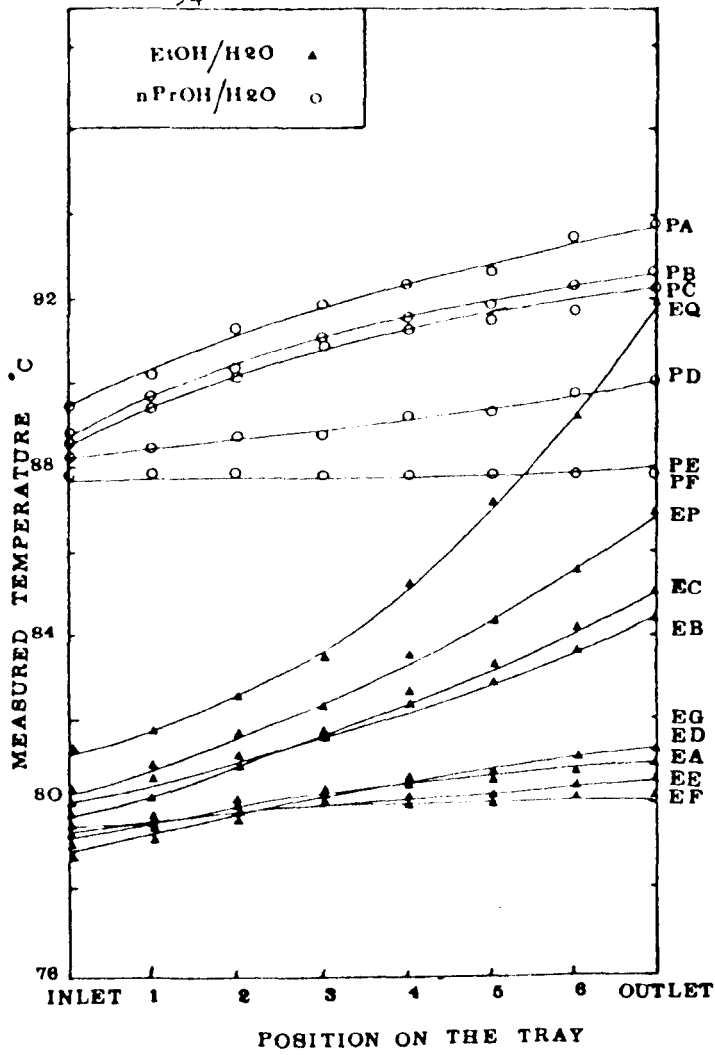
Figure 6.2   Temperature profiles
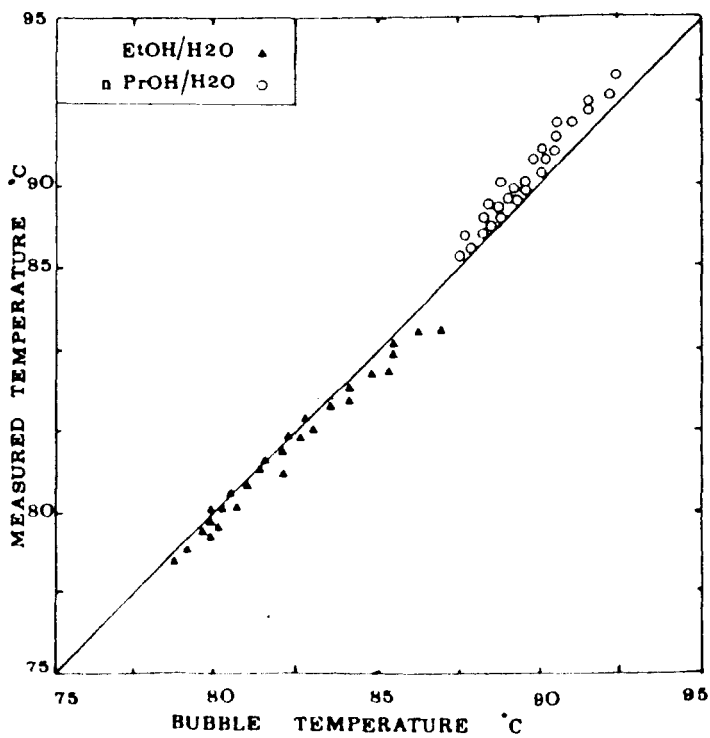
Figure 6.3 Comparison of measured and bubble temperatures
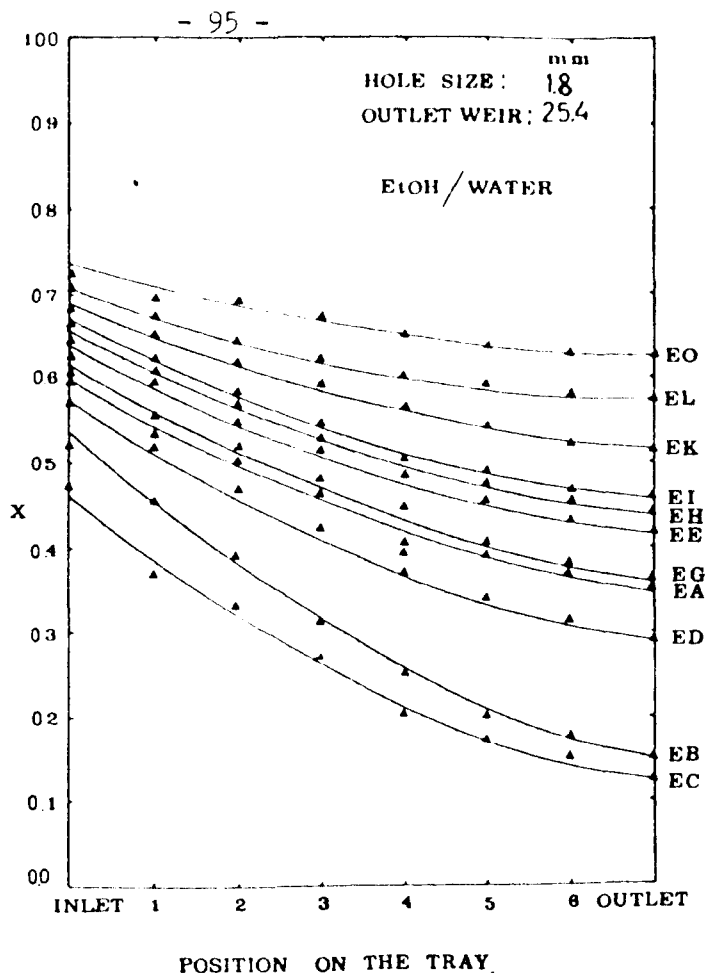
Figure 6.4 EtOH/H2O system composition profiles
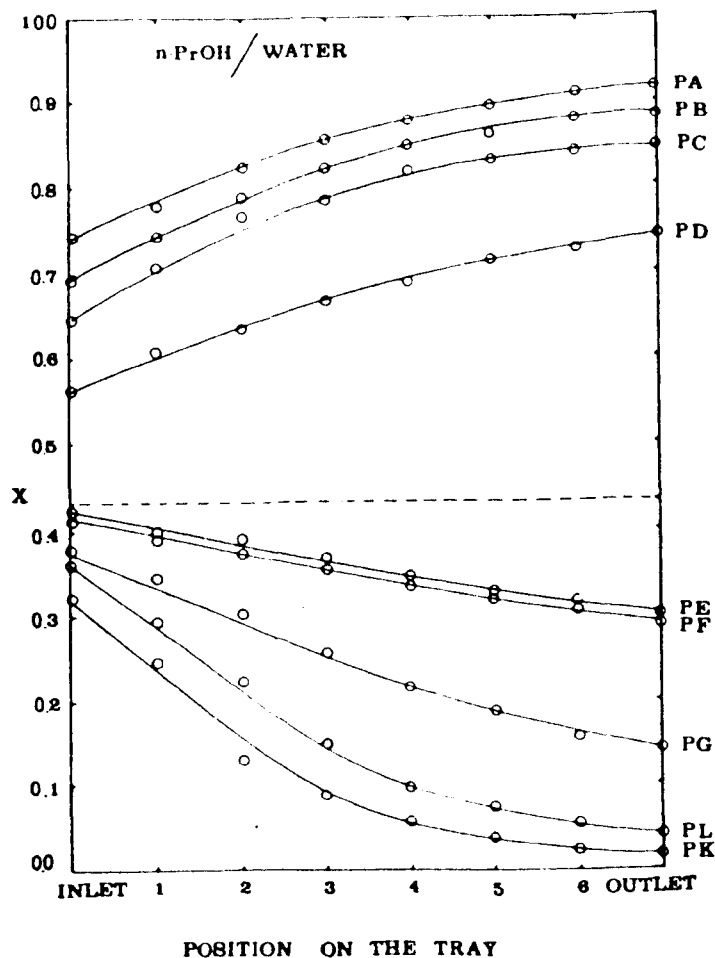
Figure 6.5 n.PrOH/H2O system composition profiles
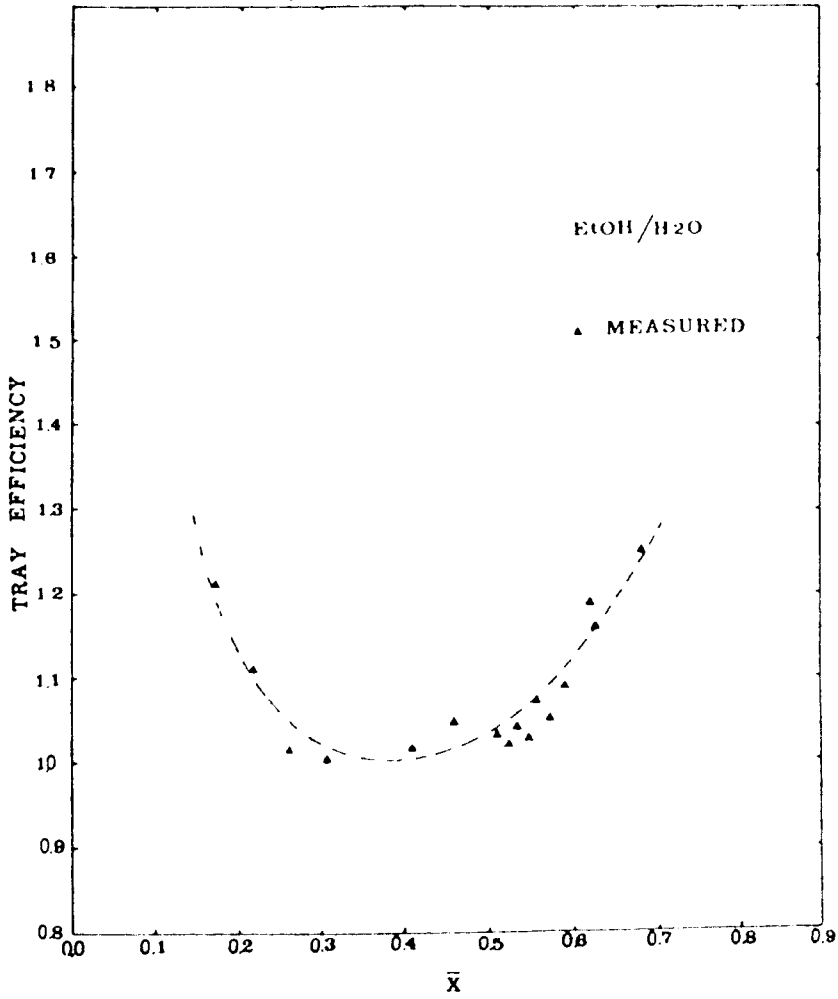
Figure 6.6   EtOH/H2O system tray efficiencies
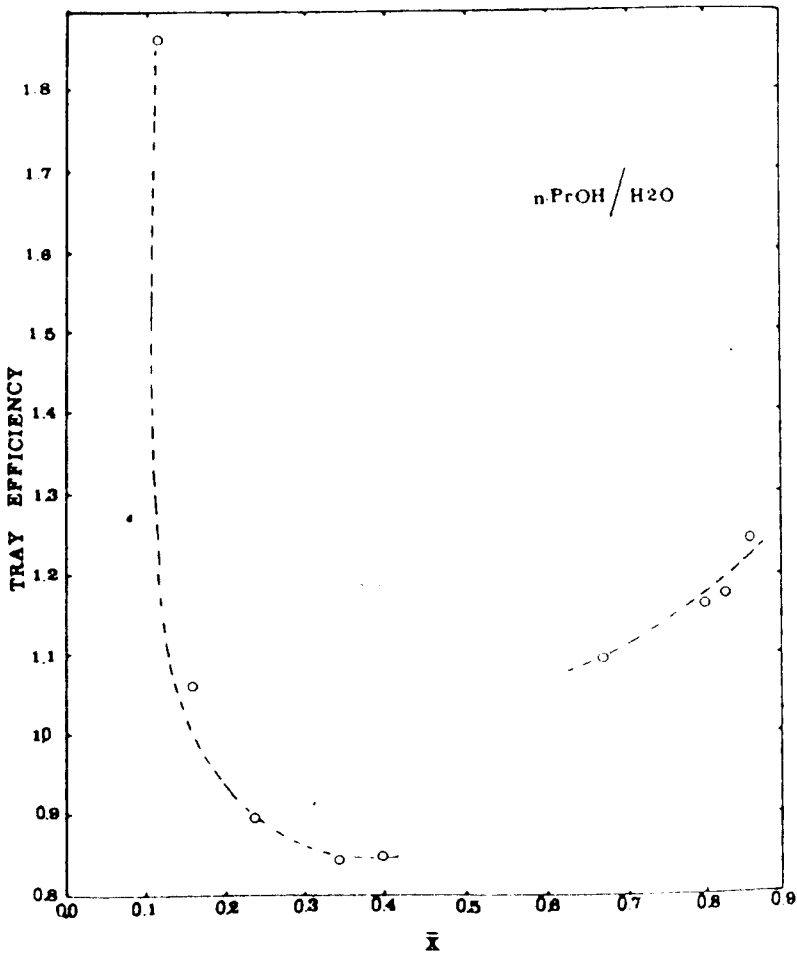
Figure 6.7   n.PrOH/H2O system tray efficiencies
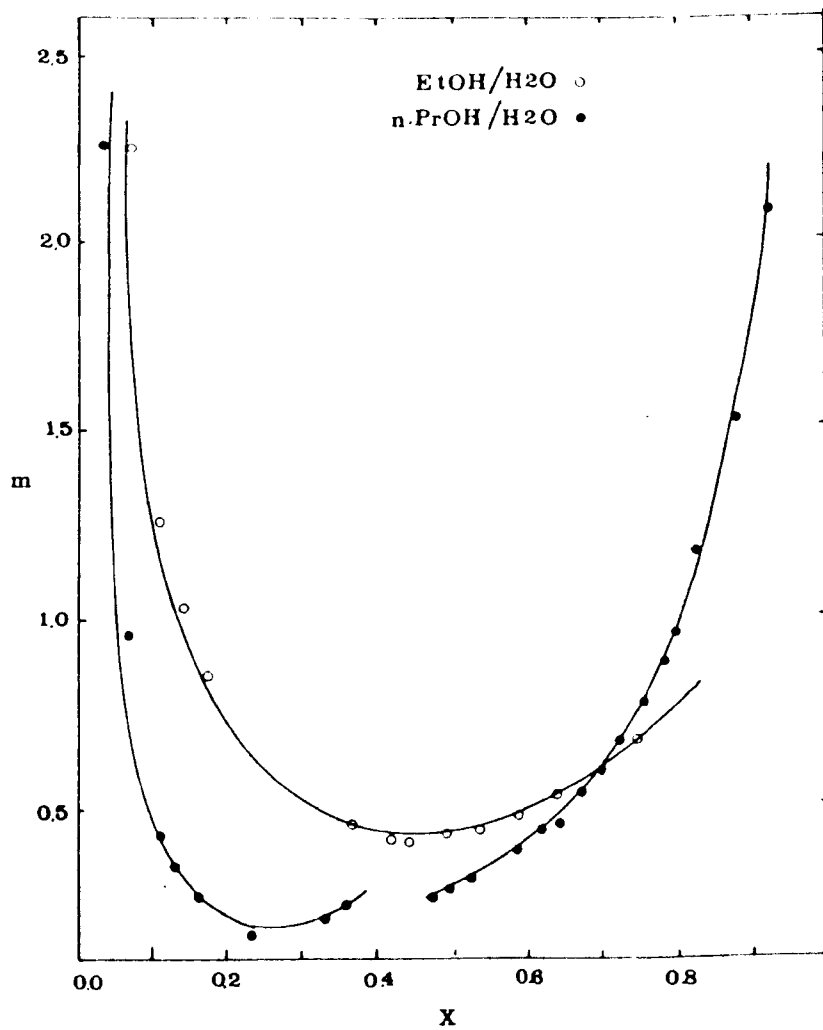
Figure 6.8 Slope of the equilibrium line
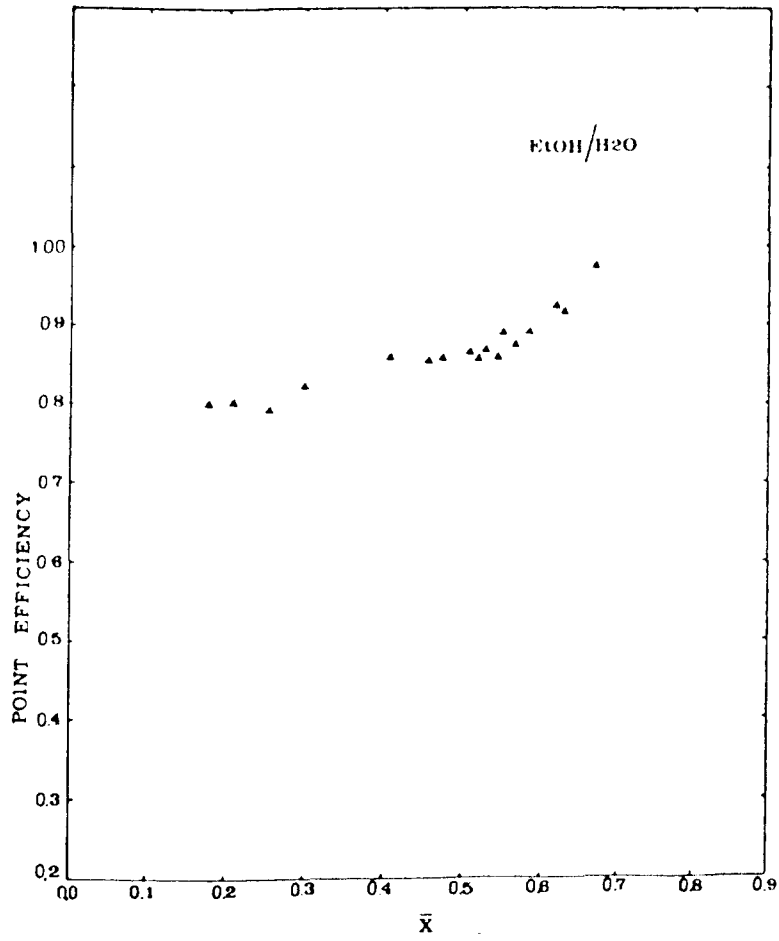
Figure 6.9 EtOH/H2O system point efficiencies
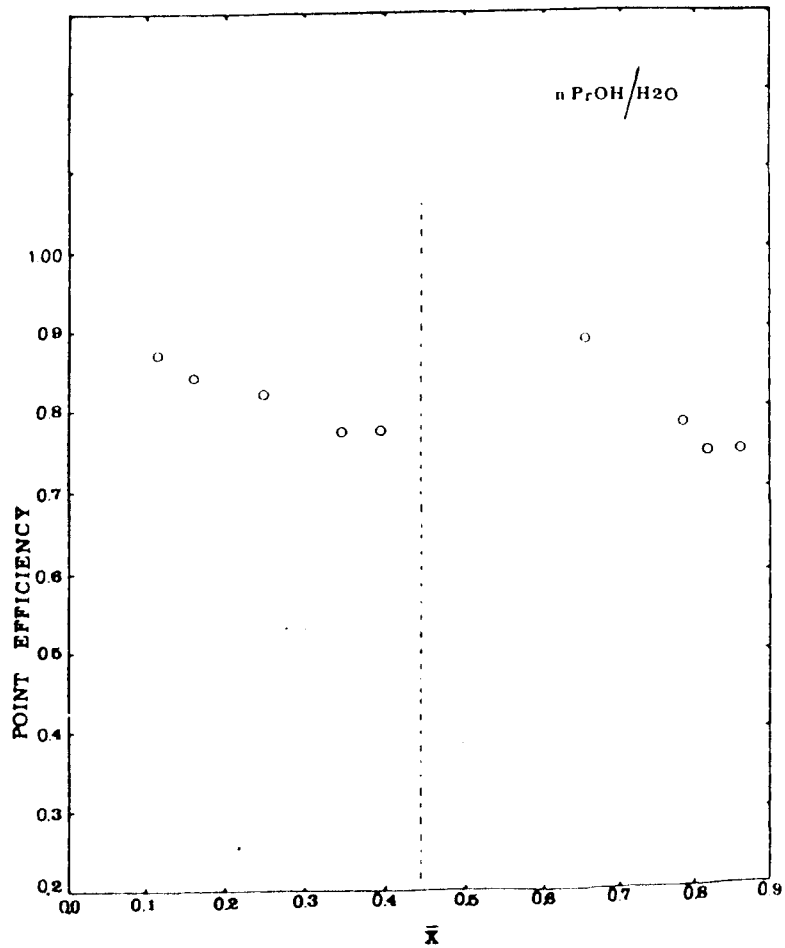
Figure 6.10 n.PrOH/H2O system point efficiencies
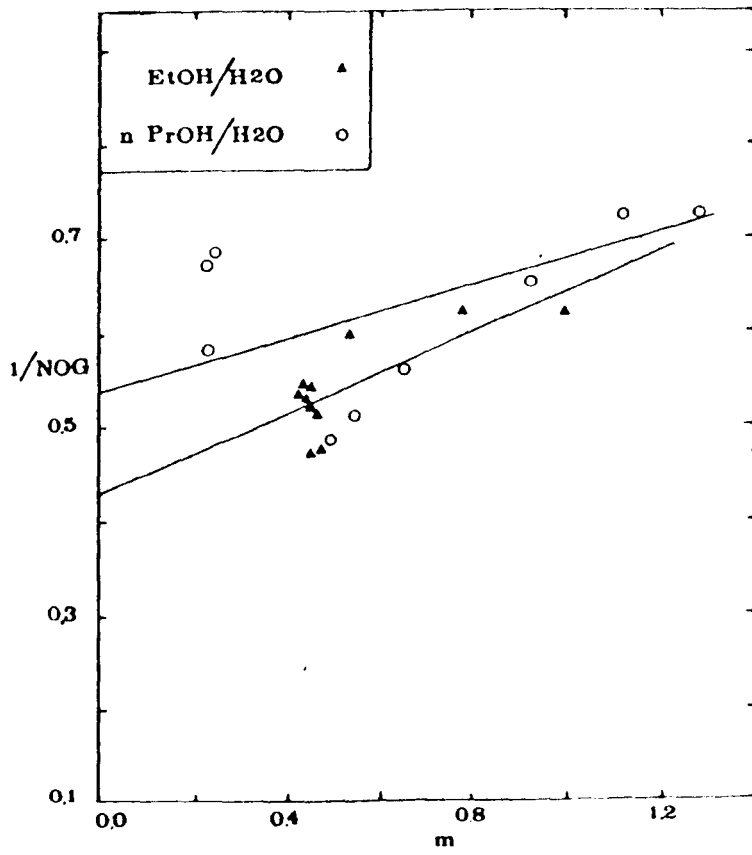
Figure 6.11   1/NOG Versus m
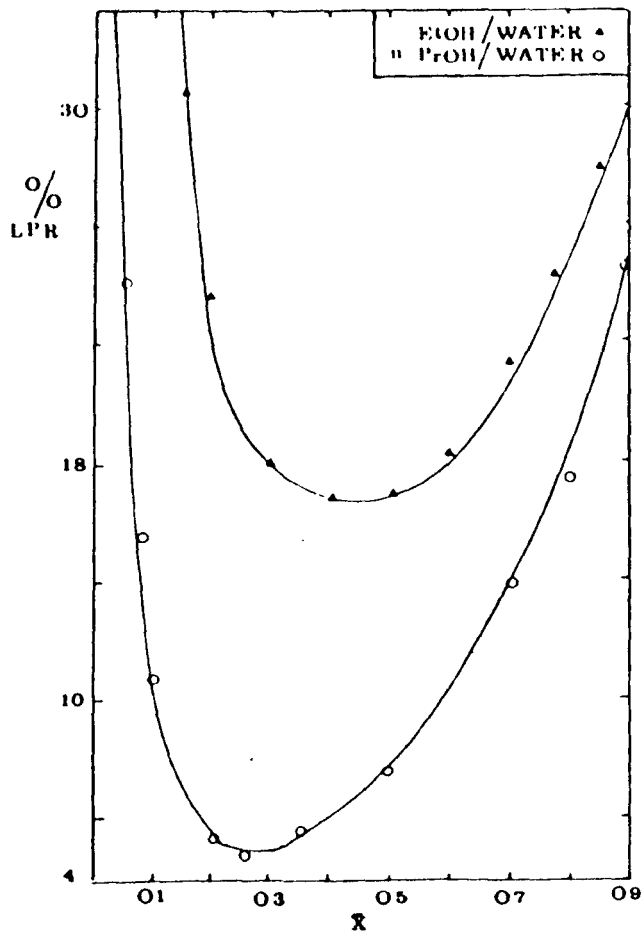
Figure 6.12 Percentage liquid phase resistance

CHAPTER 7

DISTILLATION SIEVE TRAY EFFICIENCIES

IN THE ABSENCE OF THE STAGNANT

ZONES

DISTILLATION SIEVE TRAY EFFICIENCIES IN THE ABSENCE OF THE STAGNANT ZONES

7.1   Introduction

Although the effect of the outlet weir height and hole size have been the subjects of studies by many investigators, due to experimental inconsistancies observed in most of these works it was decided to investigate these effects further. The sources of previous inconsistency were as follows:-

a)   Percentage Free Area

In comparing the effects of hydraulics a constant free area is desirable as the initial interfacial contact between the liquid and the vapour is directly related to this. Hellums et. al. (1958) and Umholtz et. al. (1958) used trays with different free area to study hole size and the outlet weir height effects.

b)   Wall Effects

In Chapter 4 the importance of removing the wall supported froth was discussed. It is very important to ensure that the hydrodynamics of the biphase in the small column is similar to that in the larger column. In the studies reported by Lockett et. al., (1979) and Pruden et. al., (1974), experiments were carried out in the presence of large froth heights dissimilar to the hydrodynamics of the larger trays, presumably due to wall effects.

c)   Stagnant Zones and Flow Non-uniformities

These detrimental effects reduce the efficiency of large circular sieve trays (Porter et. al. 1972, Lockett et. al. 1973). The distillation tray used in this investigation therefore must be rectangular.

d) Liquid Mixing on the Tray

If point efficiency is to be deduced from large tray measurements, a knowledge of the extent of the liquid mixing on the tray is required. Finch and Van Winkle (1964) assumed plug flow of the liquid on their rectangular tray to infer point efficiencies.

e) F-Factor

The F-Factor preferably should be kept constant throughout the experiments. The liquid and the vapour may experience different contact at different boil-up rates. Hofhuis and Zuiderweg (1979) identified four different regimes in a distillation column:-

- The spray regime

- The mixed froth regime

- The free bubbling regime

- The emulsified flow regime.

The investigation into hydraulic effects on the tray efficiency must lie within one of the above regimes. For atmospheric distillation the mixed froth regime is the most common.

Using the system methanol/water, an investigation into the effects of the outlet weir height and the hole size were carried out in a narrow rectangular distillation column (see Chapter 5). This avoids the problems associated with stagnant zones and flow non-uniformities in the mixed froth regime. Wall effects were absent during our experiments and the percentage free area was kept constant at 8 per cent. An eddy diffusion model (Biddulph, 1975) was used to match the composition profiles measured by experiment, and hence point efficiencies were inferred. The model took into account the extent of the liquid mixing on the tray. Tray pressure drops and liquid hold ups were also measured and compared with the recent predictions of Bennett .et.al.(1983).

7.2 Experimental

Full details of the rectangular column and the methods used to carry out the investigation are given in Chapter 5. The only addition to the column being the use of different perforation size trays, different outlet weir heights and pressure drop measurements. Trays with hole sizes 1.0, 1.8, 3.2 and 6.4 mm at an outlet weir of 12.7 mm were used to investigate the hole size effects. In addition the effect of outlet weir heights of 2 and 12.7 mm on tray/point efficiencies were also investigated using the 1.8 mm hole size tray. The details of tray are given in Table 7.1.

Table 7.1   Tray Details of the Rectangular Column

Tray thickness	2 mm
Weir length	83 mm
Liquid flowpath	991 mm
Tray spacing	154 mm
Hole diameter	1, 1.8, 3.2 and 6.4 mm
Outlet weir height	12.7 and 2 mm
% free area	8
Inlet weir height	4.8 mm

The sieve tray material is typical of that commonly used in low temperature air distillation (i.e. aluminium). The tray pressure drop was measured by a water manometer connected to vapour sample points above and below the test tray. To measure the clear liquid head the manometer was connected between a liquid sample point withdrawing liquid from the surface of the tray and the upper vapour sample point as shown in Figures 7.1 and 7.2. Figure 7.3 shows a photograph of the manometer as connected during a typical run to measure pressure drops. All the runs were carried out at total reflux and atmospheric pressure at a vapour F-Factor of about
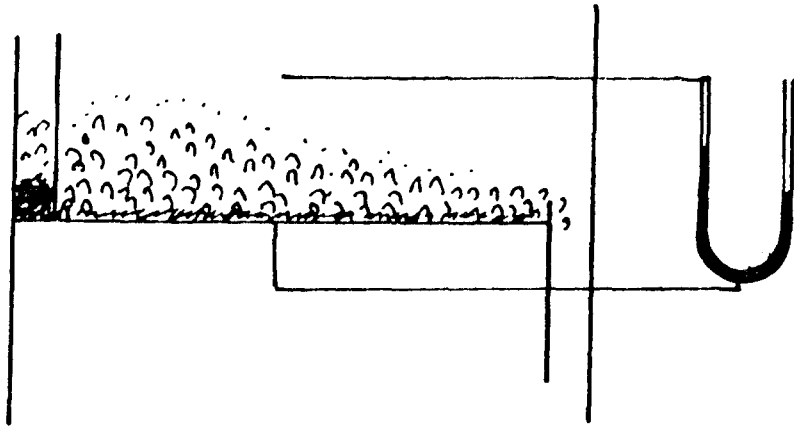
Figure 7.1   Liquid head   measurement
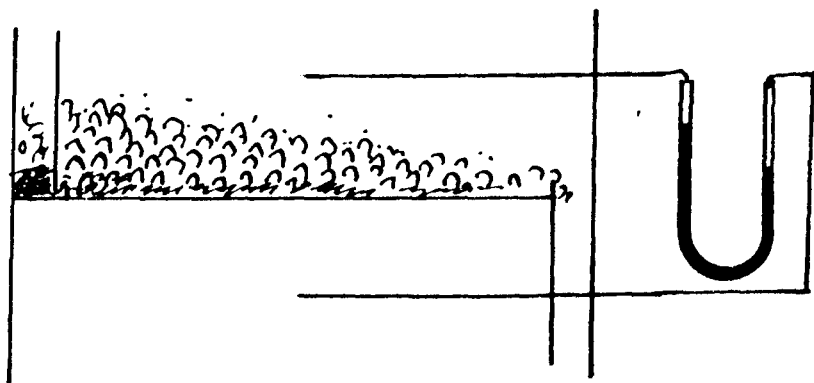
Figure 7.2   Pressure drop measurement
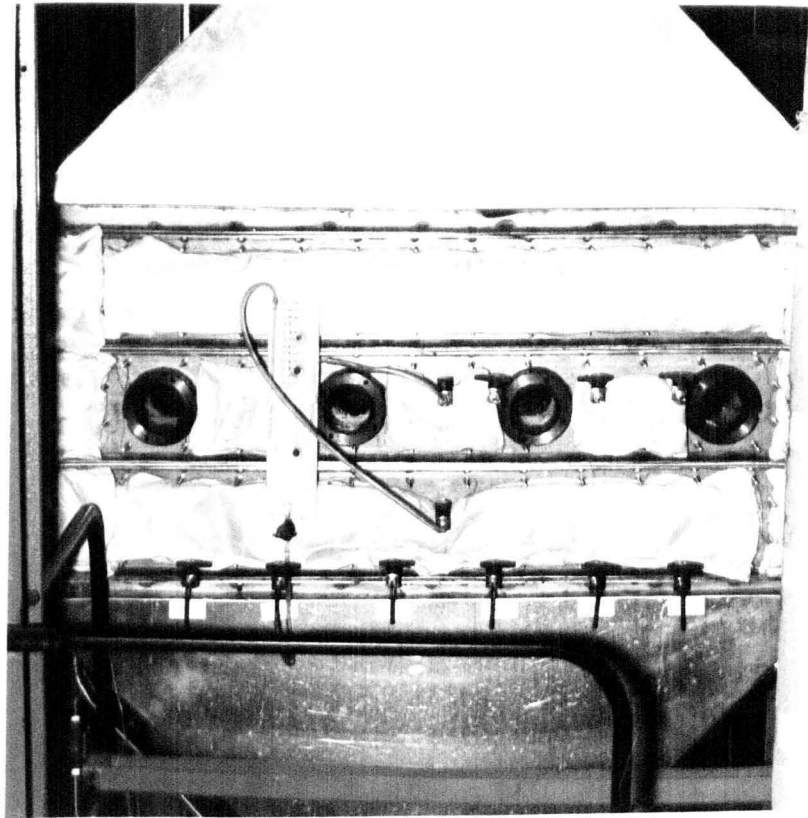
Figure 7.3   A View of the   Manometer in Operation .
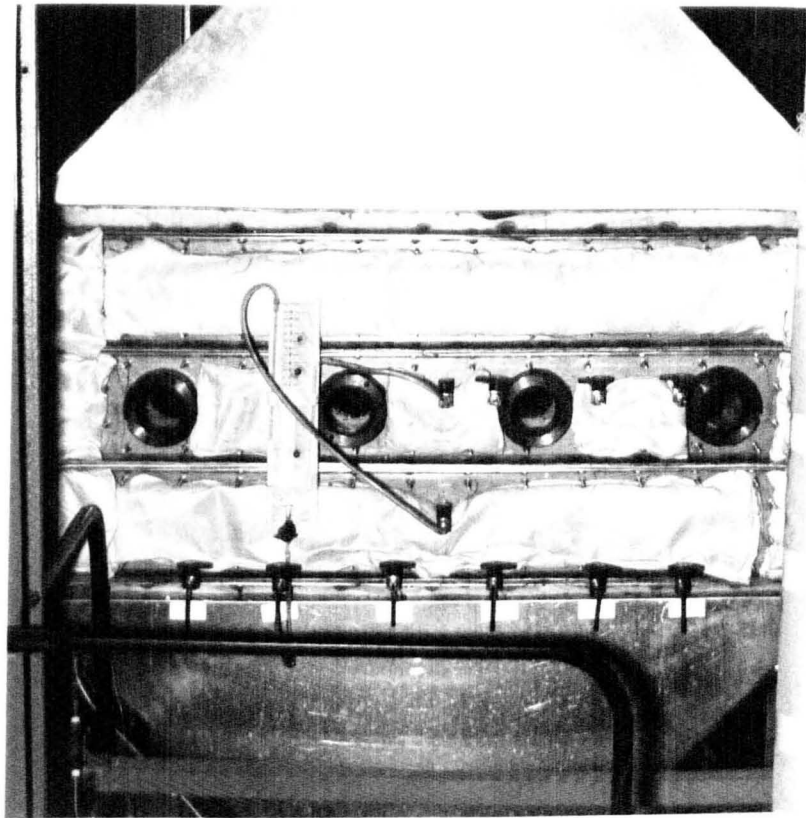
Figure 7.3   A View of the   Manometer in Operation .

$0.5 \text{ m/s } (\text{kg/m}^3)^{0.5}$, which was found to produce a nearly uniform biphase, decreasing in height from the inlet to outlet weir.

All the samples were analysed by chromatography, as described in appendix D, with an average error of 0.003% in mole fraction. The measurement of the froth height, pressure drop and liquid hold-up were also subject to the usual measurement errors.

7.3 Design of the Sieve Trays

All the trays employed had a free area of eight per cent. The 1 mm hole size tray was provided by B.O.C./Cryoplant Ltd., London. The 1.8, 3.2 and 6.4 mm trays were made in the Department workshop by drilling. A comparison of these trays is shown in the Figure 7.4.

A correlation between the percentage free area and the ratio hole pitch/hole diameter for equilateral triangular pitch was provided by Backhurst and Harker (1973).

$$\text{For 8\% Free Area, } \frac{\text{Hole Pitch}}{\text{Hole Diameter}} = 3.4$$

The calculated values of the hole pitch and numbers holes on each tray are tabulated in the table 7.2.

Table 7.2 Hole Pitch and the Number of the Holes on Each Tray

Hole Size mm	Hole Pitch mm	Number of Holes
1.8	6.1	2586
3.2	11.0	818
6.4	21.0	208
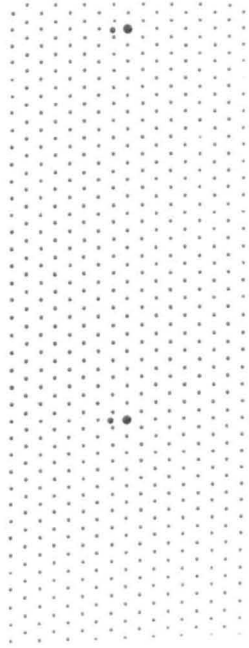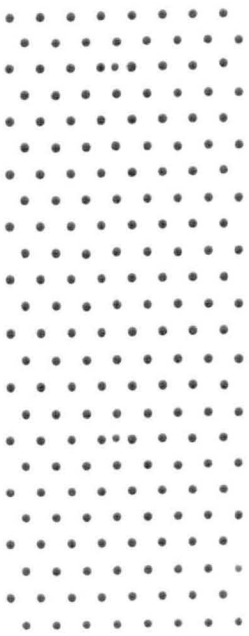
Figure 7.4   Comparison of Different Sieve Trays.
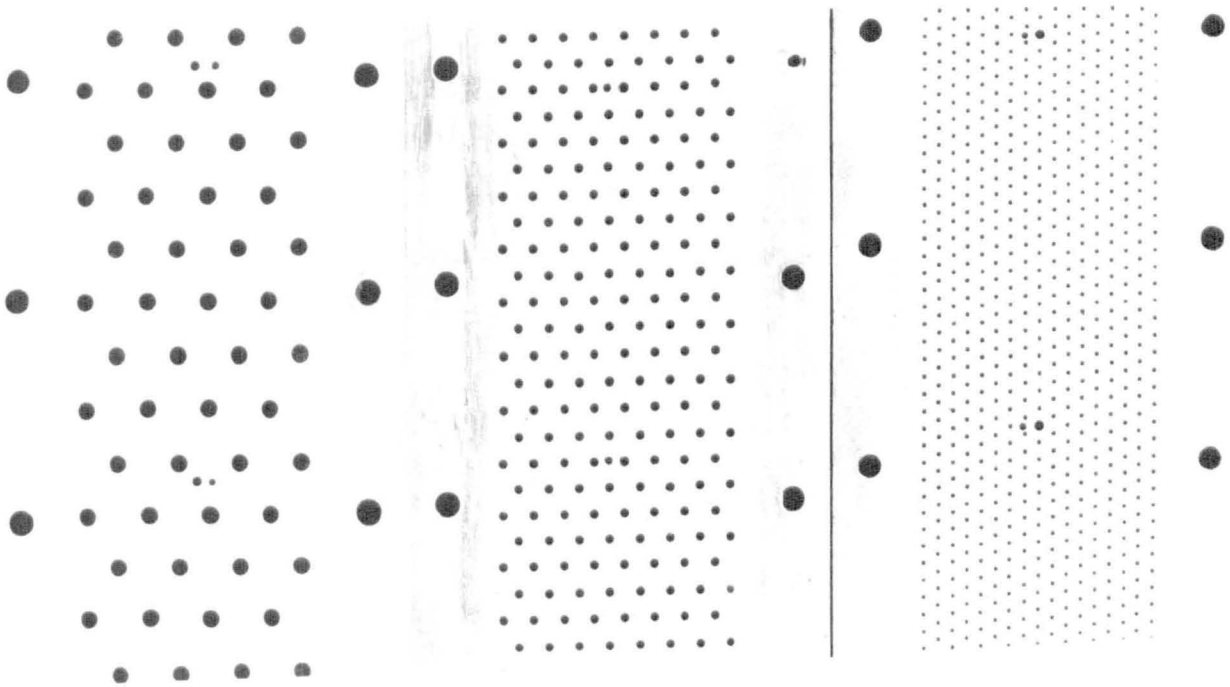
Figure 7.4 Comparison of Different Sieve Trays.

7.4 Determination of the Flow Regimes

Hofhuis and Zuiderweg (1979) have defined four flow regimes;

the spray regime : dominant in vaccuum distillation

mixed froth regime : dominant in atmospheric distillation
  (or mixed flow)

emulsified flow regime : dominant for high liquid/vapour ratios

free bubbling : dominant for operation close to weeping point.

They proposed the following relationship to identify these regimes:-

$$\Psi = \frac{q/b_o}{V_s} \left(\frac{\rho_L - \rho_v}{\rho_v} \right)^{\frac{1}{2}} \qquad 7.1$$

Where Ψ , is the flow ratio parameter, q, the liquid volumetric flowrate, and b^o the length of the outlet weir. Note that the mixed froth regime is a transition state between the spray regime, free bubbling and the emulsified regime. The flow ratio parameter representing this regime is:-

$$0.2 > \Psi > 0.1$$

Hofhuis and Zuiderweg (1979) concluded that most trays operate in the mixed flow regime. The application of the equation 7.1 to the work carried out here resulted in a flow ratio parameter of about 0.12 which is in agreement with their mixed flow conditions. Observation of the biphase further supported that the operation is in the mixed flow condition, with the sprays, froth and emulsified liquid coexistence.

7.5 Theoretical Model

A number of models have been proposed in order to represent the behaviour of the biphase on an operating tray to establish the relationship

between point and tray efficiencies. The concept of eddy diffusion has been used in this study to model the observed profiles of each component across the tray, and hence infer component point efficiencies. This model has been developed and used previously in an analysis of low temperature air distillation column by Biddulph (1975). In addition it has been applied in a study of an industrial distillation column (Biddulph (1977); Biddulph and Ashton (1977)), and was recently used in binary and multicomponent studies. (Biddulph and Dribika (1986); Dribika and Biddulph (1986)). Briefly a mass and enthalpy balance is carried out over a slice through the biphase on the tray (Figure 7.5). The eddy diffusion model is used to introduce back mixing in the liquid phase and a simple partial average model is used to account for the relatively less important influence of mixing in the vapour phase, (Diener, 1967). Liquid mixing was considered to be complete in the vertical direction. The resulting differential equations are solved numerically using a predictor/corrector method, stepping across the tray from the outlet weir to the inlet weir against the direction of the liquid flow. This is a stable iterative method and provides predicted component composition profiles of vapour and liquid phases across the tray for given values of component point efficiencies. The solution uses 50 steps across the tray making the solution stable up to values of Peclet number greater than 60. The three basic equations used were as follows:-

$$Z_i = dx_i/dw \qquad\qquad 7.2$$

$$\frac{1}{P_e}\frac{dZ_i}{dw} = Z_i - \frac{1}{L'}\frac{dL'}{dw}(y_{n',i} - x_i) - V'_{n-1}Z_L(y_{n,i} - y_{n-1,i}) \qquad 7.3$$

$$\frac{dL'}{dw} = (\frac{LdH_{L,n}}{dw} + V'_{n-1} Z_L MO - L' \sum_{i=1}^{0} H_{Ln,i} Z_i)/ (H_{Vn} - H_{Ln}) -$$

7.4

$$\sum_{i=1}^{0} H_{L\,n,i} (y_{n,i} - x_i)$$

where

$$MO = H_{Vni} - \sum_{i=1}^{0} H_{L\,n,i} (y_{n,i} - y_{n-1,i}) - H_{V,n-1}$$ 7.5

The model uses equilibrium (K)-values, and these were available from the

equilibrium data, Vapour and liquid enthalpies were available from

standard steam tables for water and from the heat of vapourisation data

for the alcohols. The procedure for the calculation of the heats of

vaporisation and hence the deduction of the liquid and vapour enthalpies

for the alcohols, together with enthalpy data on water, are given in

appendix C. A peclet no of about 39 represented the extent of liquid

mixing on the tray, as discussed in section 6.7.

7.6   Results

The measured experimental composition and temperature profiles are

presented in Figures 7.6 and 7.7 for operation in the mixed flow regime.

Observation of the biphase behaviour on the tray indicated steady operation,

with negligible entrainment and weeping.

These composition profiles were matched against the profiles predicted

by the model across the middle tray. A series of trials inferring component

point efficiencies was carried out. The trials involved computing the
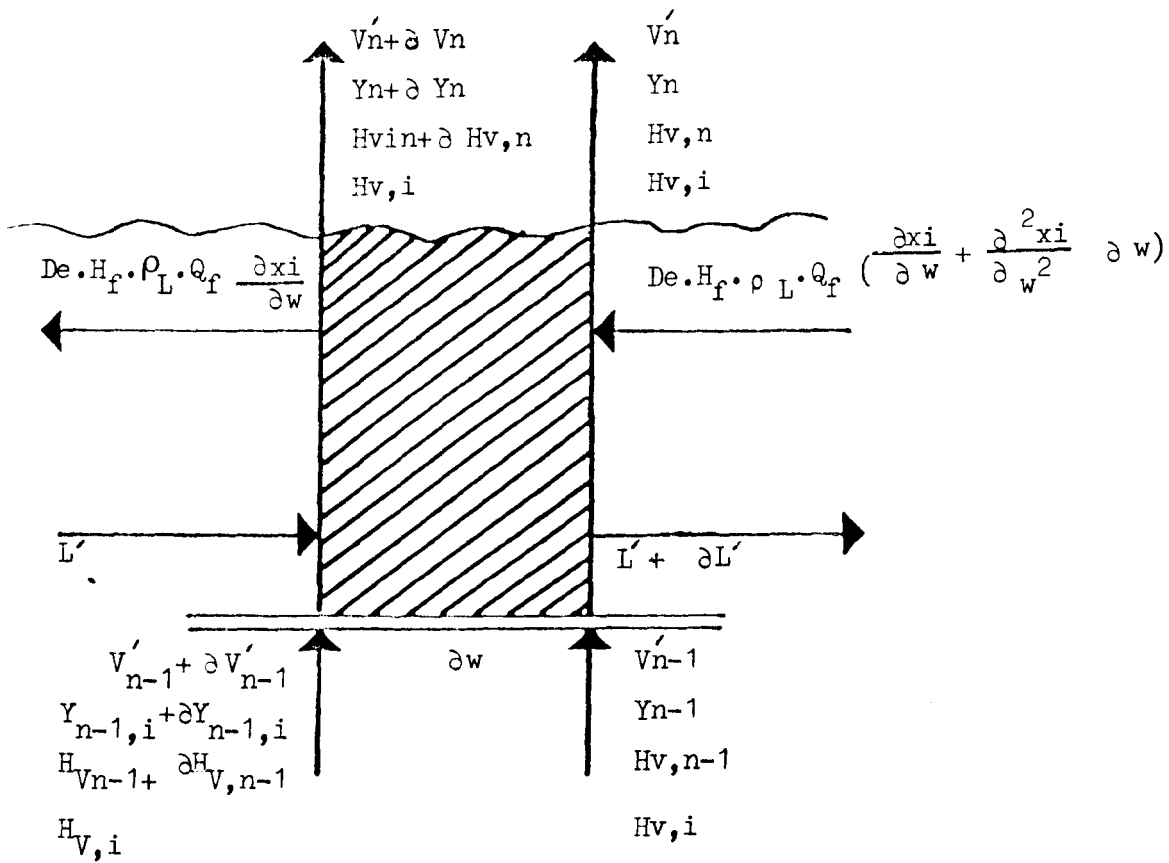
Figure 7.5   Model for Liquid Mixing Equations

vapour composition in equilibrium with the composition of the reboiler mixture, to predict the liquid composition leaving the column at total reflux. The next step involved predicting the liquid composition leaving the test tray by adjusting the bottom tray point efficiency. Finally the composition profile across the test tray was predicted by a series of trials inferring point efficiencies until a good match with the experimental component liquid composition profiles was achieved. The final liquid component composition profiles, point efficiencies and tray efficiencies were then obtained. The comparison between the experimental points and model lines were mostly quite good (Figure 7.6). At very low methanol compositions these lines do not match well with our inlet conditions. This may be due to the known high dependency of point efficiency on composition in the lower methanol range, and it is possible that different point efficiencies are operating at different points on the tray. Measurements of the point efficiency for this system, using a modified Oldershaw column avoiding surface tension wall effects, yielded lower point efficiencies in these composition ranges (Figure 4.4). The experimental liquid temperature profiles across the tray are shown in Figure 7.7, these measured temperatures being then compared with the bubble point temperatures (Figure 7.8). The bubble point temperatures were calculated taking into account the non-idealities in the phases, (Appendix B). Using the above calculations the tray efficiencies were also evaluated using the measured inlet and outlet conditions.

The effect of the outlet weir height on tray/point efficiencies using 1.8 mm tray are presented in Figures 7.9 and 7.10. The mean liquid composition was calculated using the composition profiles by:

$$\bar{x}_i = \int_0^1 x_{wi} \, dw \qquad\qquad 7.6$$

where w is the relative position on the tray.

In reducing the weir height from 12.7 to 2 mm, lower efficiencies were obtained. The observed froth height (Figure 7.11) also exhibited the same trend. Figure 7.12 shows the effect of hole size on froth height.

The study of the effect of hole size on point and tray efficiencies (Figures 7.13 and 7.14) demonstrated the tendency of the smaller holes to exhibit higher efficiencies.

The behaviour of the biphase on the tray was observed closely. The 3.2 and 6.4 mm perforated trays produced much more spray, and larger bubbles, whereas the 1 and 1.8 mm hole size trays tended to atomise fewer and smaller droplets. The biphase on the 1 mm tray was highly mobile with some back and forth motion lengthwise.

Porter and Jenkins (1979), in their comprehensive review of flow regimes, suggested that in decreasing the perforation size the capacity of the tray increases as a result of partial transition from spray to mixed flow conditions. The observations of the biphase and increase in measured clear liquid head (see later) as a result of decrease in the perforation size may support the above proposal.

The results of the tray pressure drop and liquid head measurements for different outlet weir heights are shown on figures 7.15 and 7.16 respectively. The tray pressure drop and liquid head appear to be largely unaffected by the decrease in the weir height from 25.4 to 12.6 mm, analagous to the froth height and efficiency measurements. However, the 2mm outlet weir height demonstrated lower pressure drops and liquid head. These measurements were compared with the recent prediction method of Bennett et. al. (1983) based on experimental work with low weirs and small perforation size trays. Bennett proposed the following relationship based on all the available data:

$$h_T = h_L + h_D + h_\delta \qquad\qquad 7.7$$

$$h_L = \phi_e \left[h_w + ac \left(\frac{Q_L}{\phi_e} \right)^{\frac{2}{3}} \right] \qquad 7.8$$

$$ac = 0.0327 + 0.0286 \ EXP \ (- \ 137.8 \ h_w) \qquad 7.9$$

$$\phi_e = EXP \ (- \ 12.55 \ (K_s)^{0.91}) \qquad 7.10$$

$$h_\delta = \frac{6 \ \delta}{g \ \rho_L \ D_{BMAX}} \qquad 7.11$$

$$D_{BMAX} = 1.27 \left(\frac{D_H \ \delta}{g \ (\rho_L - \rho_V)} \right)^{\frac{1}{3}} \qquad 7.12$$

$$\text{where } h_D = \frac{0.499 \ \rho_V \ V_H^2}{C_V^2 \ \rho_L \ g} \qquad 7.13$$

where h_T is the total tray pressure drop, h_L height of the liquid inventory on the tray, h_D dry pressure drop and h_δ pressure drop due to the surface tension. C_V was obtained from the correlation of Prince et. al. (1960). The mixture surface tension at the boiling point was measured by a tensiometer (Chapter 3). Our experimental pressure drops, using 2 and 12.6 mm outlet weir heights are in a close agreement with the Bennett correlation, but the correlations appear to overpredict the pressure drop at 25.4 mm outlet weir heights. This is partly because of the extra emphasis given to the liquid head element in their correlation (see Figure 7.16).

The effects of the hole size on pressure drop and liquid head on

the tray are presented in Figures 7.17 and 7.18. Although there is some scatter in the measured points, there is evidently a slight increase in pressure drop with a decrease in perforation size. The liquid head follows the same trend. These measurements are in a close agreement with the correlation presented by Bennett (1983). Note that there is a slight increase in the measured pressure drop here at low methanol concentrations due to an increase in vapour velocity to maintain stable biphase conditions on the tray. The increase in pressure drop as a result of decrease in hole size is due to surface tension effects. The dry pressure drop is unchanged since a constant tray free area was used.

Further particulars of the computed results are tabulated in the appendix A , Tables A.3.1 to A.3.11.

7.7 Discussion

a) The Effect of the Outlet Weir Height

There appears to be a decrease in the tray efficiencies at 2 mm outlet weir conditions compared with the higher weir. This decrease in tray efficiency at virtually no outlet weir is due to the decrease in liquid hold up and consequently the froth height on the tray (see Figures 7.18 and 7.11). The decrease in tray/point efficiency is probably due to a reduction in the interfacial area. This sudden drop in tray efficiency from an outlet weir condition to no outlet weir conditions has also been reported by Finch and Van Winkle (1964) and Brown and England (1961).

b) Effect of the Hole Size

Umholtz (1957), Hellums et. al. (1958), Finch and Van Winkle (1964), Pruden et. al. (1974), Fryback and Hufnagel (1960) and Burgess and Calderbank (1975) reported no significant effect of hole size on mass

transfer efficiency. However, the smallest hole size used was 1.6 mm as compared with 1 mm used here. There have been reports that smaller holes may significantly increase the tray efficiency, (Zenz, 1972). In view of the mass transfer characteristics associated with smaller holes there have been suggestions that they provide higher efficiencies due to increased mixing and mass transfer interfacial area (Patton and Pritchard (1960); Lockett et. al. (1979)). Fell and Pinczewski (1977) suggested that small holes should be used for surface tension positive systems to achieve maximum tray efficiency.

The measurements reported here reveal that there is a fairly small increase in tray/point efficiencies with decreasing hole size (see Figures 7.13 and 7.14). The increase is not as great as might be expected, considering the apparent increase in interfacial area. These differences in tray/point efficiency are minimised at high methanol concentrations, which may be due to a decrease in the surface tension of mixture (Figure 7.19). Hellums et. al. (1958) suggested that at low vapour rates the tray liquid hold up is increased, because of the capillary surface tension effects. An increase in the liquid hold up on the tray would result in higher efficiencies. The measured liquid hold-ups presented on Figure 7.18 suggest that the surface tension effects may have caused slightly higher liquid hold-ups for smaller perforated trays and consequently increased the froth heights (see Figure 7.12). From the observation of the biphase it is also evident that the 3.2 and 6.35 mm hole size trays caused more spraying, which reduces the liquid capacity on the tray. It is suggested that the increase in tray/point efficiencies with decrease in perforation size is due to:-

1. A slight increase in the tray liquid hold up and froth height.

2. An increased rate of bubble formation, which provides larger mass transfer interfacial area.

These effects may be further enhanced by the following effects:

3. Marangoni surface renewal effects at low methanol composition range, Ellis and Biddulph (1964).

4. The magnifying effect of the slope of equilibrium line at low methanol concentration. (See Figure 7.19)

The Marangoni stabilising index M, a measure of surface renewal effects stated above, is calculated from equation 4.1, Chapter 4.

It has been reported that these Marangoni surface renewal effects enhance the mass transfer, Sawistowski (1973), and they are at their highest in the lower methanol concentration range.

The perforation sizes 1, 1.8 and 3.2 mm are recommended for clean and non-corrosive services such as low-temperature distillation of air, and services where low liquid rates are expected, Smith et. al. (1981). These trays provide a large degree of flexibility and increased capacity, (Patton and Pritchard, 1960; Lemieux and Scotti, 1969 and Fell and Pinczewski, 1977). The pressure drops associated with these trays under the conditions experienced here are comparable with larger perforated tray .

c) Pressure Drop, Liquid Head

The small hole size trays used for the experiments exhibit slightly increased pressure drops compared with larger hole size trays. The increase in pressure drop with decreasing hole size is mainly due to the higher surface tension pressure drops. The measured clear liquid heads show a slight increase with decreasing hole size. An increase in outlet weir height from 2 to 12.6 mm caused a jump in pressure drop, and clear liquid head, while further increase in the outlet weir height had a negligible effect.

The Bennett et. al.(1983) pressure drop correlation predicted reasonably well the dependence on hole size at 12.6 mm outlet weir height, but it overpredicted the clear liquid head and pressure drop at an outlet weir height of 24.5 mm.
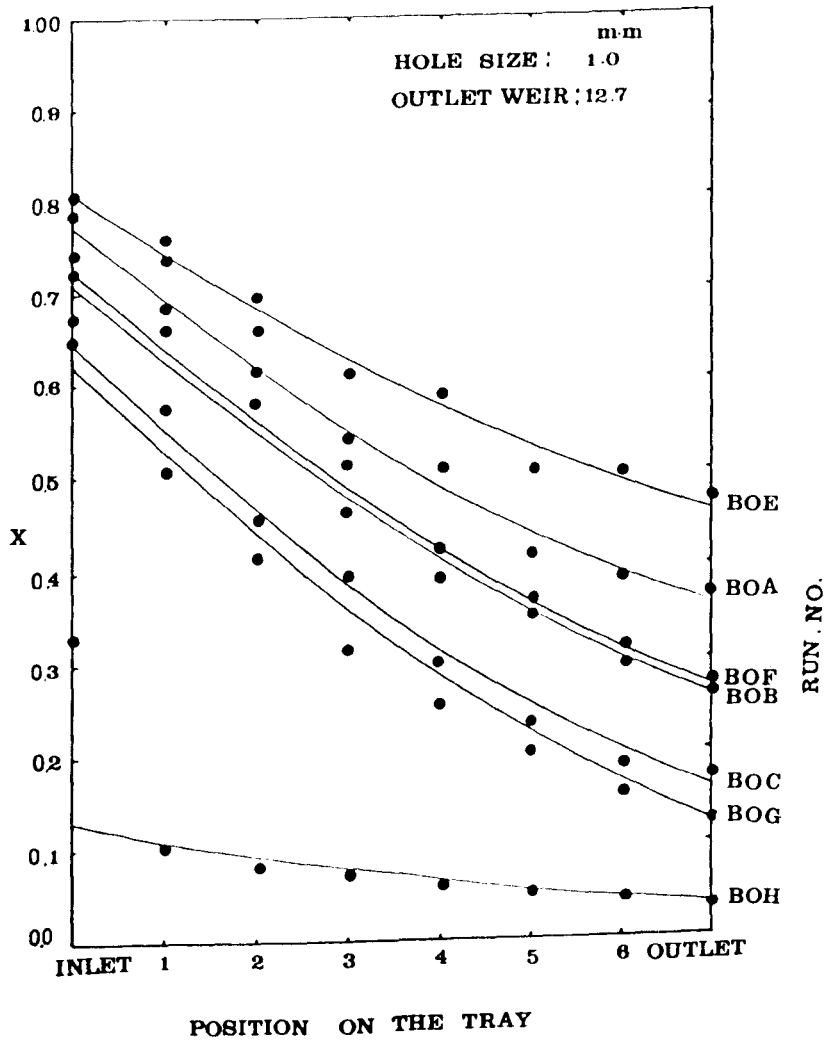
Figure 7.6   Composition profiles across the tray
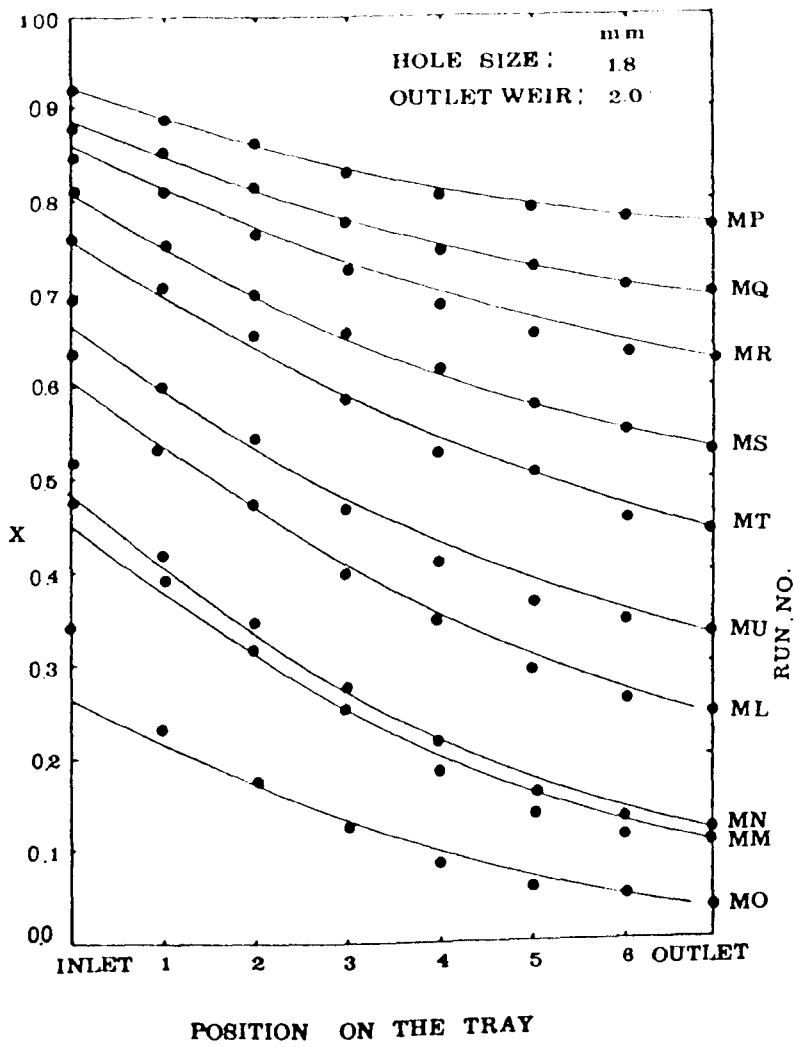
Figure 7.6
continued
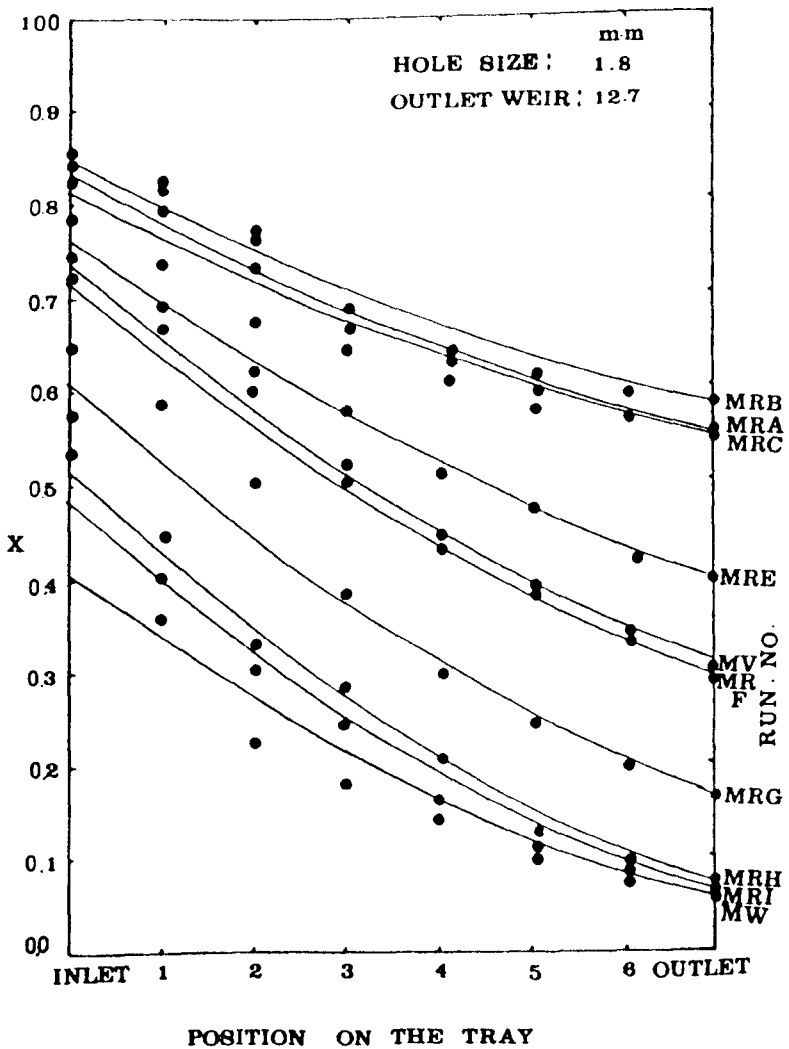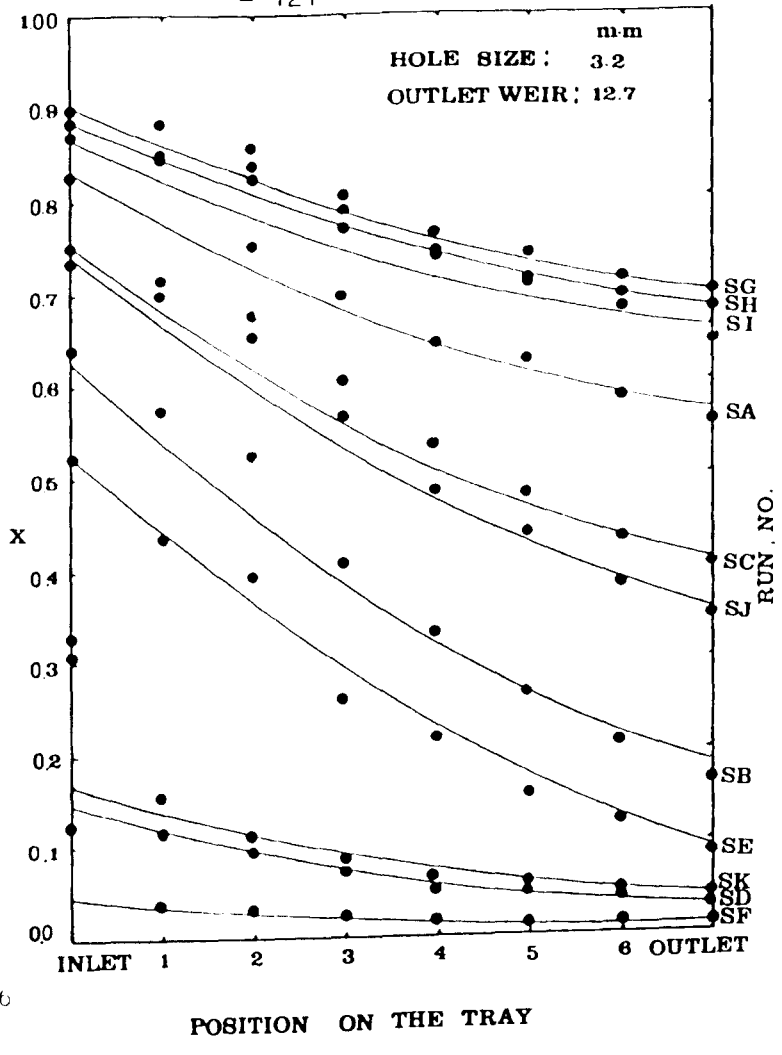
Figure 7.6
continued
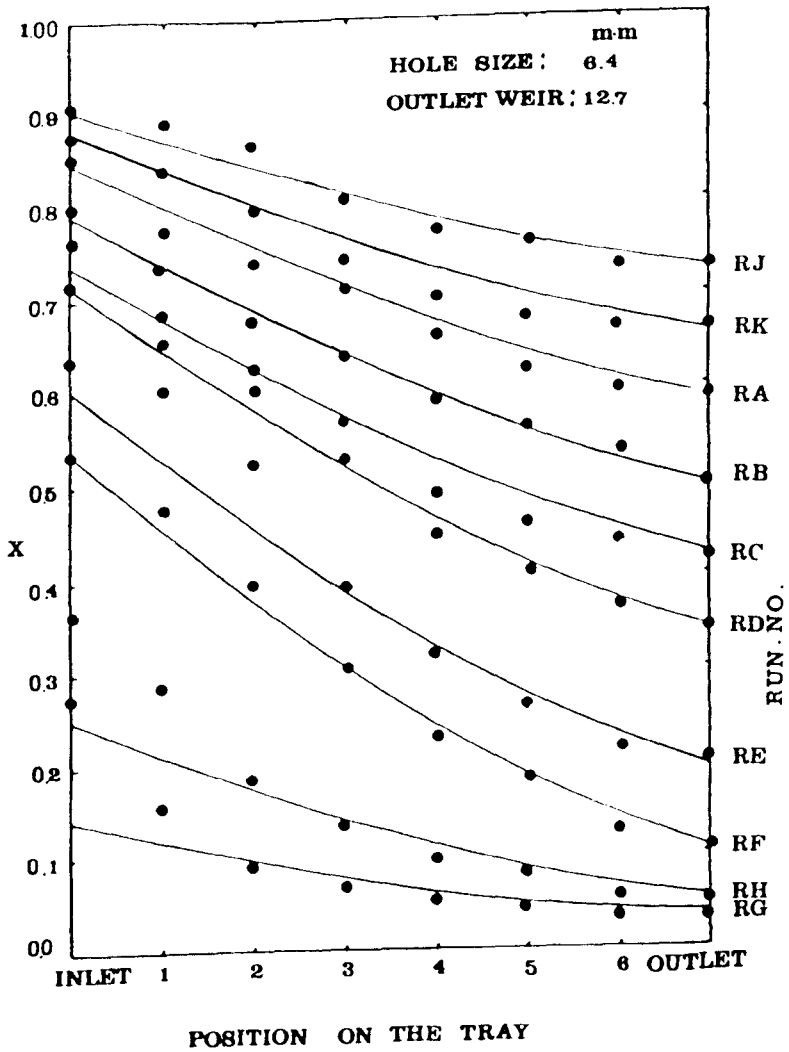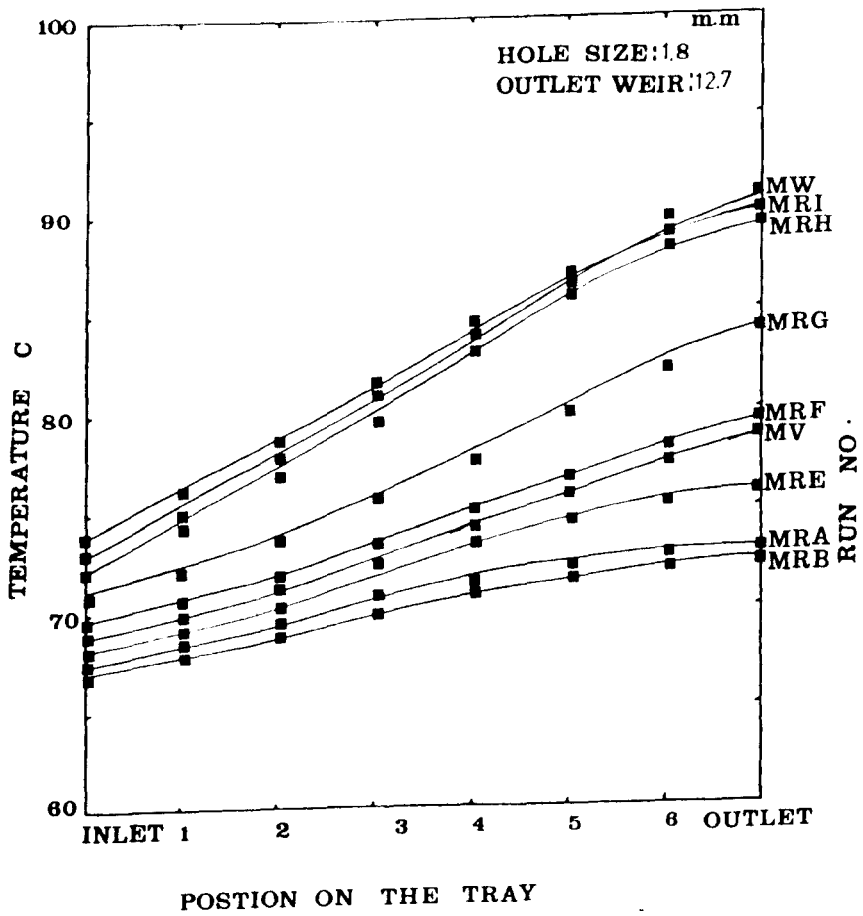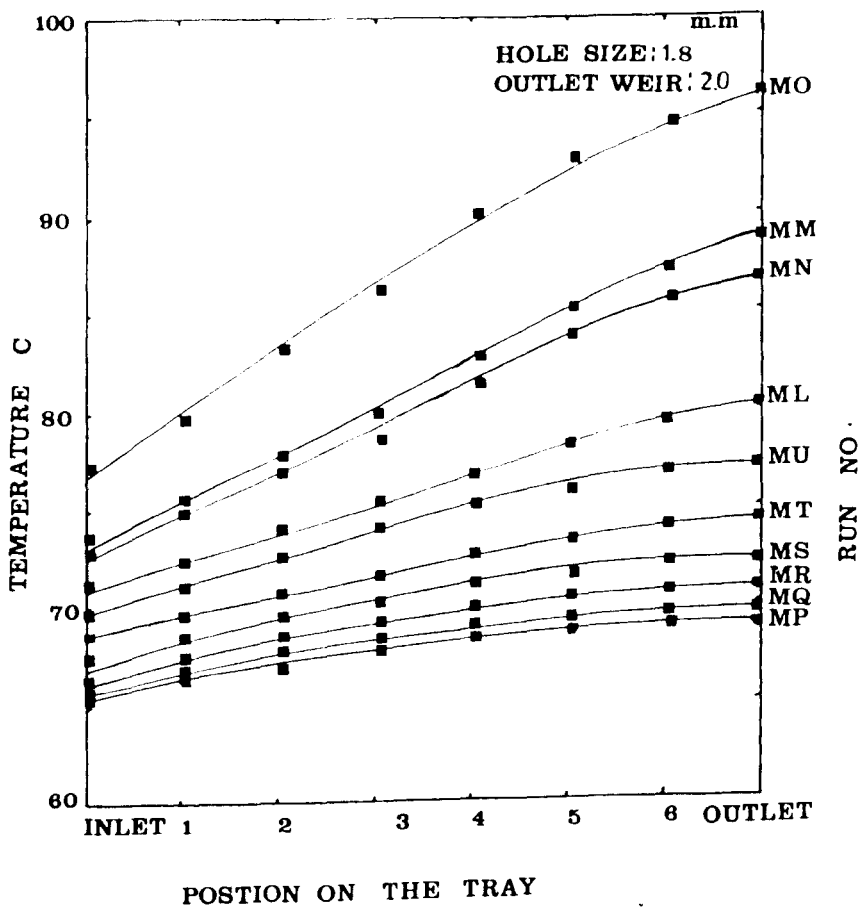
Figure 7.7 Temperature profiles across the tray
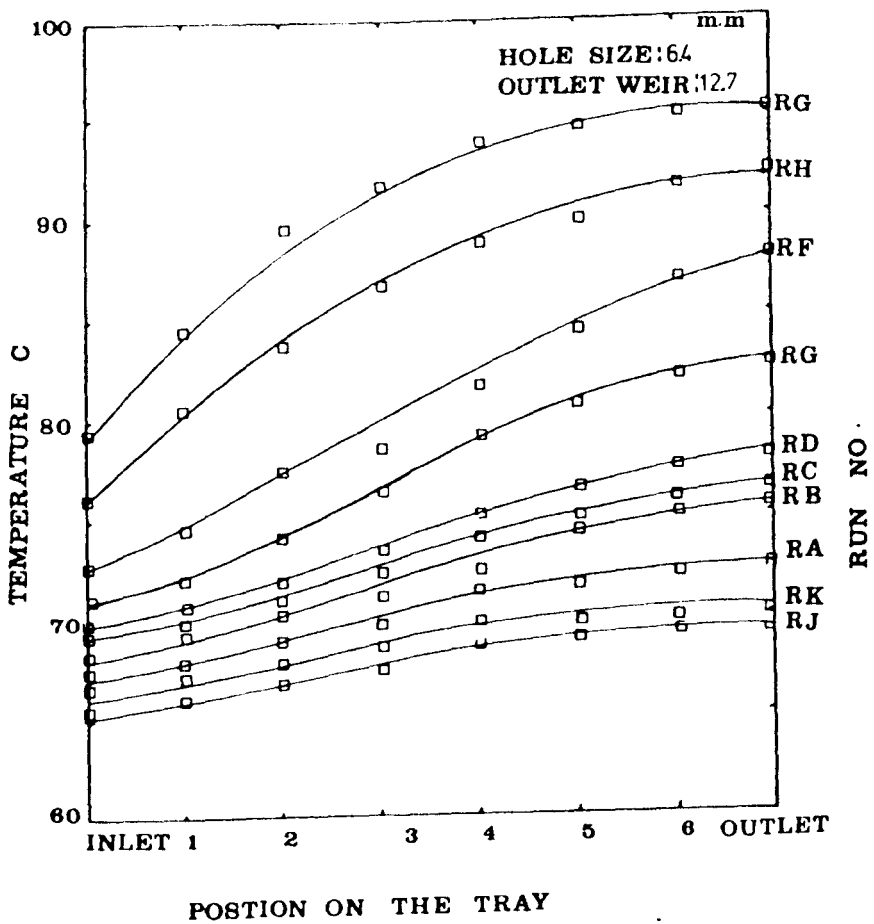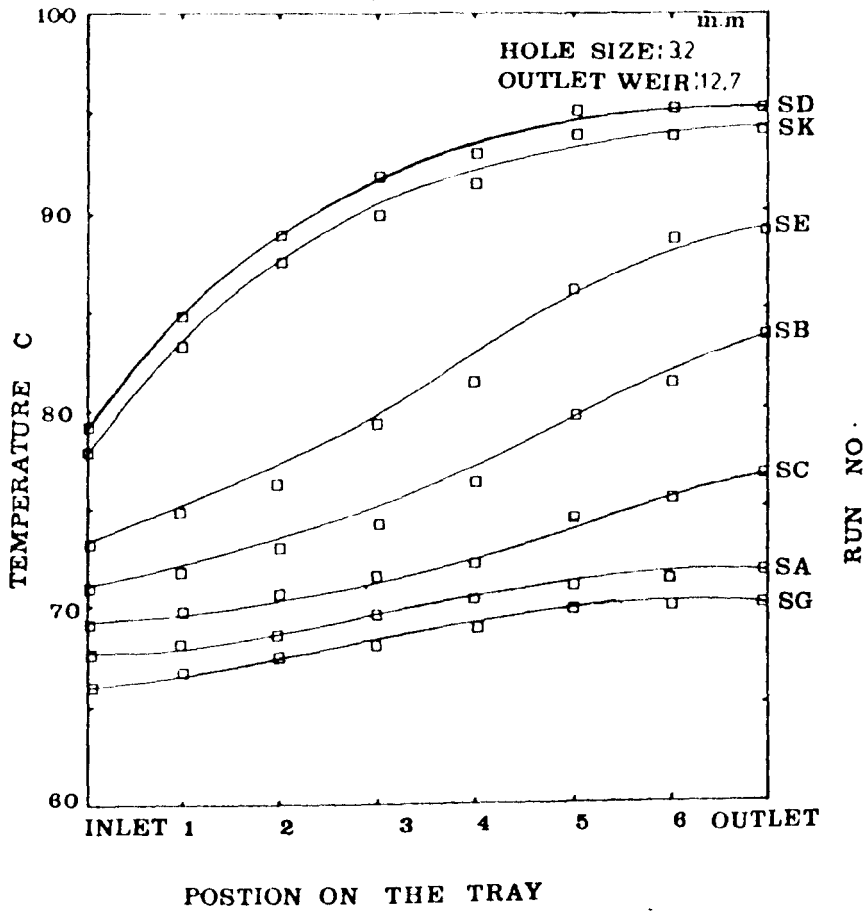
Figure 7.7   continued

- 124 -
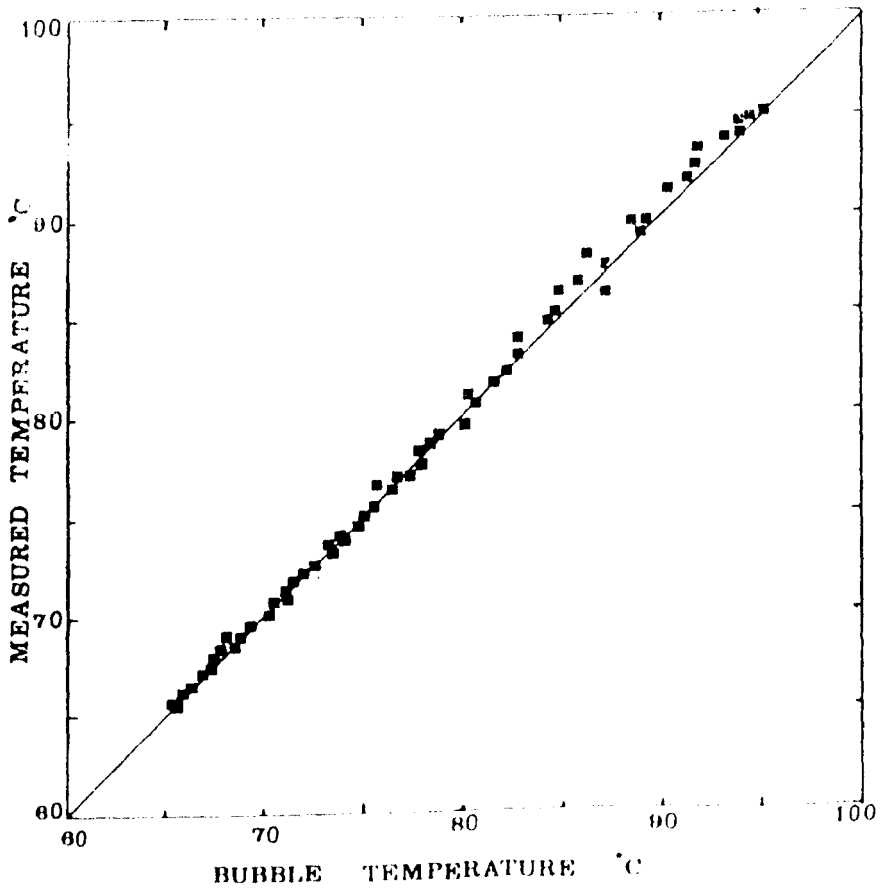
Figure 7.8 Comparison of measured and bubble temperatures
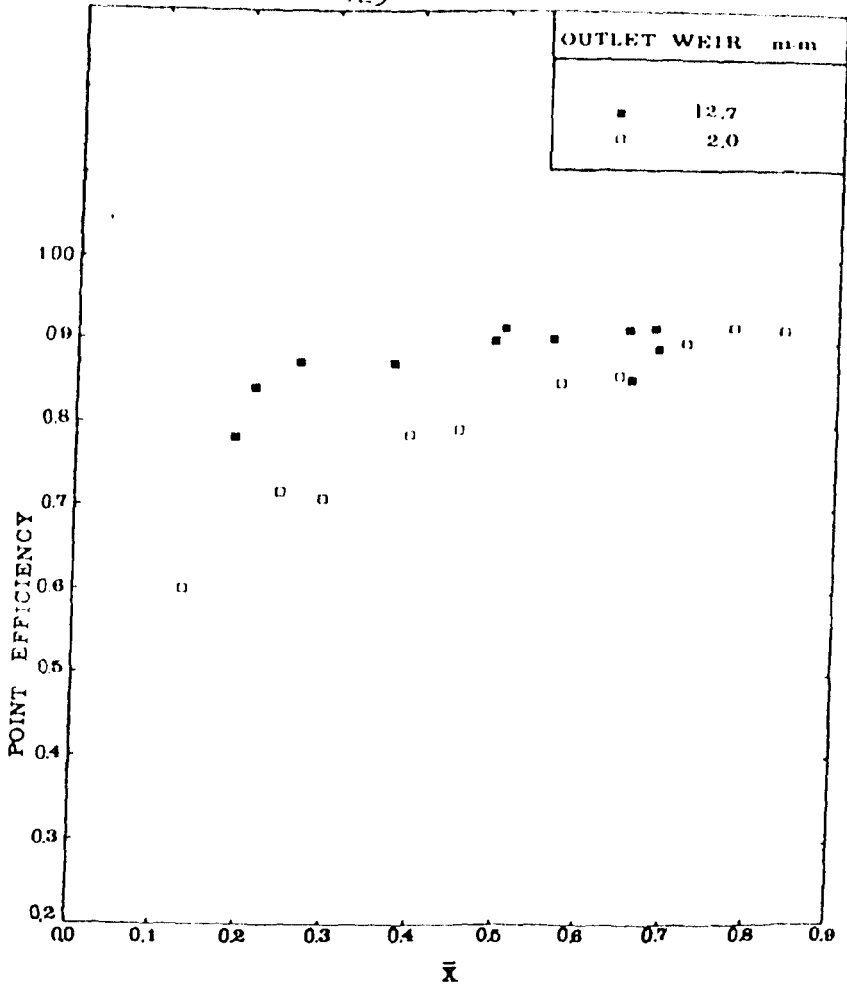
Figure 7.9 Effect of outlet weir height on point efficiencies
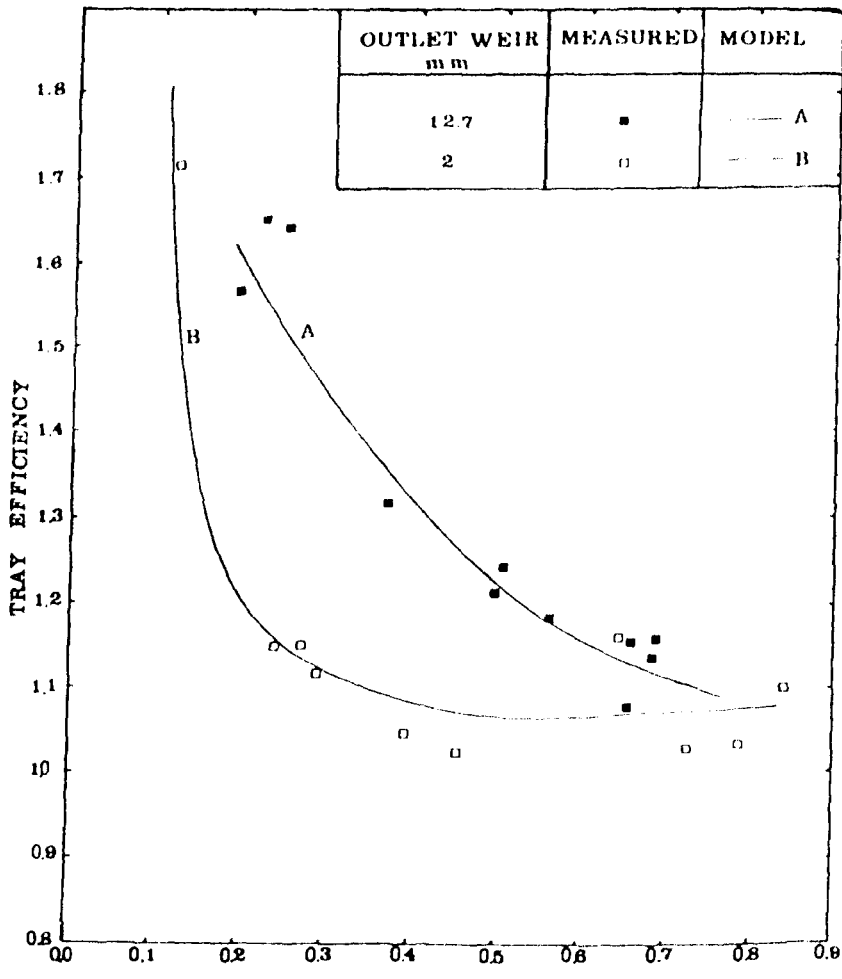
Figure 7.10 Effect of outlet weir height on tray efficiencies
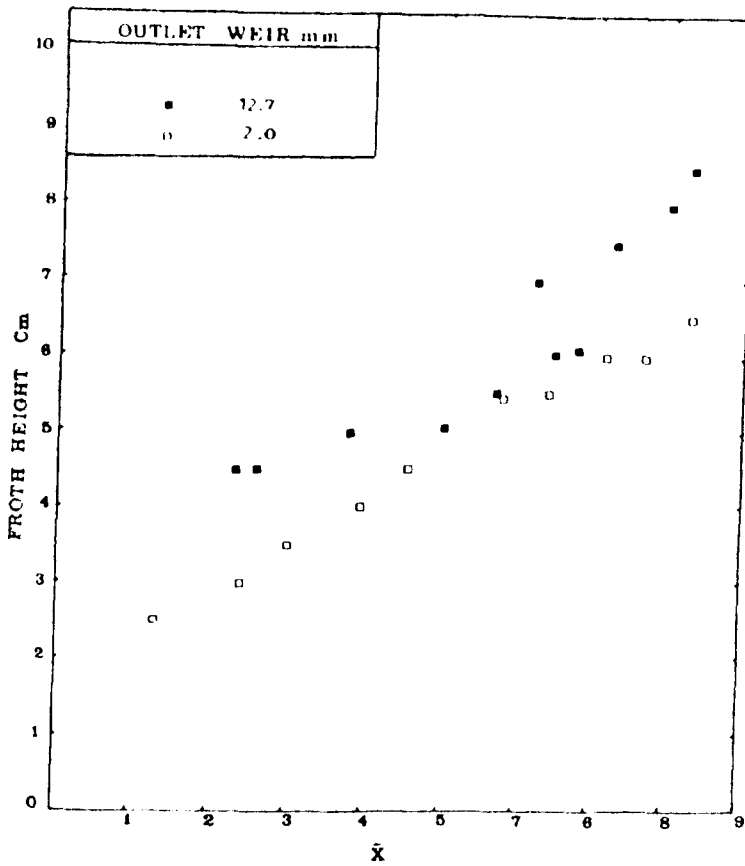
Figure 7.11 Effect of outlet weir height on observed froth height
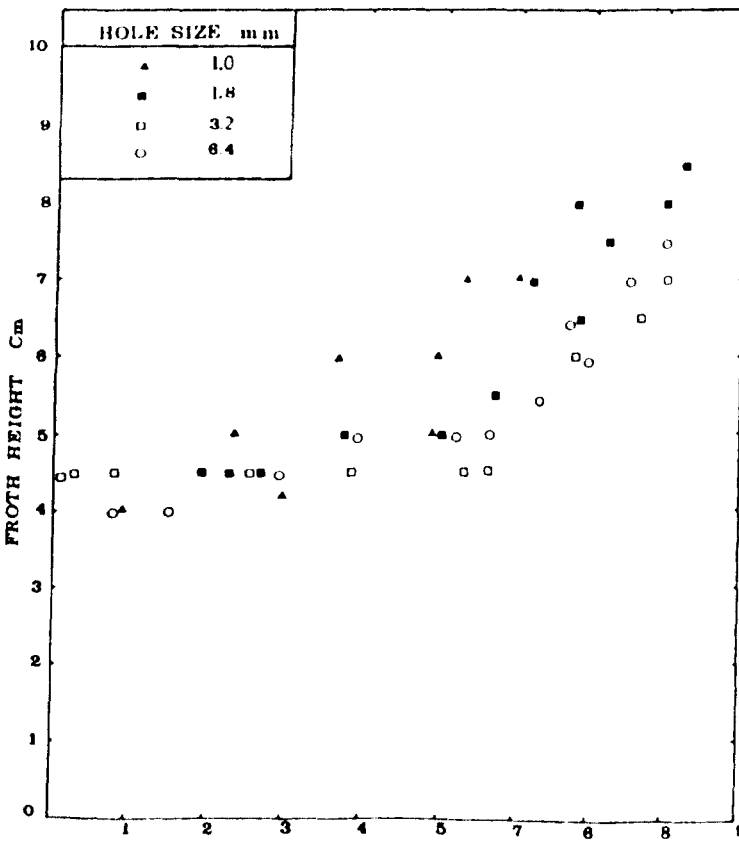
Figure 7.12 Effect of hole size on observed froth height
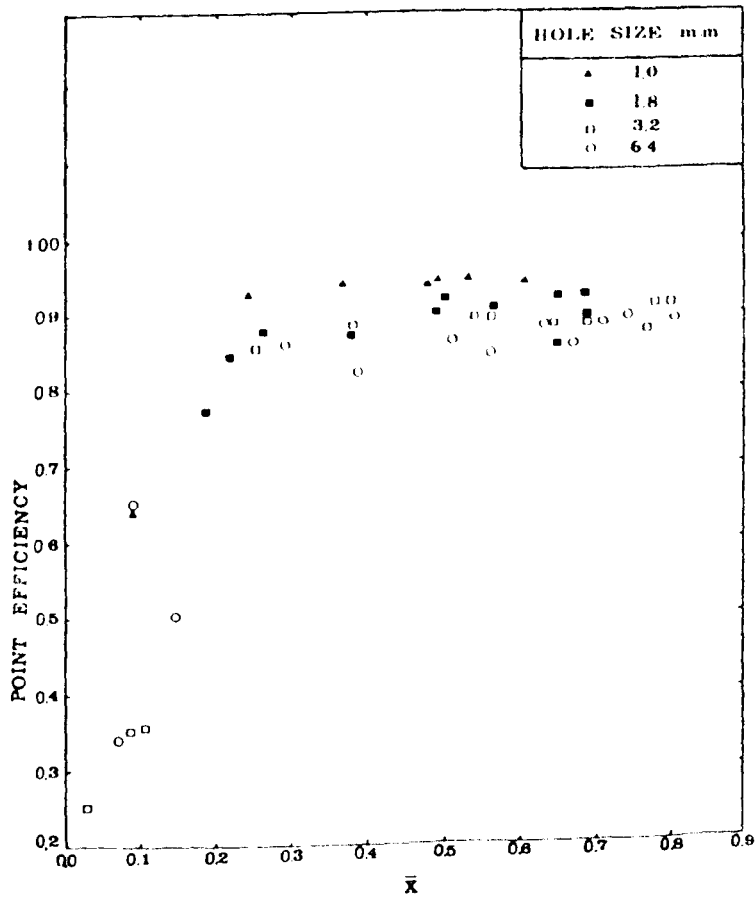
Figure 7.13 Effect of hole sise on point efficiencies
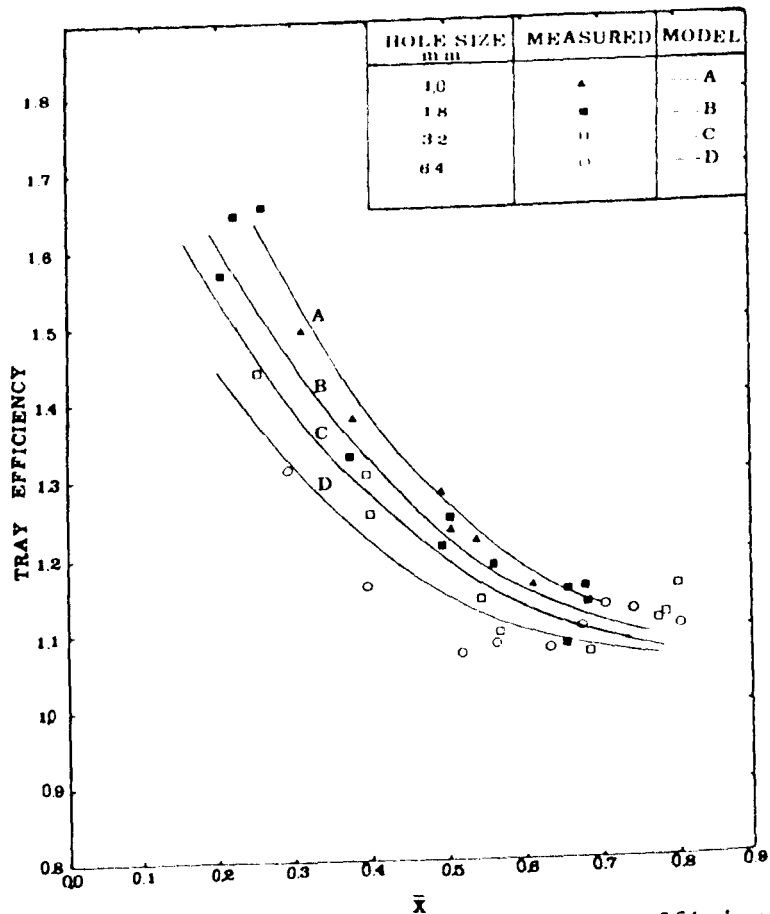
Figure 7.14 Effect of hole size on tray efficiencies
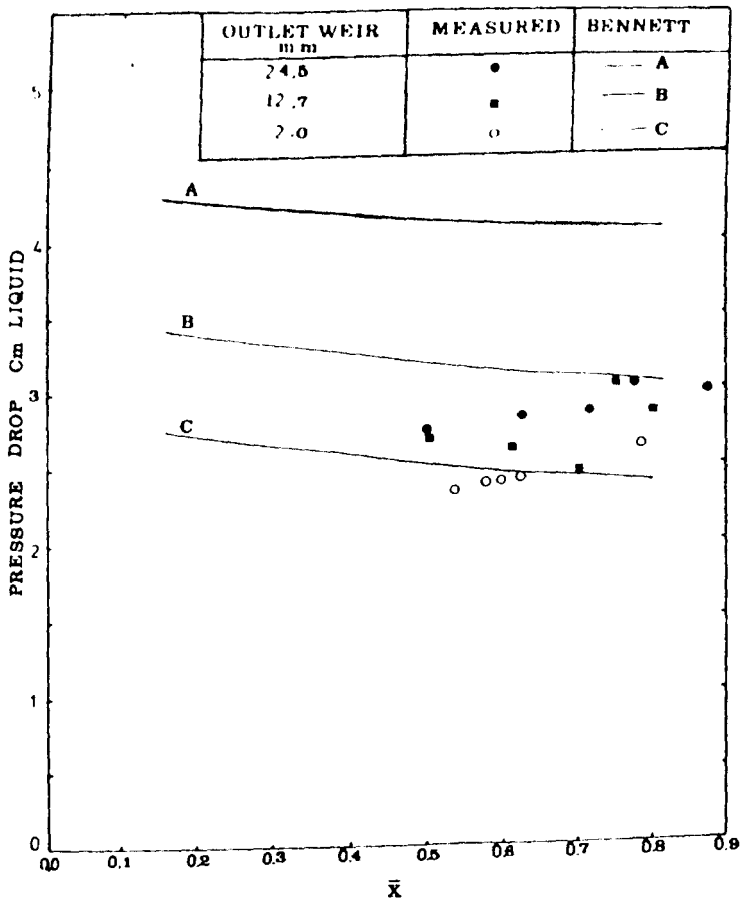
Figure 7.15 Effect of outlet weir height on tray pressure drop
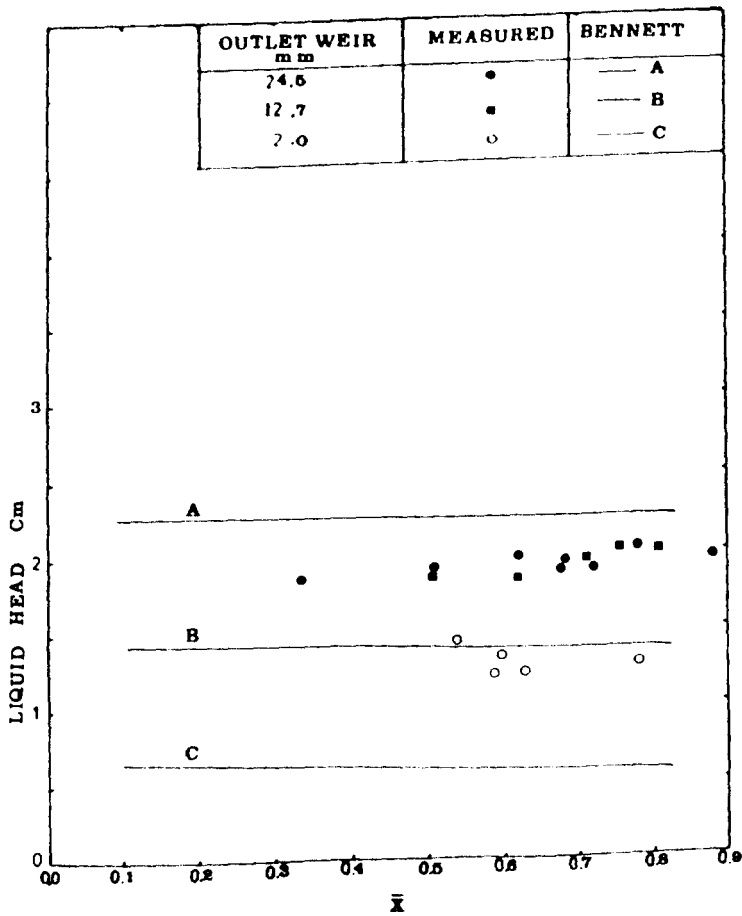
Figure 7.16 Effect of outlet weir height on tray liquid head

mm HOLE SIZE	MEASURED	BENNETT
1.0	▲	—— A
1.8	■	—— B
3.2	□	—— C
6.4	○	—·— D
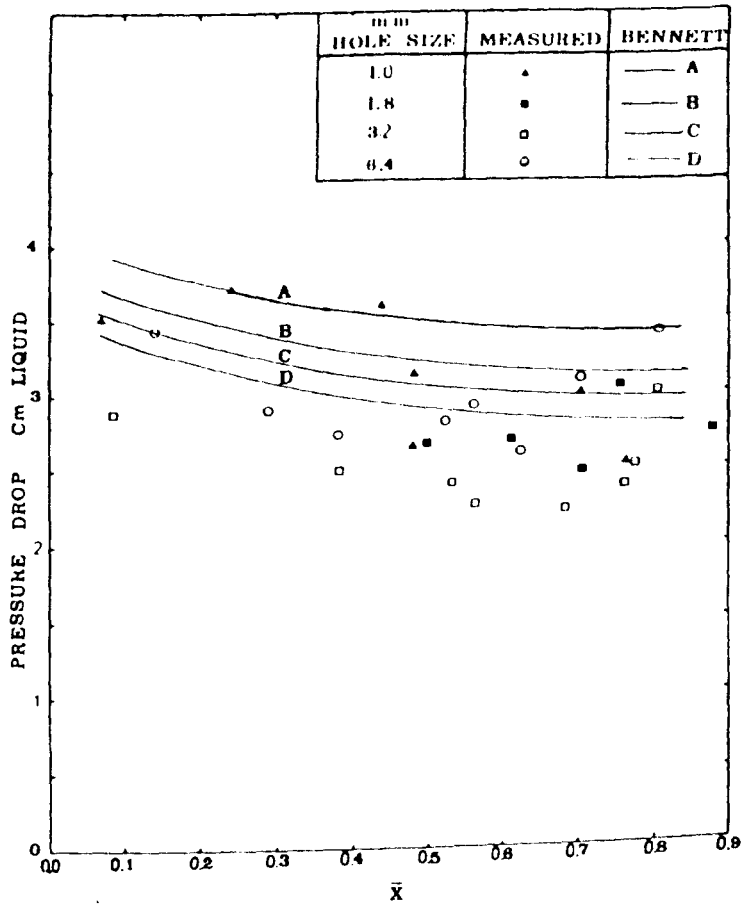
Figure 7.17   Effect of hole size on tray pressure drop

mm HOLE SIZE	MEASURED	BENNETT
1.0	▲	
1.8	■	········----
3.2	□	
6.4	○	
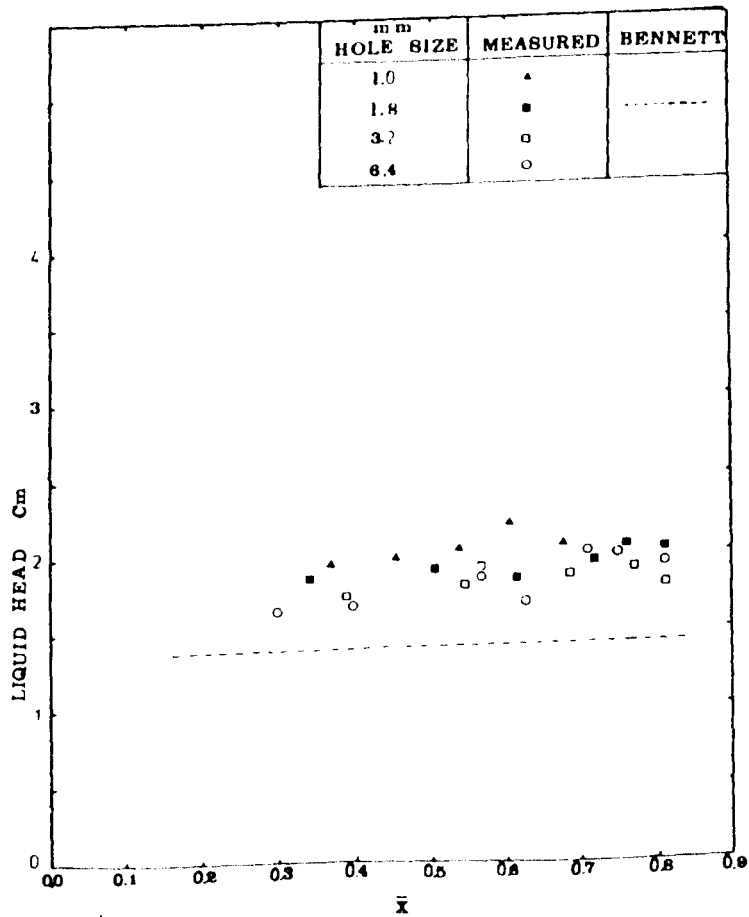
Figure 7.18 Effect of hole size on tray liquid head
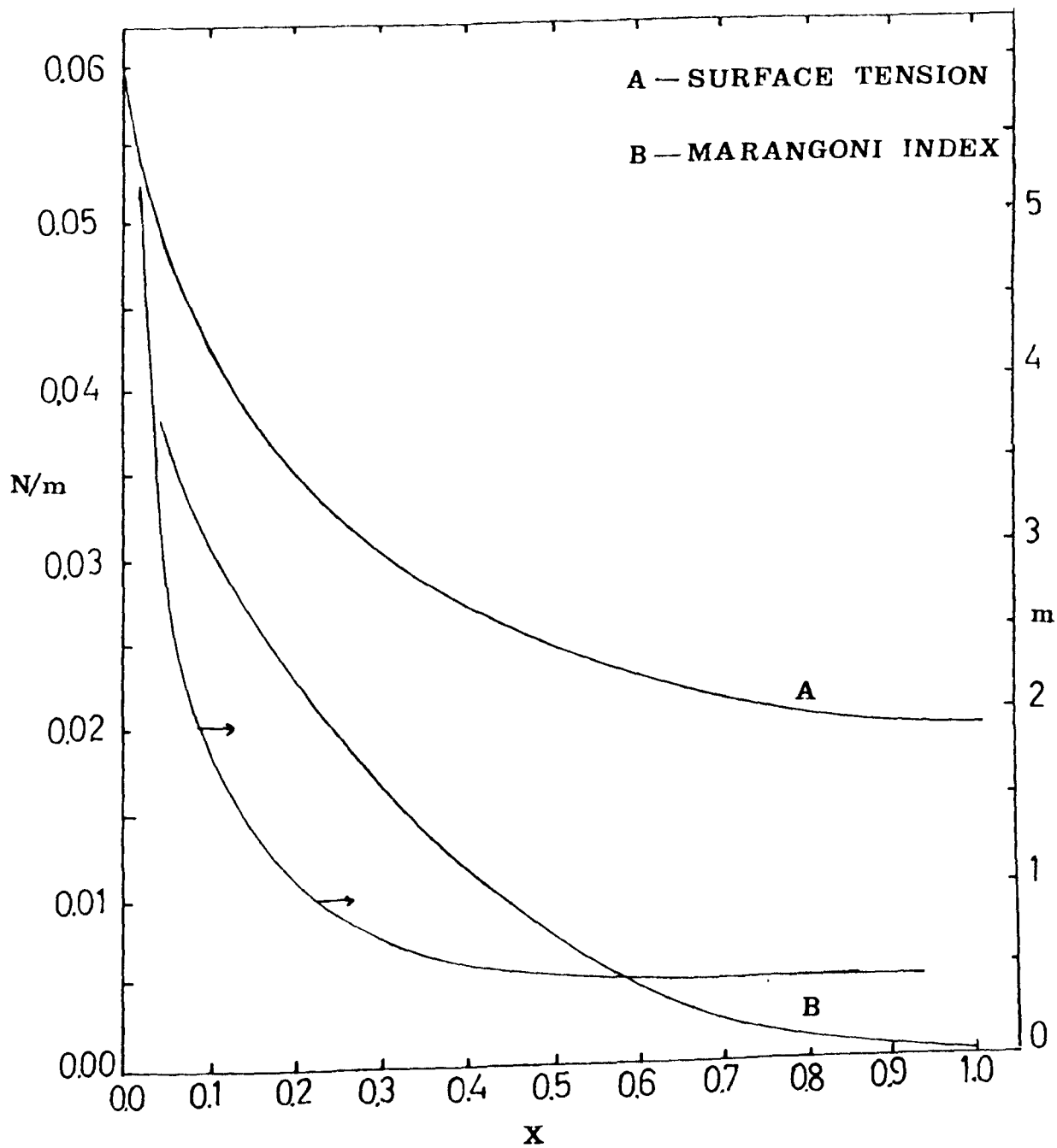
Figure 7.19 Surface tension, Marangoni Index and Slope of equilbrium
line

CHAPTER 8

SCALE-UP STUDIES

SCALE-UP STUDIES

8.1 Introduction

The development of the modified Oldershaw column (Chapter 4), providing a biphase similar to the biphase on a larger tray (see Chapters 6 and 7), was very encouraging. The point efficiencies for the systems $MeOH/H_2O$, $EtOH/H_2O$ and $n.PrOH/H_2O$ measured in this column followed the same trend as those deduced from large tray measurements. They were somewhat lower in magnitude due to the shorter contact time of the liquid and vapour in the small column. In Chapter 7, it was demonstrated that large tray with 1.8 mm perforation size and an outlet weir height of 2 mm, exactly the same as the modified column, would support a biphase almost double in height. Subsequently high point efficiencies were deduced. This observation confirmed that in order to measure point efficiencies close to those operating on a large tray, an improvement and an increase in the contact time of the gas and liquid is required, without encouraging wall effects to occur. In this chapter it is demonstrated how an increase in the outlet weir height in the modified column has improved this contact on the tray. The point efficiencies measured here are compared with those from the 1 mm perforation-size rectangular tray, reported in Chapter 7. These point efficiencies were then used directly or scaled using the Dribika and Biddulph (1986) model, and incorporated into the eddy diffusion model described in Chapter 7 simulating distillation runs on the 1 mm hole size tray as given in the same Chapter , thus deducing tray efficiencies.

8.2 Equipment

The same apparatus as described in Chapter 4 was used here. The only difference was the further modification to the modified column to accommodate outlet weir heights of 6.4 mm and 12.7 mm. Figure 8.1 shows a view of this column. The new modification was achieved by cutting the modified column in half above the tray and fitting it with a ground glass socket. The stainless steel outlet weir was then fixed by using silicon rubber near the outlet of the tray. No holes were lost from the tray.

8.3 Experimental

The experiments were carried out using the system methanol/water at a column F.Factor of about 0.4 m/s $(kg/m^3)^{0.5}$. The analysis of the samples etc., was exactly the same as described in Chapter 4.

8.4 Observation of the Biphase

On increasing the outlet weir the biphase height was increased as shown in Figure 8.2. The biphase also appeared to be holding the bubbles for a longer time prior to bursting. Satellite droplets of different sizes were produced as a result vapour jetting through the biphase or the the bubbles collapsing.

8.5 Results

As expected, there was an increase in the measured point efficiencies throughout the composition range as a result of increasing the outlet weir height from 2 mm to 6.4 mm (see Figure 8.3). This increase was

Figure 8.1   A View of the Improved Modified Oldershaw Column.
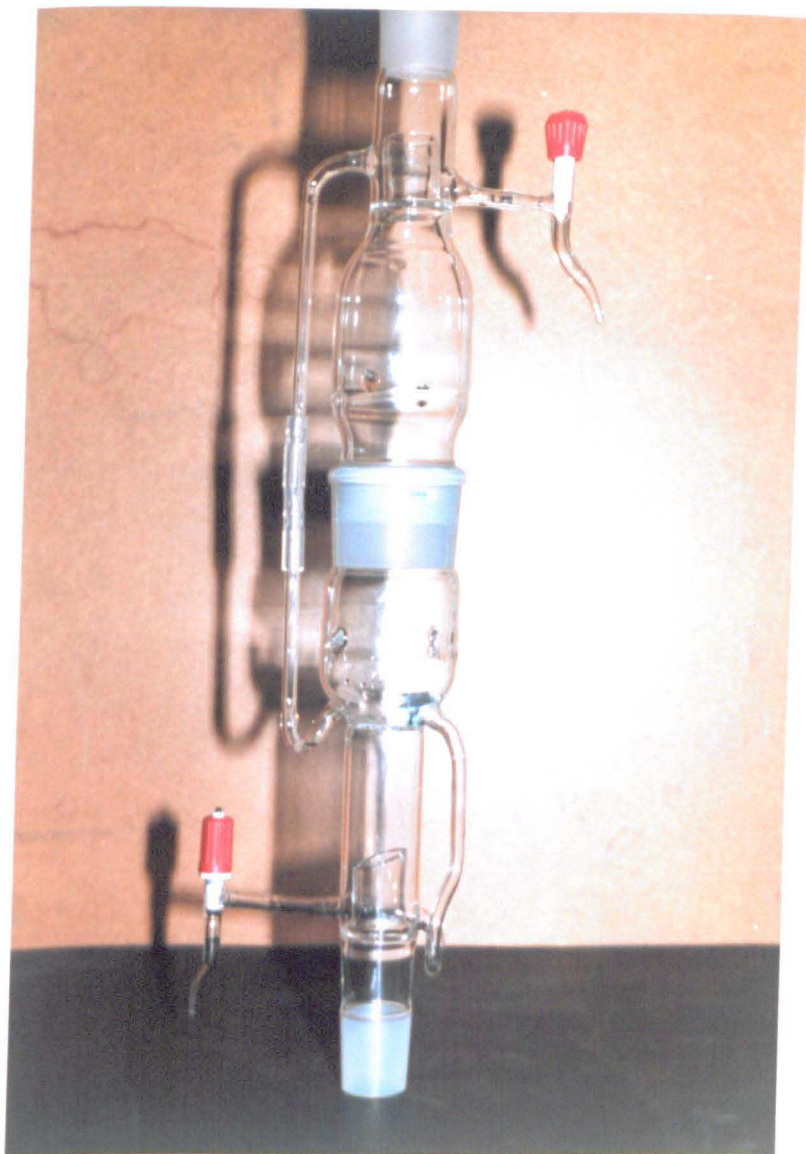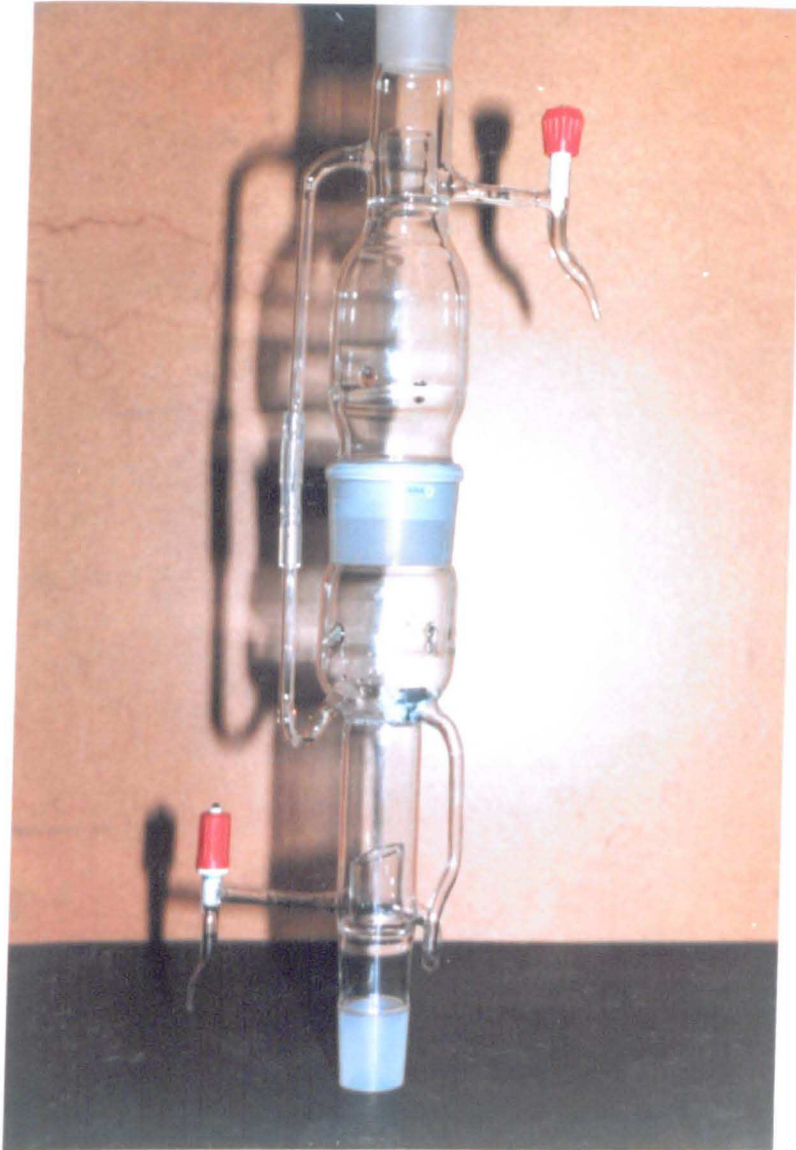
Figure 8.1   A View of the Improved Modified Oldershaw Column.

especially marked in the low methanol composition range. This is
because there is a reduction in liquid load due to the increase in the
liquid density to maintain the F.Factor constant in this range. When
there was no outlet weir poor contact between the gas and the liquid was
achieved on the plate. On increasing the outlet weir this problem is
reduced. Further increase of the outlet weir height from 6.4 mm to
12.7 mm resulted in a further jump in point efficiency due to an increase
in the biphase height (see Figures 8.2 and 8.3).

Further increases in outlet weir were not studied as the biphase
could have reached the top of the column expansion above the tray and
wall effects could have reappeared. These point efficiencies are compared
with 1 mm perforation size rectangular tray results (see Chapter 7) in
Figure 8.3. All the results obtained are tabulated in appendix A.

8.6   Tray Efficiencies Using Modified Column Point Efficiencies

The point efficiencies measured at an outlet weir height of 12.7 mm
in the modified column were used to develop a correlation using a least
mean square polynomial fitting method. The following equation was obtained:-

$$Eog = 0.902 - 0.359 \ x + 0.376 \ x^2 \qquad\qquad 8.1$$

The point efficiencies calculated from this equation are shown on Figure
8.3, represented by a dotted line.

These efficiencies were then incorporated into the eddy diffusion
model described in Chapter 7, simulating conditions under which the 1 mm
perforation tray distillation was carried out in order to evaluate tray
efficiencies. These tray efficiencies are compared with the model
prediction of actual 1 mm hole size rectangular tray measurements in

Figure 8.4.

There is a 10 to 20 per cent difference between the tray efficiencies, which would provide a fairly accurate, safe design of a distillation column.

8.7 Scale-up Work

Dribika and Biddulph (1986), using the application of the penetration theory, developed a scale-up equation for translating efficiencies from one column to another. The equation is as follows:-

$$\frac{NOG1}{NOG2} = \left[\frac{h_L^1 - H_f^1}{h_L^2 - H_f^2} \right]^{0.5} \qquad 8.2$$

When 1 and 2 referred to the modified Oldershaw column and rectangular columns respectively.

The measured froth heights are tabulated in appendix A, Tables A.4.1 and A.4.2 were used to develop the following equations by a least mean square method:-

$$H_f^1 = 1.884 + 4.022 \, x1 - 2.477 \, x^2 \qquad 8.3$$

$$H_f^2 = 3.458 + 4.15 \, x \qquad 8.4$$

The tray liquid hold-up was calculated by the Bennett et. al. (1983), correlation, Chapter 7 equation 7.8.

The overall number of transfer units or the point efficiencies, were then calculated using the equation 6.8, Chapter 6.

The resulting point efficiencies are plotted in Figure 8.3. These point efficiencies compare very well with the large tray point efficiencies. The eddy diffusion model was then used as in 8.6, to predict tray

efficiencies for the 1 mm perforation size large tray. These predicted efficiencies are only 2-4 per cent lower than actual large tray effic- iencies, (see Figure 8.4).

8.8 Discussion

The increase in the outlet weir height in the modified Oldershaw column, as expected, caused a marked increase in the measured point efficiencies. These point efficiencies are now compatible with the ones operating on a larger distillation tray. For a more accurate design the scale-up equation 8.2 can be used. The only difficulty in using the equation is a lack of information about the biphase height on the large tray, and the way the liquid flows across a circular tray. This equation was developed using experimental results from the rectangular tray column where detrimental flow non-uniformities and stagnant zones characteristic of large circular trays do not exist. In Chapter 7, it was concluded that the hole size had a relatively small influence on tray efficiencies. This means that the modified column could be used for the design of larger perforation size trays. Fair et. al. (1983), quoted that higher mass transfer efficiencies obtained in an Oldershaw column are due to the small perforation size. They derived the following scale-up relationship, comparing the mass transfer of such a column with larger columns, on the basis of the same approach to flooding:-

$$\frac{(Kog)_1 \, a_1}{(Kog)_2 \, a_2} = 8 \qquad\qquad 8.5$$

As our study of the effect of the hole size in Chapter 7 indicated this relationship, although correct, may have been mis-interpreted. As

the hole size has a relatively small effect on mass transfer efficiencies, $(Kog)_1$ should have the same value as $(Kog)_2$. The remaining terms a1 and a2 should therefore be responsible, if we assume the same flow conditions were achieved in their Oldershaw and large tray column. The interfacial contact between the liquid and gas is directly related to liquid hold up and the biphase height, and this is the only major difference between the mass transferred on a larger tray column compared with the small laboratory Oldershaw column.
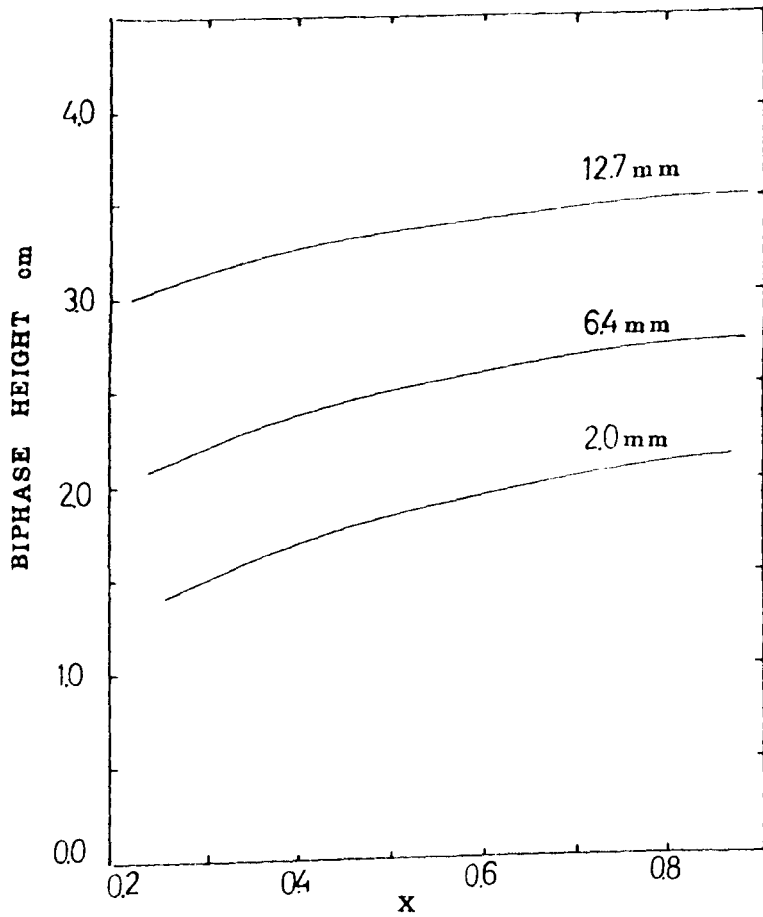
Figure 8.2   The effect of outlet weir height on the biphase
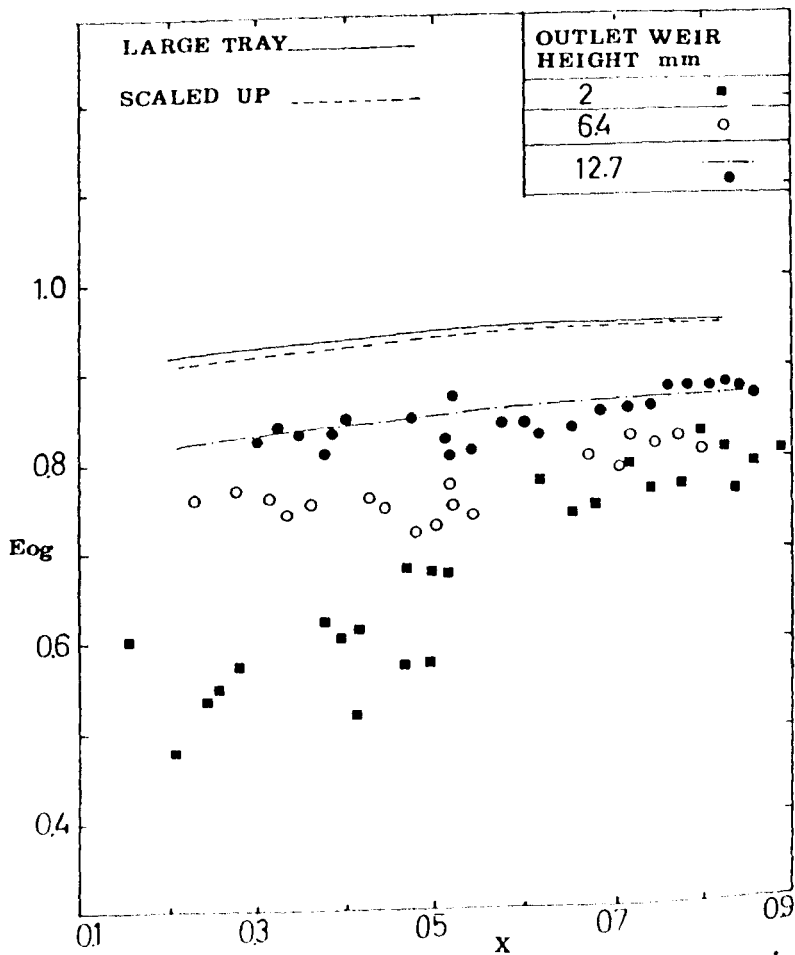
Figure 8.3 The effect of the outlet weir height on point
efficiencies
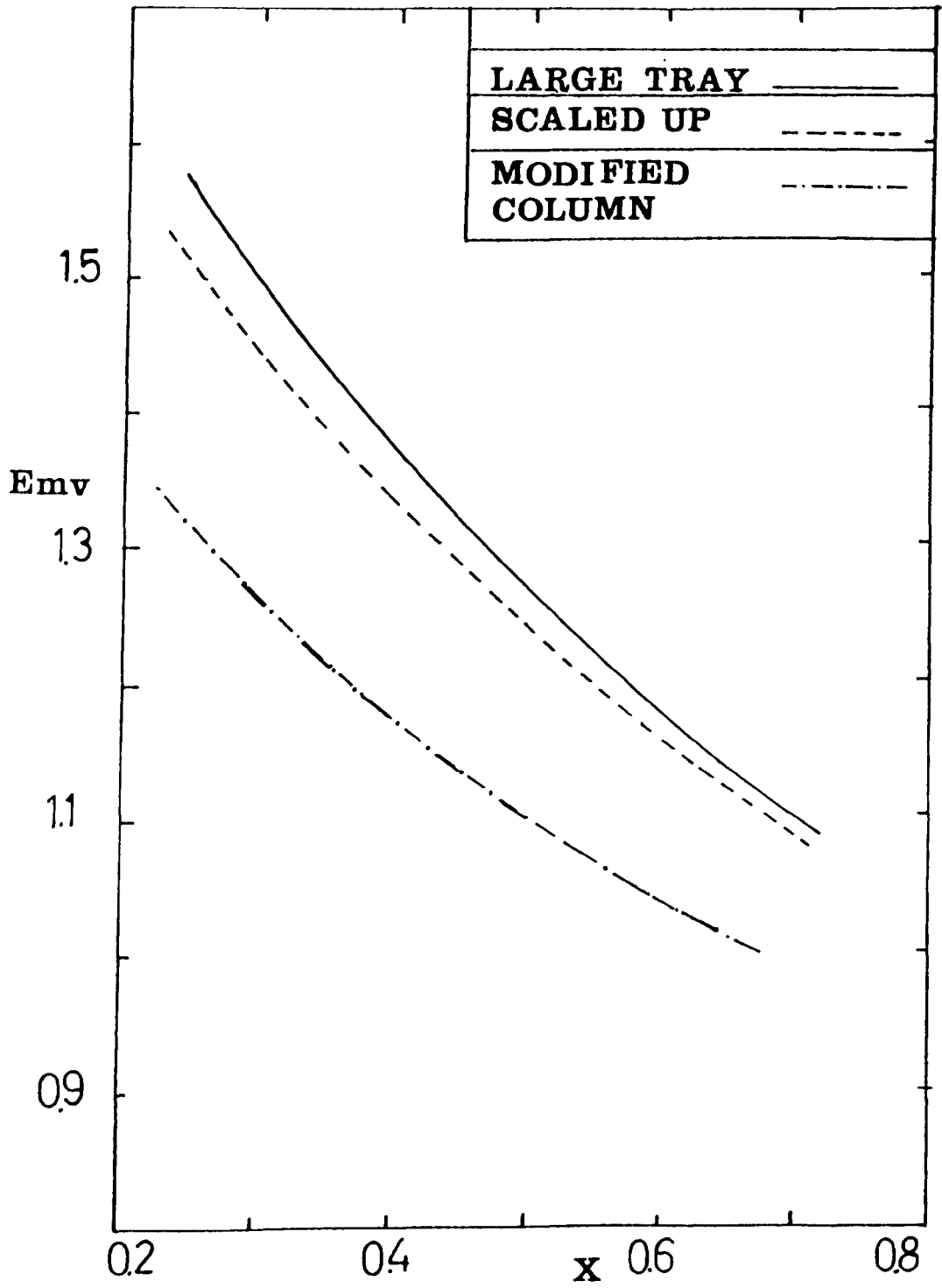
Figure 8.4 Tray Efficiencies

CHAPTER 9

STUDY OF NON-IDEAL TERNARY

DISTILLATION EFFICIENCIES

STUDY OF NON-IDEAL TERNARY DISTILLATION EFFICIENCIES

9.1 Introduction

Multicomponent systems are divided into two catagories. Firstly,
thermodynamically ideal where the system is constituted from molecules
of a similar nature and structure. Close members of a homolegous series
or components with the same order of polarity would fall into this category.
Secondly, thermodynamically non-ideal systems, where components of different
molecular structure and polarity constitute the system. Toor (1957)
showed theoretically that for thermodynamically non-ideal ternary systems,
there are marked differences between the binary and ternary mass transfer
arising from interactions between the diffusing species. This was partly
explained, in the earlier investigations into multicomponent efficiencies
by Nord (1948) and Qureshi and Smith (1958) where different component
efficiencies were reported. This was because, in a non-ideal system
individual components have different diffusion coefficients and in addition
diffusional interactions play an important role. Figure 9.1 shows a
comparison of diffusivities of binary alcohol-alcohol and alcohol-water
pairs of interest in this investigation (see appendix C for calculations).
As there are large differences between the diffusivities of these pairs,
according to Toor (1957) significant interaction effects can be expected
in a multicomponent mixture of alcohol-water which may result in individual
components showing different point efficiencies.

In multicomponent systems, independently of the thermodynamic behaviour,
individual components operate with different effective equilibrium line
slopes which can result in different individual component tray efficiencies
(Biddulph 1975). Dribika (1986) confirmed this expectation experimentally
by distilling an ideal ternary system MeOH/EtOH/n.PrOH.

In this chapter, the results from two ternary non-ideal systems of

MeOH/n.PrOH/H_2O and MeOH/EtOH/H_2O are reported, using the modified Oldershaw column (Chapter 4) and the rectangular distillation column (see Chapter 5). The intention is to broaden knowledge of the behaviour of non-ideal multicomponent system efficiencies. The feasability of using small column efficiencies to predict large tray applications is also investigated. Furthermore, the middle components of such systems are known to exhibit maxima in concentration (Cilianu et. al. 1974; Dribika 1986), and the adequacy of the Murphree definition of point efficiency to represent these conditions has been tested. Lockett (1986), in his recent review, has emphasised the need to test multicomponent efficiency prediction methods against data from large-scale columns using the predictive methods (Diener and Gerster 1968; Krishna et. al., 1977 and Medina et. al., 1979) based on the application of the Maxwell-Stefan equations for diffusion, the adequacy and accuracy of these methods for large tray measurements are tested in this chapter.

9.2   Vapour Liquid Equilibrium (VLE) Data

The VLE measurements on the systems MeOH/n.PrOH/H_2O and MeOH/EtOH/H_2O were carried out by Ochi and Kojima (1969) and Delzene (1958) respectively, compiled by Gemhling and Onken (1977). The Wilson model, incorporating binary parameters of the pairs constituting each ternary system, was used to test the predictions against the reported measurements. This comparison is shown in the Table 9.1.

Thermodynamically consistant parameters used for the required calculation were reported in Chapter 4, Table 4.1, and in addition the following thermodynamically consistent Wilson parameters were used as tabulated in Table 9.2.

Table 9.1   Comparison of the differences between the measured and predicted bubble temperature and vapour equilibrium composition

System	$\sum \left| T_{b,EXP} - T_{b,PRED} \right| /n$ °C	$\sum \left| Y^*_{EXP} - Y^*_{PRED} \right| /n$
$MeOH/EtOH/H_2O$	0.43	0.0222
$MeOH/EtOH/H_2O$	0.79	0.0011

Table 9.2   Binary Wilson Parameters

System	Wilson Parameters	Reference
Methanol-Ethanol	326.951, 284.643	Gemhling and Onken (1977 Part 1)
Ethanol-n.Propanol	385.395, 299.258	Dribika and Biddulph (1986)

9.3.a   Equipment

The modified Oldershaw column has been described in Chapter 4, and the rectangular column has been described in Chapter 5. The rectangular tray details are given in Chapter 6, Table 6.1.

9.3.b Experimental

All the experiments were carried out at atmospheric pressure and total reflux, with a superficial F-Factor of about 0.5 m/s $(Kg/m^3)^{0.5}$ to ensure steady operation in the mixed froth regime. Further details of the experimentation are given in Chapters 4 and 6. The samples were analysed by gas chromatography, as reported in appendix D, with an accuracy of $\pm$ 0.0043 mole fraction and $\pm$ 0.0053 mole fraction for MeOH/EtOH/H$_2$O and MeOH/n.PrOH/H$_2$O systems.

9.4 Prediction of Individual Component Point Efficiencies Application to the System: MeOH/n.PrOH/H$_2$O

These methods are based on interpretations of the Maxwell-Stefan equations for diffusion and their application to ternary distillation using binary data. The individual component point efficiencies are predicted by applying these equations (Diener and Gerster (1968), Krishna et. al., (1977), Krishna (1977) and Medina et. al. (1979). A summary of these methods is given by Lockett (1986). The following assumptions are made:-

   i) Equimolar mass transfer

  ii) No influence of finite mass transfer rates on the mass transfer coefficient

 iii) Neglecting thermodynamic correction factors.

It is also assumed that gas-phase resistance to mass transfer is controlling. The following steps are taken to carry out the required calculations:-

a) Evaluation of binary overall, liquid phase and vapour phase Number of Transfer Units. These can be obtained experimentally by carrying out experiments under the same hydrodynamic conditions. This is the approach taken here whereby the binary experimental data in the rectangular distillation are used. These binary data can also be calculated using standard procedures available (see Chan and Fair (1984)).

b) Evaluation of Equivalent Ternary Transfer Units (Method of Diener and Gerster (1968)

Diener and Gerster (1968), suggested the following equations:-

$$NTG11 = NG.13 \ (Y1 \ NG23 + (1 - Y1) \ NG12))S \qquad 9.1$$

$$NTG12 = Y1 \ NG \ 23 \ (NG13 \ - NG12)/S \qquad 9.2$$

$$NTG21 = Y2 \ NG \ 13 \ (NG23 \ - NG12 \ )/S \qquad 9.3$$

$$NTG22 = NG \ 23 \ (Y2 \ NG13 \ + (1 - Y2) \ NG12 \ )/S \qquad 9.4$$

where:

$$S \quad = Y1 \ NG23 \ + Y2 \ NG13 \ + Y3 \ NG12 \qquad 9.5$$

Equations 9.1 to 9.5 are used to compute the ternary equivalent liquid phase number of transfer units (NTL) using binary liquid phase transfer units (NLij), substituting (NTL) by (NTG), and (NLij) by (NGij). Note also that a theory has not yet been developed to take into account the thermodynamic non-idealities in the liquid phase. This is the main reason why the vapour phase resistance to mass transfer is required from the binaries,if the above theory is to be used. Finally Krishna (1980) questioned the work by Medina et. al. (1979) regarding the effect of surface tension on mass transfer, as the multicomponent theory does not

take this to account. The surface tension of the ternary MeOH/n.PrOH/H$_2$O measured at boiling point, Figure 3.6, indicates that the surface tension gradients are only significant at a very low water concentration, and will not have any significant effects at higher alcohol concentrations.

c) Ternary equivalent slope of the equilibrium line (mij) are calculated from theoretical tray column simulations taken from two adjacent trays n + 1 and n:

$$m11 = \frac{Y_{1,n+1} - Y_{1,n}}{x_{1,n+1} - x_{1,n}} \qquad\qquad 9.6$$

$$m12 = \frac{Y_{1,n+1} - Y_{1,n}}{x_{2,n+1} - x_{2,n}} \qquad\qquad 9.7$$

$$m21 = \frac{Y_{2,n+1} - Y_{2,n}}{x_{1,n+1} - x_{1,n}} \qquad\qquad 9.8$$

$$m22 = \frac{Y_{2,n+1} - Y_{2,n}}{x_{2,n+1} - x_{2,n}} \qquad\qquad 9.9$$

d) Ternary overall-gas-phase transfer units (NOGij) are then calculated by combining the ternary gas and liquid phase transfer units and incorporating in the same manner as for a binary system using the two film theory. Diener and Gerster (1964) give further details of the equations used.

e) Evaluation of the elements of the matrix

$$\text{EXP} \begin{bmatrix} -\text{NOG} \end{bmatrix} = \text{EXP} \begin{bmatrix} -\text{NOG11} & -\text{NOG12} \\ -\text{NOG21} & -\text{NOG22} \end{bmatrix}$$

$$= \begin{bmatrix} \text{G11} & \text{G12} \\ \text{G21} & \text{G22} \end{bmatrix} \qquad\qquad 9.10$$

The equations G11, G12, G21 and G22 are derived using Silvester's theorem, and are given by Diener and Gerster (1968), with a slightly different form by Krishna et. al. (1977).

Calculations of vapour compositions leaving the test tray, Y_{1n}, Y_{2n} and Y_{3n}.

f) Calculations of the individual component point efficiencies Eog_1, Eog_2 and Eog_3.

The numbers of liquid phase and vapour phase transfer units were available from experiments using the rectangular column for the binaries constituting the system MeOH/n.PrOH/H_2O from Dribika (1986) and Table 6.3 for the system n.PrOH/H_2O. These experiments were all carried out at similar hydrodynamic conditions. Table 9.3 summarises the values of N_L and N_G.

Table 9.3   Values of N_G and N_L

System	N_G	N_L
MeOH/H_2O	2.56	12.5
MeOH/n.PrOH	1.61	5.83
n.PrOH/H_2O	1.88	7.05

The vapour phase was controlling the mass transfer for all these binary systems.

9.4.2   Method of Medina et. al. (1979)

All the basic steps as indicated by the equations 9.1 to 9.5 and 9.10 are taken to calculate the overall number of transfer units, replacing NOGij by NGij. The point efficiencies for the binary systems of interest were measured by Dribika (1986), and for the systems $n.PrOH/H_2O$ measured as reported in Chapter 6. These data were correlated by a least mean-square polynomial method to give the following equations:-

System $MeOH/H_2O$

$$E_{og} = 0.8482 + 0.101 \ X \qquad\qquad 9.11$$

System MeOH/n.PrOH

$$E_{og} = 0.6449 + 0.166 \ X \qquad\qquad 9.12$$

System $n.PrOH/H_2O$

$$E_{og} = 1.0048 - 1.74 \ X + 4.4 \ X^2 - 3.19 \ X^3 \qquad\qquad 9.13$$

Note that all the above binary measurements were carried out under the same running conditions as the ternary measurements.

The composition of the vapour leaving the test tray was evaluated by the following equations:-

$$Y_{n,1} = Y^*_{n,1} + G11 \ (x_{n,1} - Y^*_{n,1}) + G12 \ (x_{n,2} - Y^*_{n,2}) \qquad 9.14$$

$$Y_{n,2} = Y^{*}_{n,2} + G21 \left(x_{n,1} - Y^{*}_{n,1} \right) + G22 \left(x_{n,2} - Y^{*}_{n,2} \right) \qquad 9.15$$

$$Y_{n,3} = 1 - Y_{n,1} - Y_{n,2} \qquad 9.12$$

The individual component point efficiencies were calculated using the Murphree equation.

$$Eog_{n,i} = \frac{\left(Y_{n,i} - X_{n,i} \right)}{\left(Y_{n,i}{}^{*} - X_{n,i} \right)} \qquad 9.16$$

9.4.3   Method of Krishna et. al. (1977)

The equations 9.1 to 9.5 and 9.10 were used to compute the ternary equivalent gas phase numbers of transfer units, using the N_G values as tabulated in Table 9.3

The individual component point efficiencies were then calculated using the following equations:-

$$Eog_1 = Eog_{11} + Eog_{12}/\Gamma \qquad 9.17$$

$$Eog_2 = Eog_{22} + Eog_{21}/\Gamma \qquad 9.18$$

where:

$$Eog_{11} = 1 - G_{11} \qquad 9.19$$

$$Eog_{12} = - G_{12} \qquad 9.20$$

$$Eog_{21} = -G_{21} \hspace{6cm} 9.21$$

$$Eog_{22} = 1 - G_{22} \hspace{5cm} 9.22$$

Γ is the ratio of driving forces of components 1 and 2.

9.5 Deduction of Point/Tray Efficiencies

The "Eddy diffusion" model (Biddulph 1975), described in detail in Chapter 7, was used to simulate the ternary experiments carried out in the rectangular column. The mixing study data are reported in 6.7. The vapour and liquid enthalpy values are given in appendix C. The 'K' values were calculated from V.L.E. data computations, taking into account the non-idealities in both phases (see appendix B). The point/tray efficiencies were thus inferred by matching with the observed composition profiles across the tray.

To predict the composition profiles across the tray for a given run using the predicted or measured point efficiencies the same procedure as described in Chapter 7 was used. The reboiler and bottom tray conditions were simulated as in the experimental runs. The point efficiencies of two components were used to predict the composition profiles across the tray, ensuring that the component which exhibited the maximum in concentration was not one of these, as there are large errors involved in computation of Murphree point efficiency for such component (Medina et. al. 1979). In an n-component mixture only (n-1) efficiencies can be specified. Note that the K-values were computed separately for each run as they were composition dependent.

9.6   Modified Column Point Efficiencies

The Murphree equation 9.16 was used to calculate the point efficiencies.

9.7   Results

9.7.1   Modified Oldershaw column

The Murphree point efficiencies for these two ternary systems are tabulated in Tables 9.4 and 9.5 as a function of their composition and second and third component K values.

9.7.1.1   System: MeOH/n.PrOH/H_2O Results

The biphase height was closely examined for all the runs. The biphase height varied from 1.5 to 2.5 cm. It was at its lowest and seemed to be less bubbly for the runs 202 to 207. Examining these runs reveals that at these concentrations the system would have been slightly negative, with water transferring from liquid to the vapour phase (see the K-values of water in Table 9.4), according to the classification of Zuiderweg and Harmens (1958). For the rest of the runs the biphase was bubbling more and these were slightly positive according to Zuiderweg classifications. The biphase increased in height from 1.5 to 2.5 cm as more water was added to the reboiler. In Figure 9.2 the point efficiency of methanol is plotted against its concentration on the test plate. There is a decrease in methanol point efficiency corresponding to the negative runs. This is because the plate seemed to have a larger capacity for the positive systems than for the negative (Fell and Pinczewski 1977). The work in Chapter 8

Table 9.4   Modified Oldershaw Column Point Efficiencies System:
MeOH/n.PrOH/H_2O

RUN NO.	X1	X2	K3	K2	Eog1	Eog2	Eog3
202	0.2707	0.5911	1.23	0.56	0.60	0.66	1.26
203	0.2231	0.5454	1.14	0.61	0.56	0.66	1.56
204	0.1911	0.5139	1.08	0.65	0.56	0.68	2.58
206	0.1431	0.4784	1.03	0.17	0.57	0.72	-2.81
207	0.1699	0.4357	0.92	0.75	0.57	0.71	0.08
208	0.1511	0.4292	0.91	0.78	0.57	0.72	0.20
209	0.1322	0.4145	0.89	0.83	0.58	0.76	0.29
210	0.1143	0.4100	0.89	0.87	0.60	0.80	0.42
211	0.0977	0.3919	0.88	0.92	0.65	0.82	0.56
212	0.0818	0.3912	0.88	0.95	0.71	0.90	0.65
213	0.063	0.3986	0.90	0.97	0.78	0.80	0.78
214	0.0522	0.4032	0.91	0.99	0.77	1.21	0.73
215	0.0985	0.3598	0.84	0.97	0.73	1.40	0.65
216	0.0867	0.3626	0.85	0.99	0.76	2.31	0.71
217	0.0692	0.3627	0.86	1.03	0.78	0.70	0.77
218	0.0572	0.3403	0.84	1.11	0.80	0.71	0.77
219	0.0443	0.2877	0.79	1.30	0.82	0.63	0.71
220	0.0491	0.3226	0.82	1.18	0.84	0.75	0.80
221	0.1040	0.2750	0.75	1.16	0.78	0.59	0.72
222	0.1850	0.2233	0.68	1.08	0.78	0.08	0.71
223	0.2837	0.1688	0.61	0.98	0.76	3.56	0.71
224	0.3360	0.1499	0.58	0.90	0.71	0.86	0.73
225	0.4501	0.1011	0.52	0.74	0.74	0.86	0.73
226	0.5271	0.0723	0.40	0.67	0.66	0.43	0.68
227	0.5725	0.0587	0.47	0.64	0.72	0.62	0.73
228	0.6322	0.041	0.45	0.56	0.73	0.68	0.76
229	0.6891	0.0256	0.43	0.50	0.75	0.73	0.76
230	0.7359	0.0156	0.43	0.46	0.78	0.83	0.78
231	0.7542	0.0110	0.42	0.9	0.69	0.84	0.73
232	0.7862	0.0062	0.42	0.42	0.78	0.91	0.77
233	0.7722	0.0221	0.44	0.42	0.73	0.27	0.76
235	0.7864	0.0403	0.43	0.39	0.87	0.86	0.87
236	0.8424	0.027	0.44	0.36	0.79	0.81	0.79
237	0.8651	0.0211	0.44	0.35	0.79	0.80	0.79

- 154 -

Table 9.5   Modified Column Point Efficiencies System: MeOH/EtOH/H_2O

RUN NO.	X1	X2	K2	K3	Eog1	Eog2	Eog3
281	0.1427	0.1889	1.78	0.56	0.89	0.76	0.82
283	0.3691	0.1149	1.23	0.49	0.73	0.73	0.73
284	0.4442	0.0872	1.11	0.47	0.75	0.98	0.76
286	0.5892	0.0486	0.91	0.45	0.78	0.26	0.79
287	0.6585	0.0309	0.83	0.44	0.79	0.56	0.79
288	0.6868	0.0252	0.81	0.44	0.80	0.39	0.81
289	0.6108	0.1105	0.83	0.47	0.76	0.50	0.79
290	0.5441	0.1805	0.85	0.50	0.34	0.53	0.78
291	0.6009	0.1507	0.81	0.49	0.72	0.53	0.77
292	0.655	0.1219	0.77	0.48	0.74	0.55	0.79
293	0.6800	0.1102	0.75	0.47	0.74	0.53	0.78
294	0.6559	0.1275	0.76	0.48	0.69	0.52	0.73
295	0.6220	0.1578	0.78	0.49	0.72	0.57	0.76
296	0.550	0.2196	0.81	0.52	0.74	0.61	0.79
297	0.5120	0.2536	0.83	0.54	0.73	0.62	0.72
298	0.4631	0.2958	0.85	0.56	0.73	0.64	0.76
299	0.4407	0.3036	0.87	0.56	0.72	0.64	0.75
300	0.3910	0.351	0.89	0.59	0.73	0.64	0.76
301	0.3651	0.3619	0.91	0.57	0.73	0.65	0.97
302	0.3090	0.4219	0.93	0.63	0.72	0.66	0.74
303	0.2609	0.4219	0.95	0.66	0.69	0.58	0.72
304	0.2439	0.4706	0.97	0.66	0.74	0.66	0.75
305	0.2296	0.4678	0.98	0.66	0.75	0.94	0.74
306	0.2148	0.464	1.01	0.66	0.73	1.20	0.75
307	0.2001	0.4641	1.03	0.66	0.75	0.74	0.76
308	0.1872	0.4628	1.05	0.66	0.71	0.77	0.75
309	0.1716	0.4598	1.06	0.66	0.74	0.71	0.73
310	0.1547	0.4534	1.1	0.66	0.76	0.69	0.73
311	0.1321	0.4316	1.18	0.65	0.76	0.76	0.76
312	0.1266	0.3883	1.26	6.3	0.76	0.67	0.72

also supports this conclusion. The individual point efficiencies for this system are also different from each other as expected. This system shows maxima in concentration for the middle components (water in case of the runs 202 to 207). The point efficiencies of these components were found to exceed the interval(0 - 1.0). In the Figures 9.3 and 9.4 the point efficiencies of n.PrOH and H_2O are plotted against their 'K' values. These point efficiencies are outside the boundary(0 - 1.0)as the volatility of the component passes through unity (i.e. its concentration maxima). However, at high methanol concentrations these differences in individual point efficiencies were found to be rather small for some of the runs, (e.g. Runs 229, 235, 236, 237, 238 and 239). This is in support of the theory of interaction effects, as at high methanol concentrations the number of the polar, i.e. water, and large molecular components, i.e. normal propanol, are markedly reduced.

9.7.1.2   MeOH/ EtOH/ H_2O System Results

The biphase was observed to be bubbly and the height almost constant at 2.3 cm throughout the composition range studied. The point efficiencies for this system are plotted against the methanol concentration in Figure 9.5. The differences in point efficiencies for this system are almost negligible at high methanol concentration, as expected, but at low ethanol concentration, the point efficiencies of this component are reduced with the other two components showing little change at an average value of 0.75. There was one run, 306, where the K-value of ethanol reached unity and its point efficiency exceeded the (0 - 1.0)region to reach 1.2, which can be explained as before.

9.7.2 Rectangular Column Results

9.7.2.1 MeOH/n.PrOH/H_2O System Results

The composition and temperature profiles across the tray for this system are plotted in Figures 9.6 and 9.7. A comparison of the measured and observed bubble-point temperatures for this system is also shown in Figure 9.8. The measured and observed bubble-point temperatures agree very well. Table 9.6 also gives the mean composition of each component, calculated as in Chapter 6. The average observed biphase height for each run is also included.

Table 9.6 Average Composition and Biphase Heights

RUN NO.	$\bar{X}1$	$\bar{X}2$	$\bar{X}3$	Biphase Height (cm)
WA	0.1533	0.5213	0.3255	4.0
WB	0.2847	0.4126	0.3027	4.0
WC	0.3611	0.3557	0.2832	4.5
WD	0.2474	0.3927	0.3098	5.0
WE	0.1460	0.2015	0.6525	7.0
WF	0.0785	0.1343	0.7870	7.0
WG	0.2127	0.2103	0.5769	7.0
WI	0.1572	0.2388	0.6041	7.5

For the runs WA and WB, water was transferring weakly from the liquid to the vapour phase and the system was negative according to the usual classification. In runs WC and WD, water had reached its maxima in concentration and the system was neutral. For the runs WE to WI the system was positive. The froth height of the runs WA to WE were also lower, as positive systems are known to encourage greater capacities on a seive tray with small holes (Fell and Pinczewski, 1977).

The tray efficiencies of the individual components for each run were calculated from the inlet and outlet composition measurements. They were found to be significantly different (see Table 9.7). The point and tray efficiencies were also inferred from fitting the measured composition profiles to the eddy diffusion model, and are included in Table 9.8. These individual component point efficiencies were found to be significantly different for the runs WA, WB, WC, WD and WI, whereas for the runs WE, WF and WG constant individual component point efficiencies were operating across the tray. The measured and model tray efficiencies for the components not exhibiting maxima in concentration also compare very well.

The point efficiencies were also predicted using the three methods described in 9.4, using the average conditions obtained on the tray. These point efficiencies are compared with the predictions from the model in Table 9.8. Included are also point efficiencies measured in the modified column. For some of the runs the composition in the small column were very similar to the average composition, in the rectangular column. These were runs 206, 246 and 222 matching with runs WA, WC and WG respectively.

The average deviation of these point efficiencies from the model are also included in this table. It may suggest that the methods of Diener and Gerster (1968) and Medina et. al. (1979) to predict the point efficiencies are more accurate with the modified column and the results from the Krishna et. al. (1977) model follow closely. Note that the statistical test did not include the efficiencies of the components passing through a maximum in concentration, as experimental errors are predominant here.

These point efficiencies from each prediction method were then incorporated into the eddy diffusion model simulating the large column experimental runs to predict the composition profiles across the test tray. These composition profiles are included in Figure 9.6 and are compared

Table 9.7   Comparison of Tray Efficiencies   System: MeOH/n.PrOH/H_2O

RUN	Emv_1					Emv_2					Emv_3				
	Measured	Model	Medi	Diener	M.C.	Measured	Model	Medi	Diener	M.C.	Measured	Model	Medi	Diener	M.C.
WA	1.22	1.28	1.27	1.05	0.90	1.16	1.33	0.89	0.95	0.96	1.73	1.42	0.20	0.76	1.07
WB	1.17	1.11	1.27	1.09	–	1.16	1.10	0.94	0.92	–	1.73	1.29	9.6	6.9	–
WC	1.19	1.05	1.22	1.07	0.87	1.27	1.01	0.98	0.93	0.90	1.24	1.24	2.25	1.67	0.75
WD	1.19	1.17	1.27	1.08	–	1.12	1.17	0.95	0.91	–	1.42	1.18	4.7	2.82	–
WE	1.41	1.40	1.88	–	–	0.59	0.33	0.34	–	–	1.02	0.88	1.13	–	–
WF	1.50	1.51	1.78	–	–	0.77	0.86	1.22	–	–	0.98	1.05	0.98	–	–
WG	1.49	1.54	1.53	1.66	1.40	0.43	0.02	0.22	0.12	-0.25	1.16	1.11	1.17	1.12	0.93
WI	1.5	1.45	1.59	–	–	0.37	0.17	0.56	–	–	1.11	0.89	1.14	–	–
$\dfrac{Emv_i - Emv_{i\,ea}}{n}$		0.06	0.14	0.13	0.22		0.18	0.25	0.25	0.4		0.18	0.05	–	–

Table 9.8   Comparison of Point Efficiencies   System: $MeOH/n.PrOH/H_2O$

RUN	Eog_1					Eog_2					Eog_3				
	Model	Kri	Medi	Diener	M.C.	Model	Kri	Medi	Diener	M.C.	Model	Kri	Medi	Diener	M.C.
WA	0.70	0.84	0.72	0.63	0.57	0.92	0.81	0.73	0.71	0.72	2.48	0.62	0.78	1.27	-2.81
WB	0.70	0.84	0.76	0.69	–	0.86	0.81	0.71	0.70	–	0.13	0.94	0.92	0.64	–
WC	0.70	0.85	0.77	0.71	0.61	0.75	0.82	0.72	0.70	0.69	0.6	0.92	0.91	0.73	0.52
WD	0.73	0.85	0.76	0.69	–	0.84	0.82	0.71	0.69	–	0.462	0.93	0.91	0.69	–
WE	0.7	0.91	0.85	–	–	0.7	0.84	0.87	–	–	0.70	0.89	0.84	–	–
WF	0.75	0.92	0.85	–	–	0.75	0.85	0.85	–	–	0.75	0.88	0.85	–	–
WG	0.83	0.90	0.83	0.87	0.78	0.83	0.84	1.33	1.33	0.73	0.83	0.85	0.90	0.89	0.72
WI	0.77	0.89	0.82	–	–	2.23	0.84	0.96	–	–	0.70	0.89	0.84	–	–
$(Eog_{,i}-Eog_{imodel})$		0.14	0.06	0.03	0.08		0.08	0.13	0.16	0.12		0.13	0.11	–	–

with the experimental points. This comparison again agrees with the earlier suggestion that the method of Diener and Gerster (1968) and Medina et. al. (1977) are more suitable. The tray efficiencies inferred from the simulations are included in Table 9.7 and compared with measured and model tray efficiencies, with the Diener and Gerster (1968) showing the least deviation from the measurements.

9.7.2.2 MeOH/EtOH/H$_2$O System Results

The temperature and composition profiles measured for this system are plotted on figures 9.7 and 9.9 respectively. A comparison of the measured and the bubble-point temperatures, including the ones corresponding the inlet and outlet downcomers, are also included. These bubble-point temperatures, as for the previous system, compare very well with the measurements with most of them slightly higher due to the heat transfer from the vapour phase, (see Figure 9.8).

These composition profiles the same way as before were simulated using the eddy diffusion model to infer point/tray efficiencies. These efficiencies, together with the measured tray efficiencies and the average liquid composition on the tray, are included in Table 9.9. The biphase of mixed liquid, froth and droplets had an average height of about 8 cm for this highly positive ternary system. The average deviation of the tray efficiencies predicted by the model from the measured values are also given in Table 9.10. The agreement is excellent.

Table 9.10   Mean Deviation in Modelling Component Tray Efficiencies

	MeOH	EtOH	H$_2$O
$\dfrac{E_{mvi} - E_{mvi\ model}}{n}$	0.065	0.084	0.047

Table 9.9   Experiment and predicted results   System MeOH/EtOH/H_2O

Runs	Mean liquid composition across the tray			Experimental component tray efficiencies			Component point efficiencies			Predicted component tray efficiencies by the model		
	MeOH	EtOH	H_2O	MeOH	EtOH	H_2O	MeOH	EtOH	H_2O	MeOH	EtOH	H_2O
XA	0.5229	0.0993	0.3778	1.226	0.730	1.190	0.88	-1.20	0.97	1.188	0.726	1.163
XC	0.4676	0.1084	0.4339	1.157	0.6878	1.116	0.80	-2.80	0.93	1.080	0.705	1.05
XD	0.4108	0.2193	0.3699	1.244	0.026	1.150	0.86	-0.20	1.02	1.263	0.190	1.174
XE	0.2595	0.3792	0.3613	1.316	0.694	1.121	0.86	0.86	0.86	1.442	0.463	1.115
XF	0.2283	0.4172	0.3545	1.392	0.774	1.180	0.88	0.88	0.88	1.535	0.487	1.171
XG	0.1960	0.4195	0.3845	1.380	0.776	1.110	0.76	0.86	0.75	1.228	0.621	1.020
XH	0.2004	0.391	0.4087	1.310	0.784	1.115	0.75	0.90	0.76	1.209	0.641	1.001
XI	0.1827	0.4482	0.3691	1.302	0.847	1.106	0.80	0.90	0.81	1.340	0.787	1.090
XJ	0.5614	0.2051	0.2335	1.159	1.325	1.126	0.81	0.67	0.87	1.132	1.437	1.075
XK	0.5498	0.2266	0.2236	1.170	1.280	1.140	0.81	0.67	0.87	1.132	1.437	1.075
XL	0.2419	0.2252	0.5329	1.314	0.992	1.168	0.81	0.99	0.85	1.229	0.913	1.097

The efficiencies of the components passing through a maximum in concentration are excluded from this analysis, (i.e. ethanol runs XA, XC, XD and XE).

The individual component point efficiencies for this system, as expected, were different from each other, but there were some runs where equal component point efficiencies were operating across the tray. These differences in component point efficiencies are again attributed to different diffusional mobilities of the individual components (Krishna, 1977; Krishna and Standart, 1979). The middle component, ethanol, point efficiencies were found to be composition dependent, taking values also outside the (0 - 1.0) interval, when composition maxima occured. This is due to the effect of experimental errors in evaluating Murphree point efficiencies (Medina et. al. 1979, see also Chapter 10). The individual component tray efficiencies, as expected (Biddulph 1975), were significantly different from each other even, with equal component point efficiencies operating across the tray, which emphasises the effect of limited liquid back mixing on individual component composition gradients (the same as for the system $MeOH/n.PrOH/H_2O$).

An attempt was also made to predict the tray efficiencies and composition profiles of some of the runs by simulating these runs, but using the modified Oldershaw column point efficiencies. Runs 296, 302 and 308 were found to operate with approximately similar compositions as runs (XJ and XK), XE and XI respectively, and their point efficiencies, similarly to the previous system, follow the same trend as the inferred values from the rectangular column. The deviation of these point efficiencies for individual components are included in Table 9.11. The efficiencies of the modified column, as expected, were lower than the larger column (see Chapter 8).

Table 9.11   Deviation Between Modified Column and Rectangular Column
Point Efficiencies

Runs	MeOH	$(Eog,_{iRecta} - Eog_{i\ modi})$		
		EtOH	H_2O	
XJ and 296	0.07	0.09	0.08	
XK and 296	0.07	0.05	0.09	
XE and 302	0.13	0.20	0.12	
XI and 308	0.09	0.23	0.08	
Average Mean Deviation	0.09	0.14	0.09	

Slightly higher deviation of the intermediate component is due to
the effect of experimental error on point efficiencies. The predicted
composition profiles, using these point efficiencies, are included in
Figure 9.9. The comparison is very good. Table 9.12 also shows the tray
efficiencies for individual components and their deviations from the
measured values. This comparison gives further encouragement to use
small column point efficiencies in the future design of columns operating
on multicomponent distillation systems.

Table 9.12   Tray Efficiencies of Rectangular Column using Modified
Column Point Efficiencies

Simulation Run	E_{mvi}	E_{mv2}	E_{mv3}	Tray Efficiency Deviation		
				1	2	3
XE	1.12	0.38	0.88	0.20	0.31	0.24
XI	1.11	0.67	0.91	0.21	0.18	0.19
XJ	1.00	1.19	0.96	0.16	0.13	0.18
XK	1.00	1.24	0.96	0.170	0.04	0.18
Average Deviation				0.19	0.17	0.20

9.8 Discussion

a) As expected, the individual components in these two ternary systems showed different point efficiencies due to the diffusional interactions arising from different molecular structure and polarity. However, there were some runs where equal component point efficiencies were operating across the tray, for both of the distillation columns used. This behaviour could be a result of the interaction effects of reverse diffusion, diffusion barrier or osmotic diffusion, due to large non-idealities and the very different diffusional characteristics of alcohol/alcohol and alcohol/water systems (see Figure 9.1). This is in agreement with the theory of Toor (1957), Krishna et. al. (1977) and Krishna and Standart (1979).

b) The intermediate components, ethanol in the case of MeOH/EtOH/H_2O system and either H_2O or n.PrOH in case of the MeOH/n.PrOH/H_2O system, were capable of transferring from vapour or liquid or could exhibit a concentration maxima in the composition profile across the tray. In most of the runs the intermediate component showed the highest point efficiencies. The point efficiencies of the intermediate component were also found to go outside the interval (0 - 1.0) when concentration maxima occurred. This is the direct result of errors in evaluating the Murphree point efficiencies. However, these values will not have any effect on the prediction of the composition of that component (Medina et. al. 1979).

c) As expected, there were larger non-idealities in the system MeOH/n.PrOH/H_2O, as the structure of the components constituting this system are different from those in the system MeOH/EtOH/H_2O.

d) The system MeOH/n.PrOH/H$_2$O was capable of exhibiting both positive and negative surface tension behaviour, although the surface tension driving force was fairly low for the composition ranges studied (see Figure 3.6). The biphase in the positive runs seemed more bubbly, whereas for the negative runs less bubbling but more spraying was observed. These observations are in agreement with works of Zuiderweg and Harmens (1958) and Bainbridge and Sawistowski (1964). However, the foamy biphase suggested by Zuiderweg and Harmens (1958) was never observed. The biphase in the negative runs was generally smaller in height than the positive system runs, which explains why lower point efficiencies were obtained. In Chapter 8 the effect of biphase height on the point efficiency is described in detail. If the surface tension behaviour of the ternary system MeOH/n.PrOH/H$_2$O can be assumed to be similar to the binary n.PrOH/H$_2$O and the ternary MeOH/EtOH/H$_2$O similar to MeOH/H$_2$O (see Chapter 3), this means that there are larger surface tension gradients in the latter. The higher, measured point efficiencies for the MeOH/EtOH/H$_2$O system, especially for the non-interacting component methanol in the rectangular column, is probably due to greater surface renewal effects. The measurements in the modified column give a more confused picture due to the smaller gas and liquid contact (see Chapter 8) on the test tray.

e) The eddy diffusion concept (Biddulph 1975) was found to model the differences in component tray efficiencies, including the higher and the lower efficiency values. This model is flexible and requires n-1, component point efficiencies. This means that the component which shows a maximum in concentration can be left out, as its concentration is independent of the point efficiency to carry out the simulation.

f) One of the most important features of the work carried out in this chapter, is the illustration of differences between component tray efficiencies, despite the fact that equal component point efficiencies were operating across the rectangular tray. This is a result of the limited back mixing on the tray. This influences the individual component composition gradient across the tray. Similar predictions were noted in a study of an air distillation column and an aromatic column, Biddulph (1975), Biddulph and Ashton (1977) respectively. These experimental findings confirm such predictions. The fact that component tray efficiencies can vary widely from one another in multicomponent systems, due to the thermodynamic non-idealities or the effect of back mixing, can obviously casts serious doubts on the validity of the normal design approach of using constant and equal component tray efficiencies.

g) Individual component point/tray efficiencies and composition profiles were predicted using the methods of Krishna et. al. (1977), Medina et. al. (1979) and Diener and Gerster (1968) respectively. From these methods the largest deviation from the measured values was obtained with the Krishna et. al. (1977) method. This is due to using the number of gas phase transfer units (N_{Gij}) in the original computations to fulfil the assumption of no liquid phase resistance to mass transfer. The other two methods are also based on the same assumption, however as the overall number of transfer units (NOGij) take into account the number of liquid phase transfer units (N_{Lij}), better predictions were obtained. An attempt is also made to model the rectangular column distillation runs using modified column point efficiencies. These efficiencies were chosen from a number of runs made using this column with approximately similar compositions on the tray. The deviations of the tray efficiencies and the composition profiles obtained were similar to those using the prediction

methods. However, the work on this column indicated (see Chapter 8) that better point efficiencies may be obtained using this column fitted with a 12.7 mm outlet weir. These efficiencies may be scaled up to values very close to the ones operating across the rectangular tray.
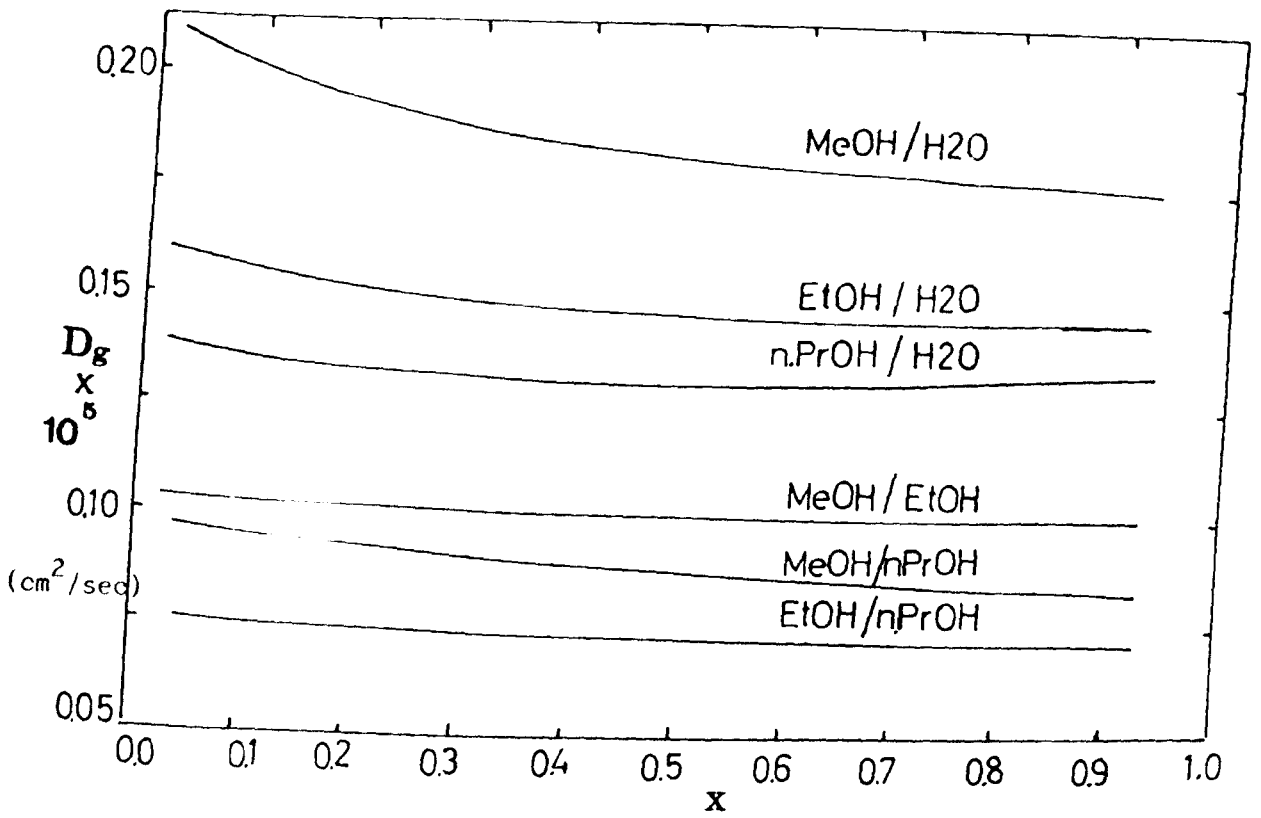
FIGURE 9.1: Binary diffusion coefficients
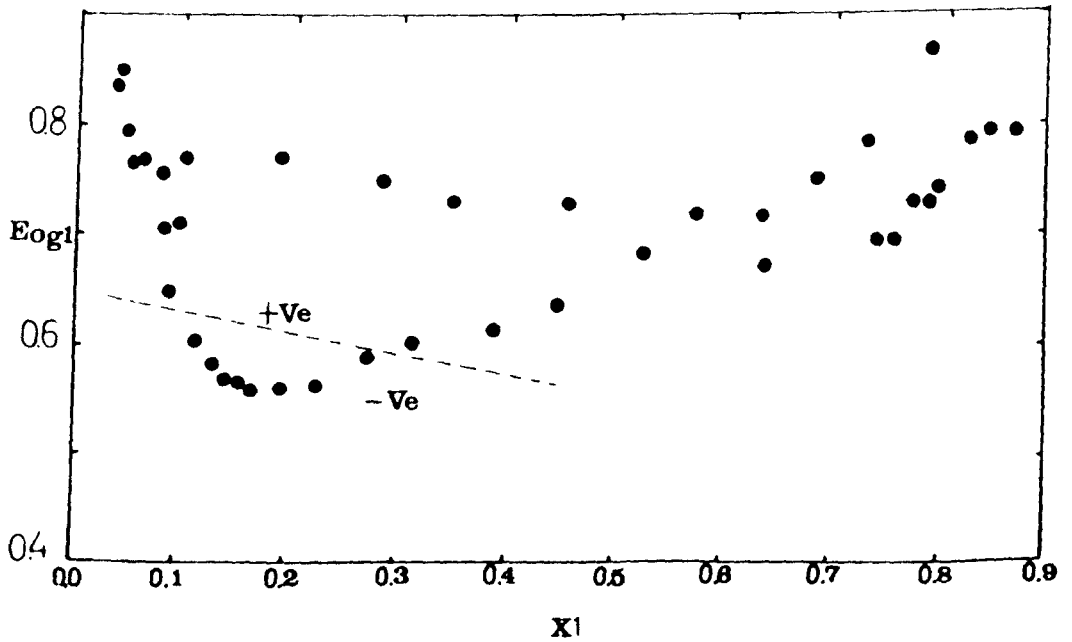
FIGURE 9.2: Point Efficiencies of Methanol in the Ternary MeOH/n.PrOH/H_2O
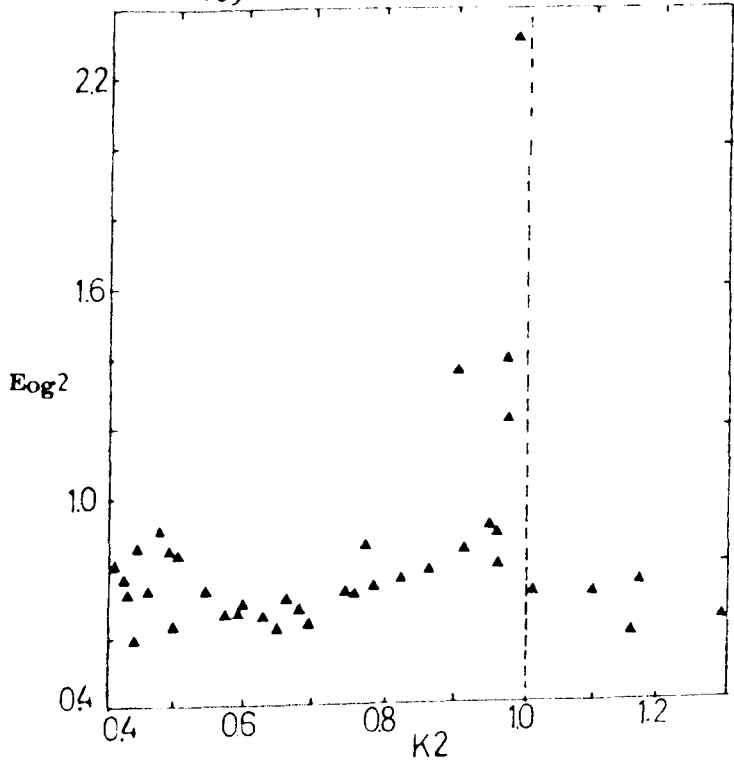
FIGURE 9.3: Point efficiencies of ethanol versus its volatility in the ternary MeOH/n.PrOH/H$_2$O
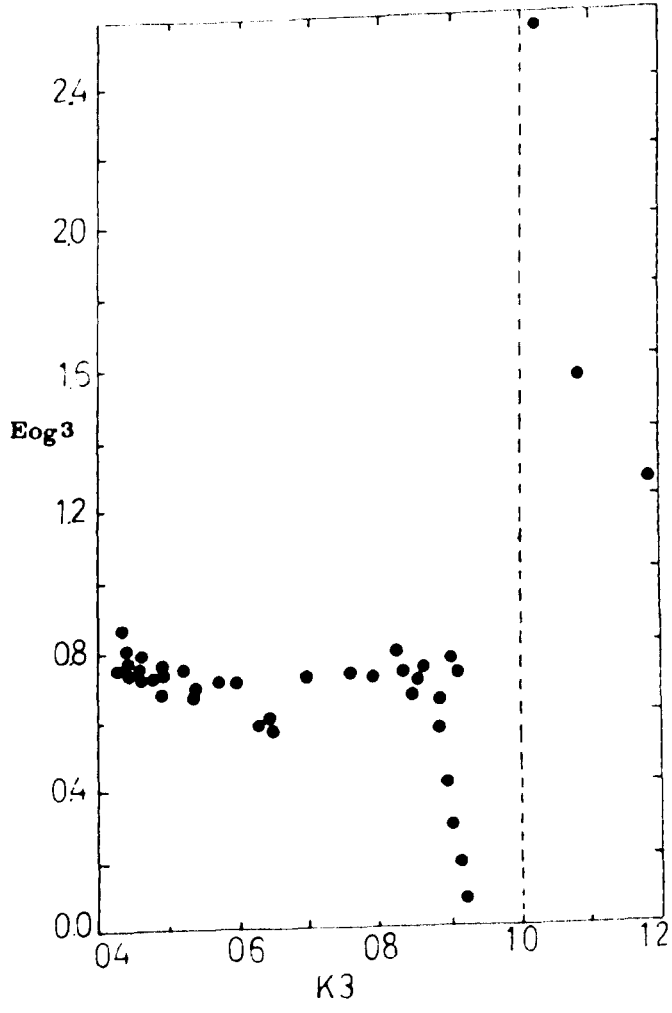
FIGURE 9.4: Efficiencies of water versus its volatility in the ternary MeOH/n.PrOH/H$_2$O
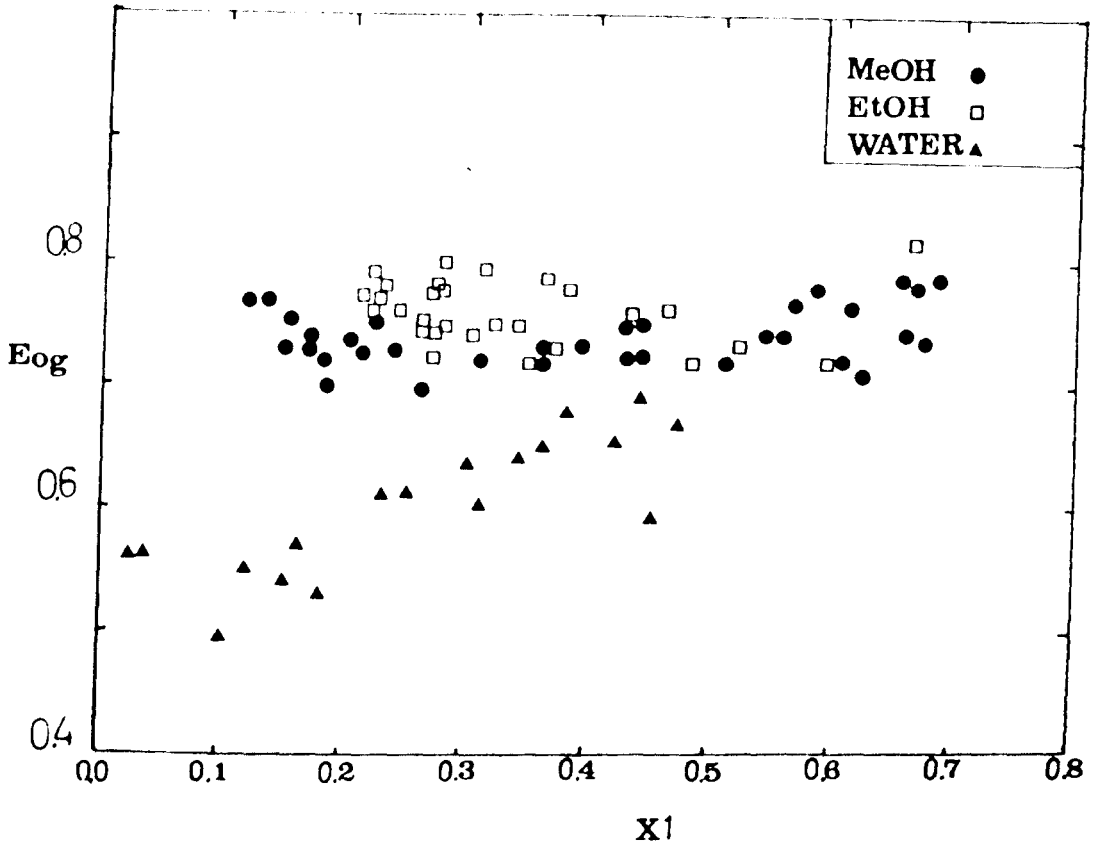
FIGURE 9.5: Point efficiencies of the ternary MeOH/EtOH/H$_2$O
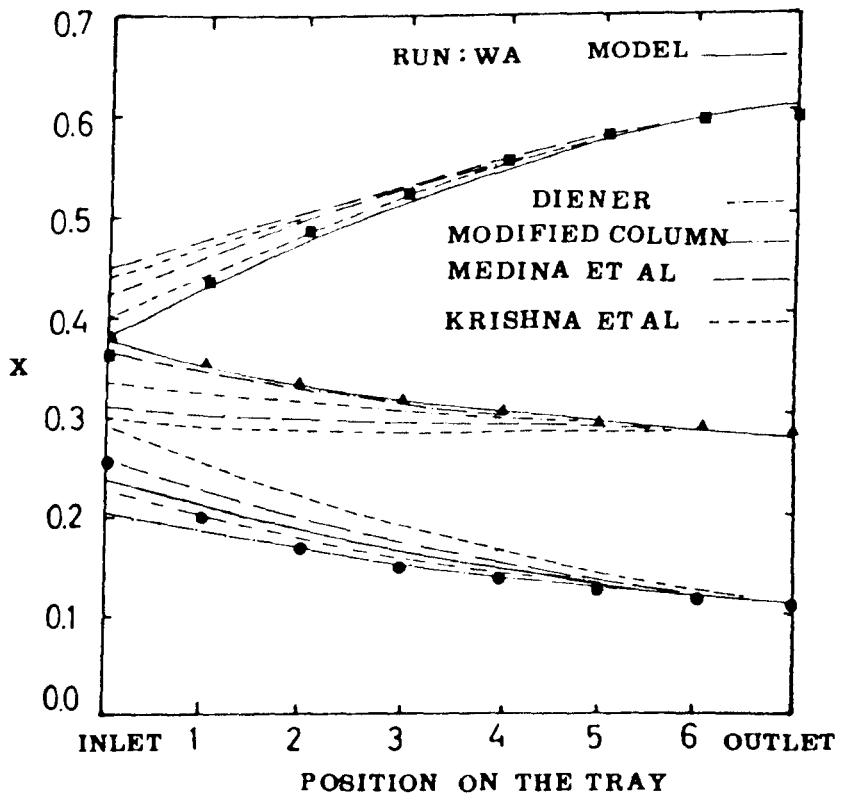
FIGURE 9.6: Composition profiles of the ternary MeOH/n.PrOH/H$_2$O
across the tray
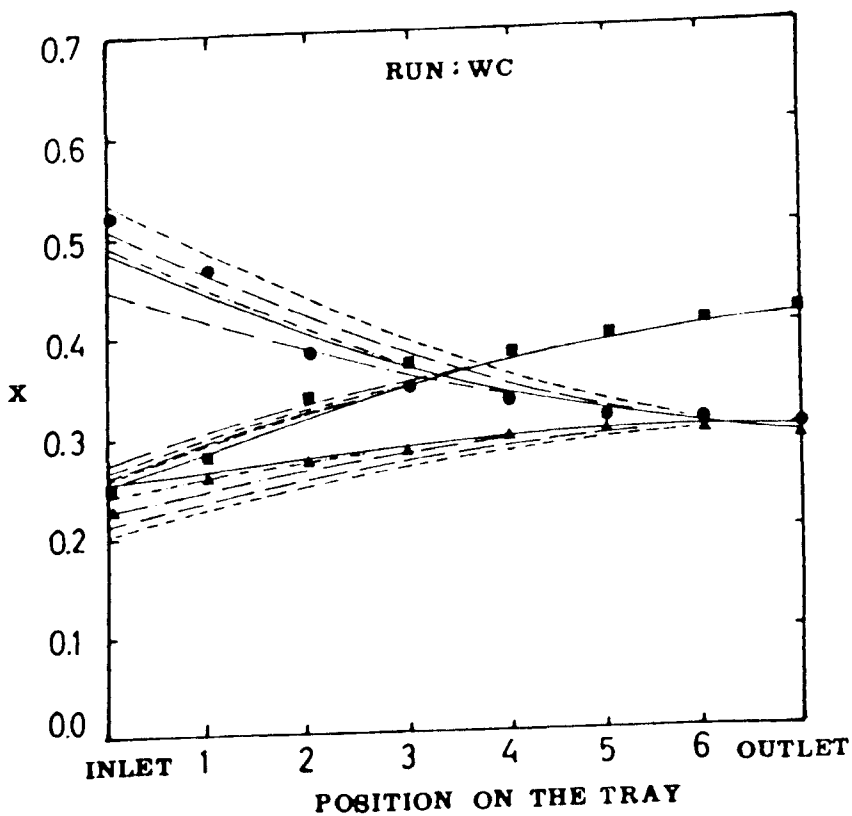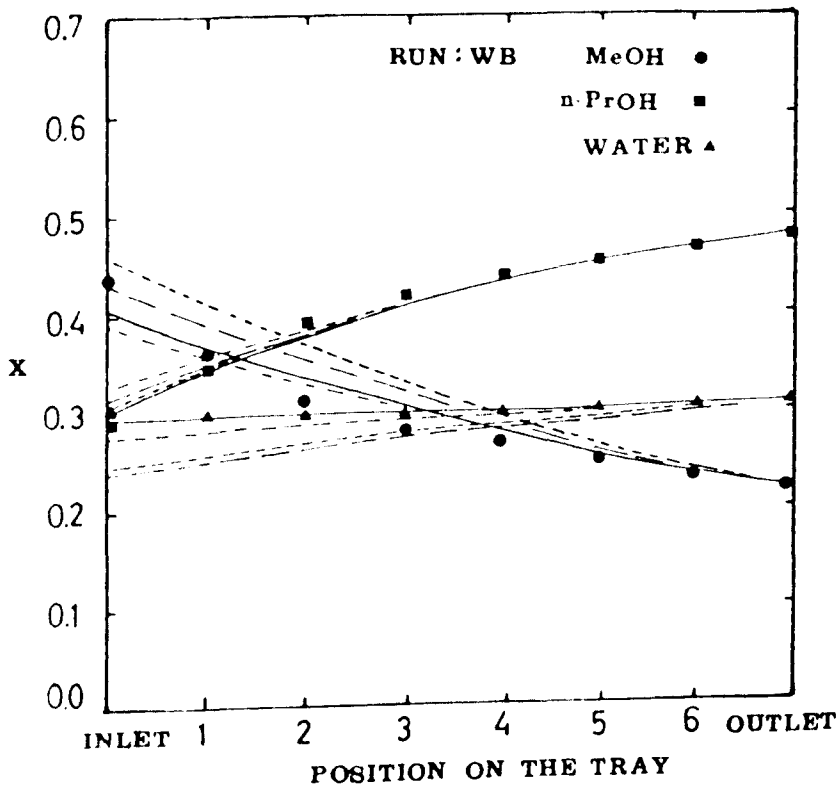
Figure 9.6 continued
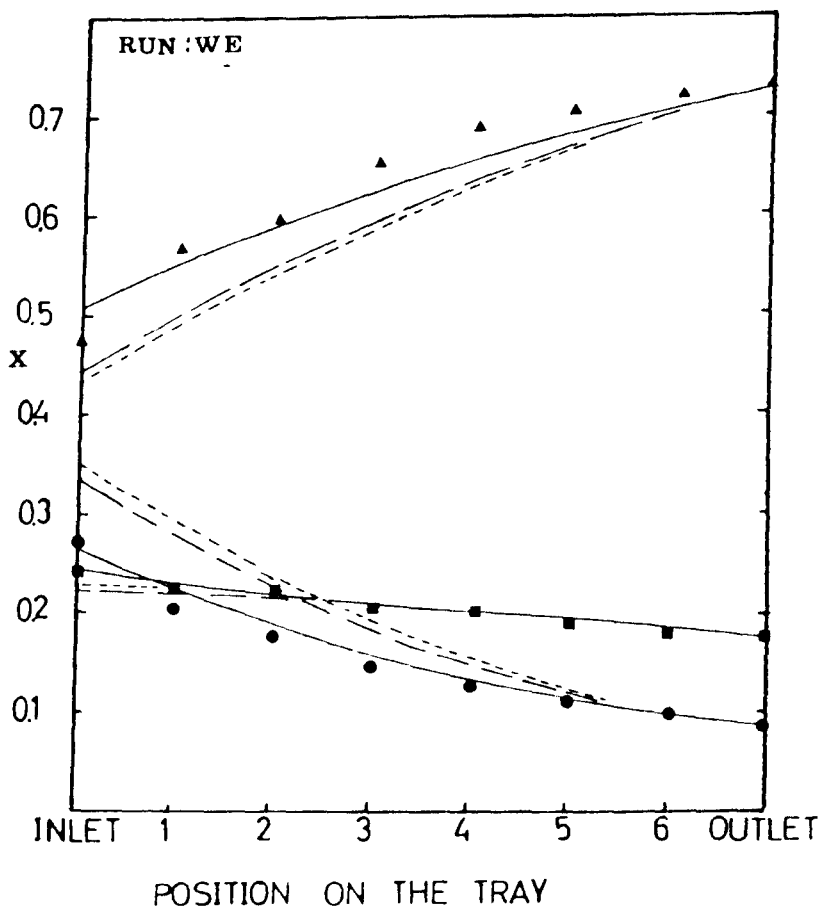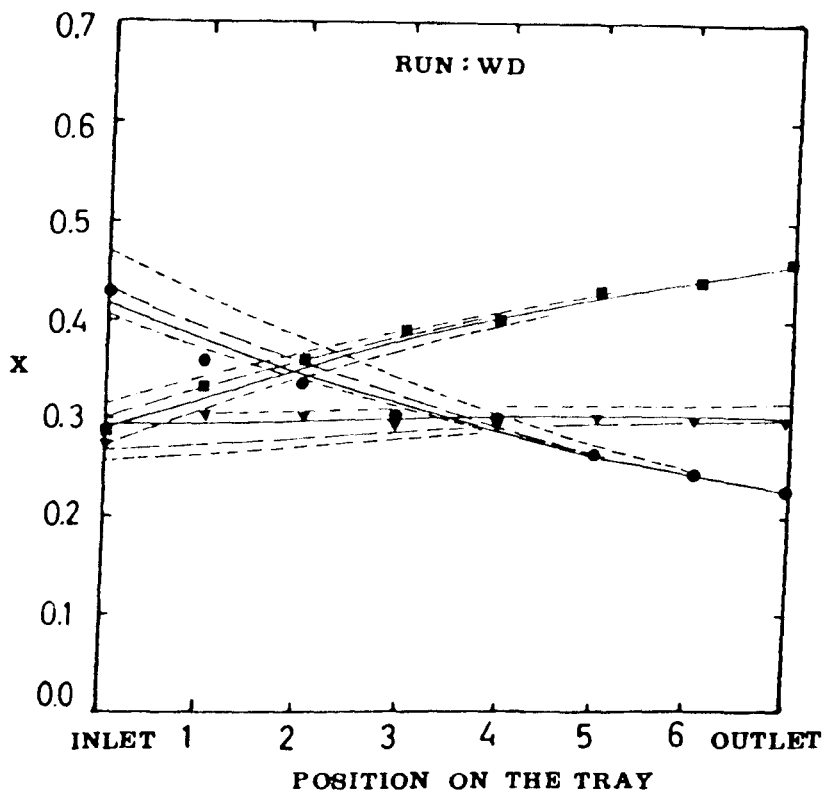
Figure 9.6 continued
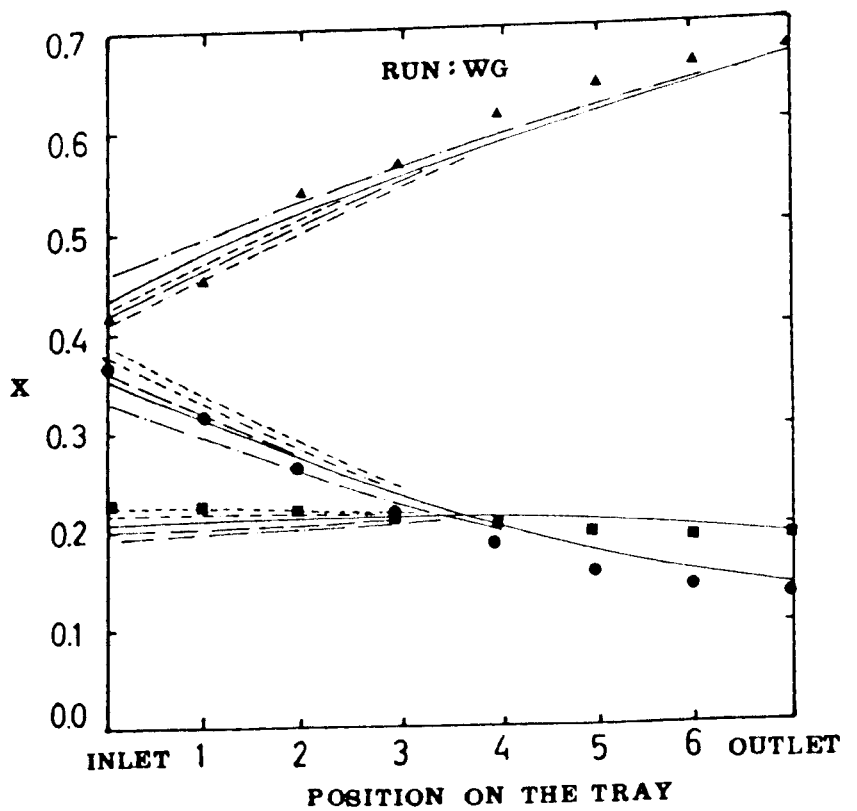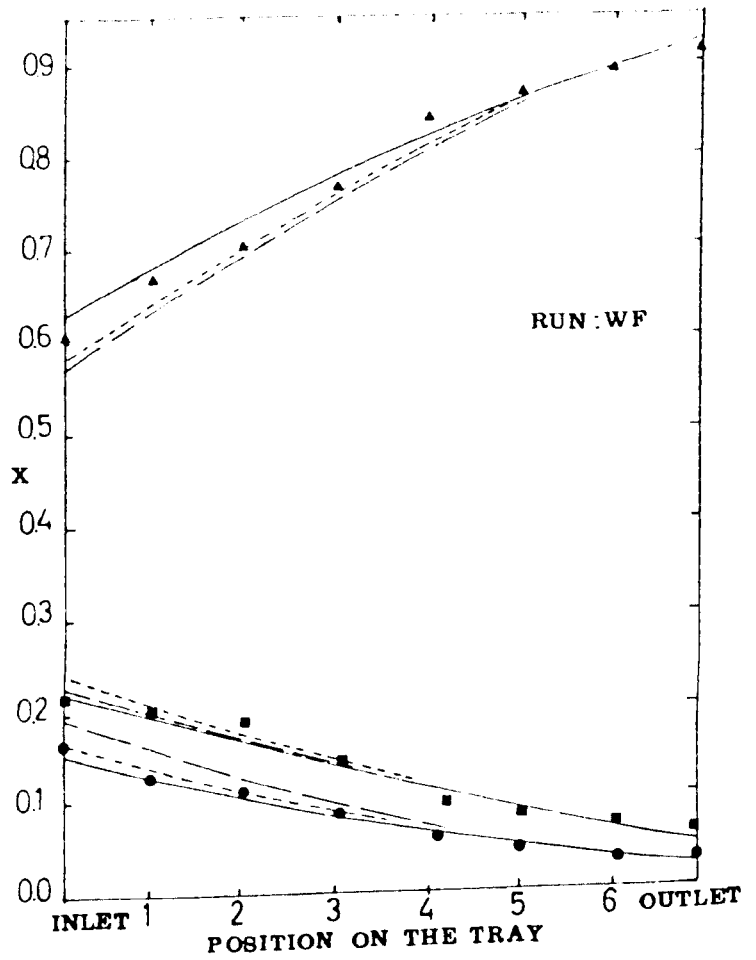
Figure 9.6 continued
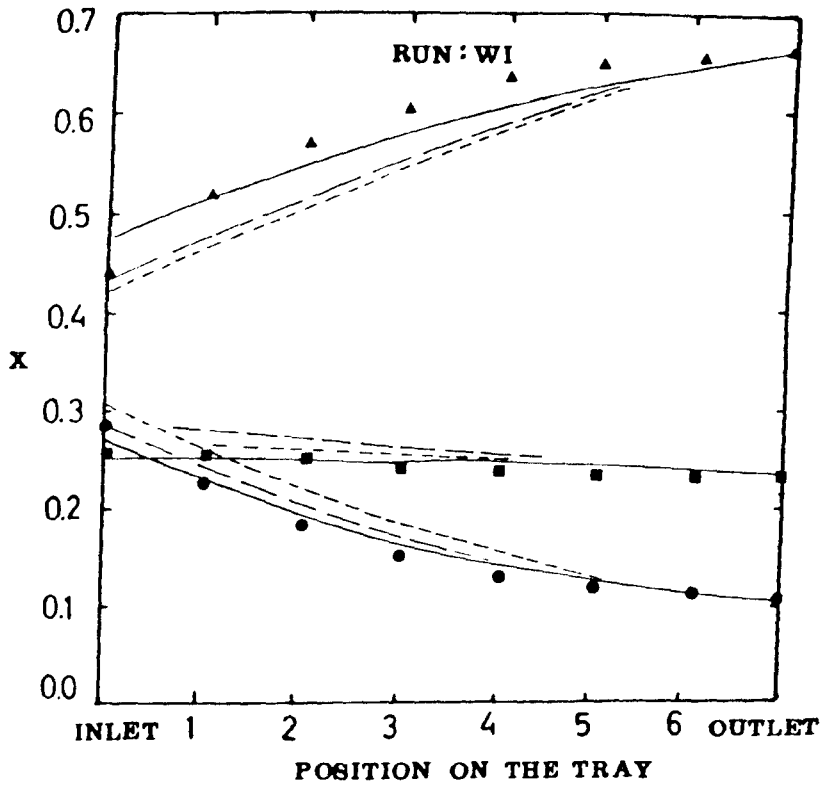
Figure 9.6 continued
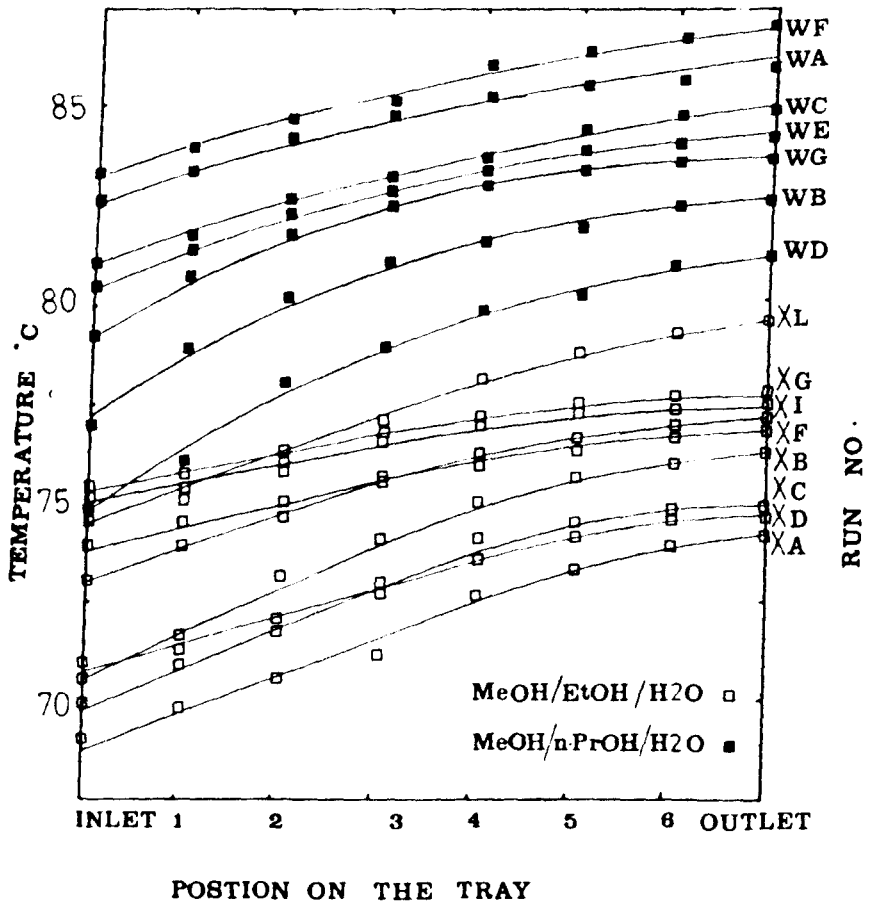
FIGURE 9.7: Temperature Profiles
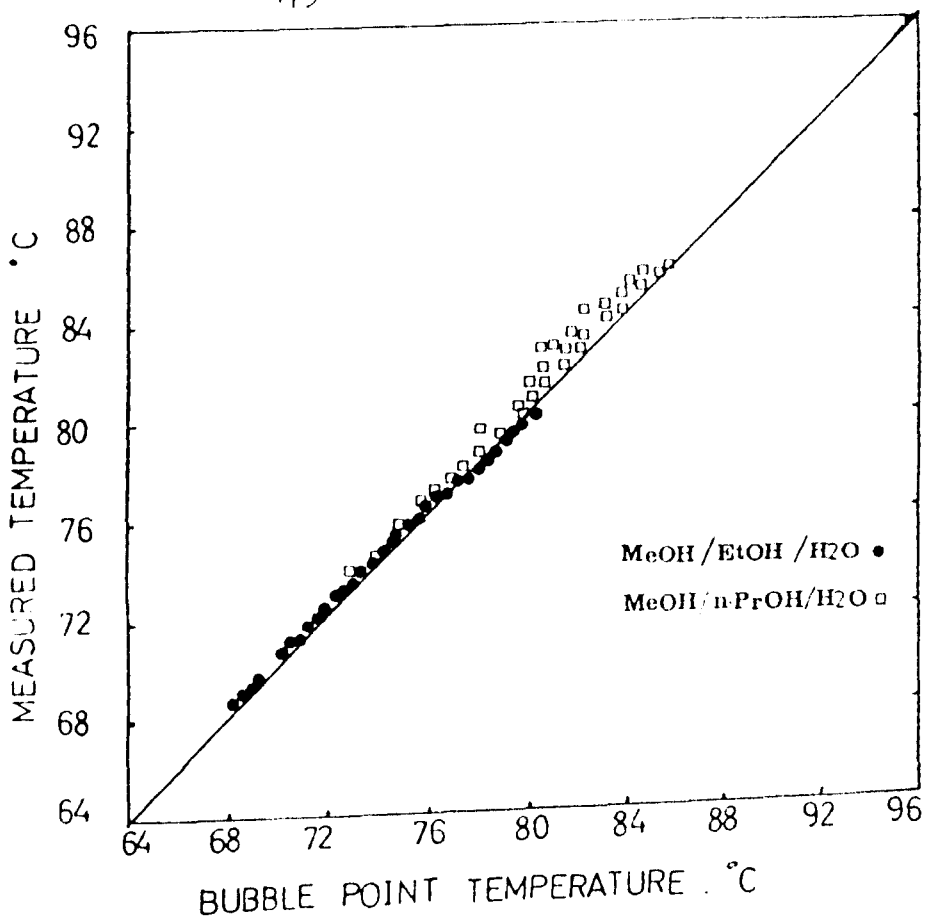
FIGURE 9.8; Comparison of measured and bubble temperatures
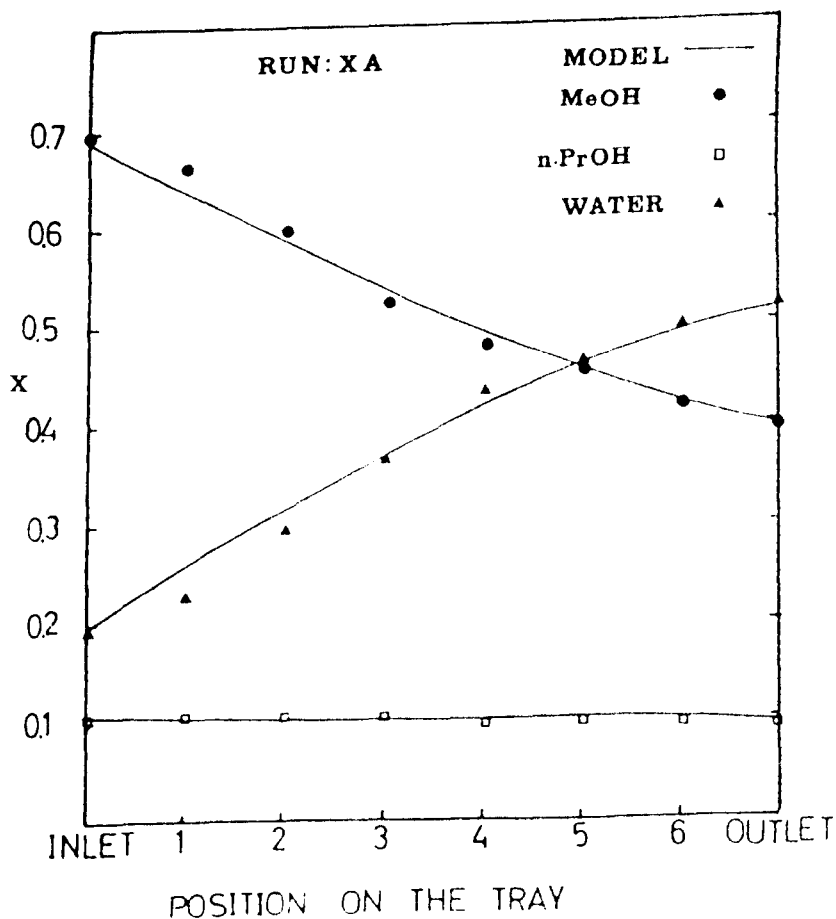
FIGURE 9.9: Composition profiles of MeOH/EtOH/H_2O system across the tray
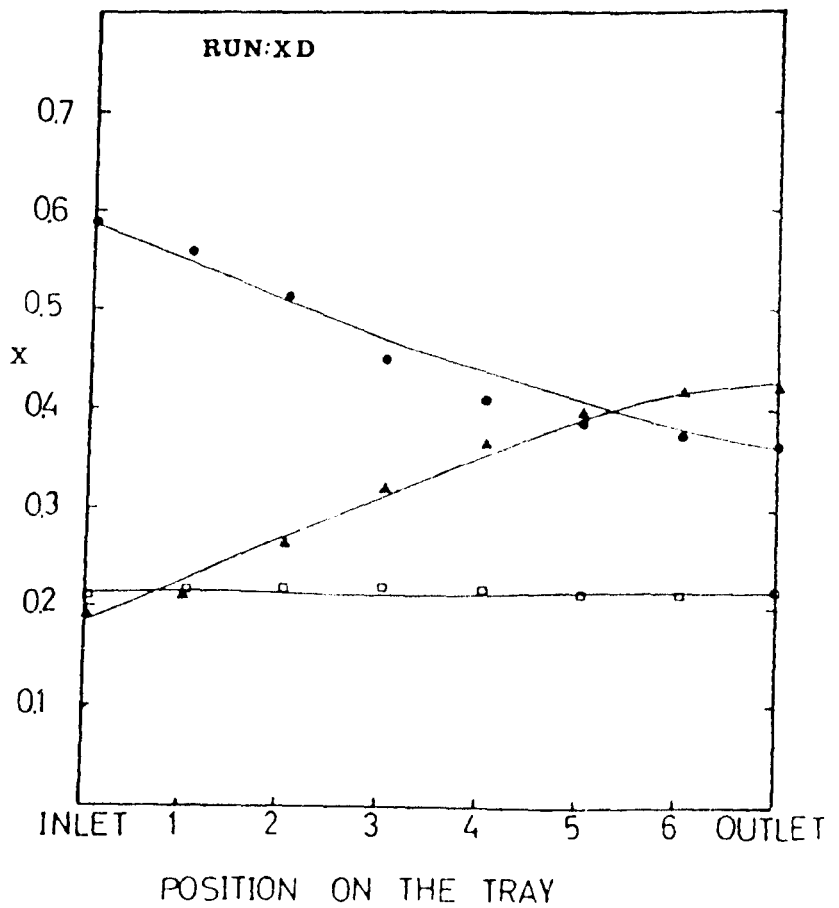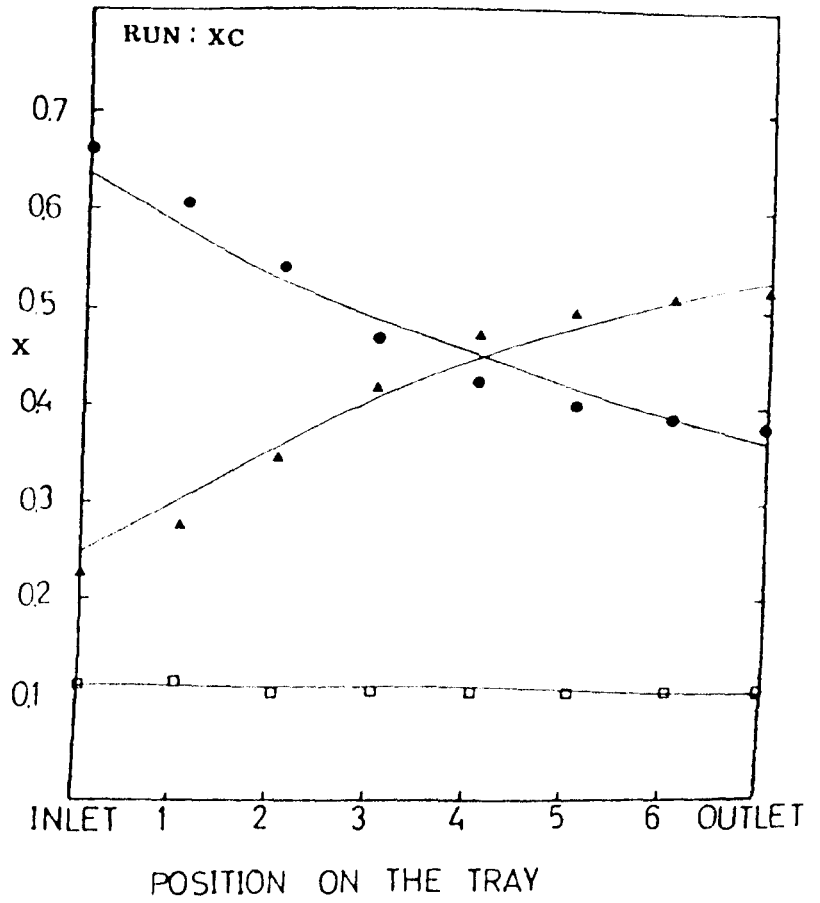
Figure 9.9 continued

Figure 9.9 continued

Figure 9.9 continued

Figure 9.9 continued

RUN:XK

POSITION ON THE TRAY

RUN:XL

POSITION ON THE TRAY
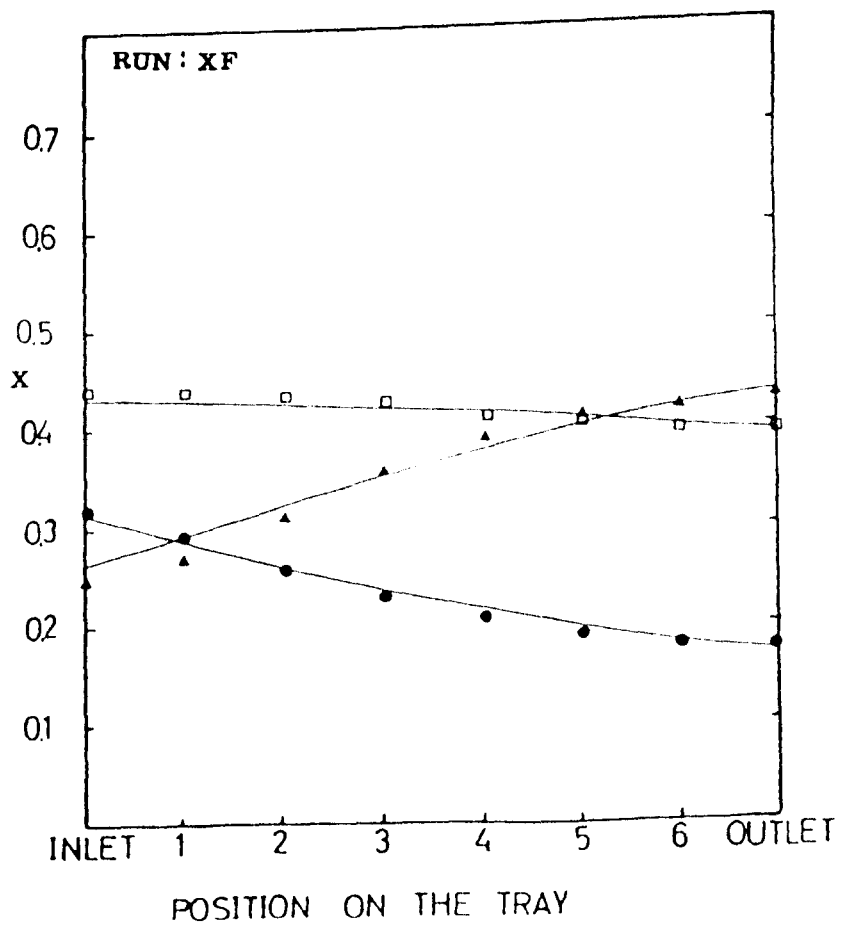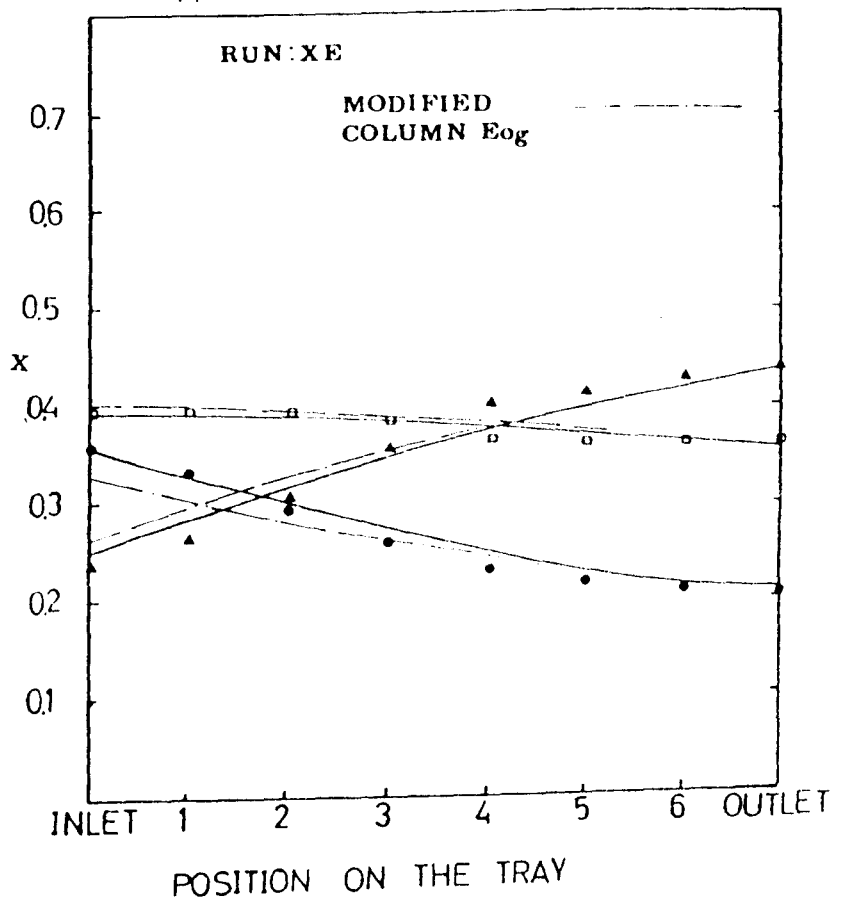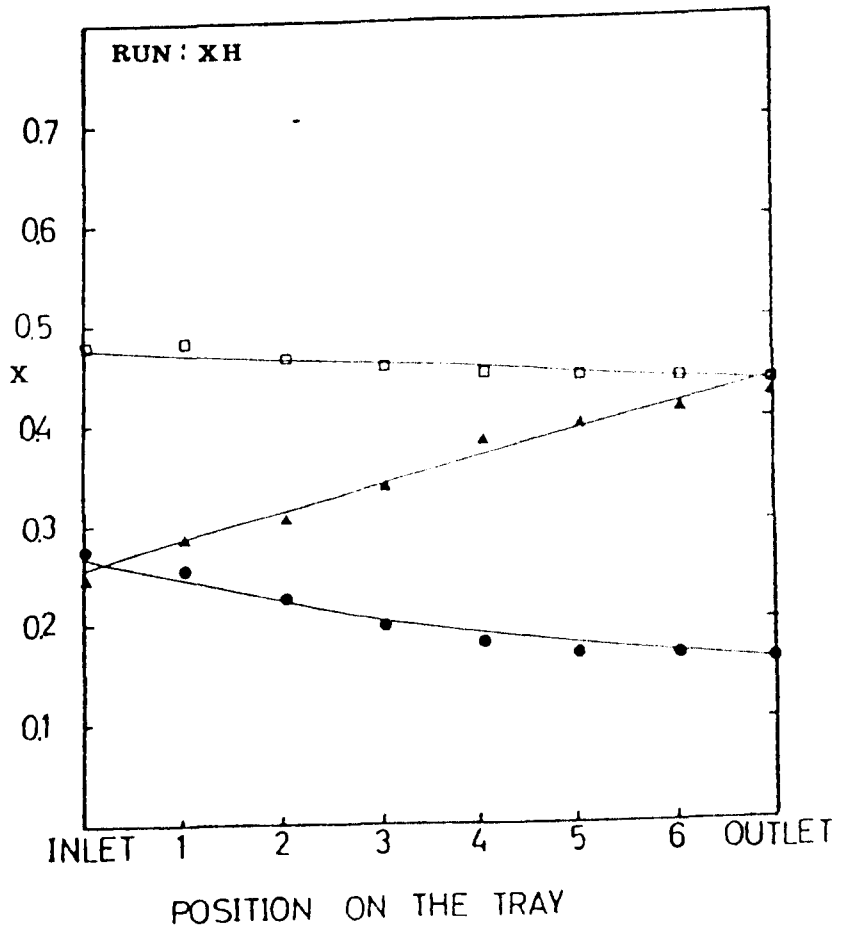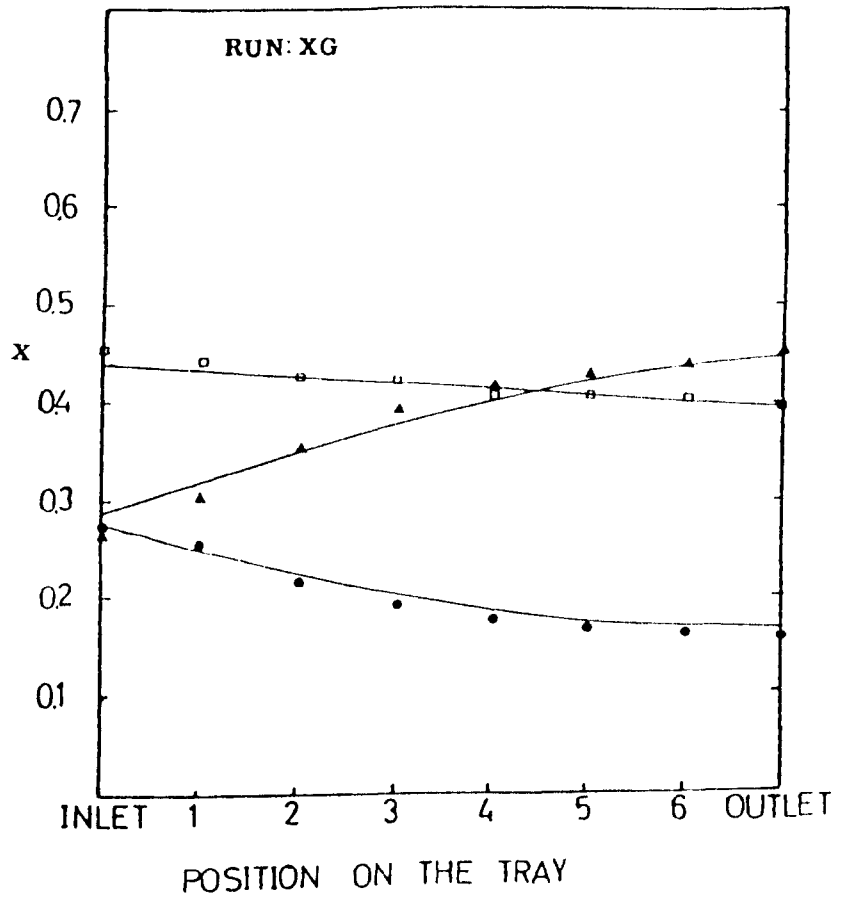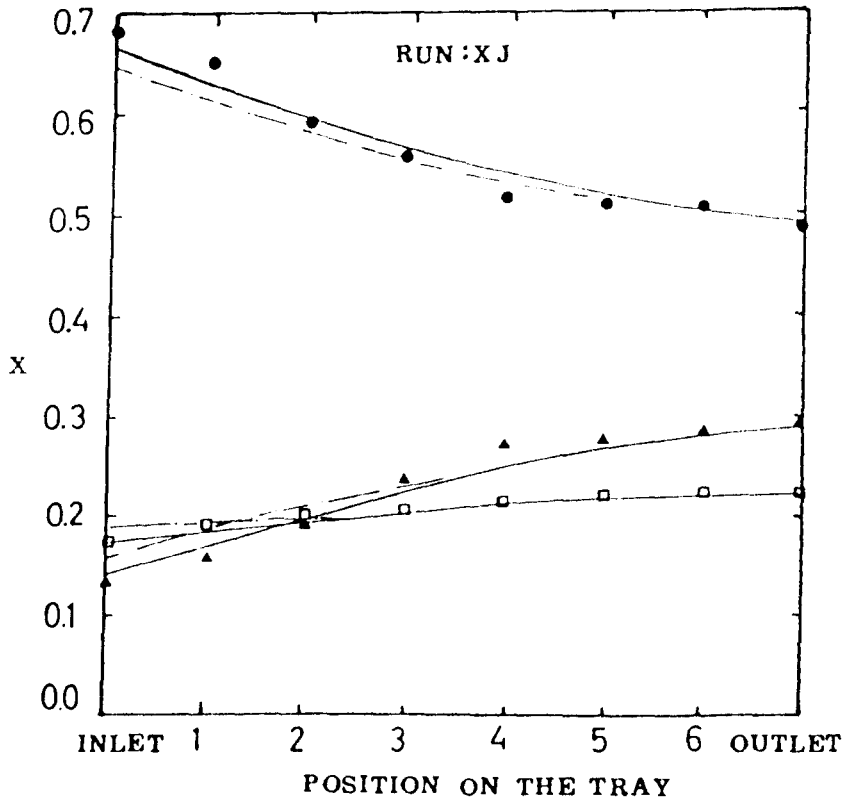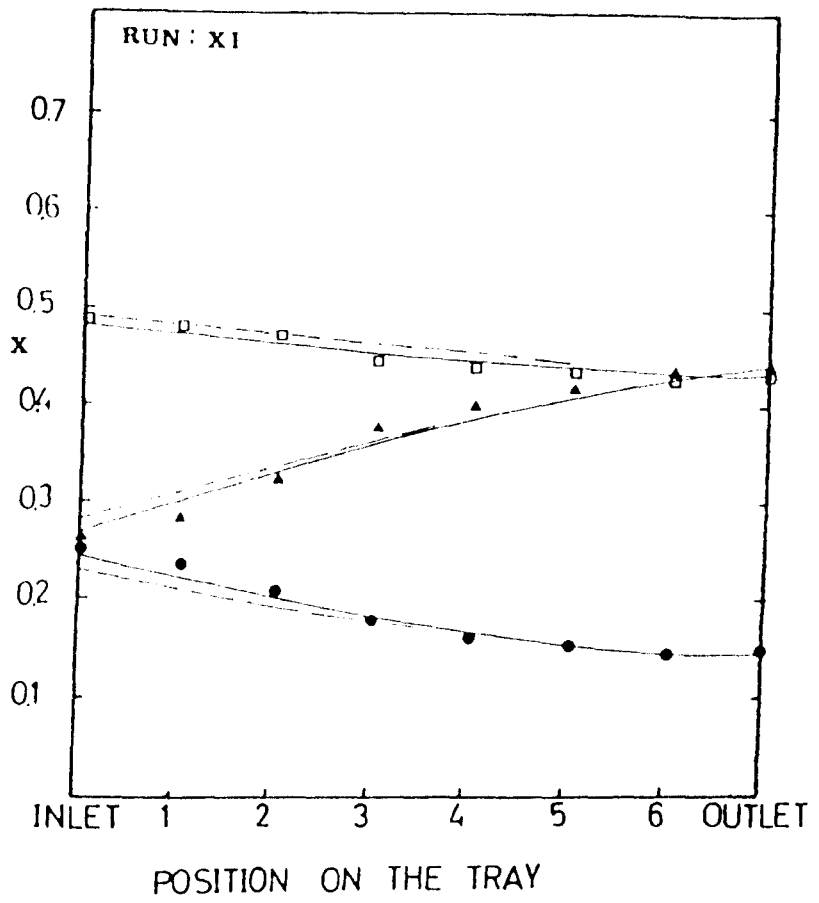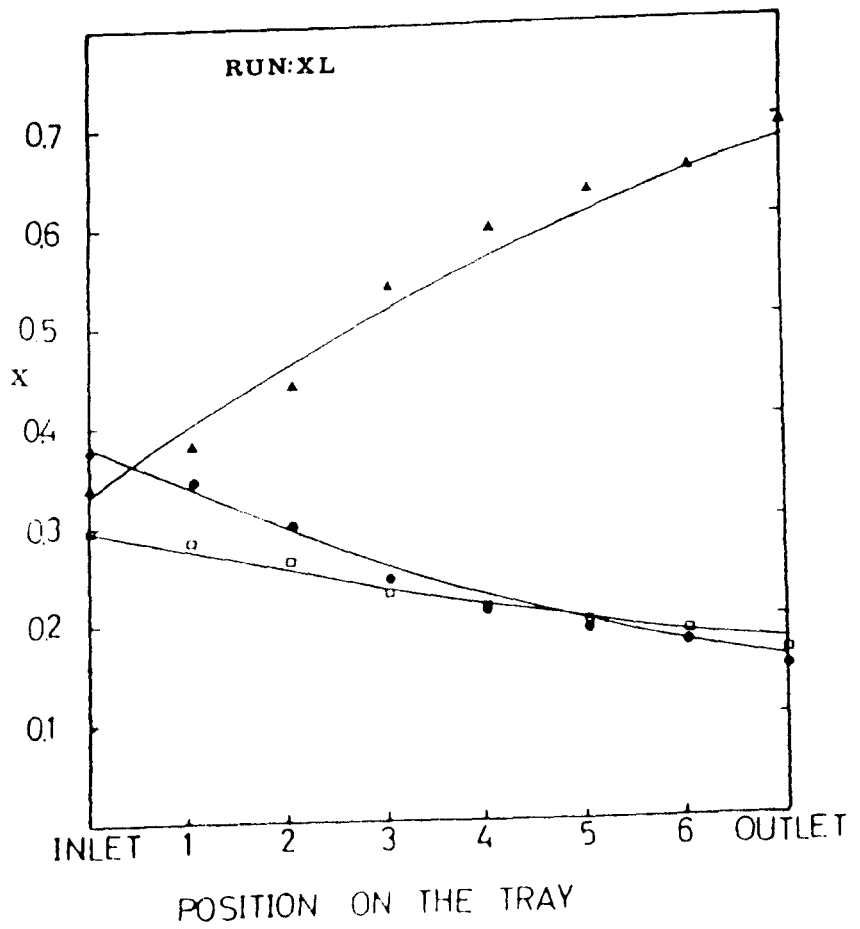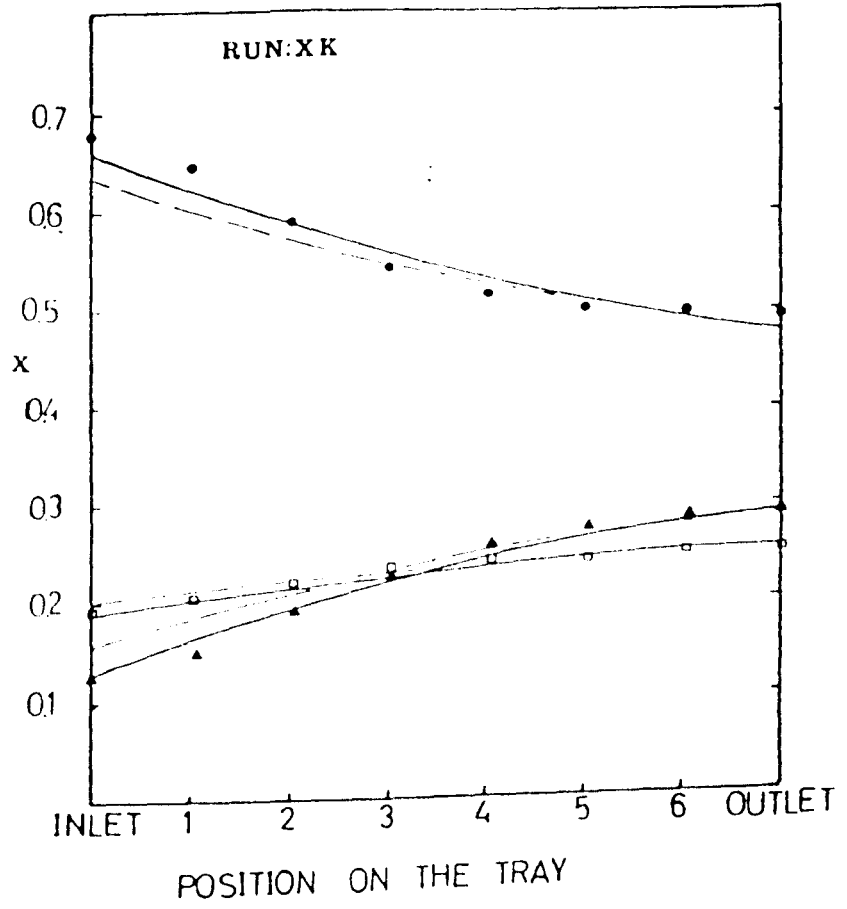
Figure 9.9 continued

CHAPTER 10

EFFICIENCIES OF A QUATERNARY SYSTEM

EFFICIENCIES OF A QUATERNARY SYSTEM

10.1 Introduction

The number of efficiency studies in multicomponent distillation is limited. The majority of these studies concern ternary systems and even less attention has been paid to systems with more components. (Gelbin 1965, Young and Weber, 1972).

In this chapter a distillation efficiency study of a thermodynamically non-ideal quaternary system of $MeOH/EtOH/n.PrOH/H_2O$ is introduced. For the first time the effect of liquid back mixing on the tray efficiencies of such a system is studied. This system was especially chosen to extend the knowledge of multicomponent distillation efficiencies where large non-idealities are present. This is due to large differences between the molecular sizes and polarities of these components, hence different point efficiencies were expected to operate due to the presence of interactions in both liquid and vapour phases. Figure 9.1 compares the binary gas diffusivities of the components constituting this system. As there are large differences between the diffusional mobilities of the alcohol-water and alcohol-alcohol pairs, according to Toor (1957), Krishna et. al. (1977), significant interactions are expected in this system in the vapour phase. In addition, the point efficiencies in this system are also expected to be composition dependent due to a greater liquid phase resistance associated with aqueous systems (Mostafa, 1979, Dribika, 1986). The middle components of this system are also expected to have maxima in concentration the same way as in the ternary systems (Cilianu et. al., 1974, Chapter 9). The adequacy of the Murphree definition of point efficiency to account for such behaviour has been tested. In Chapter 9, it was implied or demonstrated that some prediction methods can be used to estimate point efficiencies for the ternary system, from first principles, or if enough binary data

were available. These methods had their deficiencies as the non-idealities in the liquid phase were not known and hence not taken into account in the equations. It was also demonstrated that using point efficiencies measured in the modified Oldershaw column, predictions of the same order of accuracy as the predictive methods available were possible. In this chapter the same strategy is used to compare the point efficiencies obtained from a comparison of the small and large rectangular distillation columns.

Distillation runs were carried out in three plate-type distillation columns. Firstly the familiar rectangular column, secondly the modified Oldershaw column and thirdly a ten plate bubble cap column (the only non-sieve tray distillation device used for this thesis).

10.2 V.L.E. Data

The vapour-liquid equilibrium data for this system were not available in the literature, but binary measurements had been carried out and thermodynamically consistant Wilson parameters have been established (see Tables 4.1 and 9.2). In order to study the feasability of using these parameters, it was decided to measure the V.L.E. data for this system and to compare these with the predictions from the Wilson model using these parameters. An Ellis-Froome (1954) still was used to carry out the experiments at atmospheric pressure (see appendix B). A statistical test comparing the measured and predicted equilibrium data established the applicability of these parameters (see Table 10.1).

A computer model taking into account the non-idealities in the phases (Prausnitz et. al. 1967) was used to carry out the required computation of the vapour equilibrium composition (see appendix B).

Table 10.1   Statistical Analysis of Measured and Predicted Equilibrium
Data

Component No.	$\Sigma (X_i - X_{ip})/n$	███████	$\begin{vmatrix} x_{i_{min}} - x_{ip} \end{vmatrix}$
1	± 0.0115	0.0284	0.0003
2	± 0.0058	0.0342	0.0019
3	± 0.0117	0.0171	0.0008
4	± 0.0109	0.0199	0.0004

$\Sigma \, T\text{-}T_p / n$ ███████

$\begin{vmatrix} T\text{-}T_p \end{vmatrix}$ max   =   ███████

$\begin{vmatrix} T\text{-}T_p \end{vmatrix}$ min   =   ███████

10.3   Equipment

The details of the modified Oldershaw column and the rectangular columns are given in Chapters 4 and 5 respectively. The outlet weir of the 1.8 mm hole size tray was 25.4 mm in height (see Table 6.1).

███████   10 Plate Bubble Cap Column

The stainless steel column has 10 bubble cap plates, and a window is fitted above each plate. Each plate is provided with sample points and thermocouple points, the latter being located slightly above the plate in such a way as to allow temperature measurements of the biphase. Each elliptical tray contains 7 bubble caps and the tray spacing is 22.9 cm. The column and the bubble tray arrangements are shown in Figures 10.1 and 10.2. Further details of the column are given in Table 10.2.
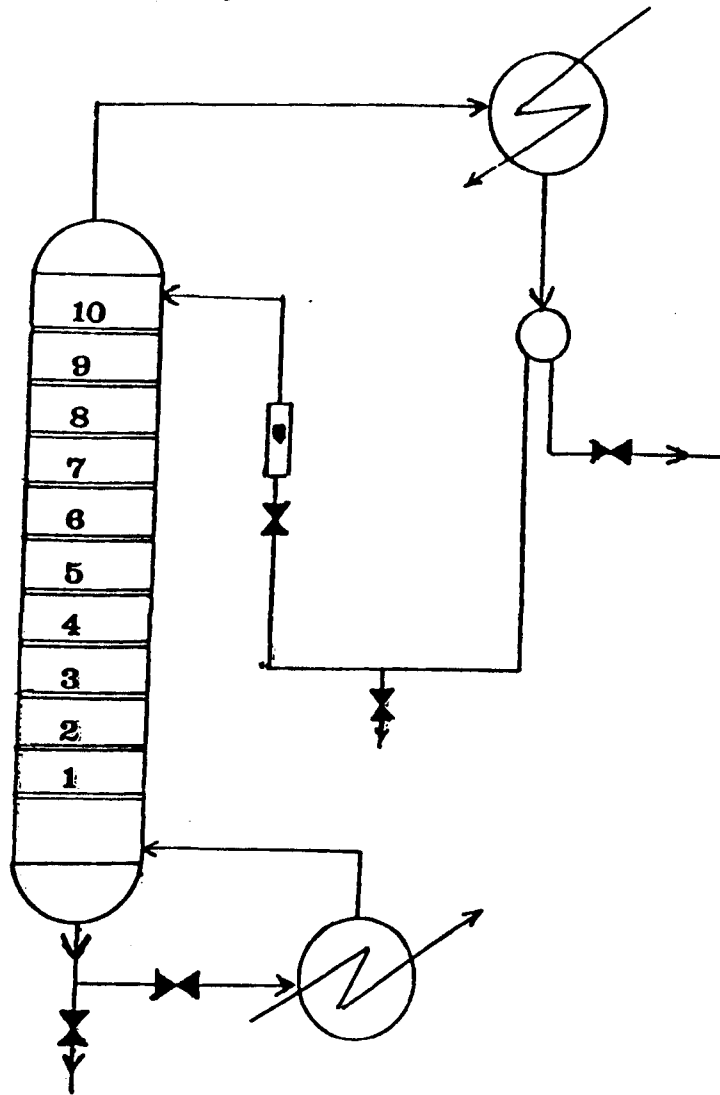
Fig. 10.1: **BUBBLE CAP COLUMN ARRANGEMENT**

○ **BUBBLE CAP**

⊛ **WEIR**
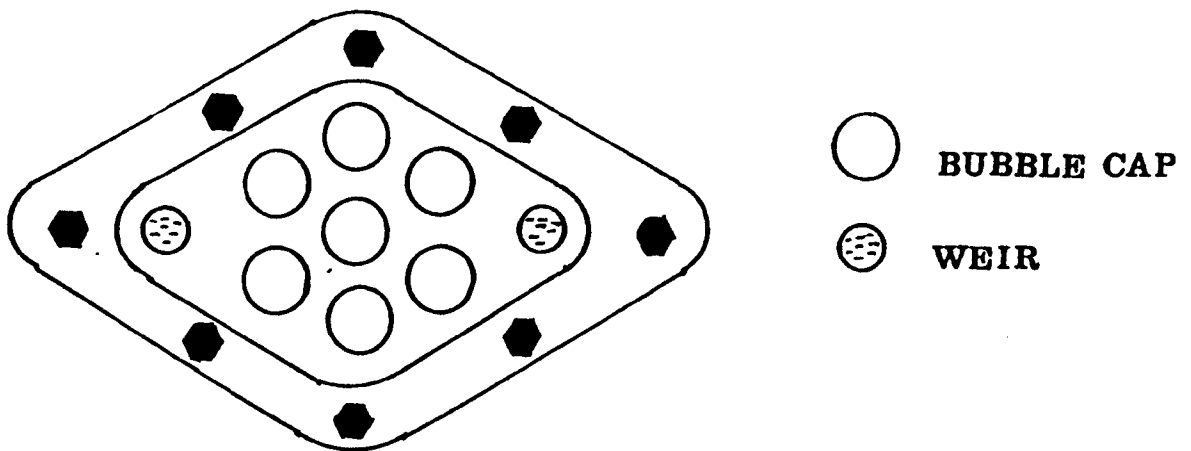
Fig. 10.2: **TRAY DETAILS**

The stainless steel reboiler is provided with an external steam jacket and an internal heating coil. The reboiler, having a capacity of 40 litres, was three-quarter filled with the test mixture. The condensers connected in series provided a total cooling area of 2 m^2, the reflux returning to the column via a calibrated rotameter. The column was insulated with glass wool and aluminium cladding to minimise heat losses.

Table 10.2   Tray Details of the 10 Bubble Cap Plate Column

Total Plate Area	197.4 cm^2
Plate Spacing	20.5 cm
Weir Height	2.54 cm
Downcomer Area	7.8 cm^2
Riser Diameter	3.1 cm
Total Riser Area	54.0 cm^2

10.4   Experimental

The experiments were carried out at total reflux and atmospheric pressure. Sufficient time was allowed to reach steady state conditions, the boil up rate and temperatures being noted in regular intervals. The operation of the columns was carried out at a vapour F-Factor of about 0.5 m/s $(kg/m^3)^{0.5}$, which provided stable hydrodynamic conditions on the tray. A wide range of composition was covered, and samples were collected into prechilled bottles and analysed by G.L.C. techniques giving an average error of $\pm$ 0.0045 in mole fraction, (see appendix D for further analysis details).

10.4.1 Theoretical Model

The eddy diffusion model (see Chapter 7) was used to match the composition profiles across the rectangular tray and along the bubble cap column.

10.5 Results

Observation of the biphase behaviour on the tray indicated steady hydrodynamic operation, with negligible entrainment and weeping. The main results from the studies in the three different columns were as follows:

10.5.1 Modified Oldershaw Column Efficiencies

The Murphree point efficiency, defined below, was calculated for the individual components.

$$E_{og} = \frac{y_{i,n+1} - y_{i,n}}{y^*_{i,n+1} - y_{i,n}} \qquad 10.1$$

where $y_{i,n}$, is the vapour inlet and $y_{i,n+1}$ is the vapour outlet mole fraction. The point efficiencies and the compositions are presented in Table 10.3. A wide range of composition was investigated and Figure 10.3 illustrates the variation of the point efficiency of methanol in the quaternary mixtures. These efficiencies are composition dependent and exhibit similar trends to those shown in the binaries methanol-water and methanol-n.propanol, (Chapters 4 and 7), that is a decrease in point efficiency at low methanol composition. The scatter in these results is

Table 10.3 Experimental Measurements of Modified Oldershaw Column

RUN NO	X1	X2	X3	X4	Eog1	Eog2	Eog3	Eog4
249	0.2610	0.0414	0.3475	0.3502	0.69	0.64	0.78	0.53
250	0.2584	0.0863	0.3232	0.3322	0.61	0.55	0.71	0.44
251	0.2154	0.2216	0.2778	0.2853	0.60	0.54	0.69	0.38
252	0.1953	0.2995	0.2471	0.2581	0.56	0.73	0.66	0.36
253	0.1662	0.3842	0.2216	0.2281	0.60	0.81	0.70	0.30
254	0.1423	0.4456	0.2039	0.2082	0.63	1.05	0.71	0.44
255	0.1116	0.4151	0.1811	0.2922	0.63	0.68	0.72	0.54
256	0.1010	0.4635	0.1639	0.2715	0.58	0.83	0.71	0.56
257	0.0864	0.5330	0.1398	0.2407	0.61	0.74	0.71	0.52
258	0.0762	0.4980	0.1533	0.2725	0.93	0.64	0.84	0.75
259	0.2019	0.3897	0.1291	0.2793	0.64	1.13	0.73	0.60
260	0.3607	0.2731	0.1060	0.2602	0.66	0.62	0.73	0.63
261	0.3795	0.2303	0.1018	0.2887	0.68	0.60	0.79	0.66
262	0.4496	0.1891	0.0916	0.2698	0.70	0.61	0.76	0.70
263	0.4782	0.1641	0.0938	0.2638	0.54	0.73	0.75	0.43
264	0.5331	0.1191	0.0981	0.2498	0.62	0.48	0.70	0.61
265	0.5321	0.0957	0.1057	0.2665	0.69	0.61	0.71	0.69
266	0.4539	0.0883	0.1293	0.3284	0.71	0.46	0.75	0.71
267	0.3968	0.0825	0.1521	0.3686	0.70	0.21	0.75	0.67
268	0.3387	0.1071	0.1650	0.3892	0.68	0.75	0.76	0.66
269	0.3157	0.0819	0.1986	0.4037	0.66	0.70	0.80	0.63
270	0.3527	0.0643	0.1924	0.3906	0.69	0.72	0.76	0.66
271	0.4406	0.0491	0.1514	0.3589	0.73	0.36	0.78	0.72
272	0.4101	0.0488	0.1603	0.3808	0.73	1.23	0.77	0.72
273	0.3343	0.0478	0.1851	0.4328	0.77	0.67	0.92	0.72
274	0.3859	0.0805	0.1451	0.3905	0.72	0.97	0.79	0.71
275	0.3228	0.0782	0.1634	0.4356	0.73	0.66	0.80	0.70
276	0.2894	0.0753	0.1734	0.4619	0.71	0.71	0.90	0.68
277	0.2148	0.2723	0.1002	0.4127	0.74	0.71	0.85	0.71
278	0.1786	0.3647	0.0692	0.3875	0.69	0.78	0.86	0.69
279	0.1450	0.4401	0.0469	0.3680	0.67	0.78	0.90	0.68
280	0.1293	0.4799	0.0367	0.3540	0.67	0.79	0.87	0.89

caused by the influence of varying composition of the other components. The middle component, ethanol, shows the largest variation in point efficiency, due largely to errors occurring in the calculation as the K-value approaches unity, (Figure 10.4). Medina et. al. (1979) showed that experimental errors can be very significant under these conditions, since the numerator and the denomenator of equation 10.1 are of the order of the experimental error. As expected, the individual components of this non-ideal system were also shown to exhibit different point efficiencies.

The K-values required were provided from the V.L.E. data. The liquid and vapour enthalpies were available from steam tables and Chopey Hicks (1984), (see appendix C). A Peclet number of 39 was used, as before, incorporated into the model to account for the liquid back-mixing on the rectangular tray. For the simulation of the ten plate column, complete liquid mixing was assumed and hence a Peclet number of zero was used. This is reasonable as the tray bubbling area in the bubble cap column is small. The biphase height was also measured to be approximately 2.2 cm throughout.

10.5.2   Bubble Cap Column Efficiencies

A few experimental runs were made using the 10 plate bubble-cap column to establish concentration profiles along the column when large changes in individual component concentrations occurred. The active area of the tray is small enough to assume complete mixing in the liquid phase. A total of four runs were made at atmospheric pressure and total reflux, the resulting composition profiles being presented in Figure 10.5. The profiles could be satisfactorily simulated by using equal component efficiencies for runs A and B, whereas runs C and D required unequal individual component point efficiencies in some composition regions. The

consequence of using the best equal component point efficiencies is shown in Figure 10.5, run C (dashed line), and this resulted in significant deviations from the measured composition profiles. The experimental component point efficiencies are compared with the computer predictions (using unequal and equal (dashed lines) point efficiencies for run C) of point efficiencies, in Figure 10.6. These experimental component point efficiencies vary from one tray to another, probably due to the errors involved in sampling, and so no definite conclusion regarding the comparison of component point efficiencies can be reached using these data. However, the computer simulation of these runs does indicate that unequal individual component point efficiencies do best represent runs C and D. It can also be seen that for these two runs point efficiencies greater than one were required for water on some trays, but these values were strongly dependent on the choice of efficiencies for the other three components.

10.5.3   Rectangular Column Efficiencies

The measured concentration profiles were matched with those predicted using the eddy diffusion model to infer point efficiencies. This involved guessing and re-guessing component point efficiencies until a good match was achieved. Table 10.4 summarises the results of all these measurements. Figures 10.7 and 10.8 illustrate the composition and temperature profiles. A comparison is also made (Figure 10.9) between the measured temperatures and computed bubble point temperatures for this system, showing a tendency to values slightly above the bubble point temperature. This is probably the result of heat transfer from the vapour phase. Table 10.5 also compares the deviation between the measured and predicted values of tray effic-iencies. As before, it appears that different individual component point

TABLE 10.4 Experimental and Predicted Results of Rectangular Column

RUN	MEAN COMPOSITION				TRAY EFFICIENCY								POINT EFFICIENCY			
	X1	X2	X3	X4	MEASURED				MODEL							
					Emv1	Emv2	Emv3	Emv4	Emv1	Emv2	Emv3	Emv4	Eog1	Eog2	Eog3	Eog4
VA	0.1959	0.0455	0.4067	0.3518	1.32	1.21	1.39	-11.60	1.14	1.16	1.31	-11.98	0.68	0.95	0.90	0.16
VB	0.2373	0.0668	0.3229	0.3733	1.26	0.97	1.40	0.92	1.18	1.07	1.37	0.74	0.71	0.88	0.94	0.34
VC	0.2712	0.0804	0.2854	0.3629	1.27	0.87	1.38	1.09	1.23	0.89	1.36	1.03	0.74	0.82	0.92	0.56
VD	0.2824	0.0898	0.2649	0.3629	1.27	0.88	1.43	1.06	1.02	0.83	1.41	0.96	0.74	0.82	0.95	0.53
VE	0.1076	0.0649	0.2092	0.6182	1.59	1.42	0.44	1.03	1.75	1.27	0.46	1.07	0.80	0.80	0.80	0.80
VF	0.1646	0.0776	0.1985	0.5593	1.31	1.16	0.04	1.03	1.27	1.05	0.46	0.94	0.72	0.80	0.30	0.79
VG	0.1710	0.0702	0.1885	0.5703	1.21	1.03	-0.39	0.99	1.09	1.05	0.001	0.94	0.65	0.79	0.60	0.69
VI	0.3049	0.1640	0.1011	0.4300	1.34	0.82	2.52	1.15	1.26	0.77	-0.24	0.80	0.78	0.98	0.80	0.79

- 191 -

efficiencies were operating across the tray for the majority of the runs. The measured individual component tray efficiencies were significantly different, with equal or unequal point efficiencies operating across the tray. The average froth height on the tray was about 7 cm throughout.

Table 10.5   Statistical Comparison of Measured and Model Tray Efficiencies

Component	$\sum (E_{mvi}, \text{ measured} - E_{mvi}, \text{ model})/n$
1	± 0.11
2	± 0.07
3	± 0.03
4	± 0.12

10.6   Discussion

10.6.1

The study of this highly non-ideal system highlights the possible effects of diffusional interactions which, according to Toor (1957) and Krishna et. al. (1977), arise from the presence of reverse diffusion, osmotic diffusion or diffusion barrier. It is assumed that these effects must be responsible for such large variation in individual component point efficiencies. The system used here is particularly interesting as there are two "middle" components which can transfer from the liquid to vapour or vice versa. These middle components also reach maxima in concentration where their mass transfer reach minima. In the majority of the tests n.Propanol was transferred from the vapour to the liquid and its point efficiencies were in general higher than the other components. Ethanol,

however, showed a more confused picture. There were some experiments, (A, B and VE), where approximately equal component point efficiencies appeared to be operating across the tray. The maximum variation in individual component point efficiencies was obtained when one of the middle components reached its composition maximum. In this region errors become very significant.

10.6.2

The Murphree definition of point efficiency clearly has its limitations, especially for the components reaching a maximum in concentration. Under these circumstances the magnitudes of the numerator and the denominator of equation 10.1 become comparable with the experimental errors (Medina et. al. 1979), and meaningless values of point efficiency are obtained for that component. By using the mathematical model over a range of composition, more reliable point efficiencies can be obtained for the component which has reached its maximum in concentration (Figure 10.6). However, it is also important to note that when a component reaches a maximum in concentration, its vapour composition becomes independent of the point efficiency and the efficiency obtained by equation 10.1, although possibly unusual, has little influence on the evaluation of the vapour composition.

10.6.3

The component tray efficiencies in this system are significantly different from each other. Run VE shows large differences between individual component tray efficiencies despite approximately equal component point efficiencies operating across the tray. These differences result

from the effect of limited backmixing (Biddulph, 1975 and Biddulph and Ashton, 1977).

10.6.4

The eddy diffusion concept was found to model and predict the profiles and the differences in component tray efficiencies. Table 10.5 shows the deviation in measured and predicted component tray efficiencies. The efficiencies of the components which exhibited a maximum in composition were excluded from this evaluation as errors had infl:... d the computation of the tray efficiencies (Medina et. al. 1979). I. can be seen that these deviations are reasonable.

10.6.5

The point efficiencies were found to be composition dependent, as in the case of some of the constituent binaries, namely ethanol-water, methanol-water, n.Propanol-water and n.Propanol-water (see Chapters 4 and 6).

10.6.6

The measured tray efficiencies, shown in Table 10.4, indicate that high efficiencies can be obtained if the detrimental influences of flow non-uniformities and stagnant zones, which are known to reduce the tray efficiency, are eliminated. This provides further evidence for the high efficiencies available to the design engineer if these effects can be eliminated to improve the hydraulic behaviour of conventional circular trays.

10.6.7

The point efficiencies measured in the modified Oldershaw Column are lower than the point efficiencies deduced from the rectangular column experiments. This is the result of shorter contact time between the vapour and liquid in the smaller column (see Chapter 8). The individual components follow similar variations in point efficiencies in both columns. Table 10.6, compares these differences for three pairs of similar composition experiments. The more and least volatile components demonstrate the least differences in point efficiencies. The middle components show larger differences which are the result of the experimental errors on the computation of point efficiencies for these components as they exhibit either neglibible or small volatilities. If a small column is to be used for direct measurements of point efficiency for the design of a multi-component distillation column, it will involve a number of experiments covering a wide range of composition, identifying the components exhibiting maxima in composition and measure point efficiencies for these components on the other side of the maximum. This will reduce the possibility of experimental errors in point efficiency measurements.

These point efficiencies were then incorporated into the eddy diffusion model to simulate their corresponding runs, and hence predict composition profiles across the tray. The lines are included in the composition profile diagram (Figure 10.7) for the runs VI, VD and VC. The prediction seems very reasonable considering the low liquid hold up and hence lower point efficiencies obtained in the modified column. The tray efficiencies predicted for individual components are also included in the Table 10.6, together with their deviation from the original rectangular tray measurements.

The improvement in the liquid hold-up, and hence the point efficiencies, measured in the modified column (Chapter 8) may suggest that even better results are possible with relative ease and accuracy.

Table 10.6 Deviation between the Modified Oldershaw Column and Rectangular Column Point/Tray Efficiencies and Tray Efficiencies of the Rectangular Column Using the Modified Column Eog's

Runs	$Eog,_{irecta} - Eog,_{imodif}$				$Emv,_i$ Modif				$Emv,_{irecta} - Emv._{imodif}$			
	1	2	3	4	1	2	3	4	1	2	3	4
VI and 268	0.1	0.23	0.04	0.13	1.03	0.61	2.52	0.83	0.32	0.21	0.01	0.32
VD and 250	0.13	0.27	0.29	0.09	0.92	0.53	0.95	0.83	0.35	0.34	0.47	0.23
VC and 249	0.05	0.18	0.14	0.03	1.11	0.64	1.08	1.06	0.16	0.34	0.30	0.04
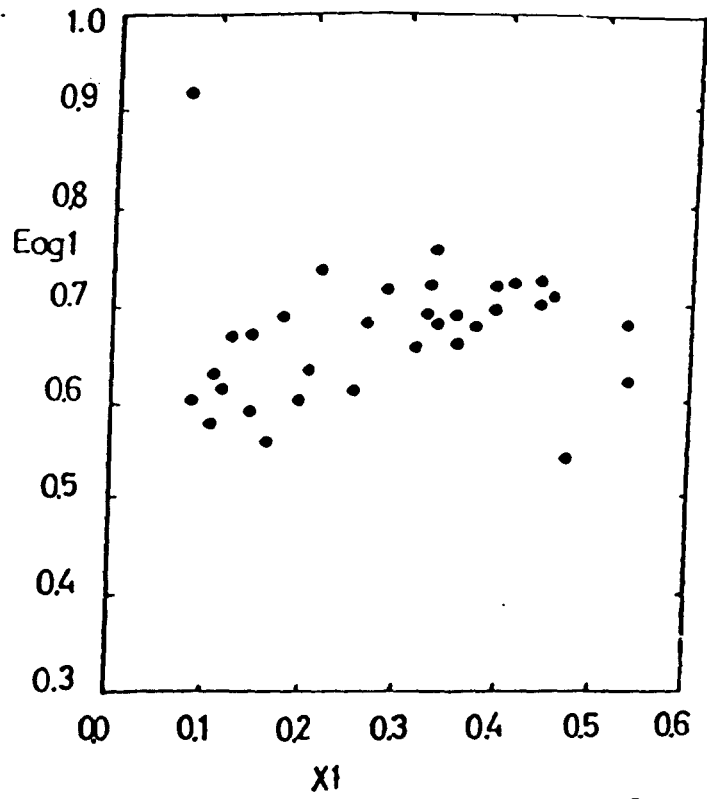
FIGURE 10.3 Point efficiencies of Methanol in the Quaternary System
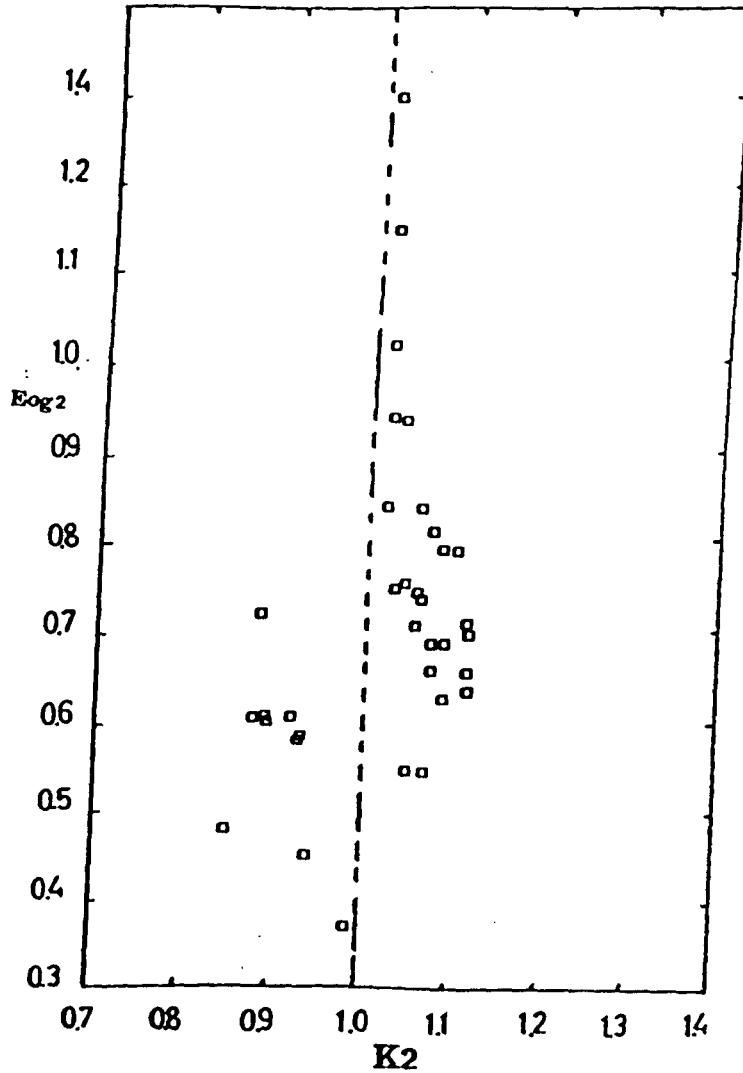
FIGURE 10.4 Point efficiencies of ethanol in the quaternary system
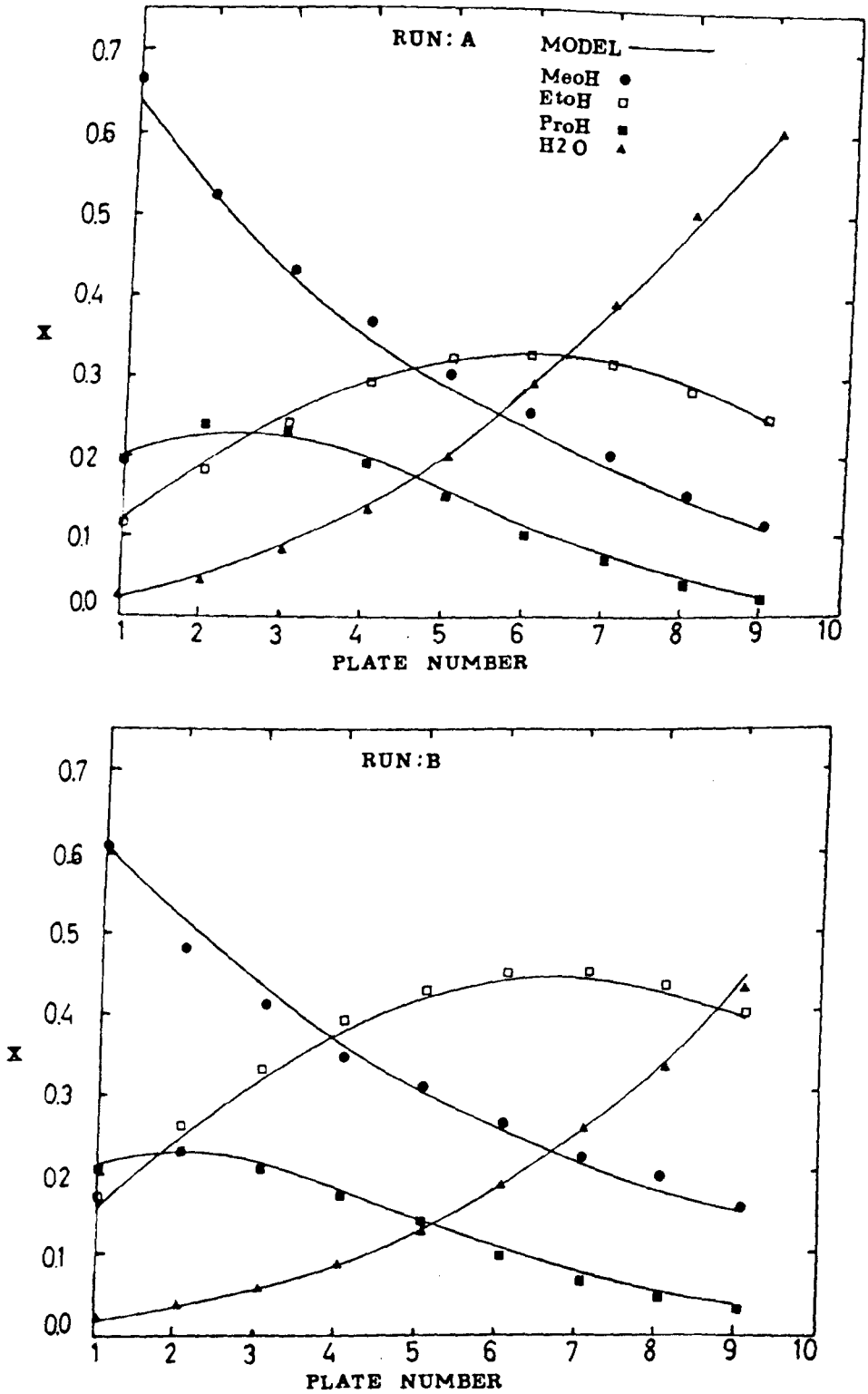
FIGURE 10.5 Composition profiles along the bubble cap column
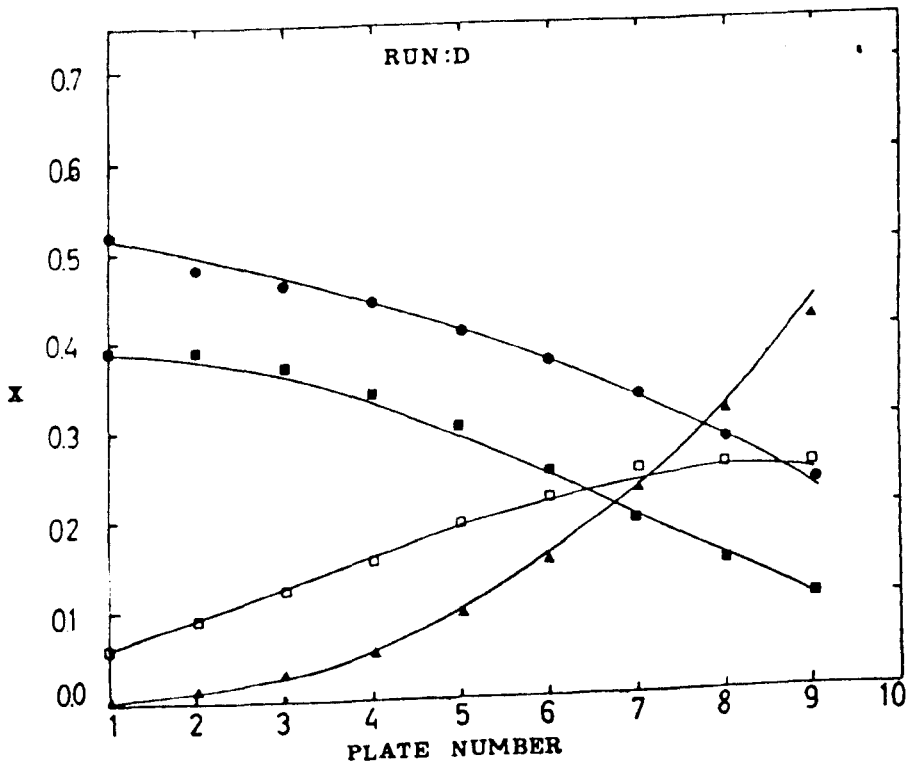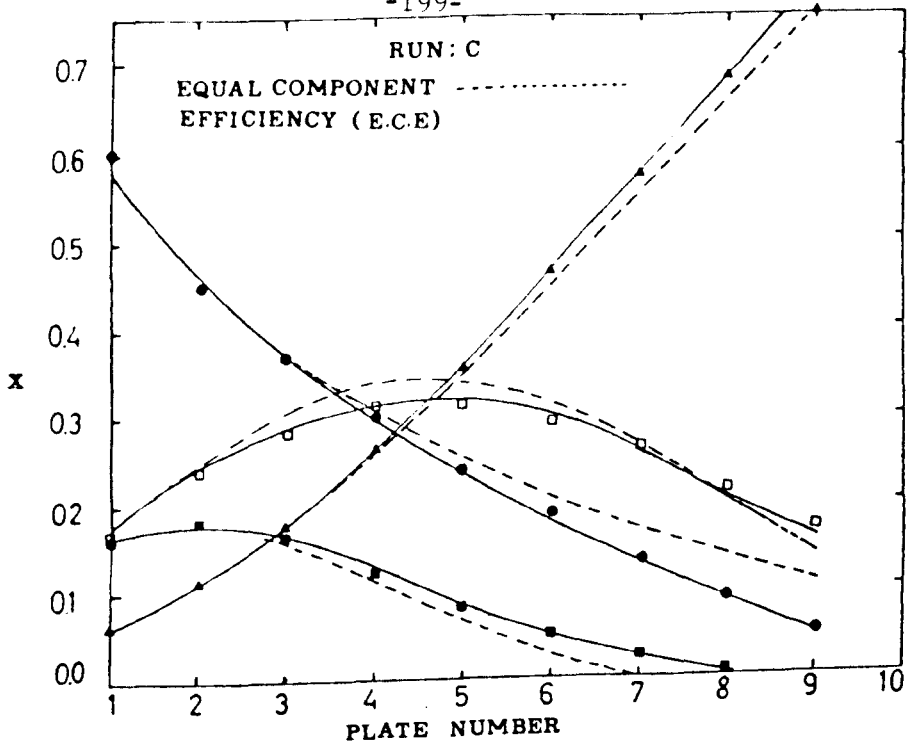
FIGURE 10.5 continued
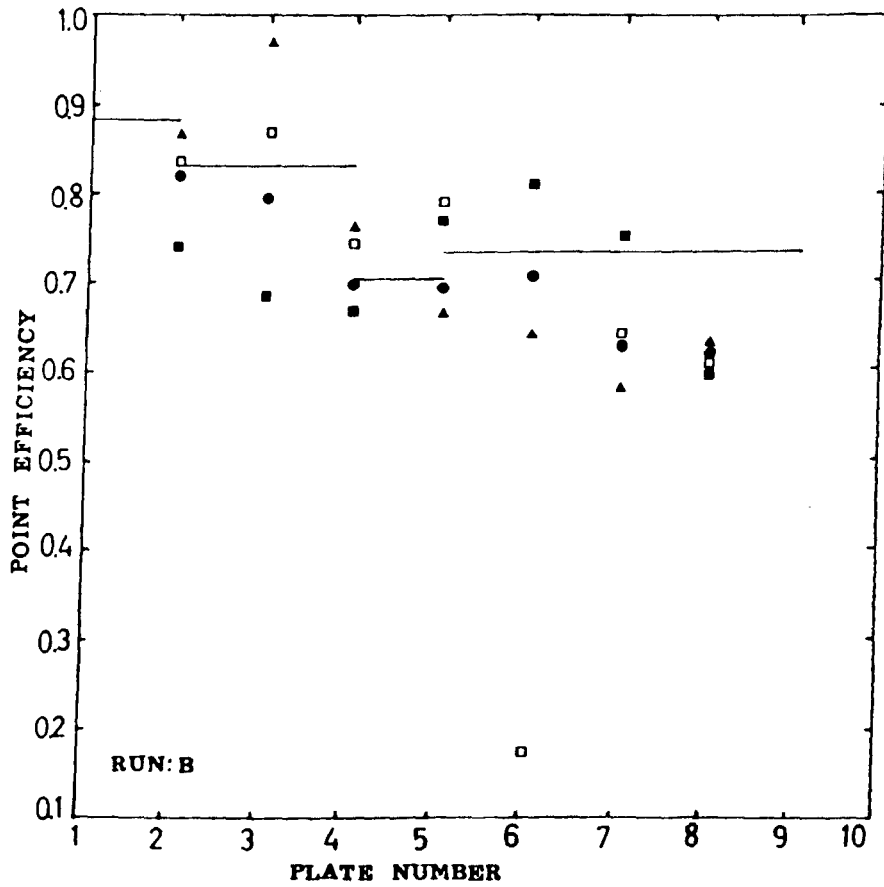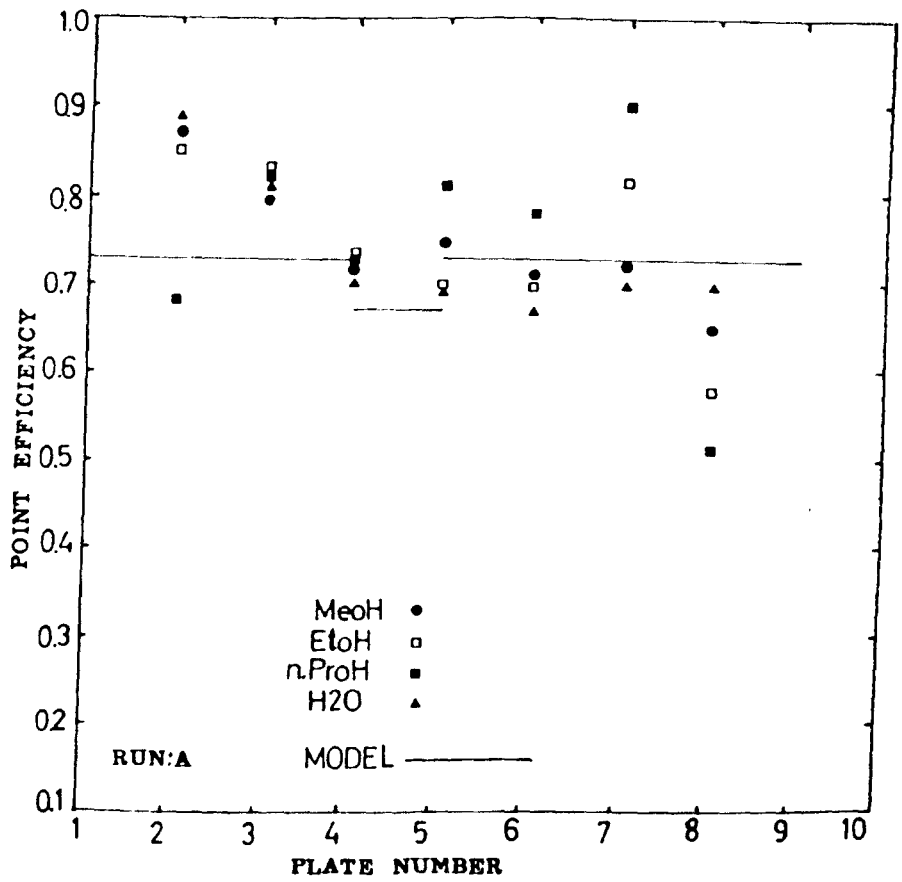
FIGURE 10.6 Point efficiencies along the bubble cap column
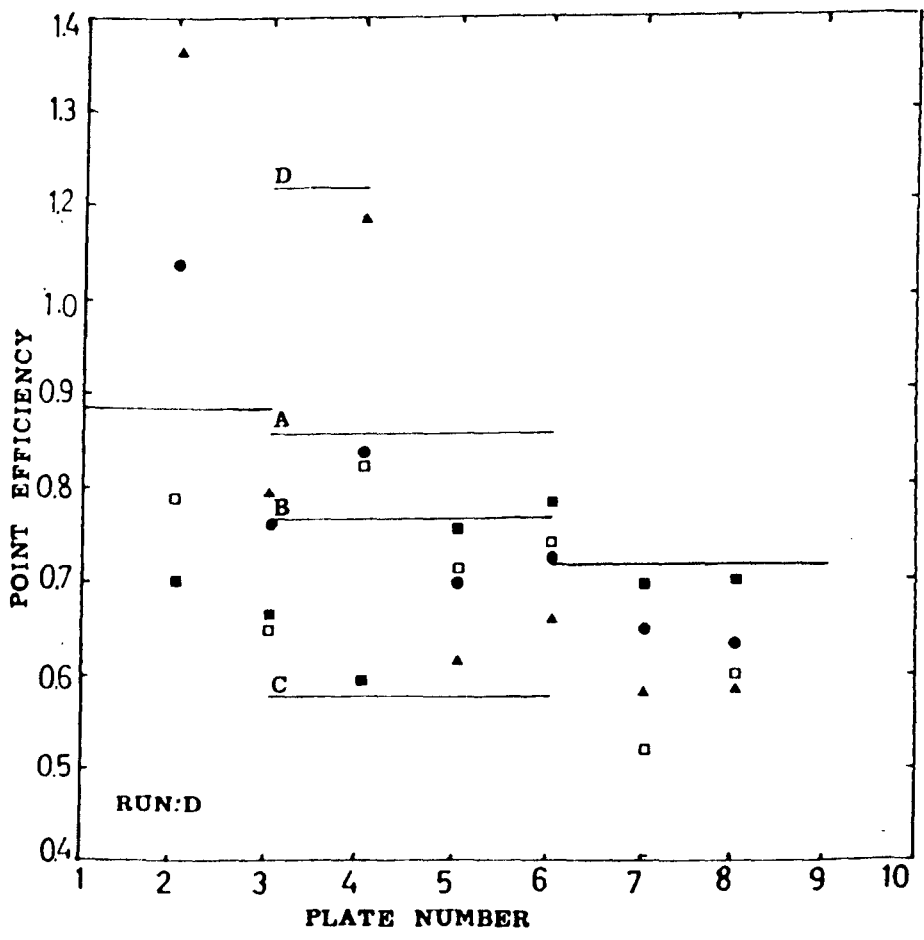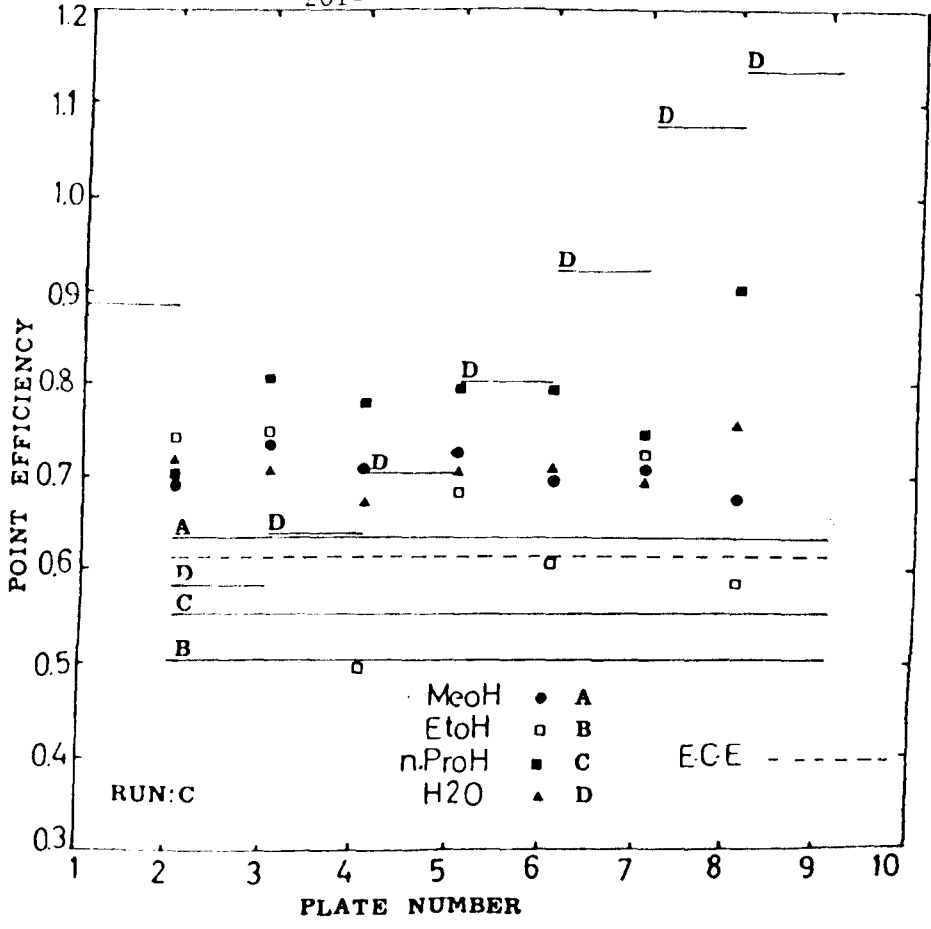
Figure 10.6 continued
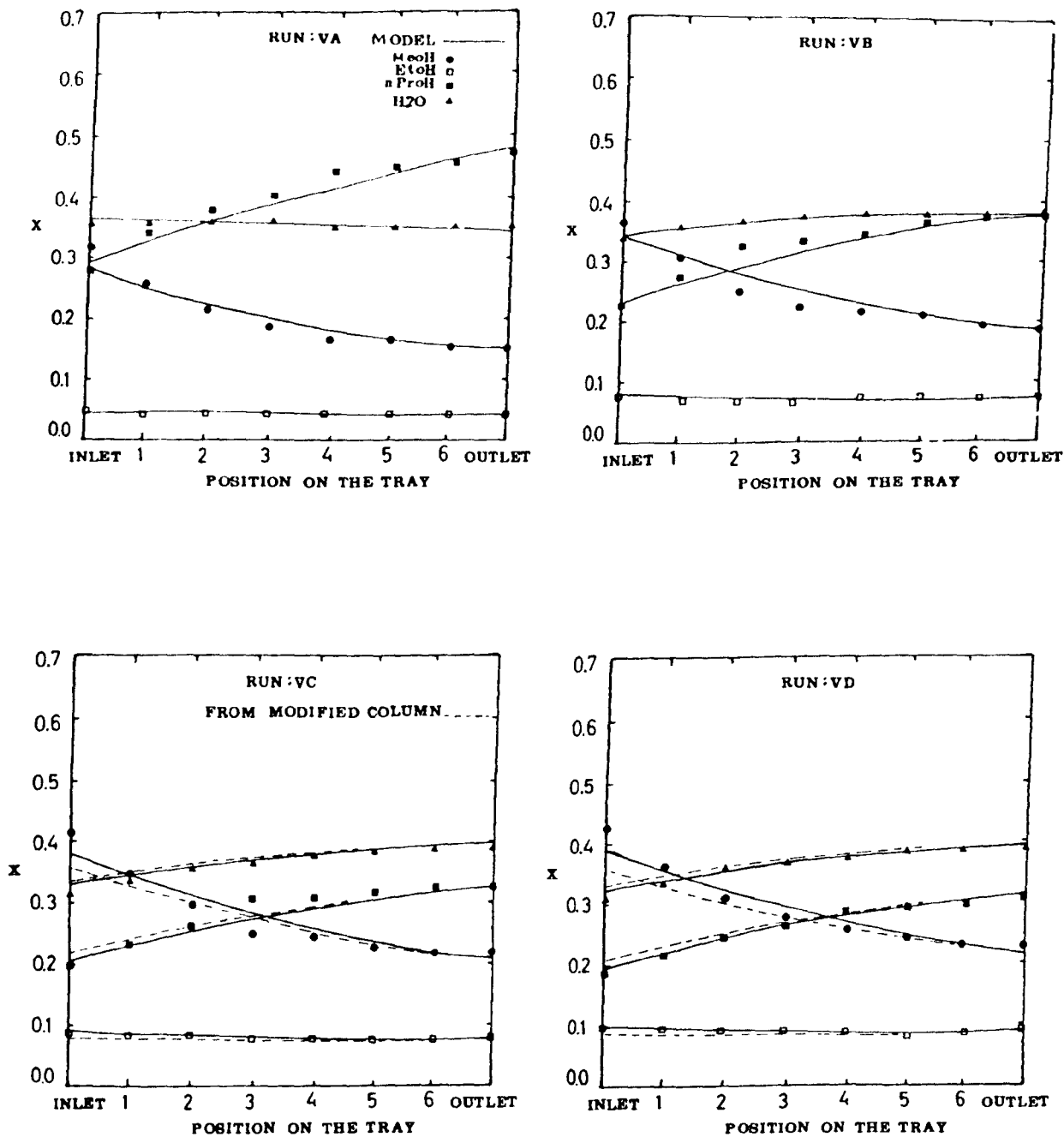
FIGURE 10.7 Composition profiles across the rectangular tray
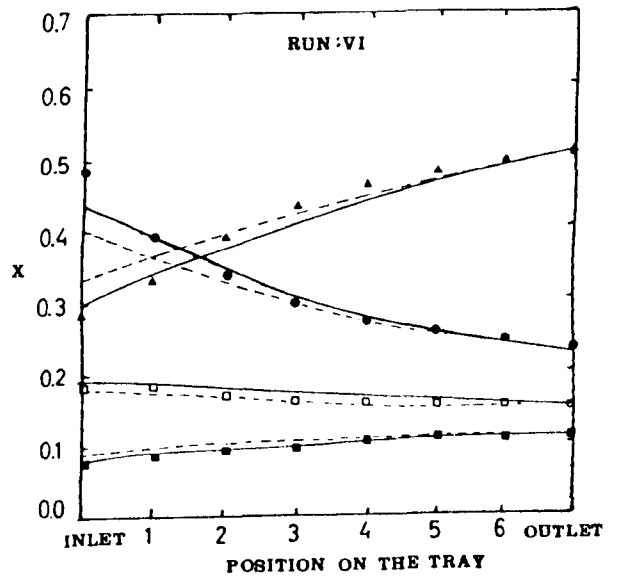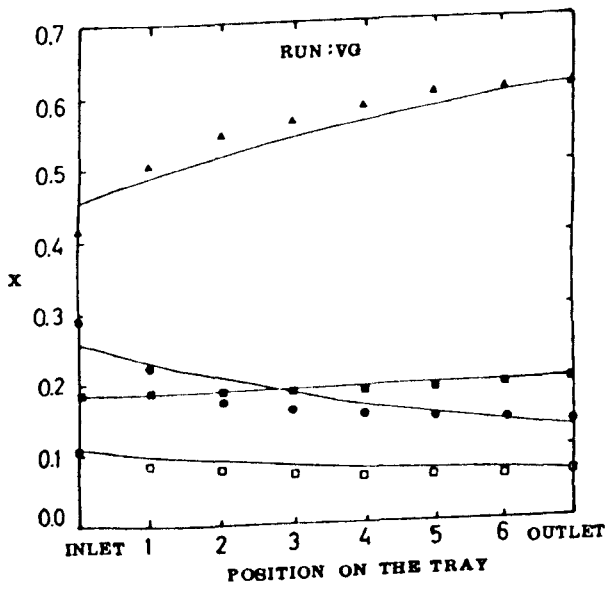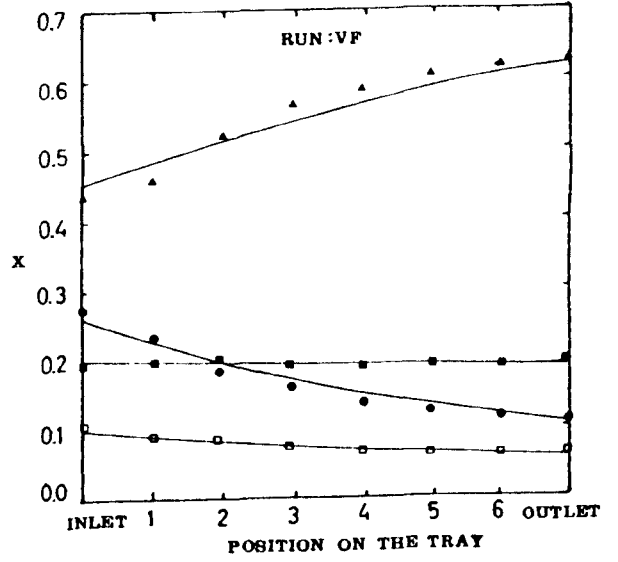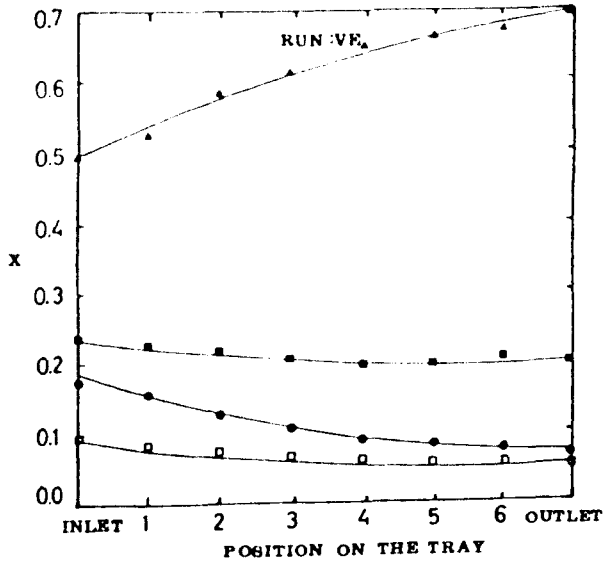
FIGURE 10.7 continued
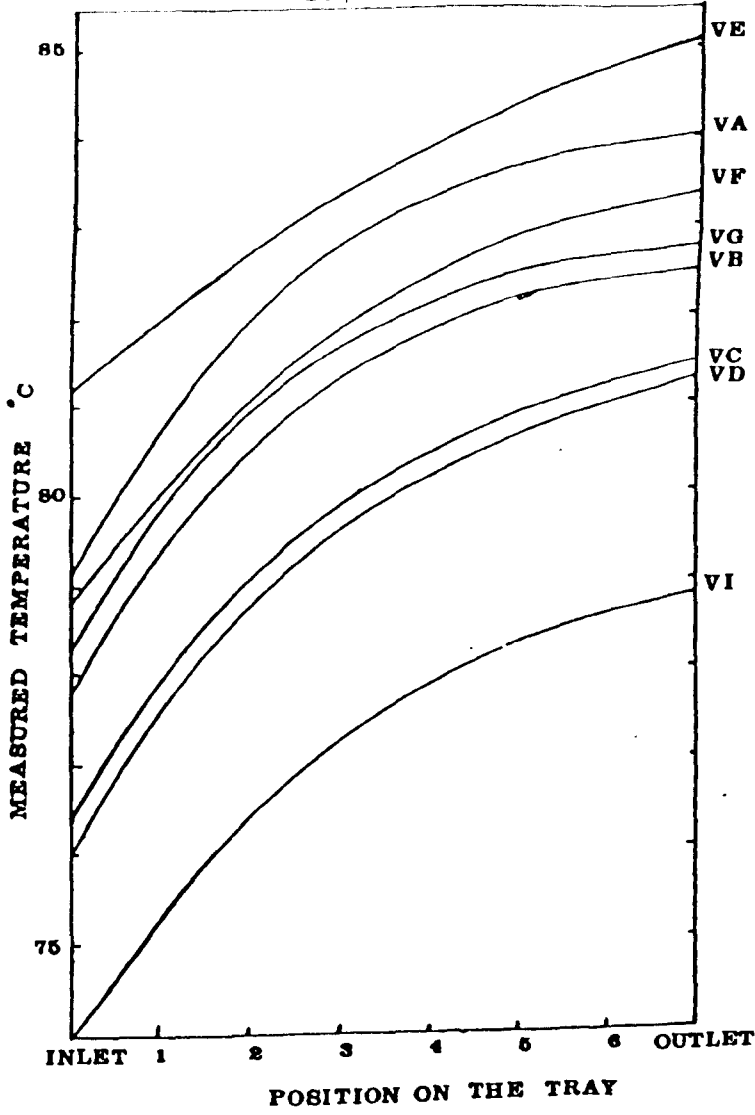
FIGURE 10.8 Temperature profiles across the rectangular tray
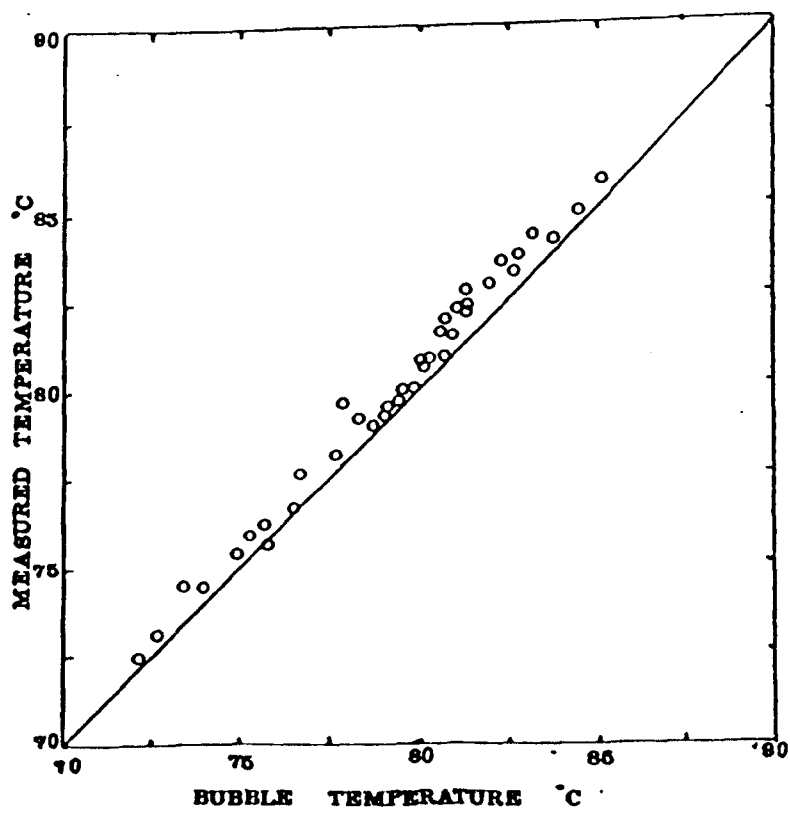
FIGURE 10.9 Comparison of measured and bubble temperatures

CHAPTER 11

EFFICIENCIES OF THE EXPANDED ALUMINIUM

TRAY (EXPAMET 607 A)

EFFICIENCIES OF THE EXPANDED ALUMINIUM TRAY (EXPAMET 607 A)

11.1   Introduction

Porter and co-workers in 1972 and 1973 pointed out the existence of flow non-uniformities on large circular sieve trays and their detrimental effects on tray efficiencies. Although many years have passed since this revelation little work has been carried out to actually remove the stagnant zones and improve the liquid flow across the tray. The only flow improving tray currently in operation is designed by the Union Carbide Co., (Smith and Delnicki, 1975; Weiler and Lockett, 1985). This slotted tray, which uses the vapour momentum to shift the slow moving liquid at the sides of the tray, is reported to have improved the tray efficiency. However, this tray is proprietary and not generally available.

The Expamet tray material tested here was chosen from a wide range of material samples, and is believed to be the first material of its type to have been used as a distillation tray. In this chapter the Expamet tray is discussed in detail and the results of distillation tests under different hydraulic conditions to measure its efficiencies are reported. Haselden and Too (1985) used a different flattened form of the Expamet tray for their baffled tray tests, but this was used for a different purpose.

11.2   Expamet 607 A

This aluminium material is produced by a slitting and deforming process which generates diamond-shaped holes and also corrugates the sheet. The length of the sheet increases because no metal is rejected. This corrugation forms diamond-shaped holes (see Figure 11.1 and 11.2) at an angle to the sheet. The material has a thickness of 0.56 mm and a

Figure 11.1 A View of the Expamet(607 A) Material.
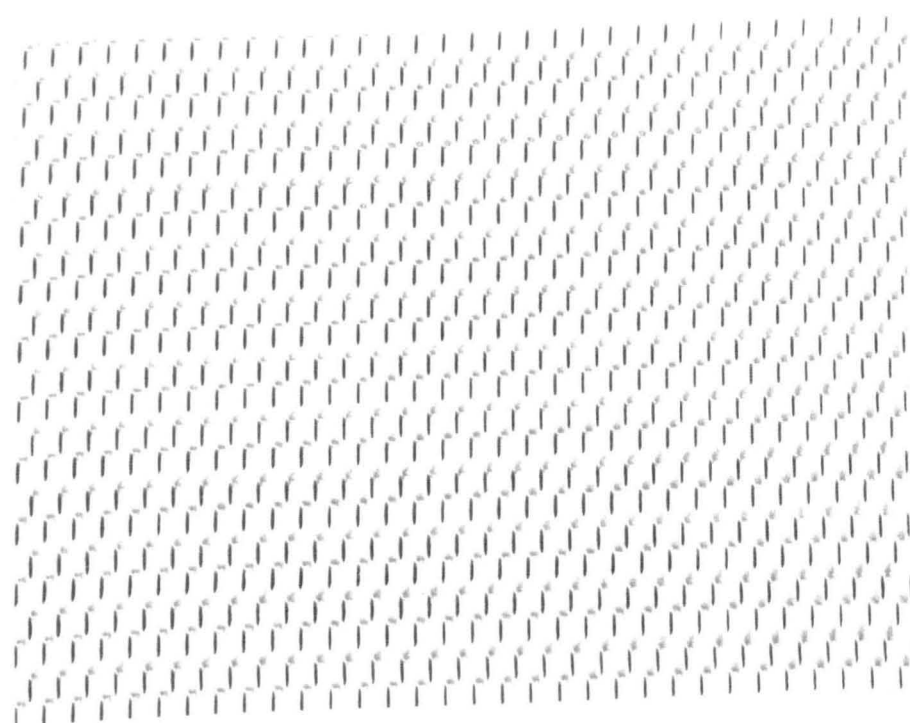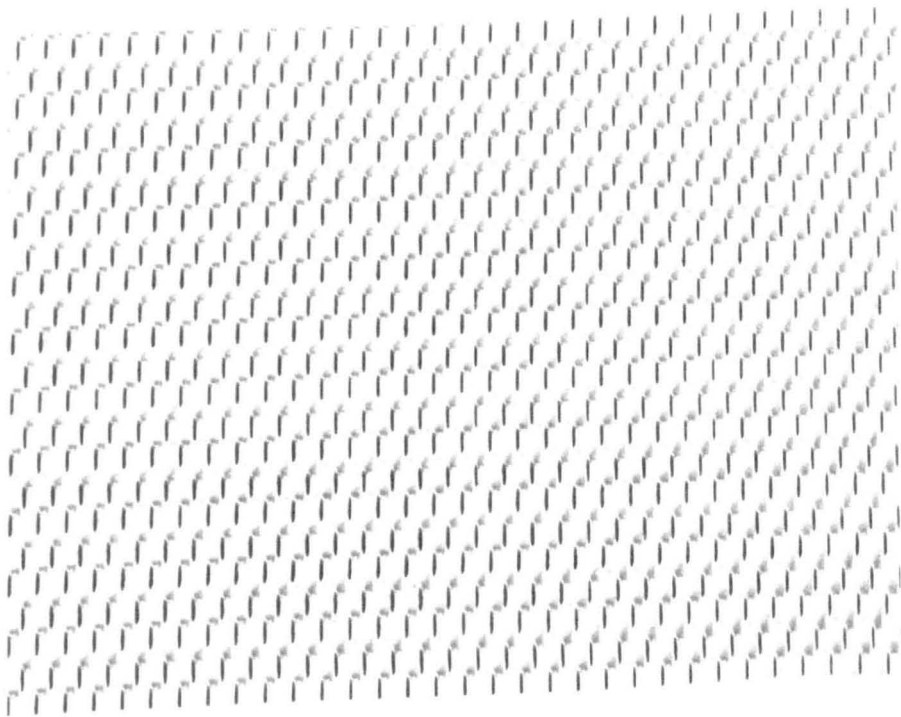
Figure 11.1 A View of the Expamet(607 A) Material.

weight of approximately 1.37 kg/m^2. The material has a free area of approximately 51%. This was calculated from individual hole measurement at approximately 45° to the normal using a travelling microscope. The average dimension of a typical hole is shown in Figure 11.2. Figure 11.1 also shows a photograph of a section of this material. It is hoped that this tray will actually direct the liquid on the tray as the vapour is forced to change its direction by about 45° in the direction of the biphase flow on the tray.

11.3 Experimental

The rectangular tray (Chapter 5) was used to test this material using the system methanol-water. The pressure drop was measured by using a water manometer. In addition, froth heights and boil-up rates were measured as before. The samples were analysed by using a G.L.C. technique (see appendix D). The samples were collected in the pre-cooled bottles.

11.4 Results

The high percentage free area available on this tray meant that increased F-Factors were required to achieve a satisfactory biphase on the tray. The results of all the runs including, the Murphree tray efficiencies, F-Factors, froth heights and pressure drops are tabulated in Table 11.1. These pressure drops are also compared with an equivelant 1.8 mm hole size tray at the same F-Factors, calculated using the Bennett et. al. (1983) correlation. It is evident that this tray provides much lower pressure drops under distillation conditions compared with a standard sieve tray due to its lower hole velocities. The composition and temperature profiles are also presented on the Figure 11.3 and 11.4.

11.4.1 Hydraulic Tests and Observations

Run: ZI, No Outlet Weir

At vapour F-Factors about 0.4 m/s $(kg/m^3)^{\frac{1}{2}}$, the first half of the tray was bubbling irregularly, the second half was dominated by very fast moving liquid. On lowering the F.Factor irregular bubbling increased with some stagnant liquid present. On increasing the F-Factor fast moving liquid was encouraged and dominated a larger proportion of the tray.

Run: ZJ, 6.4 mm Outlet Weir

The reverse of the Run ZI was observed with irregular bubbling dominating the second half of the tray from the inlet and fast moving liquid on the first half. A larger proportion of the irregular bubbling was dominated by fairly stagnant liquid.

Run: ZK, 12.7 mm Outlet Weir with Four Equally Spaced Intermediate Weirs of the Same Height

The main purpose of this test was to avoid local accummulation of the liquid. At an F-Factor of about 0.75 reasonably bubbling biphase enclosed by the intermediate weirs was observed. That accounted for $^3/_5$th of the tray. The other $^2/_5$th of the tray was dominated by the fast moving liquid.

Runs: ZL, ZM and ZN $^2/_5$th of the Tray Active Area was Blanked

A bubbling area enclosed by four equally spaced 12.7 mm intermediate weirs was left in the centre of the tray. This was to encourage higher vapour hole velocities as low rates were thought to be the reason behind bad bubbling on the tray. This tray has hole velocities of about 20% of the conventional sieve trays. This change created a biphase with better bubbling characteristics. The optimum bubbling was found for the

runs ZL and ZN. Run ZM was carried out at lower F-Factors where a larger proportion of the tray was bubbling irregularly. On increasing the F-Factor above the conditions of the runs ZL and ZN, fast moving liquid was encouraged at the expense of poorer bubbling.

Runs: ZO, ZP and ZQ, 37.5 mm Outlet Weir

The intermediate weirs were kept at the same height as before. This change was made to ensure a larger liquid resistance against the vapour momentum. The fast moving liquid region was completely eliminated or obscured as a result of this change, with much better biphase behaviour. The biphase also showed some recirculation of the liquid from the outlet weir which resulted in a peaked biphase on the tray.

11.5   Discussion

1. Although the biphase stability on the tray was successfully improved a lot of work still remains to be done to find the best loading conditions under which this tray may operate. One of the limitations of using the rectangular column was operation at total reflux, where there is no control over finding the best liquid and vapour ratios. In addition higher boil up rates were not possible.

2. The observation of the biphase, especially when low outlet weir was used, showed that the liquid on the tray was moving very fast from inlet to outlet as a result of vapour being deflected at an angle. This is the main objective of using this tray. However, the fast forward movement of the liquid meant a very short contact time between the liquid and the gas in the tray as a result of smaller biphase residence time on the tray.

3. In order to reduce the fast forward movement of the liquid on the tray intermediate weirs were used with subsequent partial blanking of the tray. This improved the gas and liquid contact on the tray as the intermediate trays reduced the fast movement of the liquid. In addition the liquid hold up on the tray also seemed to have increased, which presumably helped to reduce the fast liquid movement.

4. In further increasing the outlet weir the fast forward movement of the liquid disappeared as a result of the further increase in the liquid hold up, or was obscured. The biphase also seemed to be recirculating after hitting the outlet weir. This observation is in agreement with composition profiles shown on the figure 11.3, as a negligible change in composition is observed. We may also note that the sharp reduction in composition from the inlet downcomer to the tray is due to its long path before entering the tray, as a result of blanking the first part of the tray, and also some liquid from the tray was recirculating back on the blanked part.

Table 11.1   Expanded Aluminium Tray (607 A)

Efficiency Tests by the Rectangular Column

RUN	$\bar{x}$	EmV	F-Factor $m/s(kg/m^3)^{0.5}$	Froth Height (cm)	h_T(cm liquid) measured)	Bennett
ZI	0.63	0.74	0.40	2.5	2.4	4.2
ZJ	0.63	0.70	0.67	2.5	2.4	4.3
ZK	0.25	0.70	0.76	2.5	2.2	4.1
ZL	0.63	0.70	0.93	3.0	2.2	5.7
ZM	0.63	0.69	0.78	3.0	2.4	4.6
ZN	0.54	0.69	0.83	3.0	2.4	4.8
ZO	0.53	0.82	1.01	4.5	3.1	6.5
ZP	0.45	0.82	1.00	4.5	3.8	6.3
ZO	0.20	0.91	1.10	4.5	4.1	7.0
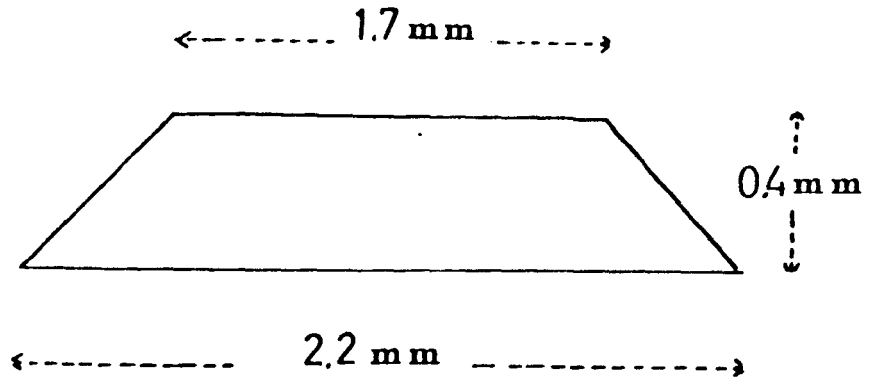
ire 11.1 A typical hole
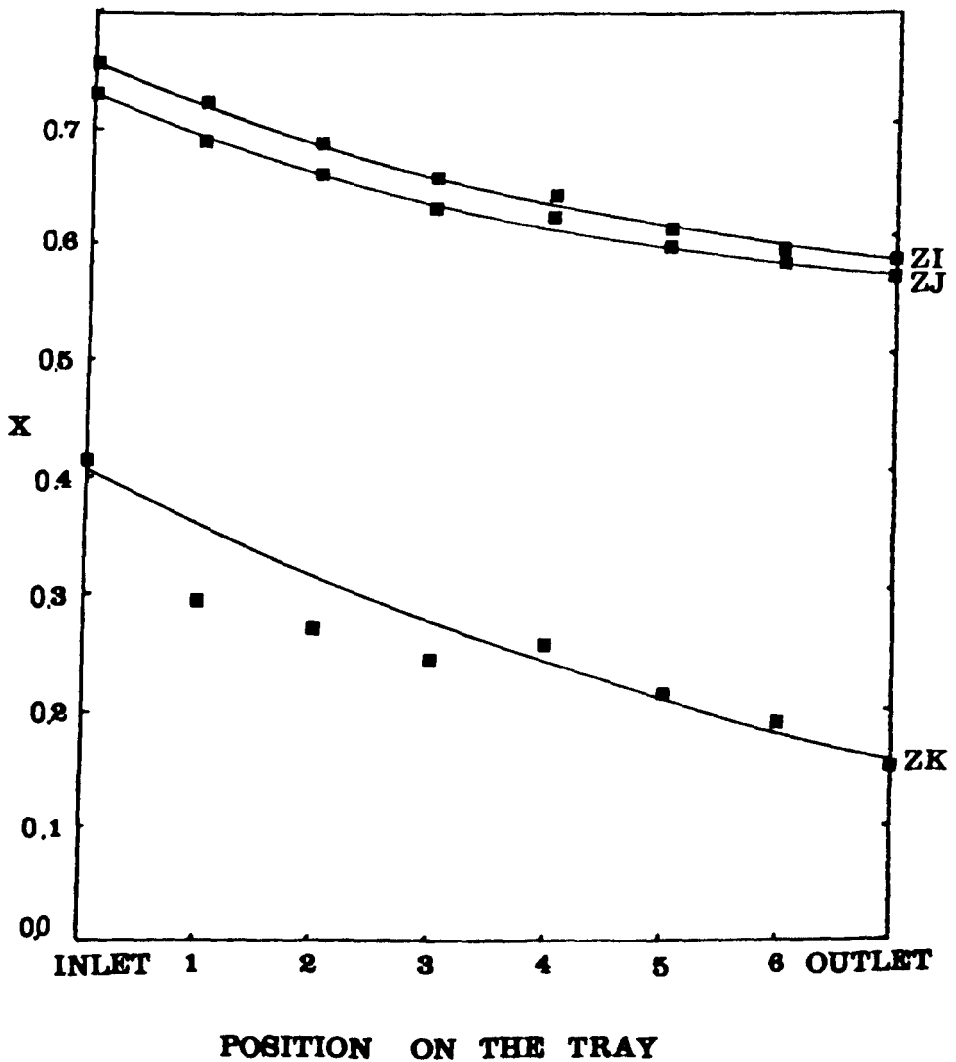
Figure 11.3   Composition profiles across the tray
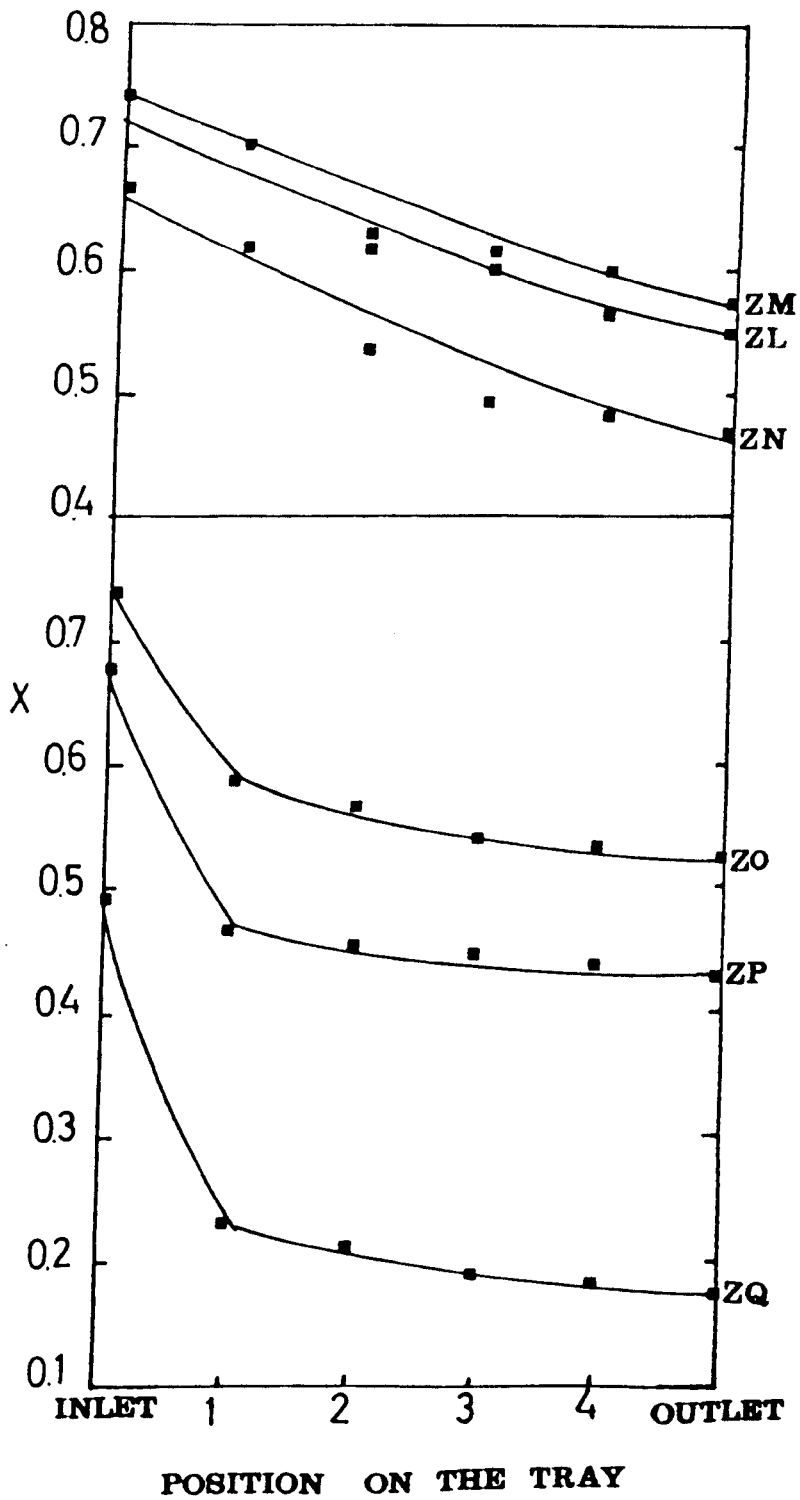
Figure 11.3 continued
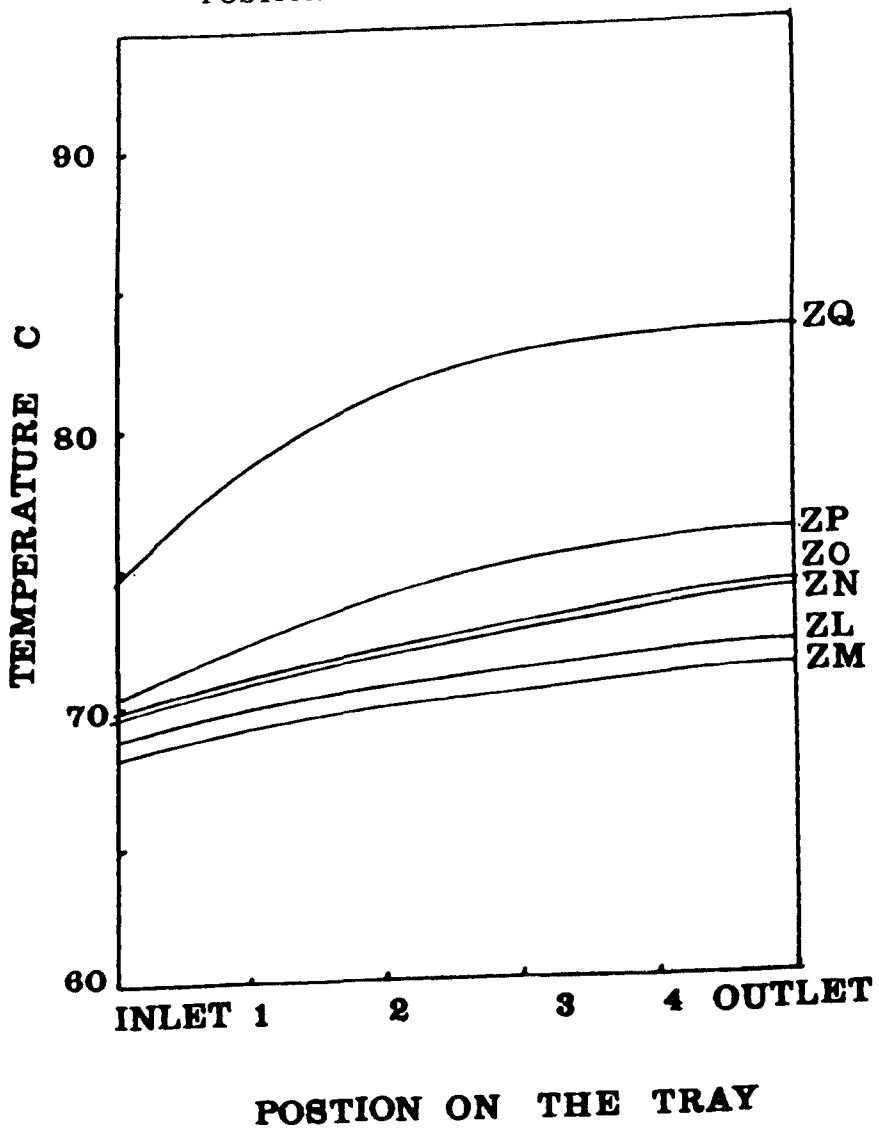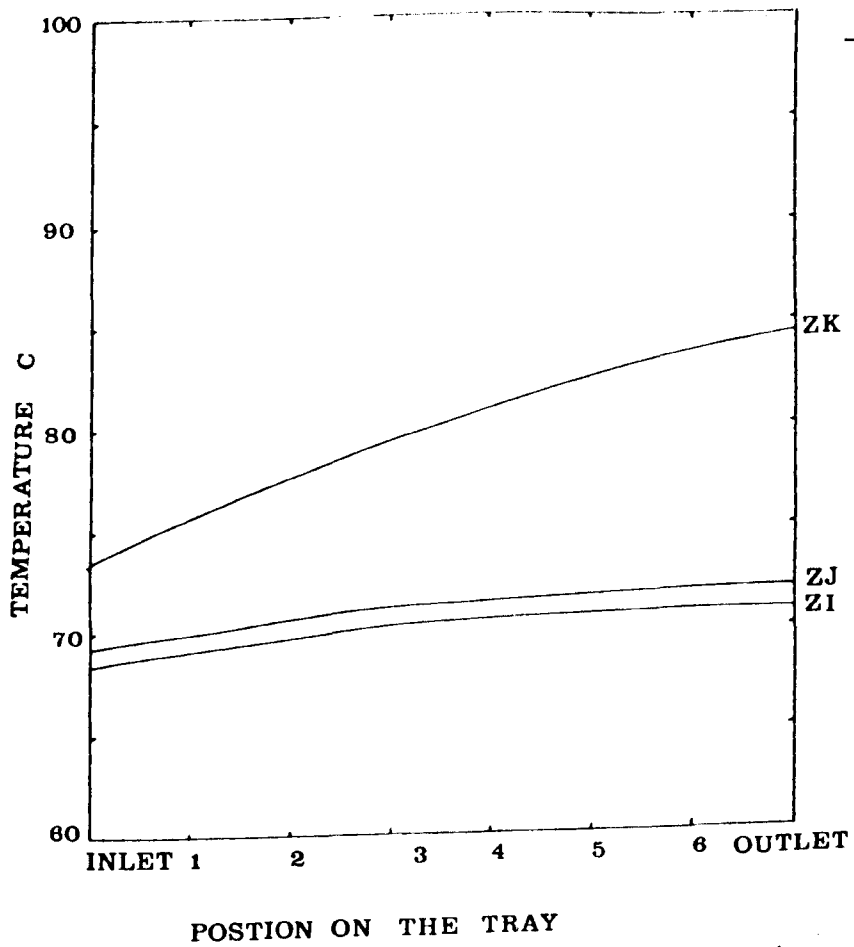
Figure 11.4   Temperature profiles

CHAPTER 12

CONCLUSIONS AND RECOMMENDATIONS

CONCLUSIONS AND RECOMMENDATIONS

12.1 Conclusions

a) A series of experiments was conducted to study the effect of the outlet weir height and hole size on tray and point efficiencies under similar hydrodynamic conditions. Composition and temperature profiles were measured in the absence of stagnant zones, flow non uniformities and problems of wall supported froth. The composition profiles were then matched against the predictions by an eddy diffusion model taking into account the effect of the liquid back mixing on the tray, to infer point efficiencies. The measurements indicate that there is an increase in the tray/point efficiencies with increasing outlet weir height from 2 to 12.6 mm. The study of the effect of hole size on tray/point efficiencies included a 1 mm perforated tray for the first time. It was found that there was an increase in tray/point efficiencies, with decreasing perforation size. This difference was however narrowed at high methanol concentrations. It is suggested that the slight increase in tray liquid hold-up and froth heights accompanied by a marked increase in the initial bubble formation rate which provides extra interfacial area are responsible. These effects are magnified by the steep slope of the equilibrium line and Marangoni surface renewal effects at the lower methanol concentrations. The pressure drop and liquid hold-up were also measured under these conditions. There is an increase in pressure drop on decreasing the perforation size due to the surface tension forces. Economic considerations will dictate the hole size used in tray design.

b) The modified column designed and developed here appears to be suitable for point efficiency measurements for any distillation system, including high surface tension positive and negative systems. It eliminates the surface tension induced "wall supported froth", and minimises the wetted

wall effects. The column appears to provide steady operating conditions. This development is a useful step in the simulation of conditions i.e. mixed flow regime of liquid, froth and spray, on a large tray.

c) In order to improve the contact between the gas and liquid on the modified column tray, its outlet weir height was increased from 2 mm to 12.7 mm. This increased the biphase height, and consequently the point efficiencies, without encouraging wall effects to occur. These efficiencies were about 10 per cent lower than the point efficiencies measured on a similar large rectangular tray under similar hydrodynamic conditions. Using the recent model of Dribika and Biddulph (1986), the modified column point efficiencies were scaled-up. This led to a marked improvement in predicted tray efficiencies to within 2 to 4% of actual measurements. This means that the modified Oldershaw column, with a 12.7 mm outlet weir height, can actually measure point efficiencies very similar to those on a larger tray operating under similar hydrodynamic conditions.

d) The surface tension study of the positive, neutral and negative systems suggests that highly surface tension positive systems exhibit higher point efficiencies due to Marangoni effect.

e) An important feature of this work is the high point and tray efficiencies obtained for different hole size, large rectangular trays. Point efficiencies of 85 to 95% indicate that there is only very narrow room for improvement. This provides further evidence for the higher tray efficiencies available to the design engineer, if the detrimental effects of stagnant zones and flow non-uniformities were eliminated.

f) Two highly non-ideal ternary systems and a quaternary system were studied using the modified Oldershaw and the large rectangular tray columns. Considerable differences between the individual component point

efficiencies were obtained, either by direct measurement using the modified column, or by matching the composition profiles obtained from the rectangular tray column with an eddy diffusion model. The differences between the component point efficiencies are probably caused by the interactive nature of mass transfer in these systems. These systems also exhibited equal component point efficiencies in some composition ranges. The point efficiencies were composition dependent.

g) Significant differences between component tray efficiencies were also observed, even when equal component point efficiencies existed across the tray. The eddy diffusion model, taking into account the extent of the liquid back mixing, simulated these differences in individual component tray efficiencies confirming previous theoretical expectations.

h) The composition profiles for the system MeOH/n.PrOH/H_2O were predicted across the rectangular tray column using three methods derived from the Maxwell and Stephen mass transfer equation. The composition profiles were in good agreement with the measurements. However, as the comparison is only based on a one metre flow path, the actual design of a distillation column using these methods is conservative. The prediction of the composition profiles using the point efficiencies measured in the original version of the modified Oldershaw column also gave similar observations for both of the ternaries and the quaternary system.

i) The preliminary work on the expamet 607 A tray showed its main characteristic of directing the liquid flow using the vapour momentum. This tray has low pressure drop characteristics due to its high free area. The narrow diamond shaped holes also avoid weepage despite high free area due to the capillary surface tension forces.

12.2   Recommendations

a)   The improved form of the modified column was shown to provide experimental point efficiencies for the system MeOH/H_2O very close to those operating across the large rectangular distillation tray. Further work is required to test other systems and seek further improvement of the liquid and the gas in the biphase.

b)   It was shown in the original version of the modified Oldershaw column that multicomponent point efficiencies can be measured using this arrangement. Further work is required using the improved form of the modified column to measure multicomponent point efficiencies more confidently. This is a very important step forward as there is no prediction method available to predict point efficiencies for the systems comprising more than 3 components, and the methods for ternary systems are restrictive and complex.

c)   It was shown that multicomponent systems can exhibit different component point efficiencies, possibly due to interaction effects. It was also shown that the individual component tray efficiencies are also different, due to the effect of the limited liquid back mixing, with or without equal point efficiencies operating across the tray. This casts serious doubts on the validity of the normal design approach of constant tray efficiencies. New measured data must be taken to incorporate unequal point and tray efficiencies into the design procedure for multicomponent systems.

d)   The study of the effect of the hole size in point efficiencies of the system MeOH/H_2O revealed a rather small increase in point efficiencies as a result of the decrease in perforation size. The tray pressure drop increased. For clean and low liquid rate operations, a 3.2 mm hole size

tray seems to be more economical than smaller perforation size trays, as its point efficiencies are comparable with the 1.8 mm hole size tray and they can provide lower pressure drops than do 1.8 mm and 1.0 mm trays. Further work into the economical aspects of using these trays is required for a clearer picture.

e)   Another feature of the results obtained, using the rectangular tray column, is the high tray efficiencies in virtually all the systems studied. This provides evidence for the higher tray efficiencies available to a design engineer, if the effects of the flow non-uniformities and stagnant zones which are known to reduce the tray efficiencies of larger circular trays. Thus studies of the hydraulics of circular trays should be extended.

f)   The work on the expamet 607 A tray was introduced in Chapter 11. Further hydraulic tests are required to find the hydraulic condition under which a more hydrodynamically stable biphase can be obtained. It would also be worthwhile to look at other Expamet material to consider as possible tray material, in particular numbers 801 A, 604 A, 605 A and 606 A.

REFERENCES

Adam, N. K., 'The Physics and Chemistry of Surfaces', 3rd Ed., 374, (1941)

Aittema, L. T. J., Kemia-Kemi, 8, 5, 298, (1985).

Aquilar, A. M.; Rosello Segado. A; Patino, J. M. R; Hormigo Leon, A., Ingenieria Quimico, 127, University of Seville, Dept. Phys. Chem., Jan. (1983), Spain.

Andrew, S. P. S., I. Chem.t. Symp. Manchester, U.K., 15, March 21 (1969).

Ashley, M. T.; Haselden, G. G., Trans. Instn. Chem. Engrs., 50, (1972).

Backhurst, J. R; Harker, J. H., 'Process Plant Design', Heinemann Educational Books Ltd. U.K. (1973).

Bainbridge, G. S; Sawistowski, H., Chem. Eng. Sci., 19, 992, (1964).

Barker, P. E; Self, M. F., Chem. Eng. Sci., 17, 541, (1962).

Bell, R. L., A. I. Ch. E. Journal, 18, 3, 491, May (1972).

Bell, R. L., A. I. Ch. E. Journal, 18, 3, 498, May (1972).

Bennett, D. L; Pakesh, A; Cook, P. J., A. I. Ch. E. Journal, 29, 3, 434, May (1983).

Biddulph, M. W., Ph.D. Thesis, University of Birmingham, (1966).

Biddulph, M. W., A. I. Ch. E. Journal, 21, 2, 327, March (1975).

Biddulph, M. W., Hydrocarbon Processing, 145, Oct. (1977).

Biddulph, M. W; Ashton, N., Chem. Eng. J., 14, 7, (1977).

Biddulph, M. W; Dribika, M. M., A. I. Ch. E. Journal, 32, 6, (1986).

Boyes, A. P; Ponter, A. B., J. Chem. Eng. Data, 15, 235, (1970).

Boyes, A. P; Ponter, A. B., Chem. Eng. Sci., 25, 1952, (1970).

Boyes, A. P; Ponter, A. B., Ind. Eng. Chem. Fund., 10, No. 4, 641, (1971).

Boyes, A. P; Ponter, A. B., Ind. Eng. Chem. Process. Des. Dev. 10, No. 1, 140, (1971).

Boublik, T; Friend, V; Hala, E., 'The Vapour Pressures of Pure Substances', Elsevier, Amsterdam, (1973).

Brown, B. R; England, B. L., Int. Inst. Ref. Commun. London, 20, Sept. (1961).

Bubble-Tray Design Manual; A. I. Ch. E. Manual, (1958).

Burgess, J. M; Calderbank, P. H., Chem. Eng. Sci., 30, 1107, (1975).

Chan, H; Fair, J. R., Ind. Eng. Chem. Proc. Des. Dev., 23, 820, (1984).

Catchpole, J. P., Ph.D. Thesis, University of Birmingham, (1962).

Cermak, J., Collec. Czech. Chem. Commun., 35, 1844, (1970).

Chopey, N. P; Hicks, P. G., 'Handbook of Chemical Engineering Calculations', (1984).

Cilianu, S; Brauch, V; Schlunder, E., Verfuhrenstechnic 8, 3, 84, (1974).

Delzene, A. D., Ind. Eng, Chem., 3, 2, 224, (1958).

Diener, D. A; Gerster, J. A., Ind. Eng. Chem. Process, Des. Dev., 7, 3, 339, (1968).

Diener, D. A., Ind. Eng. Chem., 6, 4, 499, Oct. (1967).

Dribika, M. M; Rashed, L. G; Biddulph, M. W., J. Chem. Eng. Data, 30, 2, 146, (1985).

Dribika, M. M., Ph.D. Thesis, University of Nottingham, (1986).

Dribika, M. M; Biddulph, M. W., A. I. Ch. E. Journal 32, 11, 1864, Nov. (1986).

Eagle, R. S; Lemieux, G. J., Chem. Eng. Progress, 60, 1, 74, Oct. (1964).

Ellis, S. R. M; Biddulph, M. W., Trans. Inst. Chem. Eng. 45, T?23, (1967).

Ellis, S. R. M; Bennett, R. J., J. Inst. Petrol., 43, 433, 19, 'an (1960).

Ellis, S. R. M; Catchpole, J. P., Dechem Monogr., 55, 43, (1964).

Ellis, S. R. M; Contractor, R. M., J. Inst. Petrol., 45, 147, (1959).

Ellis, S. R. M; Froome, B. A., Chemistry and Industry, Feb. 27, (1954).

Ellis, S. R. M; Legg, R. J., Can. J. Chem. Eng., 6, Feb. (1962).

Fair, J. R; Null, H. R; Bolles, W. L., Ind. Eng. Chem Process, Des. Dev. 22, 1, 53, (1983).

Fane, A. G; Sawistowski, H., I. Chem. E. Symp. Ser. 32, 1:8, (1969).

Fell, C. J. D; Pinczewski, W. V., Chem. Eng. 45, Jan. (1977).

Finch, R; Van Windle, M., Ind. Eng. Chem. Process,Des. and Dev., 2, 106, April (1964).

Free, K. W; Hutchison, H. P., Inst. Chem. Engrs, Symp. Ser, 32, 232, (1960).

Friend, L; Lemieux, E. J., Oil and Gas Journal, 54, 88, July 23 (1956).

Fryback, M. G; Hufnagel, J. A., Ind. Eng. Chem., 52, 8, 654, Aug. (1960).

Gallant, R. W., 'Physical Properties of Hydrocarbones' 2, (1968-1970).

Gelbin, D., Bri. Chem. Eng., <u>10</u>, 5, 301, (1965).

Gemhling, S; Onken, U., 'Vapour-liquid Equilibirum Data, Dechem. Chemistry Series', Frankfurt, 1, 2a, (1977).

Hart, D. J; Haselden, G. G., I. Chem. E. Symp. Ser. 32, 1:19, (1969).

Haselden, G. G; Thorogood, R. M., Trans. Inst. Chem. Eng. <u>42</u>, T81, (1964).

Haselden, G. G; Too, K. S., I. Chem. E. Symp. Ser., 94, 157, (1985).

Hofhuis, P. A. M; Zuiderweg, F. J., I. Chem. E. Symp. Ser., 56, 2.2.1, (1979).

Huang, C. J; Hodson, J. R., Petrol Refining, <u>37</u>, 2, 104, (1958).

Hunt, C; Hanson, D. N; Wilke, C. R., A. I. Ch. E. Journal, <u>1</u>, 4, 441, (1955).

Jasper, J. J., J. Phys. Chem. Ref. Data, 1, 14, (1972).

Jeromin, L; Holik, H; Knapp, H., I. Chem. E. Symp. Ser., 23, 5.49.4., (1969).

Kern, D. Q., 'Process Heat Transfer', McGraw-Hill, (1950).

Kirschbaum, Forsch. Gebiete Ingenieur, 5, 245, (1934).

Konstantinov, E. N; Nikolaev, A. M., Kim-i-Kim, Tekh., <u>1</u>, 492, (1964).

Kreis, H; Raab, M., I. Chem. E. Symp. Ser., 56, 3.2163, (1979).

Krishna, R; Chem. Eng. Sci., <u>32</u>, 1197, (1977).

Krishna, R; Martinez, H. F; Sreedhar, R; Standart, G. L., Trans. I. Chem. E., <u>55</u>, 178, (1977).

Krishna, R; Standart, G. L., Chem. Eng. Commun., <u>3</u>, 201, (1979).

Kutsarov, R; Tasev, Z. H., Hung. Journal of Ind. Chem. Veszprem, 14, 53, (1986).

Lemieux, E. J; Scottie, L. J., Chem. Eng. Progress, 65, 3, 52, (1969).

Lim, C. T; Porter, K. E; Lockett, M. J., Trans. Inst. Chem. Engrs., <u>52</u>, 193, (1974).

Linddell, J., Chem. Eng. 36, April (1984).

Lockett, M. J., 'Distillation Tray Fundamentals', Cambridge University Press, (1986).

Lockett, M. J; Lim, C. T; Porter, K. E., Trans. Instn. Chem. Engrs, <u>51</u>, 61, (1973).

Lockett, M. J; Safekourdi, A., Chem. Eng. Journal, 11, 111, (1976).

Lockett, M. J; Kirkpatrick, R. D; Uddin, M. S., Trans. Instn. Chem. Engrs. 57, 25, (1979).

Lockett, M. J; Ahmed, I. S., Chem. Eng. Des. Dev., 61, 110, March (1983).

Lockett, M. J; Uddin, M. S., Trans. Instn. Chem. Engrs., 58, 166, (1980).

Martin, H. W., Chem. Eng. Progress, 60, 10, 50, (1964).

Maripur, V. O; Ratcliff, G. A., J. Chem. Eng. Data, 17, 366, (1972).

Mayfield, F. D., Church, W. L.; Green, A. C; Rasmussen, R. W., Ind. Eng. Chem. 44, 9, 2238, (1952).

Medina, A. G; Ashton, N; McDermott, C., Chem. Eng. Sci., 33, 331, (1978).

Medina, A. G; McDermott, C; Ashton, N., Chem. Eng. Sci., 34, 861, (1979).

Medina, A. G; McDermott, C; Ashton, N., Chem. Eng. Sci., 33, 1489, (1978).

Miskin, L. G; Ozlap, U; Ellis, S. R. M., Brit. Chem. Eng. Proc. Tech. 17, 2, 153, (1972).

Mix, T. W; Dweck, J. S; Weinberg, M; Armstrong, R. C., A. I. Ch. E. Symp. Ser., 76, 192, (1980).

Moens, F. P., Chem. Eng. Sci., 27, 275, (1972).

Moens, F. P; Bos, R. G., Chem. Eng. Sci., 27, 403, (1972).

Mostafa, H. A., Trans. I. Chem. E., 57, 55, (1979).

Neuburg, H. J; Chuang, K. T., Can. J. Chem. Engr., 60, 504, Aug. (1982).

Nord, M., Trans. Am. Inst. Chem. Engrs., 42, 863, (1943).

Ochi, K; Kojima, K; Kagaku kogacu, 33, 352, (1969).

Oldershaw, C. F., Ind. Eng. Chem. Anal. Ed., 13, 265, (1941).

Patton, B. A; Pritchard, B. L., Petrol Refiner, 39, 95, (1960).

Porter, K. E; Lockett, M. J; Lim, C. T., Trans. Instn. Chem. Engrs. 59, 91, (1972).

Porter, K. E; Jenkins, J. D., I. Chem. Eng. Symp. Ser., 56, 5.1/1, (1979).

Porter, K. E; Davies, B., Private Communication, (1986).

Prausnitz, J. M; Eckert, C. A; Orge, R. V; O'Connell, J. P., 'Computer Calculations for Multicomponent Vapour-liquid Equilibria', (1967).

Prince, B. G. H., Int. Chem. E. Symp. Ser. 32, 177, (1960).

Pruden, B. B; Hayduk, W; Laudie, H., Can. J. Chem. Eng., 52, Feb. (1974).

Qureshi, A. K; Smith, W., J. Inst. Petrol., 44, 413, May (1958).

Reid, R. C; Prausnitz, J. M; Sherwood, T. K., 'The Properties of the Gas and Liquids', New York, McGraw-Hill, 3rd Ed. (1977).

Sakata, M; Yanagi, T., I. Chem. E. Symp. Ser. 56, 3.2/21, (1979).

Sargent, R. W. H; Bernard, J. O. T; McMillan, W. P; Schroter, R. C., Symp. in Distillation, London, (1964).

Sawistowski, H., Chemie-Ing-Tech 45 Jahrg, 18, 1093, (1973).

Smirnov, N. A; Vestin, J., Lenningrad Univ., U.S.S.R., Fiz, Khim, 81, (1959).

Smith, B. D., 'Design of Equilibrium Stage Processes', McGraw-Hill, (1963).

Smith, V. C; Delnicki, W. V., Chem. Eng. Progress, 71, 8, 68, Aug. (1975).

Smith, V. C; Upchurch, J. C., Chem. Eng. Progress, 48, Sept. (1981).

Stabinkov, V. N; Matgushev, B. Z; Protsyak, T. B; Yushanko, M., Pushch. Prom. 'Kiev', 15, (1972).

Standart, G. L., Chem. Eng. 716, Nov. (1974).

Sugden, S., Journal of Chemical Society, 121, 858, (1922).

Sugden, S., Journal of Chemical Society, 125, 27, (1924).

Tamura, M; Kurata, M; Hisashi, O., Bulletin, Chem., Soc., Jap., 28, 83, (1955).

Thomas, J. W; Haq, M. A., Ind. Eng. Chem. Process. Des. Dev. 15, Nov. (1976).

Toor, H. L., A. I. Ch. E. Journal, 3, 2, 198, June (1957).

Toor, H. L; Burchard, J., A. I. Ch. E. Journal, 6, 2, 202, June (1960).

Tsonopoulos, C., A. I. Ch. E. Journal, 20, 2, 263, March (1974).

TRC Tables, 'Selected Values of Properties of Chemical Compounds', Thermodynamics Research Centre Data Project, Texas A. and M. University, College Station, Texas U.S.A., (1981).

Umholtz, C. L; Van Winkle, M., Ind. Eng. Chem., 49, 2, 226, Feb. (1957).

Veatch, F; Callaham, J. L; Idol, J. D; Milberger, E. C., Chem. Eng. Progress, 56, 65, (1960).

Vogelpohl, A., I. Chem. E. Symp. Ser, 56, 2.1, 25, (1979).

Vogelpohl, A; Crettor, R., Chem. Ing. Tech, 44, 15-16, 1936, (1972).

Weiler, D. W; Kirkpatrick, R. D; Lockett, M. J., Chem. Eng. Progress, 63, Jan. (1983).

Weiler, D. W; Delnicki, W. V: England, B. L., Chem. Eng. Progress, 69, 10, 67, Oct. (1973).

Weiler, D. W; Lockett, M. J., I. Chem. E. Symp. Ser. 94, 141, (1985).

Winterfeld, P. H; Scriven, L. E; Davis, H. T., A. I. Ch. E. Journal, 24, 6, 1010, Nov. (1978).

Yanagi, T; Scott, B. D., Chem. Eng. Progress, 69, 10, 75, Oct. (1973).

Young, G. C; Weber, J. H., Ind. Eng. Chem. Process, Des. Dev., 11, 3, 440, (1972).

Zens, F. A., Chem. Eng. 120, Nov 13, (1972).

Zuiderweg, F. J; Harmens, A., Chem. Eng. Sci., 9, 89, (1958).

Zuiderweg, F. J., 37, 10, 1441, (1982), Chem. Eng. Sci.

Zuiderweg, F. J., Chem. Eng. Res. Des., 61, 388, (1983).

APPENDIX A

1) All the results of the Oldershaw and Modified Column.

2) All the results of $EtOH/H_2O$, $n.PrOH/H_2O$ runs with rectangular column.

3) All the results of hydraulic studies.

4) All the results of the improved modified column.

Table A.1.1   MeOH/H_2O Experimental Results using the Standard

Oldershaw Column

RUN NO.	X_B	X_T	Y_B^*	$P_{(atm)}$	H_f (cm)	Eog_1
73	0.9841	0.9909	0.9932	0.9921	5.0	0.75
74	0.9662	0.9841	0.9856	0.9939	7.0	0.92
75	0.9457	0.9771	0.9768	0.9971	10.0	1.01
76	0.9263	0.9700	0.9686	0.9970	12.0	1.03
77	0.9088	0.9637	0.9612	0.9900	13.0	1.05
78	0.8807	0.9537	0.9492	0.9890	4.0	1.07
79	0.8560	0.9388	0.9388	0.9736	13.5	0.99
80	0.8393	0.9355	0.9317	0.9736	14.0	1.02
81	0.7687	0.9161	0.9012	1.0110	14.0	1.11
82	0.7098	0.9072	0.8756	1.0110	14.0	1.19
83	0.6971	0.8864	0.8702	1.0020	14.0	1.09
84	0.6841	0.8748	0.8645	1.0000	14.0	1.06
85	0.5714	0.8203	0.8135	0.9997	14.0	1.03
86	0.6841	0.8748	0.8641	1.0000	14.0	1.16
87	0.5448	0.8369	0.8009	0.9997	14.0	1.14
88	0.3487	0.7499	0.6953	0.9961	14.0	1.18
89	0.2956	0.7094	0.6586	1.0105	14.0	1.24
90	0.2315	0.6718	0.6060	1.0105	14.0	1.18
91	0.1809	0.6418	0.5528	1.0105	14.0	1.06
92	0.1553	0.5863	0.5195	1.0132	14.0	1.14

Table A.1.2 EtOH/H_2O Experimental Results Using Standard Oldershaw Column

RUN	X1B	X1T	Y1B*	P(atm)	$H_{f}(cm)$	Eog
39	0.9968	0.9601	0.9641	1.0150	6.0	1.12
40	0.9386	0.9379	0.9330	1.0150	7.0	0.13
41	0.9195	0.9092	0.9144	1.0037	7.5	1.95
42	0.8742	0.8030	0.8737	1.0037	7.5	0.89
43	0.8296	0.8520	0.8379	0.9807	9.5	2.70
45	0.8117	0.8291	0.8246	0.9914	10.0	1.35
46	0.7867	0.8410	0.8070	1.0013	11.5	2.67
47	0.7649	0.7853	0.7922	1.0039	13.0	0.75
48	0.7224	0.7902	0.7653	0.9934	13.5	1.60
49	0.7007	0.7596	0.7524	0.9908	15.0	1.14
50	0.6700	0.7334	0.7351	0.9849	15.0	0.97
51	0.6554	0.7247	0.7272	0.9848	15.5	0.97
52	0.6296	0.7207	0.7135	1.0016	15.5	1.09
53	0.6095	0.7116	0.7032	1.0095	15.5	1.09
54	0.6108	0.7083	0.7039	1.0082	15.5	1.05
55	0.5884	0.6878	0.6928	1.0111	14.5	0.95
56	0.5826	0.6967	0.6900	1.0076	13.5	1.06
57	0.5694	0.6829	0.6838	1.0076	14.0	1.00
58	0.0776	0.4134	0.3770	1.0076	2.0	1.12
59	0.1476	0.5456	0.4719	1.0076	11.0	1.23
60	0.2212	0.5676	0.5254	1.0020	12.0	1.14
61	0.2581	0.5725	0.5456	1.0014	12.0	1.09
62	0.2667	0.5871	0.5500	0.9971	12.0	1.14
63	0.3470	0.6030	0.5870	0.9922	12.0	1.07
64	0.3948	0.6072	0.6073	0.9940	12.0	1.00
65	0.3987	0.6078	0.6087	1.0092	12.0	1.00
66	0.4257	0.6107	0.6205	0.9895	12.5	0.95
67	0.4240	0.6229	0.6198	0.9882	12.5	1.02
68	0.4652	0.6380	0.6371	0.9974	12.5	1.01
69	0.4913	0.6409	0.6484	0.9974	12.5	0.95
70	0.5033	0.6574	0.6546	0.9975	13.0	1.02
71	0.5422	0.6633	0.6712	0.9892	13.0	0.975
72	0.5382	0.6737	0.6694	0.9892	13.0	1.03

Table A.1.3   n.PrOH/H_2O Experimental Results Using the Standard
Oldershaw Column.

RUN NO.	XB	YB*	XT	P(atm)	H_f(cm)	Eog_1
1	0.0474	0.3124	0.2433	1.0147	2.5	0.74
2	0.0970	0.3609	0.2515	1.015	3.0	0.59
3	0.0686	0.3396	0.3135	1.0084	3.0	0.90
4	0.0819	0.3518	0.3365	1.0080	5.0	0.94
5	0.0733	0.3438	0.3318	1.0085	5.5	0.98
7	0.0985	0.3617	0.3403	1.0131	6.5	0.92
8	0.1179	0.3704	0.3504	1.0131	7.2	0.92
9	0.1365	0.3769	0.3635	1.0107	8.5	0.94
10	0.1789	0.3883	0.3655	1.0066	9.0	0.89
11	0.2048	0.3940	0.4192	1.0066	10.0	1.13
12	0.2044	0.3939	0.2299	0.9993	11.0	0.97
13	0.1936	0.3916	0.3835	0.9993	12.0	0.96
14	0.2291	0.3989	0.3818	1.0036	13.0	0.90
15	0.2076	0.3946	0.3866	1.0067	13.0	0.96
16	0.2414	0.4014	0.3890	1.0033	15.0	0.92
17	0.2031	0.3936	0.3923	1.0033	15.0	0.99
19	0.2329	0.3997	0.3846	0.9998	13.0	0.91
20	0.2941	0.4116	0.3918	0.9998	14.0	0.83
21	0.3254	0.4178	0.4010	1.0019	14.0	0.82
22	0.8531	0.6778	0.7656	0.9895	2.8	0.50
23	0.7546	0.5807	0.6431	0.9854	2.5	0.64
24	0.6825	0.5335	0.5680	0.9854	2.5	0.77
25	0.5930	0.4908	0.5147	0.9863	2.5	0.85
26	0.5513	0.4760	0.4872	0.9863	2.5	0.96
27	0.5186	0.4653	0.4672	0.9908	2.5	0.96
28	0.5034	0.4607	0.4672	0.9908	2.5	0.99
29	0.4829	0.4549	0.4509	1.0055	2.5	1.14
30	0.4656	0.4502	0.4519	1.0055	2.5	0.91
31	0.4597	0.4487	0.4373	1.0122	2.5	2.03
32	0.4403	0.4437	0.4479	1.0142	6.0	2.25
33	0.4433	0.4444	0.4389	1.0132	8.5	-3.95
34	0.4424	0.4442	0.4341	1.0132	8.0	-4.65
35	0.4407	0.4435	0.4467	1.0147	9.0	1.95
36	0.4359	0.4425	0.4348	1.0197	11.0	-0.167
37	0.4331	0.4419	0.4316	1.0197	13.0	-0.17

Table A.2.1   MeOH/H_2O Experimental Results Using the Modified

Oldershaw Column

RUN NO.	x_B	x_r	Y_B^*	P(atm)	Eog_1
93	0.4159	0.6147	0.7344	1.0178	0.62
94	0.4647	0.6666	0.7607	1.0151	0.68
95	0.4957	0.6887	0.7764	1.0151	0.68
96	0.5140	0.7003	0.7857	1.0151	0.68
97	0.3742	0.5856	0.7105	1.0095	0.62
98	0.2766	0.4924	0.6444	1.0072	0.58
99	0.2479	0.4519	0.6213	0.9986	0.54
100	0.2113	0.3923	0.5870	0.9980	0.48
101	0.2267	0.4739	0.6021	0.9964	0.65
102	0.1608	0.3852	0.5282	0.9922	0.61
103	0.3936	0.6057	0.7226	0.9922	0.64
104	0.6772	0.8174	0.8614	1.0029	0.76
105	0.6557	0.8027	0.8518	1.0046	0.74
106	0.6182	0.7893	0.8350	1.0046	0.78
107	0.9169	0.9822	0.9856	1.0072	0.81
108	0.9529	0.9682	0.9799	1.0072	0.56
109	0.9272	0.9591	0.9689	1.0073	0.76
110	0.8909	0.9422	0.9535	1.0073	0.81
111	0.8554	0.9225	0.9383	1.0133	0.81
112a	0.8356	0.9084	0.9299	1.0133	0.74
*112b	0.8268	0.9267	0.9261	1.0211	1.0
113	0.7950	0.8942	0.9124	1.0211	0.84
114	0.7728	0.8746	0.9029	1.0211	0.78
115	0.7395	0.8548	0.8885	1.0211	0.77
116	0.7153	0.7153	0.8779	1.0211	0.81

* 112b, by Standard Oldershaw Column.

NOTE: Froth height was about 2 cm throughout all the experiments with the modified column.

Table A.2.2   EtOH/H_2O Experimental Results Using Modified Oldershaw

Column

RUN	X1B	X1T	Y1B*	P(atm)	Eog
159	0.1590	0.4001	0.4819	1.0105	0.75
160	0.2140	0.3689	0.5209	1.0105	0.51
161	0.2190	0.3735	0.5244	0.9947	0.51
162	0.2439	0.4192	0.5383	0.9947	0.60
163	0.2620	0.4492	0.5472	1.0145	0.66
164	0.2816	0.4515	0.5483	1.0145	0.64
165	0.3469	0.4936	0.5864	1.0184	0.61
166	0.3701	0.5144	0.5964	1.0184	0.64
167	0.3933	0.5351	0.6063	1.0171	0.67
168	0.4373	0.5709	0.6246	1.0328	0.71
169	0.4703	0.5989	0.6388	1.0328	0.76
170	0.4897	0.6127	0.6473	1.025	0.78
171	0.4981	0.6187	0.6510	1.025	0.79
172	0.8641	0.8685	0.8654	1.016	3.51
174	0.8366	0.8478	0.8434	1.0065	1.65
175	0.7786	0.8026	0.8013	1.0040	1.06
176	0.7455	0.7738	0.7296	0.9986	0.83
177	0.7128	0.7520	0.7595	1.0128	0.84
178	0.6834	0.7308	0.7425	1.0128	0.80
179	0.6602	0.7168	0.7297	1.0026	0.81
180	0.6408	0.7055	0.7194	1.000	0.82
181	0.6150	0.6891	0.7061	0.9921	0.81
182	0.5933	0.6756	0.6954	0.9927	0.81
183	0.5787	0.6686	0.6884	0.9796	0.82
184	0.542	0.6472	0.6711	0.9895	0.81

Table A.2.3   n.PrOH/H_2O Experimental Results Using the Modified

Oldershaw Column

RUN	X1B	X1T	Y1B*	P (atm)	Eog$_1$
117	0.1540	0.2768	0.3820	0.9927	0.54
118+	0.11898	0.2401	0.3708	0.9947	0.48
119+	0.1785	0.2580	0.3882	0.9868	0.38
120-	0.1410	0.2639	0.3784	0.9829	0.52
121+	0.2342	0.3011	0.3999	0.9895	0.40
122	0.2179	0.2940	0.3967	0.9934	0.43
123+	0.2894	0.3462	0.4107	1.0019	0.47
124	0.2731	0.3593	0.4975	1.0019	0.64
125+	0.3369	0.3693	0.4202	1.0105	0.39
126	0.3285	0.3966	0.4185	1.0105	0.68
127+	0.3595	0.3995	0.4190	1.0029	0.61
128	0.3487	0.3840	0.4221	1.0053	0.48
129+	0.3856	0.4056	0.4306	1.0053	0.45
130	0.3724	0.4086	0.4278	1.0131	0.65
131+	0.3887	0.4073	0.4314	1.0112	0.44
132	0.4005	0.4075	0.4340	1.0112	0.21
133+	0.3926	0.4024	0.4322	1.0092	0.25
134	0.3934	0.4164	0.4329	1.0092	0.59
135+	0.3957	-.4201	0.4329	1.0105	0.59
136	0.4057	0.4184	0.4348	1.0105	0.35
141+	0.8720	0.7795	0.7040	1.0000	0.55
142	0.8695	0.7809	0.7005	1.0000	0.52
143+	0.7849	0.6854	0.6050	1.0092	0.44
144	0.7918	0.6969	0.6114	1.0092	0.53
145+	0.7231	0.6343	0.5593	1.0197	0.54
146	0.7207	0.6363	0.5576	1.0197	0.52
147+	0.6816	0.5976	0.5340	1.0227	0.57
148	0.6898	0.6080	0.5387	1.0227	0.54
149+	0.6445	0.5801	0.5148	1.0229	0.50
150	0.6479	0.5704	0.5164	1.0229	0.59
151+	0.6098	0.5504	0.4991	1.0226	0.53
152	0.6138	0.5593	0.5008	1.0226	0.48
153+	0.5808	0.5094	0.4872	1.0132	0.76
154	0.5869	0.5105	0.4894	1.0132	0.78
155+	0.5424	0.5206	0.4734	1.0145	0.32
156	0.5448	0.5194	0.4792	1.0145	0.36
157+	0.5293	0.5237	0.4748	1.0186	0.19
158	0.5314	0.5031	0.4686	1.0186	0.45

+ F.Factor = 0.4 $\left(ms^{-1} (Kg/m^3)^{0.5} \right)$

Table A.2.4   MeOH/n.PrOH Experimental Results Using the Modified

Oldershaw Column

RUN NO.	XB	YB*	XT	P	H_f (cm)	Eog
188	0.8788	0.9573	0.9342	1.0053	2.0	0.71
189	0.8593	0.9501	0.9243	1.0053	2.0	0.72
190	0.8081	0.9305	0.8953	1.0079	2.0	0.71
191	0.7706	0.9155	0.8711	1.0079	2.0	0.69
192	0.6887	0.8807	0.8211	0.9947	2.0	0.69
193	0.6209	0.8484	0.7768	0.9921	2.0	0.69
194	0.5576	0.8146	0.7307	0.9921	2.0	0.67
195	0.4776	0.7656	0.6648	0.9763	2.0	0.65
196	0.4095	0.7160	0.6007	0.9763	2.0	0.62
197	0.3616	0.6742	0.5548	1.000	2.0	0.62
198	0.3122	0.6251	0.5040	1.0138	2.0	0.61
199	0.2785	0.5876	0.4599	1.0138	2.0	0.58
200	0.2273	0.5226	0.3991	1.0151	2.0	0.58
201	0.202	0.4851	0.3628	1.0151	2.0	0.57

Table A.3.1 Results of 1.8 mm Hole Size Tray Experiments: System MeOH/H_2O

RUN	$\bar{x}$	Emv Measured	Model	Eog	H_f(cm)
MRA	0.6569	1.07	1.03	0.85	8.5
MRB	0.6887	1.14	1.08	0.89	8.0
MRC	0.6801	1.16	1.13	0.92	6.0
MRD	0.6500	1.16	1.13	0.92	6.0
MRE	0.5668	1.19	1.14	0.90	5.5
MRF	0.4960	1.21	1.19	0.90	5.0
MRG	0.3720	1.33	1.29	0.87	4.5
MRH	0.2607	1.64	1.62	0.87	4.5
MRI	0.2256	1.66	1.62	0.84	4.5
MV	0.5048	1.25	1.21	0.92	5.0
MW	0.1981	1.56	1.61	0.78	4.5

Table A.3.2 Results of 1.8 mm Hole Size Tray at an Outlet Weir Height of 2 mm Experiments: System MeOH/H_2O

Run	$\bar{x}$	Emv Measured	Model	Eog	H_f(cm)
ML	0.3926	1.05	1.03	0.79	4.0
MM	0.2420	1.15	1.10	0.72	3.0
MN	0.291	1.12	1.08	0.74	3.5
MO	0.1326	1.71	–	0.60	2.5
MP	0.8300	1.10	1.08	0.92	6.5
MQ	0.7735	1.03	1.09	0.92	6.0
MR	0.7148	1.02	1.07	0.90	6.0
MS	0.6459	1.15	1.03	0.86	6.0
MT	0.5785	1.09	1.04	0.85	5.5
MU	0.4532	1.02	1.03	0.79	5.0

Table A.3.3   Results of 1 mm Hole Size Tray Experiments:
                System MeOH/H_2O

RUN	$\bar{x}$	Emv Measured	Model	Eog	H_f(cm)
BOA	0.5345	1.21	1.22	0.94	7.0
BOB	0.4950	1.22	1.27	0.93	6.0
BOC	0.3660	1.36	1.46	0.94	6.0
BOD	0.2355	1.36	1.59	0.92	5.0
BOE	0.6040	1.14	1.17	0.93	7.0
BOF	0.4878	1.27	1.30	0.94	5.0
BOG	0.3090	1.48	1.50	0.92	4.0
BOH	0.0867	1.26	1.31	0.65	4.0

Table A.3.4   Results of 3.2 mm Hole Size Tray Experiments:
                System MeOH/H_2O

RUN	$\bar{x}$	Emv Measured	Model	Eog	H_f(cm)
SA	0.6840	1.07	1.05	0.88	6.0
SB	0.3870	1.30	1.25	0.88	4.5
SC	0.5693	1.09	1.09	0.89	4.5
SD	0.0875	1.39	-	0.35	4.5
SE	0.2515	1.44	1.45	0.85	4.5
SF	0.0294	1.77	-	0.25	4.5
SG	0.7940	1.15	1.07	0.91	7.0
SH	0.7770	1.13	1.06	0.91	6.5
SI	0.7650	1.11	1.02	0.87	6.5
SJ	0.5350	1.13	1.14	0.89	4.5
SK	0.0101	1.31	-	0.3	4.5

Table A.3.5   Results of 6.4 mm Hole Size Tray Experiments:
System MeOH/H_2O

RUN	$\bar{x}$	Emv Measured	Model	Eog	H_f(cm)
RA	0.7036	1.13	1.07	0.88	6.0
RB	0.6378	1.08	1.08	0.88	5.5
RC	0.5642	1.08	1.04	0.84	5.0
RD	0.5111	1.07	1.09	0.86	5.0
RE	0.3898	1.15	1.15	0.82	5.0
RF	0.2920	1.31	1.46	0.86	5.0
RG	0.0760	1.38	–	0.34	5.0
RH	0.1495	1.37	–	0.50	4.5
RJ	0.8020	1.11	1.06	0.89	7.5
RK	0.7414	1.13	1.07	0.89	7.0
RL	0.6754	1.10	1.03	0.85	6.5

Table A.3.6   Pressure Drop and Liquid Hold-up for 1.8 mm Diameter Hole
                Size Tray with 12.7 mm Outlet Weir Height: System MeOH/H_2O

Test	$\bar{x}$	h_T cm liquid Measured	h_T cm liquid BENNETT	h_L cm liquid Measured	h_L cm liquid BENNETT	h_δ(cm liquid) BENNETT
A1	0.81	2.2	3.16	1.6	1.34	1.16
A2	0.75	2.4	3.19	1.6	1.34	1.16
A3	0.71	2.0	3.18	1.6	1.34	1.14
A4	0.60	2.3	3.19	1.5	1.33	1.113
A5	0.50	2.3	3.23	1.6	1.32	1.11
MV	0.36	2.3	3.3	1.6	1.29	1.10
MW	0.23	-	3.5	-	1.27	1.10

Table A.3.7   Pressure Drop and Liquid Hold-up for 1.8 mm Hole Size Tray
with 2 mm Outlet Weir Height: System $MeOH/H_2O$

Test	$\bar{x}$	h_T (cm liquid) Measured	h_T (cm liquid) BENNETT	h_L (cm liquid) Measured	h_L (cm liquid) BENNETT	h_δ (cm liquid) BENNETT
MX	0.59	2.39	2.46	1.20	0.57	1.12
MY	0.53	2.35	2.47	1.41	0.57	1.12
A6	0.78	2.635	2.40	1.26	0.58	1.15
A8	0.63	2.41	2.43	1.21	0.58	1.13
A9	0.59	2.39	2.45	1.31	0.57	1.12
-	0.37	-	2.58	-	0.9	1.12
-	0.24	-	2.74	-	1.00	1.13

Table A.3.8   Pressure Drop and Liquid Hold-up for 1.8 mm Hole Size Tray
with 25.4 mm Outlet Weir Height: System MeOH/H_2O

Test	$\bar{x}$	h_T (cm liquid)		h_L (cm liquid)		h_δ (cm liquid)
		Measured	BENNETT	Measured	BENNETT	BENNETT
T1	0.87	2.95	4.11	1.93	2.30	1.20
T2	0.77	3.00	4.11	2.00	2.28	1.15
T3	0.71	2.83	4.11	1.85	2.28	1.14
T4	0.61	2.80	4.12	1.95	2.26	1.13
T5	0.67	2.58	4.14	1.83	2.26	1.13
T6	0.51	2.69	4.15	1.87	2.23	1.11
T7	0.34	2.57	4.20	1.79	2.18	1.11

Table A.3.9 Pressure Drop/Liquid Hold-up for 1 mm Hole Size Tray with
12.7 mm Outlet Weir Height: System MeOH/H_2O

Test	$\bar{x}$	h_T (cm liquid)		h_L (cm liquid)		h_δ (cm liquid)
		Measured	BENNETT	Measured	BENNETT	BENNETT
1	0.71	2.96	3.42	–	1.34	1.39
2	0.49	3.14	3.48	–	1.38	1.35
3	0.44	3.60	3.49	–	1.30	1.34
4	0.27	3.70	3.62	–	1.27	1.40
5	0.09	4.7	3.92	–	1.23	1.36
BOA	0.53	–	3.45	2.0	1.32	1.35
BOB	0.49	–	3.47	1.97	1.30	1.34
BOC	0.37	–	3.55	1.93	1.29	1.34
BOD	0.24	–	3.68	1.96	1.26	1.37
BOE	0.60	–	3.45	2.20	1.33	1.35
BOF	0.48	2.44	3.48	1.86	1.31	1.33
BOG	0.31	2.24	3.60	1.57	1.28	1.33
BOH	0.09	3.49	3.94	1.60	1.23	1.41

Table A.3.10   Pressure Drop/Liquid Hold-up for 3.2 mm Hole Size Tray
with 12.7 mm Outlet Weir Height: System MeOH/H_2O

Test	$\bar{x}$	h_T (cm liquid) Measured	h_T (cm liquid) BENNETT	h_L (cm liquid) Measured	h_L (cm liquid) BENNETT	h_δ (cm liquid) BENNETT
SA	0.68	2.20	2.97	1.83	1.34	0.94
SB	0.38	2.49	3.09	1.70	1.31	0.91
SC	0.57	2.25	3.01	1.78	1.33	0.92
SD	0.08	2.86	3.50	1.59	1.25	0.95
SE	0.25	-	3.20	-	1.30	0.91
SF	0.03	-	3.70	-	1.24	1.05
SG	0.79	3.02	2.96	1.76	1.40	0.95
SH	0.78	2.51	2.96	1.75	1.40	0.95
SI	0.77	2.37	2.98	1.87	1.34	-
SJ	0.54	2.35	3.03	1.76	1.33	0.95

Table **A.** 5.11   Pressure Drop/Liquid Hold-up for 6.4 mm Hole Size Tray

with 12.7 mm Outlet Weir Height: System MeOH/H_2O

Test	$\bar{x}$	h_T (cm liquid) Measured	BENNETT	h_L (cm liquid) Measured	BENNETT	h_δ (cm liquid) BENNETT
RA	0.70	3.07	2.78	1.96	1.34	0.70
RB	0.64	2.55	2.8	1.70	1.33	0.74
RC	0.56	2.96	2.8	1.78	1.33	0.74
RD	0.51	2.81	2.85	1.64	1.32	0.73
RE	0.38	2.73	2.9	1.59	1.30	0.72
RF	0.29	2.88	3.00	1.64	1.29	0.77
RG	0.07	-	3.3	-	1.23	0.73
RH	0.14	-	3.1	-	1.24	0.74
RJ	0.80	3.41	3.1	1.89	1.25	0.75
RK	0.74	3.70	2.78	1.97	1.34	0.75

Table A.4.1   Point Efficiencies of the Modified Oldershaw Column with

6.5 mm. Outlet Weir Height, System: Methanol–Water

RUN	x_1	y_1^*	E_{og}	H_f (cm)
320	0.5541	0.8054	0.73	2.5
321	0.5381	0.7978	0.74	2.5
322	0.5339	0.7956	0.76	2.5
323	0.5128	0.7853	0.72	2.2
324	0.4938	0.7759	0.71	2.2
325	0.4653	0.7613	0.74	2.2
326	0.4397	0.7483	0.75	2.2
327	0.3741	0.7112	0.74	2.1
328	0.3559	0.7001	0.73	2.1
329	0.3157	0.6738	0.75	2.1
330	0.2882	0.6519	0.76	2.0
331	0.2429	0.6174	0.75	2.0
332	0.8013	0.9153	0.75	2.6
333	0.7838	0.9079	0.81	2.5
334	0.7593	0.8973	0.80	2.5
335	0.7269	0.8833	0.81	2.5
336	0.7186	0.8796	0.77	2.5
337	0.6839	0.8644	0.78	2.5

Table A.4.2   Point Efficiencies of the Modified Oldershaw Column with

12.7 mm Outlet Weir Height System: MeOH/H_2O

RUN	XB	YT*	Eog Measured	Scaled	H_f (cm)
338	0.6289	0.8395	0.81	0.92	3.5
339	0.6129	0.8325	0.83	0.92	3.5
340	0.5952	0.8244	0.83	0.92	3.5
341	0.5641	0.8100	0.79	0.91	3.5
342	0.5381	0.7972	0.87	0.91	3.5
343	0.5100	0.7835	0.81	0.91	3.5
344	0.5339	0.7952	0.79	0.91	3.5
345	0.4917	0.7744	0.84	0.91	3.3
348	0.3877	0.7184	0.79	0.91	3.2
349	0.4078	0.7300	0.84	0.91	3.0
350	0.3964	0.7235	0.82	0.91	3.0
351	0.3610	0.7023	0.82	0.91	3.0
352	0.3312	0.6833	0.83	0.91	3.0
353	0.3049	0.6652	0.82	0.96	3.5
355	0.8491	0.9359	0.87	0.96	3.5
356	0.8325	0.9286	0.87	0.95	3.5
357	0.8176	0.9223	0.87	0.94	3.5
358	0.7864	0.9088	0.87	0.94	3.5
359	0.7691	0.9013	0.85	0.94	3.5
360	0.7426	0.8899	0.84	0.93	3.5
361	0.7215	0.8807	0.84	0.93	3.5
362	0.6934	0.8686	0.84	0.93	3.5
363	0.6661	0.8565	0.82	0.92	3.5

APPENDIX B

B.1 Calculation of Vapour-Liquid-Equilibria and Volumetric Properties

The computer programme was provided by Prausnitz et. al. (1967), in Fortran language and applied previously by Dribika (1986). The programme using accurately the thermodynamic non-idealities in the vapour and the liquid phases, was capable of computing the bubble point and volumetric properties for n components. It involved the following steps:-

For two phases which are at the same temperature, the equation of equilibrium for any component i, is

$$\varphi_i \, Y_i^{\,*} \, P \;=\; \gamma_i \, x_i \, f_i^{\,OL} \qquad\qquad B1$$

This is the key equation for the calculation of n. component vapour-liquid Equilibria (VLE).

a) Computation of vapour phase fugacity coefficient φ_i.

$$\ln \varphi_i = \frac{2}{\nu} \sum_{j=1}^{n} Y_i \, B_{ij} - \ln Z \qquad\qquad B2$$

The compressibility and the molar volumes are related by:-

$$Z = \frac{P}{RT} = 1 + \frac{B_{mix}}{\nu} \qquad\qquad B3$$

(Truncated Virial Equation of State)

$$B_{mix} = \sum_{i=1}^{N} \sum_{j=1}^{N} Y_i \, Y_j \, B_{ij} \qquad\qquad B4$$

(Second Virial Coefficient)

Method of the computation of B_{ij}, was the only modification to this computer programme. It was calculated using the correlation of Tsonopouls (1974) for polar-polar systems.

$$B_{ij} = \frac{RT_{Cij}}{P_{Cij}} \left[F(0) \, T_R + \omega \cdot F(1) \, T_R + F(2) \, T_R \right] \qquad \text{B5}$$

$$F(0)T_R = 0.1445 - 0.330/T_R - 0.1385/T_R^2 - 0.0121/T_R^3 \qquad \text{B6}$$

$$F(1)T_R = 0.073 + 0.46/T_R - 0.50/T_R^2 - 0.097/T_R^3 - 0.0073/T_R^8 \qquad \text{B7}$$

$$F(2)T_R = \alpha_{ij}/T_R^6 - \beta_{ij}^*/T_R^8 \qquad \text{B8}$$

The values of α and β, the parameters polar contribution term to $F(2)T_R$ in equation B8 were provided by the author as given in Table B1.

Table B1   Parameters of Polar Contribution

Comp.	H_2O	MeOH	EtOH	n.PrOH
α_i^*	0.0279	0.0878	0.0878	0.0878
β_i^*	0.0229	0.0560	0.0572	0.0447

The cross coefficient B_{ij} is calculated using the equation B5 by making the following simplifying assumptions:-

$$T_{Cij} = (T_{Ci} \, T_{Cj})^{\frac{1}{2}} \qquad \text{B9}$$

$$\omega_{ij} = 0.5 \, (\omega_i + \omega_j) \qquad \text{B10}$$

$$P_{Cij} = 4 \, T_{Cij} \left[\frac{P_{Ci} \, \nu_{ci}}{T_{Ci}} + \frac{P_{Cj} \, \nu_{cj}}{T_{Cj}} \right] \Big/ \, (\nu_{ci}^{\frac{1}{3}} + \nu_{cj}^{\frac{1}{3}})^3 \qquad \text{B11}$$

$$\alpha^*_{ij} = 0.5 \, (\alpha^*_i + \alpha^*_j) \qquad \text{B12}$$

$$\beta^*_{ij} = 0.5 \, (\beta^*_i + \beta^*_j) \qquad \text{B13}$$

T_C, critical temperature

P_C, critical pressure

$\omega_{i,j}$ acentric factor for polar components

and T_R, reduce temperature $= T/T_C$

The critical properties and physical chemical quantities of pure components are given by Reid et. al. (1977) and tabulated in the Table B2.

Table B2   Critical properties and physical-chemical quantities of pure components

Property		MeOH	EtOH	n.PrOH	H_2O
T_C	°K	512.06	516.2	536.7	647.3
P_C	atm	79.9	63.0	51.0	217.6
ν_C	cc/mole	118.0	167.0	218.5	56.0
Z_C		0.2240	0.248	0.253	0.229
ω_i		0.557	0.635	0.624	0.344

b) <u>Computation of Liquid Phase Fugacity</u>

The fugacity of any component i in the liquid phase F_i^L (right hand side of the equation B1), is given by:-

$$F_i^L = \gamma_i \, x_i \, F_i^{OL} \qquad\qquad B14$$

or $\quad F_i^L = \gamma_i \, x_i \, F_i^{0(PO)} \, EXP \left(\dfrac{P \, \nu_i^L}{RT} \right) \qquad\qquad B14$

where

$$F_i^{(PO)} = \varphi_i^S \, P_i^S \, EXP \left(- \dfrac{\nu_i^L \, P_i^S}{RT} \right) \qquad\qquad B15$$

Substitute B15 in B14

$$F_i^L = \gamma_i \, x_i \, \varphi_i^S \, P_i^S \, EXP \dfrac{\nu_i^L \, (P - P_i^S)}{RT} \qquad\qquad B16$$

φ_i^s , is calculated using equation B2, P_i^S from Antoine equation:

$$\ln P_i^S = C_1 + \dfrac{C_2}{C_3 + T} \qquad\qquad B17$$

The values of Antoine constants were provided by Boublik et. al. (1973) as given in Table B3:-

Table B3   Antoine Equation Constants

Component	C1	C2	C3
MeOH	8.08097	1582.71	239.726
EtOH	8.11220	1592.866	226.184
n.PrOH	7.74416	1437.686	198.463
H_2O	8.07131	1730.630	233.426

Liquid molar volumes v_i, at three different temperatures were correlated from the following equation:-

$$v_i^L = r + sT + tT^2 \qquad \text{B18}$$

Where:

$$t = \frac{(T_3-T_1)(v_2^L - v_1^L) - (v_3^L - v_1^L)(T_2-T_1)}{(T_2^2-T_1^2)(T_3-T_1) -)T_3^2-T_1^2)(T_2-T_1)} \qquad \text{B19}$$

$$s = \frac{(v_2^L - v_1^L) - t(T_2^2 - T_1^2)}{T_2 - T_1} \qquad \text{B20}$$

$$r = v_1^L - s T_1 - t T_1^2 \qquad \text{B21}$$

The molar volume data were provided by Prausnitz et. al. (1967) as tabulated in Table B4.

Table B4   Molar Volume Data

Component	T_1	v_1	T_2	v_2	T_3	v_3
MeOH	273.15	39.556	373.15	44.874	473.15	57.939
EtOH	273.15	57.141	323.15	60.356	373.15	64.371
n.PrOH	293.15	74.785	343.15	78.962	393.15	84.515
H_2O	277.13	18.06	323.15	18.278	373.15	18.844

B.1.b.1   Computation of Activity Coefficient, γ_i

The activity coefficient was calculated using the Wilson equation:-

$$\ln \gamma_i = 1 - \ln\left[\sum_{j=1}^{n} x_i \Lambda_{ij}\right] - \sum_{K=1}^{n}\left[\frac{x_K \Lambda_{Ki}}{\sum_{j=1}^{n} x_i \Lambda_{Kj}}\right] \quad B22$$

where

$$\Lambda_{ij} = \frac{v_j^L}{v_i^L} \; EXP\left[-\frac{(\psi_{ij} - \psi_{ii})}{RT}\right] \quad B23$$

ψ_{ii} and ψ_{ij} are the Wilson parameters given in Chapters 4 and 9.

B.2   V.L.E. Measurements for the Quaternary System MeOH/EtOH/n.PrOH/H_2O

The V.L.E. measurements were carried out using an Ellis Froom (1954) still. The experimental details of the measurements are given by the authors. The main purpose of this investigation was to study the feasability of using the binary Wilson parameters (see Chapters 4 and 9) to

predict quaternary V.L.E. The details of analysis of the samples were given in appendix D. The details of using the Wilson model was given earlier in this appendix. Table B5 shows the maximum and minimum absolute deviations between the prediction and measurements of the vapour equilibrium values. Within experimental accuracy these deviations seem reasonable. Further details of the V.L.E., and bubble point measurements and predictions are given in Table B6.

Table B5   Statistical analysis of measured and predicted equilibrium data

Component No.	$(X_i - X_{ip})/n$	$x_{i_{max}} - x_{ip}$	$x_{i_{min}} - x_{ip}$
1	$\pm$ 0.0115	0.0284	0.0003
2	$\pm$ 0.00587	0.0342	0.0019
3	$\pm$ 0.0117	0.0171	0.0008
4	$\pm$ 0.0109	0.0199	0.0004

$$T-T_p/n \quad = \pm\ 0.8^{\circ}C$$

$$T-T_p \quad max = \quad 2.1^{\circ}C$$

$$T-T_p \quad min = \quad 0.0^{\circ}C$$

Table B6   Quaternary V.L.E. Measurements/Predictions

RUN	X1	Y1 MEAS	Y1 BUB	X2	Y2 MEAS	Y2 BUB
Q2	0.0515	0.1124	0.1186	0.2170	0.2920	0.2882
Q4	0.0204	0.0402	0.0394	0.2073	0.2640	0.2595
Q6	0.2960	0.4547	0.4725	0.1448	0.1549	0.1423
Q8	0.3104	0.5016	0.4846	0.1244	0.1320	0.1279
Q10	0.3168	0.5089	0.5007	0.1008	0.1053	0.0995
Q12	0.4399	0.6378	0.6301	0.1103	0.1006	0.0972
Q13	0.4982	0.6950	0.6852	0.0998	0.0858	0.0838
Q14	0.5073	0.7029	0.6922	0.1203	0.1005	0.0986
Q15	0.5007	0.6989	0.6867	0.1209	0.1022	0.0996
Q16	0.5358	0.7278	0.7171	0.1131	0.0928	0.0906
Q17	0.5201	0.7052	0.6959	0.1676	0.1364	0.1336
Q18	0.4817	0.6619	0.6663	0.1610	0.1370	0.1355
Q19	0.4874	0.6671	0.6649	0.1390	0.1228	0.1189
Q20	0.2651	0.7432	0.7331	0.1193	0.0972	0.0957
Q22	0.4200	0.6111	0.6035	0.1444	0.1416	0.1397
Q25	0.3749	0.6209	0.5925	0.0894	0.0982	0.0982
Q26	0.3610	0.5952	0.5700	0.0865	0.1025	0.0992
Q27	0.2301	0.4677	0.4614	0.0569	0.0990	0.0958
Q28	0.2645	0.5202	0.5074	0.0536	0.0890	0.0847
Q29	0.2389	0.4423	0.4311	0.1310	0.1916	0.1882
Q30	0.2852	0.5137	0.4989	0.1127	0.1617	0.1552
Q31	0.2383	0.4886	0.4592	0.0964	0.1590	0.1548
Q32	0.2813	0.5285	0.5166	0.0872	0.1372	0.1305
Q33	0.2596	0.4719	0.4552	0.0833	0.1160	0.1110
Q34	0.2435	0.4165	0.4168	0.1296	0.1998	0.1656
Q35	0.2284	0.3891	0.3775	0.1995	0.2368	0.2395
Q36	0.2112	0.3481	0.3415	0.2627	0.3084	0.3012

Contd.

RUN	X3	Y3 MEAS	Y3 BUB	X4	Y4 MEAS	Y4 BUB	T_{MEAS} °C	T_{BUB} °C
Q2	0.6489	0.4362	0.4464	0.0825	0.1594	0.1469	86.5	86.5
Q4	0.4735	0.3365	0.3443	0.2989	0.3767	0.3568	84.9	84.8
Q6	0.3310	0.1636	0.1899	0.2282	0.2268	0.1953	78.0	78.0
Q8	0.2301	0.1241	0.1482	0.3351	0.2422	0.2394	77.2	77.6
Q10	0.3195	0.1609	0.1881	0.2629	0.2249	0.2177	78.0	77.34
Q12	0.2340	0.1052	0.1225	0.1564	0.1941	0.1502	75.2	74.4
Q13	0.2079	0.0877	0.1034	0.1941	0.1315	0.1276	74.4	73.2
Q14	0.2110	0.0851	0.1006	0.1115	0.1626	0.1082	74.0	73.0
Q15	0.2158	0.0866	0.1034	0.1125	0.1518	0.1103	74.0	73.1
Q16	0.1993	0.0792	0.0929	0.1518	0.1002	0.0993	73.2	72.4
Q17	0.1798	0.0682	0.0822	0.1326	0.0902	0.0884	73.2	72.4
Q18	0.1706	0.0736	0.0840	0.1867	0.1274	0.1142	73.8	73.0
Q19	0.1489	0.0666	0.0768	0.2247	0.1435	0.1394	73.6	73.1
Q20	0.1252	0.0493	0.0601	0.1904	0.1103	0.1111	72.0	71.5
Q22	0.0981	0.0517	0.0608	0.3374	0.1956	0.1980	74.5	74.2
Q25	0.0606	0.0438	0.0499	0.4751	0.2370	0.2532	74.0	73.1
Q26	0.0918	0.0635	0.0732	0.4607	0.2388	0.2577	76.9	75.4
Q27	0.0602	0.0796	0.0818	0.6528	0.3537	0.3610	77.8	76.1
Q28	0.0559	0.0691	0.0699	0.6259	0.3217	0.3379	78.9	79.3
Q29	0.0518	0.0516	0.0553	0.5786	0.3135	0.3255	78.0	78.3
Q30	0.0526	0.0526	0.0436	0.5593	0.2836	0.3025	79.2	78.1
Q31	0.0361	0.042	0.0452	0.6292	0.3183	0.3407	78.4	78.1
Q32	0.0326	0.0346	0.0375	0.5989	0.2996	0.3154	78.6	77.3
Q33	0.1151	0.0941	0.1112	0.5420	0.3173	0.3225	80.0	78.3
Q34	0.1151	0.0889	0.1032	0.5112	0.2948	0.3144	79.5	78.3
Q35	0.1070	0.0758	0.0867	0.4552	0.2983	0.2912	77.8	78.0
Q36	0.1010	0.0639	0.0759	0.4251	0.2796	0.2814	77.8	77.8

APPENDIX C

PHYSICAL PROPERTIES

C.1 Diffusion Coeffiecient of Binary Gas Systems at Low Pressure

The derivation of the Chapman or Enskog equation as described by Reid et. al. (1977) was used to calculate D_{gij}.

$$D_{gij} = 1.858 \times 10^{-3} \times T^{3/2} \frac{((M_i + M_j)/M_i M_j)^{\frac{1}{2}}}{P \, F_{ij}^2 \, \Omega_D} \qquad \text{C1}$$

where,   T   = temperature ^{o}K

P   = Pressure atm

F   = Characteristic length, A^{o}

Ω_D = Diffusion collision integral

M   = Molecular weight

D_{gij} = Binary Diffusion coefficient (m^2/Sec)

And

$$F_{ij} = \frac{F_i + F_j}{2} \qquad \text{C2}$$

$$\Omega_D = \frac{AD}{T^{*BD}} + \frac{CD}{EXPDDT^*} + \frac{ED}{EXPFDT^*} + \frac{GD}{EXPHDT^*} \qquad \text{C3}$$

$$T^* = KT/E_{ij} \qquad \text{C4}$$

$$E_{ij} = (E_i * E_j)^{\frac{1}{2}} \qquad \text{C5}$$

where

E = Characteristic Energy

From R&id et. al. (1977):-

AD = 1.06036   BD = 0.15610   CD = 0.1930

DD = 0.4764   CD = 1.03589   FD = 1.52996

GD = 1.76474   HD = 3.89411

	F	E/k
MeOH	3.626	481.8
EtOH	4.53	362.6
n.PrOH	4.549	576.7
H_2O	2.641	809.1

The calculated diffusion coefficients for the binary combination of the above components were calculated using equation C1 as shown in the Figure 9.1, Chapter 9.

C.2   Calculation of the Vapour and Liquid Enthalpies

The heat of vapourisation of a pure component at normal boiling point can be estimated with an average error of 2.2 per cent using the Riedel equation as given by Chopey Hicks, (1984).

$$\Delta H_{vb} = 1.093 \; R \; T_c \left[\frac{T_{b.r} \times 1_n \, (P_c - 1)}{0.93 - T_{b.r}} \right] \qquad C6$$

The critical properties were given in appendix B. With $T_{b.r} = T_{BUB}/T_c$, reduced temperature at boiling point.

The heats of vapourisation at reduced temperatures are calculated using the Wilson correlation:-

$$\frac{\Delta H_{vb2}}{\Delta H_{vb1}} = \left(\frac{1 - T_{R.2}}{1 - T_{R.1}}\right)^{0.38} \qquad\qquad C7$$

Where ΔH_{v1} and ΔH_{v2} are the heats of vapourisation at reduced temperatures and $T_{R.1}$ and $T_{R.2}$ are the reduced temperatures.

The heat of vapourisation is:-

$$\Delta H_{vb} = H_v - H_L \qquad\qquad C8$$

As H_v, the vapour enthalpy and H_L liquid enthalpy are arbitrary values, suitable values describing the change of the heat of vapourisation at different temperatures were chosen by trial and error. For water the vapour and liquid enthalpies were provided by the standard steam tables. These values are tabulated in the Table C1 and C2.

Table C1   Vapour Enthalpies

H_L BTU/lb.mole

Temp °C	MeOH	EtOH	n.PrOH	H_2O
66.0	18918	18189	20081.2	20289.0
75.0	19050	19220	20150.3	20413.0
100.0	19148	20482	20200.8	20730.0

Table C2   Liquid Enthalpies

H_L BTU/lb.mole

Temp ^{o}C	MeOH	EtOH	n.PrOH	H_2O
66.0	2518.0	2100.0	1200.0	2138.0
75.0	3620.0	2340.0	1600.0	2432.0
100.0	4095	3000.0	2627.0	3247.0

C.3   Liquid Densities

Pure component liquid densities at different temperatures were provided by TRC tables (1981) for the alcohols and water as follows:-

ρ_L (g/cm^3)

Temperature	MeOH	EtOH	n.PrOH	H_2O
60	0.7546	0.7550	0.7704	0.9832
70	0.7448	0.7459	0.7614	0.9778
80	0.7347	0.7362	0.7522	0.9718
90	0.7242	0.7260	0.7426	0.9653
100	0.7132	0.7151	0.7326	0.9584

These data were subject to a least mean square polynomial fitting for suitable equations of the following form:

$$\rho_i = EXP (H_i - q_i \ln T) \qquad\qquad C9$$

	H_i	q_i
MeOH	0.1704	0.1098
EtOH	0.1446	0.1033
n.PrOH	0.1421	0.0979
H_2O	0.1884	0.0499

The mixture density ρ_M was calculated using the following equation:-

$$\rho_M = \sum_{i=1}^{n} \rho_i W_i \qquad \text{C10}$$

Where Wi is the weight fraction of the component, i in the mixture.

APPENDIX D

ANALYSIS OF THE SAMPLES

D.1 Gas-Liquid-Chromatography

The samples containing up to four components at times were analysed by gas-liquid-chromatography technique. A Varian Vesta chromatographer with an automatic injection equiped with a thermal conductivity detector (TCD) was used. The column ready packed with "Porapak Q" was 290 cm long, operated isothermally at $150^{\circ}C$ for the samples containing methanol, otherwise $160^{\circ}C$ and 3 bar pressure. The TCD detector and the injector temperatures were at $200^{\circ}C$. These conditions were found to provide an excellent reproducibility, with non-overlapping peaks. Each sample was analysed twice and saved for further re-analysis, if required. $1\mu l$ of the sample was injected each time with nitrogen as carrier gas at a rate of 30 ml/Min. Figure D.1 shows the peaks and details of a typical quarternary and binary analysis.

D.2 Calibration

20, 30 and 40 samples were made for the binary, ternary and quarternary calibrations respectively, covering a wide range of composition. Each sample was weighed up on a balance with 5D accuracy. Fisons AR grade alcohols and distilled deionised water were used to make up these samples. The samples were then analysed by G-L-C technique described in D.1. The area ratios AR_j, and weight ratios W_j were correlated by a least square method to yield a calibration equation of the form:-

$$W_j = EXP \left(-e + f \, 1_n \, AR_j \right) \qquad \text{D.1}$$

Where W_j and AR_j are the ratios of the component i to the standard component. These weight ratios were then translated in terms of the mole fraction.

The accuracy of each calibration was calculated by the following equation:-

$$ACC = \frac{\sum_{1}^{n} (x_{iMEAS}\ x_{iCALIB})}{n} \qquad D.2$$

Where x_{iCALB} is the mole fraction calculated by the equation D.1, and n is the number of calibration samples. Table D.1 summarises the coefficients of the equation D1 and its accuracy ACC for the systems used in this work. Note: these calibrations were subject to regular checks, and were repeated if necessary.

Table D Coefficients and Precision of the Equation D.1

System	W_j	e	f	ACC
n.PrOH/MeOH	W1	0.9342	1.1032	± 0.0020
MeOH/H_2O	W1	0.7284	1.3081	± 0.0038
EtOH/H_2O	W1	0.7291	1.4089	± 0.0028
n.PrOH/H_2O	W1	0.4930	1.3987	± 0.0034
MeOH/EtOH/H_2O	W2	0.2370	1.4611	± 0.0043
	W3	0.6946	1.3130	"
MeOH/n.PrOH/H_2O	W2	0.6069	1.4789	± 0.0053
	W3	0.7924	1.3648	"
MeOH/EtOH/ n.PrOH/H_2O	W2	0.2016	1.377	± 0.0045
	W3	0.6406	1.429	"
	W4	0.6713	1.3067	"

CHART SPEED   0.2 CM/IN
ATTEN: 128   ZERO: 5%   5 MIN/TICK

STAT :INJECT

3.572   2.222
5.430
7.294
9.810
16.531
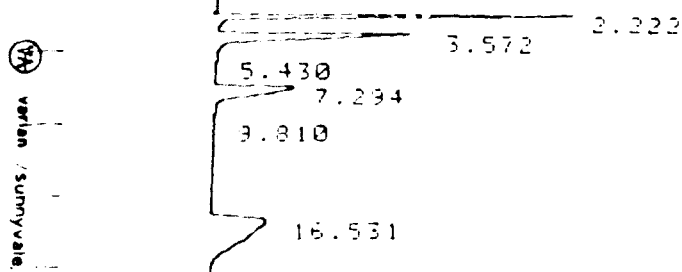
TITLE: DISTILLATION   14:52   16 MAR 86

CHANNEL NO: 1   SAMPLE: 16   METHOD: MAK

PEAK NO	PEAK NAME	RESULT FACTOR	TIME (MIN)	AREA COUNTS	SEP CODE
1	WATER	1.013400	2.222	482347	BB
2	METHANOL	INT STD	3.572	488810	BB
3	ETHANOL	1.452870	7.294	336445	BV
4	PROPANOL	0.753391	16.531	644536	BB

TOTALS: 1952140
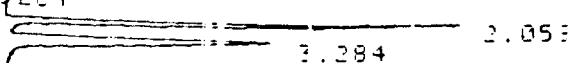

CHART SPEED   0.2 CM/IN
ATTEN: 128   ZERO: 5%   5 MIN/TICK

STAT :INJECT
WATER

3.284   2.059

TITLE: DISTILLATION   16:08   27 FEB 87

CHANNEL NO: 1   SAMPLE: ZK7   METHOD: M0

PEAK NO	PEAK NAME	RESULT FACTOR	TIME (MIN)	AREA COUNTS	SEP CODE
1	WATER	1.241220	2.059	676519	BB
2	METHANOL	INT STD	3.284	839709	BB

TOTALS: 1516230

FIGURE D.1